The phosphorolytic activity of the exosome core complex contributes to rRNA maturation in Arabidopsis thaliana

Natalia Sikorska

UNIVERSITÉ DE STRASBOURG

ECOLE DOCTORALE DE LA VIE ET DE LA SANTE

L'Institut de biologie moléculaire des plantes, CNRS

THÈSE présentée par :

Natalia SIKORSKA

soutenue le 30 Septembre 2016

pour obtenir le grade de : **Docteur de l'université de Strasbourg**

Spécialité : **Aspects Moléculaires et Cellulaires de la Biologie**

The phosphorolytic activity of the exosome core complex contributes to rRNA maturation in *Arabidopsis thaliana*

THÈSE dirigée par :

Dr GAGLIARDI Dominique Directeur de recherche, Université de Strasbourg

RAPPORTEURS :

Dr BOUSQUET-ANTONELLI Cécile Directrice de recherche, Université de Perpignan

Dr KUFEL Joanna Professeur, Université de Varsovie

AUTRES MEMBRES DU JURY :

Dr ROMBY Pascale Directrice de recherche, Université de Strasbourg

Table of contents

Acknowledgments

First and foremost, I want to thank my two great supervisors, Gag and Heike. For all the support, attention, great discussions, luxury experiments ;) and for my PhD project, which I loved to work on.

I would like to thank all the members of the Jury, Cécile Bousquet-Antonelli, Joanna Kufel and Pascale Romby, to have accepted to evaluate the work presented in this manuscript.

The members of our group have contributed immensely to my personal and professional time here in IBMP. I was very happy to share the lab with our 306 “core team”, Carlos, Caro, Hélène and little Hélène. There are also unforgettable former members, Pawel, Pierre and Gaetan, and new members, Clara and Damian. It was great to work around you guys. I was lucky to be a member of our team.

I would also like to thank Todd, Jean, Clémentine, Marion and Marco, for interesting discussions, great ideas and support.

Lastly, I would like to thank my parents for all their love and encouragement.

This manuscript is based upon work supported by LabEx NetRNA.

List of tables

List of figures

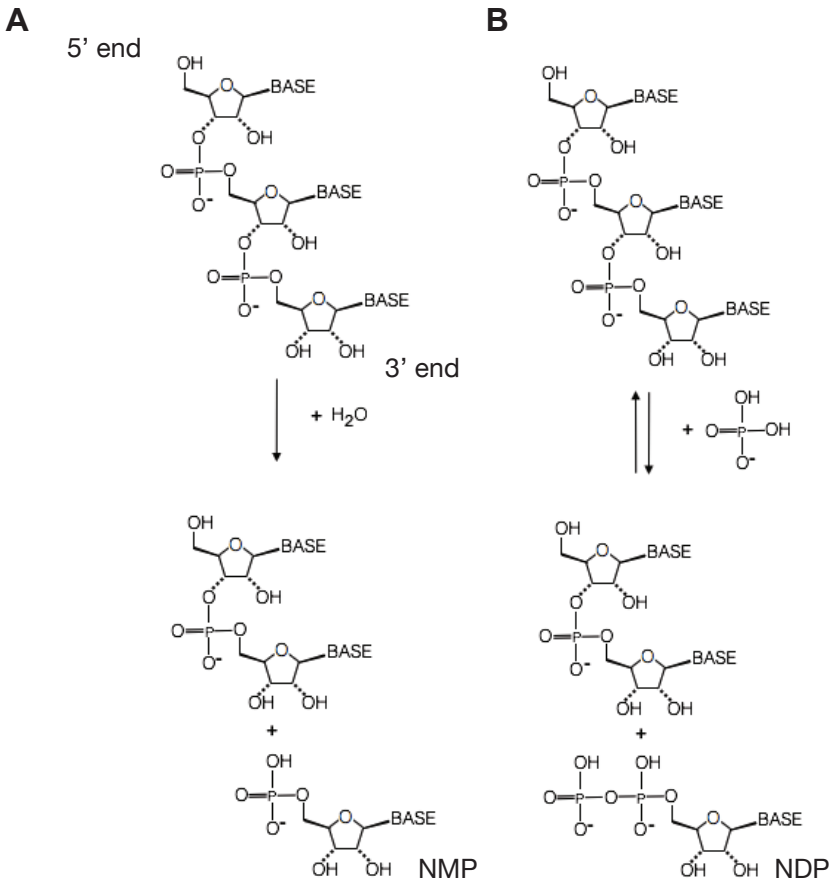

Figure 1. Mechanism used by hydrolytic ribonucleases vs phosphorolytic ribonucleases.
A. Hydrolytic ribonucleases, like Rrp44p/hRRP44/AtRRP44 and Rrp6p/hRRP6/AtRRP6L2 use water to cleave phosphodiester bonds of attacked RNA substrates and in irreversible reaction release nucleoside monophosphates (NMPs).
B. Phosphorolytic ribonucleases like RNase PH, PNPase or archaeal exosome use inorganic phosphate (Pi) to attack the phosphodiester bond of the RNA substrate and release nucleoside diphosphates (NDPs). The reaction is reversible: in presence of inorganic phosphate, RNA is degraded; in excess of NDPs, RNA is synthesized.

Introduction

I. Context

RNA degradation plays an essential role for cell homeostasis in all domains of life. RNA turnover is involved in the control of the steady-state levels of all cellular RNAs, eliminates misprocessed and non-functional RNA species and recycles maturation by-products that arise from RNA processing (Houseley and Tollervey, 2009; Lykke-Andersen et al., 2009). Another role of RNA degradation is partial trimming of RNA precursors to their mature form since most of RNA molecules require multiple co- and post-transcriptional processing steps involving endo- and exoribonucleases.

Endoribonucleases use a hydrolytic mechanism to degrade RNA, while exoribonucleases use either hydrolysis or phosphorolysis. Hydrolytic exoribonucleases use water to attack the phosphodiester bond of their substrate and release nucleoside monophosphates (NMPs). Phosphorolytic exoribonucleases degrade RNA by using inorganic phosphate (Pi) to attack the phosphodiester bond and release nucleoside diphosphates (NDPs) (Figure 1). Phosphorolysis salvages the energy of the phosphodiester bond, whereas this energy is lost upon hydrolytic degradation of RNA. Hence, the activity of phosphorolytic enzymes is reversible. Therefore, phosphorolytic enzymes degrade RNAs in the presence of excess Pi, but synthesize non-templated polynucleotide tails in the presence of excess NDPs.

In eukaryotic cells, exoribonucleolytic RNA degradation involves two major pathways, the 5'-3' pathway and the 3'-5' pathway (Houseley and Tollervey, 2009; Kilchert et al., 2015; Lykke-Andersen et al., 2009). The bulk of 5'-3' degradation is performed by the exoribonucleases of the XRN family (Jones et al., 2012; Nagarajan et al., 2013; Parker, 2012; Siwaszek et al., 2014). In yeast, flies and mammals, XRN1 is mainly cytoplasmic while XRN2/RAT1 resides in the nucleus. Plants have no homologs of XRN1 but three homologs of XRN2/RAT1, named AtXRN2-4. In

Arabidopsis, AtXRN4 is a cytoplasmic enzyme while AtXRN2 and AtXRN3 are located in the nucleus (Kastenmayer et al., 2001). The main role of the cytoplasmic members of the XRN family is the bulk turnover of both non-coding RNAs and mRNAs (He et al., 2003; Souret et al., 2004) including co-translational mRNA decay (Hu et al., 2009; Merret et al., 2015; Pelechano et al., 2015). In the nucleus, XRN proteins degrade pre-mRNAs, contribute to mRNA quality control and function in transcription termination (El Hage et al., 2008; Kim et al., 2004; Luo et al., 2006). XRN proteins contribute also to the processing, quality control and degradation of rRNAs and other non-coding transcripts (Chernyakov et al., 2008; Henry et al., 1994; Kurihara et al., 2012; Zakrzewska-Placzek et al., 2010). In plants, all three AtXRNs function as silencing suppressors by eliminating transcripts that would otherwise be recognized by the siRNA machinery (Gazzani et al., 2004; Gy et al., 2007).

The main 3'-5' degradation machinery in eukaryotic cells is the RNA exosome. The exosome is a multisubunit complex that is present in both nucleus and cytoplasm. The eukaryotic RNA exosome was originally discovered as the 3'- 5' exoribonuclease that generates the 3' end 5.8S ribosomal RNA (rRNA) in yeast (Mitchell et al., 1997, 1996). The majority of exosome subunits were named Rrp (for rRNA-processing) or Mtr (for mRNA transport). Nearly two decades after being discovered, the exosome complex is known to be involved in degradation and processing of virtually all kinds of coding and non-coding RNAs. The exosome degrades pre-mRNAs, eliminates mRNAs that are recognized by nonsense-mediated decay, nonstop decay or no-go decay pathways, and contributes to mRNA turnover (Anderson and Parker, 1998; Bousquet-Antonelli et al., 2000; Doma and Parker, 2007; Gudipati et al., 2012; van Hoof et al., 2000; Houseley and Tollervey, 2009; Schneider et al., 2012). Another important role of the exosome is the processing and degradation of small nuclear RNAs (snRNAs), small nucleolar RNAs (snoRNAs) and ribosomal RNAs (rRNAs) (Allmang et al., 1999a, 1999b; van Hoof et al., 2000).

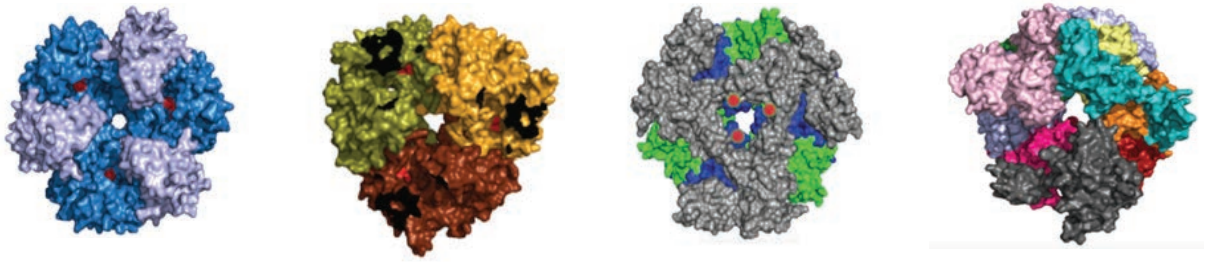

RNase PH
6 active sites

PNPase
3 active sites

archaeal exosome
3 active sites

eukaryotic exosome
(yeast and human)
catalytically inert core

Figure 2. Bacterial phosphorylases RNase PH and PNPase, archaeal exosome and eukaryotic exosome share a characteristic ring-shaped structure.
Description in the main text. (Adapted from Januszyk et al., 2014)

The exosome also degrades misfolded transfer RNAs (tRNAs) and tRNA precursors, cryptic unstable transcripts (CUTs), PROMPTs (promoter upstream transcripts), or RISC-cleaved transcripts (transcripts cleaved by RNA Induced Silencing Complex) (Branscheid et al., 2015; LaCava et al., 2005; Neil et al., 2009; Orban and Izaurralde, 2005; Preker et al., 2008; Schneider et al., 2012; Vanácová et al., 2005; Wyers et al., 2005).

II. From bacterial RNase PH to eukaryotic exosomes

A. RNase PH

The eukaryotic exosome is structurally and evolutionarily related to prokaryotic phosphorolytic 3'-5' exoribonucleases. The simplest phosphorolytic 3'-5' exoribonuclease is bacterial RNase PH, that is mainly involved in the 3' end processing of structured RNAs such as tRNAs (Harlow et al., 2004). A functional RNase PH enzyme consists of six monomers that form a characteristic ring-shaped structure with a central channel. The RNase PH ring includes six phosphorolytic active sites that are located at the interface between the six RNase PH monomers (Choi et al., 2004; Harlow et al., 2004). The characteristic ring of RNase PH is also found in other protein complexes with RNase PH-like domains such as bacterial phosphorolytic 3' exoribonuclease, polynucleotide phosphorylase (PNPase) and both archaeal and eukaryotic exosomes (Figure 2) (Januszyk and Lima, 2014).

B. PNPase

PNPase is a homotrimer. Each monomer contains a duplicated RNase PH fold, PH1 and PH2, and two RNA-binding domains of the KH and S1 types. The KH and S1 domains are located on top of the ring and participate in substrate binding and in feeding the RNA substrate through the central channel of PNPase (Stickney et al., 2005). Deletion of any or both of RNA-binding domains of *Escherichia coli* PNPase substantially reduces its RNA binding and its enzymatic activity (Stickney et

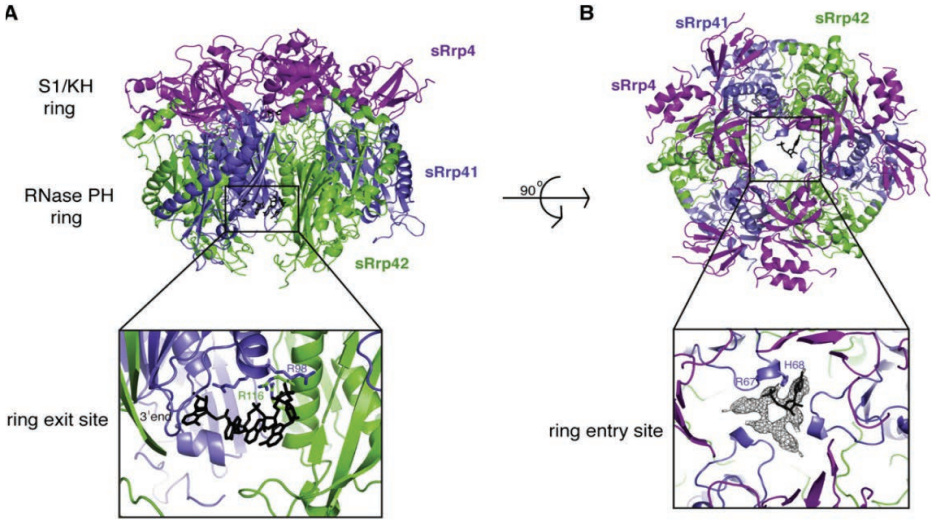

Figure 3. The ring-shaped structure of archaeal exosome with a prominent central channel.
A. Side view of the *Sulfolobus solfataricus* exosome structure (Lorentzen et al., 2007). The RNase PH-like subunits Rrp41 and Rrp42 are depicted in blue and green respectively; the S1/KH subunit Rrp4 is in magenta and RNA is shown in ball-and-stick representation in black. The zoomed-in view shows the phosphorolytic active site.
B. Top view of the *S. solfataricus* exosome, looking down the central channel. The zoomed-in view shows the RNA trapped at the entrance pore of the channel.
(Figure taken from Bonneau et al., 2009)

al., 2005). Since only the C-terminal PH2 domains harbor a catalytic site, PNPase enzymes have three active sites situated inside the channel (Shi et al., 2008). PNPase is evolutionary conserved and present in almost all species from bacteria to plants (present in the mitochondria and chloroplasts) and mammals (present in mitochondria) (Schuster and Stern, 2009; Slomovic et al., 2008, 2006, 2005). By contrast, archaea, yeast and trypanosomes do not possess a PNPase (Slomovic et al., 2006). PNPase is a highly processive enzyme that has the ability to degrade its substrates without releasing it after each catalytic cycle (removal of a single nucleotide) (Shi et al., 2008). *E. coli* PNPase favors single-stranded substrates and is impeded by secondary structures such as stem-loops. PNPase-mediated degradation of structured RNAs can be facilitated by the ATP-dependent RNA-unwinding helicase RhIB (Liou et al., 2002). *E. coli* PNPase, RhIB, endoribonuclease RNaseE and the metabolic enzyme enolase can form a high-molecular-weight complex, called the degradosome (Carpousis et al., 1994; Coburn and Mackie, 1999; Py et al., 1994). Related complexes containing endo-and exoribonucleases, an RNA helicases and a metabolic enzyme have also been found in other bacteria (reviewed in Aït-Bara and Carpousis, 2015). In both bacteria and organelles, RNA degradation by PNPase is stimulated by the addition of non-templated poly(A) or poly(A)-rich tails to the 3' ends of its substrates (Hajnsdorf et al., 1995; Haugel-Nielsen et al., 1996; Mohanty and Kushner, 2016, 2002; Schuster et al., 1999). Such tails can be added by dedicated poly(A) polymerases or by PNPase itself (Mohanty and Kushner, 2000; Slomovic et al., 2008).

C. Archaeal exosome

Archaeal exosomes are processive phosphorolytic enzymes that share mechanistic and structural similarities with bacterial PNPase (Lorentzen and Conti, 2012; Lorentzen et al., 2005). Archaeal exosomes are composed of three heterodimers of the two PH-like proteins Rrp41 and Rrp42, that form the hexameric

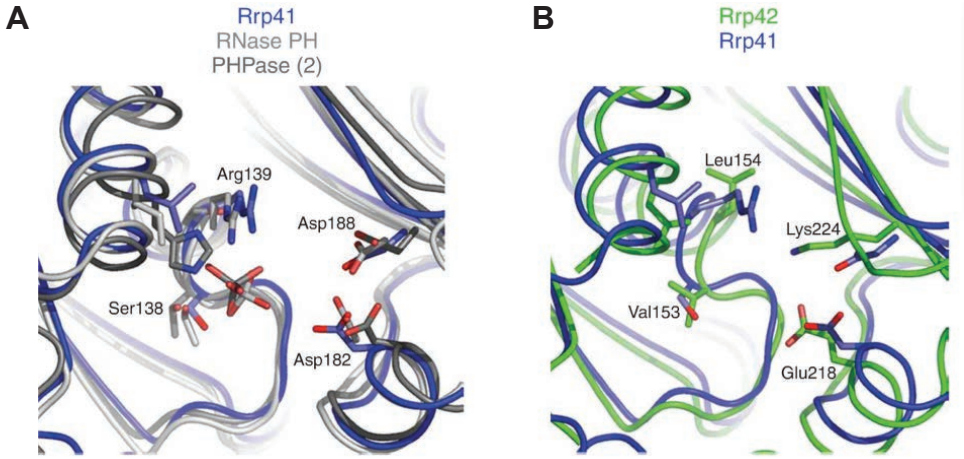

Figure 4. The residues essential for the phosphorolytic activity are conserved in bacterial RNase PH, C-terminal RNase PH-like domain of bacterial PNPase and archaeal exosome subunit Rrp41 but not Rrp42. A. Structural superposition of the active site regions of RNase PH (light gray), the C-terminal RNase PH-like domain of PNPase (dark gray) and the Rrp41 subunit of Archaeal exosome (Sulfolobus solfataricus) (blue). Residues of Archaeal Rrp41 involved in phosphate ion coordination: Ser^{138} and Arg^{139} (corresponding to Thr^{462} and Ser^{463} in PNPase and Thr^{125} and Arg^{126} in RNase PH); residues of Archaeal Rrp41 involved in the catalytic mechanism Asp^{182} and Asp^{188} (corresponding to $Asp^{181}$and Asp^{187} in RNase PH and Asp^{514} and Asp^{520} in PNPase)
B. Structural superposition of the active site regions of Archaeal Rrp41 (blue) and Rrp42 (green); Residues of Rrp42 are not compatible with phosphate binding.
(Figure adapted from Lorentzen et al., 2005)

ring with the central channel. On top of the hexameric ring three additional subunits form a cap-like structure (Figure 3). *In vivo,* the cap of archaeal exosomes contains Csl4 (for CEP1 synthetic lethal 4) and Rrp4 subunits in different combinations, giving rise to different versions of archaeal exosomes. Reconstitution experiments with exosomes containing either only Csl4 or only Rrp4 subunits revealed that Rrp4 confers poly(A) specificity to the exosome, while Csl4 preferentially binds heteropolymeric over homopoly(A) substrates (Roppelt et al., 2010). Moreover, Csl4 is responsible for the interaction of the archaeal exosome with DnaG. DnaG is related to bacterial topoisomerases and primases and present in all archaea that have been sequenced to date. In *Sulfolobus solfataricus*, DnaG binds tightly to the exosome complex and confers an additional poly(A) binding site. In addition, DnaG is required for the synthesis of non-templated tails by the archaeal exosome (Evguenieva-Hackenberg et al., 2014).

The ring components of archaeal exosomes, Rrp41 and Rrp42, share 25% sequence identity with bacterial RNase PH (Evguenieva-Hackenberg et al., 2014). Both Rrp41 and Rrp42 have an RNase PH-like fold, with more than 75% of their residues having a similar α-carbon position (Lorentzen et al., 2005). However, the superposed structures of the active sites of *E. coli* RNase PH, the C-terminal RNase PH domain of *E. coli* PNPase and *S. solfataricus* Rrp41 and Rrp42 revealed that the residues essential for the phosphorolytic activity are conserved between RNase PH, PNPase and SsRrp41 but not in SsRrp42 (Figure 4) (Lorentzen et al., 2005). Phosphorolysis requires amino acid residues involved in the coordination of the inorganic phosphate ion and residues involved in the cleavage of the phosphodiester bond (Lorentzen et al., 2005). In RNase PH, the phosphate is coordinated by Thr^{125} and Arg^{126}. In PNPase, the phosphate is coordinated by Thr^{462} and Ser^{463}. Ser^{138} and Arg^{139} coordinate the phosphate ion in *S. solfataricus* Rrp41. Besides coordination of the inorganic phosphate, the cleavage of the RNA substrates phosphodiester bond requires two negatively charged residues that are located in the close proximity to

the phosphate-coordination site: $Asp^{181}$and Asp^{187} in *E. coli* RNase PH, Asp^{514} and Asp^{520} in *E. coli* PNPase and Asp^{182} and Asp^{188} in *S. solfataricus* Rrp41 (Lorentzen and Conti, 2012, 2005). In *S. solfataricus* Rrp42 proteins, the catalytic site is disrupted with Val^{153}, Leu^{154}, Glu^{218} and Lys^{224} at the respective positions of phosphate coordination and cleavage sites, and therefore, Rrp42 is catalytically inactive (Lorentzen et al., 2005).

Hence, the archaeal exosome contains three active sites within the channel. The central channel of the *S. solfataricus* exosome has a diameter of 13 Å at its narrowest point (Lorentzen et al., 2005). Therefore, the central channel of archaeal exosomes can accommodate only single stranded RNA molecules. The distance from the entrance of the central channel to the Rrp41's active site spans 10-15 nt (Audin et al., 2016). Like bacterial PNPase, the archaeal exosome is a highly processive enzyme. Recent data from Remco Sprangers group suggest that the RNA-binding sites located in the neck region of the channel play an important role for the processivity of the archaeal exosome (Audin et al., 2016). In addition, they have shown that all three active sites inside the central channel contribute to the speed of substrate degradation by the archaeal exosome (Audin et al., 2016). Whether the number of active sites is also important for the processive character of the archaeal exosome remains to be investigated.

D. The structural organization of eukaryotic exosomes

The eukaryotic exosome consists of a conserved core complex, EXO9, which associates with various exoribonucleases and cofactors (Chlebowski et al., 2011; Lubas et al., 2012). The components of the eukaryotic exosome were originally identified in genetic screens. Subsequent co-purification experiments in yeast and human cell lines identified a nine-subunit core complex of 300-400 kDa comprising Rrp4, Rrp40, Rrp41, Rrp42, Rrp43, Rrp45, Rrp46, Mtr3 and Csl4 (Allmang et al., 2000, 1999; Mitchell et al., 1997). The structures of yeast and human

exosomes were solved by the laboratories of Christopher Lima and Elena Conti and showed that EXO9 resembles the characteristic ring-shaped structure of bacterial phosphorylases and archaeal exosomes (Liu et al., 2006; Makino et al., 2013).

The barrel of EXO9 is made of six RNase PH-like domain proteins organized in three heterodimers: Rrp41-Rrp45, Rrp46-Rrp43 and Mtr3-Rrp42. The trimeric cap situated on top of the barrel is composed of Csl4, Rrp4 and Rrp40 that contain S1 and/or KH RNA-binding domains. The diameter of the central channel of yeast exosome is 10–12 Å, making it suitable for accommodating a single-stranded RNA substrate (Liu et al., 2006; Makino and Conti, 2013).

The ring subunits of eukaryotic exosome can be divided into two groups based on their sequence similarity with archaeal Rrp41 and Rrp42 subunits. Rrp41, Rrp46 and Mtr3 show 25-35% sequence identity with archaeal Rrp41 and substantially lower similarity with Rrp42 (10-15%), whereas Rrp42, Rrp43 and Rrp45 share 30% sequence identity with the archaeal Rrp42 but only 10–15% sequence identity with Rrp41 (Lorentzen et al., 2005). The exosome was described as a "complex of exonucleases," with multiple subunits proposed to have RNase activity (Liu et al. 2006; Mitchell et al. 1997). Later work revealed that actually none of the PH-domain proteins of yeast and human EXO9 contains the residues required for phosphorolytic activity (Dziembowski et al., 2007). Residues potentially involved in structural interactions, RNA-binding and cleavage of the phosphodiester bond are conserved in yeast and human Rrp41p/hRRP41. By contrast, the Ser^{138} and Arg^{139} residues required for phosphate coordination in *S. solfataricus* RRP41 are replaced by Ile^{135} and Met^{136} in yeast Rrp41 and by Thr^{133} and Tyr^{134} in human RRP41 (Lorentzen et al. 2005; Dziembowski et al., 2007).

Indeed, yeast and human EXO9 do not possess phosphorolytic activity (Dziembowski et al., 2007; Greimann and Lima, 2007 erratum to Liu et al., 2006). Therefore, EXO9 complexes in yeast and humans rely on the activities of the associated ribonucleases Rrp6p/hRRP6 and Rrp44p/hRRP44 (Dziembowski et al.,

2007; Wasmuth and Lima, 2012; Wasmuth et al., 2014). However, all subunits of yeast and human EXO9 are essential for viability, probably because EXO9 serves as a scaffold for the assembly and regulation of active exoribonucleases and cofactors involved in exosome activation or substrate recognition.

E. The plant exosome

1) Composition of the exosome core complex in *Arabidopsis thaliana*

All nine subunits of the core exosome complex are conserved in plants. All plant genomes encode at least one of each subunit of EXO9 and many plant species have two genes for individual subunits (Lange and Gagliardi, 2012). In *Arabidopsis*, two genes encode an AtRRP40 subunit. However, only AtRRP40A (AT2G25355) was detected in immunopurified exosome complexes complexes (Chekanova et al., 2007; Lange et al., 2014) and therefore, it remains unknown whether RRP40B is incorporated into exosome complexes. The *Arabidopsis* genome encodes also two isoforms of AtRRP45. Both AtRRP45A (AT3G12990) and AtRRP45B/CER7 (AT3G60500) were shown to rescue the growth defect of yeast *rrp45* mutants suggesting that they may have partially overlapping functions (Hooker et al., 2007). Co-immunoprecipitation experiments in plants detected exosome complexes with both AtRRP45B and AtRRP45A, indicating that both AtRRP45 isoforms are functional subunits and can be incorporated into EXO9 (Lange et al., 2014, this work). While loss of AtRRP45B leads to a cuticular wax deposition defect (Hooker et al., 2007), no such phenotype is observed for plants lacking AtRRP45A. However, simultaneous down-regulation of both AtRRP45B and AtRRP45A is lethal (Hooker et al., 2007). This observation may indicate that exosome complexes containing either AtRRP45A or AtRRP45B have both distinct and overlapping functions. However, it is still unknown whether exosome complexes containing either AtRRP45B or AtRRP45A have different biochemical properties or differ in their ability to associate with different cofactors. All other subunits of EXO9 are encoded

by single genes in *Arabidopsis*. One of the subunits that were studied in *Arabidopsis* is AtMTR3, also called RRP41-like in one study (Yang et al., 2013). A T-DNA insertion located in the 7th exon of the 8 exons of the MTR3 (AT4G27490) gene leads to the expression of a truncated *MTR3* transcript and causes a delayed germination and a slow growth phenotype (Yang et al., 2013). The molecular phenotype of this hypomorphic mutant remains to be thoroughly studied.

By contrast, the essential roles of AtRRP4 and AtRRP41 have been demonstrated. Heterozygous *rrp41*/RRP41 plants produce viable seeds and aborted ovules showing that AtRRP41 is crucial for female gametogenesis in *Arabidopsis* (Chekanova et al., 2007). Knock-out of *RRP4* (AT1G03360) leads to arrest of seed growth at early stage of embryo development indicating that AtRRP4 is dispensable for gametogenesis, but essential for embryogenesis in *Arabidopsis* (Chekanova et al., 2007). However, down-regulation of *RRP4* or *RRP41* by inducible RNAi results in growth arrest and seedlings death, indicating that both subunits are essentially required for post-embryonic growth (Chekanova et al., 2007). The molecular effects of *RRP41* and *RRP4* down-regulation have been studied by genome-wide tiling arrays that revealed that loss of either AtRRP4 or AtRRP41 result in the accumulation of polyadenylated RNA substrates including mRNAs, snRNAs, snoRNAs and ribosomal RNA precursors. By contrast, plants harboring a T-DNA insertion in the CSL4 gene (AT4G27490) were viable and showed a slight accumulation only of a small subset of exosome substrates (Chekanova et al., 2007).

Moreover, knock-down of AtCSL4 did not affect the integrity of exosome complex as judged from gel-filtration experiments (Chekanova et al., 2007). Therefore, it was suggested that CSL4 is not essential for exosome function in *Arabidopsis* (Chekanova et al., 2007). Interestingly, the TbCSL4 subunit of *Trypanasome brucei* seems not to be essential neither, since its down-regulation does not destabilize the CSL4-free exosome complex (Haile et al., 2003). Hence, exosome complexes without CSL4 may still be functional in *Arabidopsis* and *Trypanosome*. One

possible explanation is that the exosome cap proteins may have overlapping functions and remaining cap proteins may take over CSL4's function.

The roles of exosome subunits in other plants are not well investigated. While studying host-pathogen response in barley (*Hordeum vulgare*) infected with the pathogenic fungus *Blumeria graminis*, Xi and colleagues isolated a barley mutant *bcd1* (for bgh-induced tip cell death 1) carrying a deletion of six genes, among them *HvRRP46* (Xi et al., 2009). The phenotype of *bcd1* mutants was restored by introducing a RRP46 transgene, which proved that loss of HvRRP46 was responsible for the mutant phenotype. Besides being susceptible to infection with *B. graminis* *bcd1* mutants suffered from pathogen-induced apoptosis in the leaf tip and accumulated polyadenylated, misprocessed rRNA precursors, a hallmark of impaired exosome function in any organism studied to date.

Taking together down-regulation or mutation of distinct plant EXO9 subunits affects different stages of plant development or other aspects of plant health such as resistance to pathogens. Whether these findings are linked to the different levels of EXO9 down-regulation due to limiting availability of individual subunits, or truly indicate that distinct subunits of EXO9 have specialized roles in plant growth and development remains to be experimentally addressed.

2) Plant EXO9 may be catalytically active

Intriguingly, dimers of the rice (*Oryza sativa*) homologue of AtRRP46 were convincingly shown to possess both a DNase and a phosphorolytic RNA degradation activity *in vitro* (Yang et al., 2010). However, one of the critical amino acids required for OsRRP46 activity *in vitro* ($OsLys^{75}$) is not conserved in *Arabidopsis*. *In vivo* studies that address the question whether such OsRRP46 dimers exist and contribute to RNA degradation *in vivo* are lacking to date. In fact, sequence alignments of exosome ring subunits from different organisms, including the enzymatic active proteins *E. coli* RNase PH and *S. solfataricus* Rrp41 identified the RRP41 subunit as the best

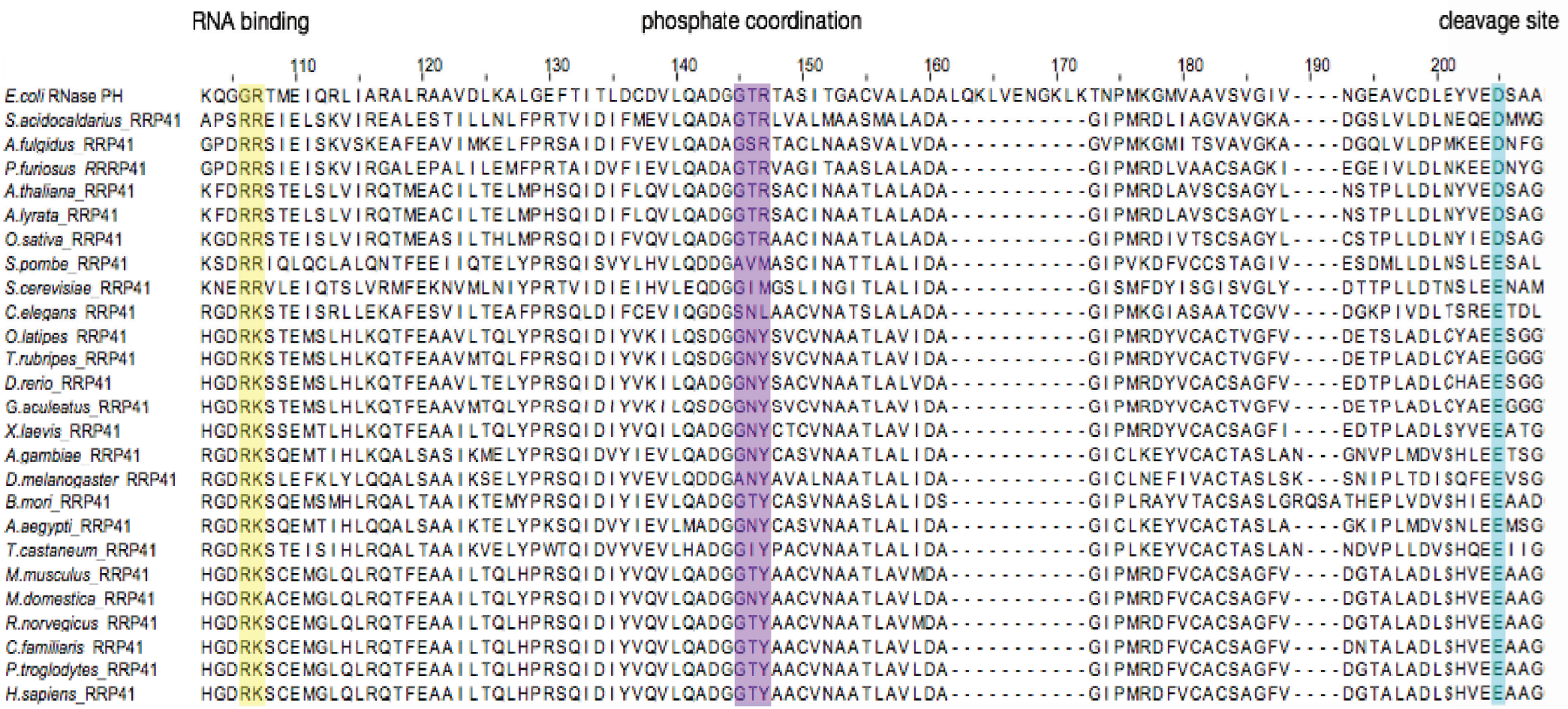

Figure 5. Regions crucial for catalytic activity of RNase PH and RNase PH-like proteins are conserved in archaeal Rrp41, *Arabidopsis* and rice RRP41, but not in yeast, animals and human. Sequence alignment of bacterial RNase PH and RRP41 proteins from archaea, Arabidopsis, yeast and animals made by Clustal Omega and visualized by Jalview. Names of organisms are listed on the left, three functional regions of RNase PH-like proteins are marked by color (RNA-binding region in yellow, phosphate coordination region in violet, cleavage site in turquoise). Only part of the sequence is shown.

candidate for conferring catalytic activity to eukaryotic exosomes (Dziembowski et al., 2007).

As mentioned before, the RRP41 subunits of most species including yeast and mammals harbor point mutations in the phosphate coordination site, and are indeed catalytically inert (Dziembowski et al., 2007; Greimann and Lima, 2007). By contrast, these residues essential for the phosphorolytic activity of RNase PH domain are conserved in the RRP41 subunit of both rice and *Arabidopsis* (Dziembowski et al., 2007). The residues involved in the coordination of the inorganic phosphate ion in *Arabidopsis*, AtRRP41 Thr^{130} and Arg^{131} and rice, OsRRP41 Thr^{132} and Arg^{133} corresponded to Thr^{125} and Arg^{126} in *E. coli* RNase PH or Ser^{138} and Arg^{139} in archaeal Rrp41. Similarly, the residues involved in the cleavage of the phosphodiester bond in *Arabidopsis* AtRRP41 Asp^{168} and Asp^{174} and rice OsRRP41 Asp^{170} and Asp^{176} mirror corresponding residues in *E. coli* RNase PH (Asp^{181} and Asp^{187}) and archaeal Rrp41 (Asp^{182} and Asp^{188}) (Figure 5). The fact that all residues essential for the phosphorolytic activity of RRP41 are conserved suggests that plant EXO9 complex, unlike most of eukaryotic exosomes, could indeed have retained a catalytic activity comparable to archaeal exosome complexes.

Actually, recombinant AtRRP41 has been claimed to be catalytically active *in vitro* as a monomer. Chekanova et al tested the catalytic activity of N-terminal GST fusion of AtRRP41 expressed and purified from *E. coli* (Chekanova et al., 2000). Unfortunately, the presented work is questionable for two main reasons. First, no catalytic mutant of AtRRP41 was used as a control. Second, recombinant proteins were expressed in a standard BL21 *E. coli* strain and purified with a single-step purification for all but one experiment. The BL21 strain expresses a functional PNPase protein, a common contaminating protein in purifications of recombinant RNases (Liu et al., 2006). Hence, it cannot be excluded that the activity that was observed after the single step purification was due to a PNPase contamination. The

only experiment that was carried out in the PNPase$^-$ *E. coli* strain was technically not convincing due to electrophoresis artefacts. Therefore, the ensemble of the data presented in the Chekanova et al. paper does not fulfil the requirements to demonstrate the catalytic activity of *Arabidopsis* RRP41.

Moreover, the structural and biochemical data from Elena Conti's group provided solid arguments against an enzymatic activity of an SsRRP41 monomer (Lorentzen et al., 2005). Using *in vitro* degradation assays they demonstrated that first, SsRRP41 confer the catalytic activity to the SsRRP41/SsRRP42 dimer, which is abolished upon mutation of the catalytic site present in SsRRP41. Second, they showed that SsRRP41 is not active as a monomer. Based on the crystal structure of the Rrp41/Rrp42 dimer from *S. solfataricus* (SsRrp41/SsRrp42) they suggested that positively charged residues involved in RNA binding are provided by both SsRrp41 and SsRrp42 subunits and form a prominent surface groove with the EXO9 central channel lined with arginines (so-called arginine patch). In conclusion, formation of the RRP41/RRP42 dimer in archaeal exosomes is a requirement for the enzymatic activity. These structural and biochemical data put additional question marks on the experiments of Chekanova et al. that claimed a catalytic activity of the *Arabidopsis* RRP41 monomer.

The main aims of this work are to investigate whether *Arabidopsis* EXO9 is active as a complex and what are its roles *in vivo,* what has not been addressed so far.

III. Ribonucleases associated with yeast and human exosomes

As mentioned above, EXO9 in yeast and human are catalytically inert. Therefore, the enzymatic activity of yeast and human exosomes is only provided by associated ribonucleases, namely Rrp44p/hDIS3 (for chromosome disjunction) and Rrp6p/hRRP6 (Dziembowski et al., 2007; Schneider and Tollervey, 2013). Both Rrp44p and Rrp6p have hydrolytic activities, i.e. they catalyze the irreversible

cleavage of phosphodiester bond using water and release nucleoside monophosphates.

A. The endo-/exoribonuclease Rrp44/Dis3

Rrp44p/hRRP44 is related to the bacterial exoribonuclease RNAse R/II and binds to the bottom of eukaryotic exosome core (Makino and Conti, 2013; Schneider et al., 2009). Rrp44p contains three RNA binding domains (one S1 and two cold shock RNA-binding domains, so called CSD1 and CSD2), and two catalytic domains, RNB (named after the gene locus encoding bacterial RNase II in *E. coli*) and PIN (named after its identification in the N-terminus of the PilT protein) (Schneider and Tollervey, 2013). The C-terminal RNB domain provides a processive 3'-5' exoribonucleolytic activity that is magnesium-dependent (Dziembowski et al., 2007; Schneider and Tollervey, 2013). The exoribonucleolytic activity is responsible for the bulk RNA degradation by Rrp44p/Dis3p. The N-terminal PIN domain provides a manganese-dependent endonucleolytic activity that was proposed to be involved in the release of structured RNA substrates stalled at the exoribonucleolytic active site of Rrp44p/Dis3 (Schneider et al., 2012; Lebreton et al., 2008; Schaeffer et al., 2009; Tomecki et al., 2010). In addition, the PIN-domain of Rrp44/Dis3 is involved in the interaction with the EXO9 core complex (Schneider et al., 2009). Rrp44 can degrade not only single stranded RNA substrates (ssRNA) but it is also able to unwind and degrade duplex and hairpin structures as long as they possess 3' single-stranded extensions (Wasmuth and Lima, 2012).

The *S. cerevisiae* genome encodes a single and essential Rrp44p protein that localizes in the nucleolus, nucleoplasm and cytoplasm. By contrast, humans possess three homologs of *S. cerevisiae* Rrp44p. The closest homolog that has both endo- and exonuclease activities is hDIS3, located both in the nucleoplasm and cytoplasm. Due to point mutations, the cytoplasmic protein hDIS3-like (DIS3L) lacks the endonuclease activity albeit is has a PIN domain that enables its interaction with

EXO9 (Staals et al., 2010; Tomecki et al., 2010). Finally, the cytoplasmic exoribonuclease hDIS3L2 lacks the PIN domain and does not associate with the exosome core. The hDIS3 isoform is essential and its mutations were correlated with occurrence of cancers such as multiple myeloma (Tomecki et al., 2014; Weißbach et al., 2015).

B. The exoribonuclease Rrp6

The second 3'-5' exoribonuclease associated with the exosome core in yeast and humans is Rrp6p/hRRP6, a homologue of bacterial RNase D. Unlike Rrp44p, Rrp6p is a distributive exoribonuclease, i.e. it releases its RNA substrate after removal of each nucleotide and needs to rebind to perform the next catalytic step. Alike Rrp44p's, the mechanism of RNA degradation by Rrp6p is hydrolytic. Rrp6p and hRRP6 proteins preferably degrade single-stranded RNA substrates, although structured substrates can also be degraded as long as they contain a single-stranded region on their 3' end. Rrp6p/hRRP6 bind to the top of the exosome barrel and its C-terminal part contacts the exosome core (Wasmuth et al., 2014). Rrp6p harbors three distinct domains, PMC2NT, DEDD and HRDC. The N-terminal PMC2NT (polycystin 2 N-terminal) domain of Rrp6p serves as a binding site for Rrp47p/C1D, an RNA-binding protein (Januszyk et al., 2011; Schuch et al., 2014). The DEDD domain of Rrp6 is required for its 3' -5' exoribonucleolytic activity (Januszyk et al., 2011). Rrp6p proteins possess also a RNAse H-fold that harbors the 3'-5' exoribonucleolytic activity and a helicase/RNase D C-terminal domain (HRDC), that is believed to mediate its interaction with nucleic acids (Assenholt et al., 2008; Callahan and Butler, 2010; Januszyk et al., 2011).

Known endogenous substrates of Rrp6p include the 7S 5.8S pre-rRNA, small nuclear RNAs and snoRNAs. Rrp6p is the only subunit of yeast exosome that is not essential, however its deletion leads to a thermosensitive slow growth phenotype and the accumulation of the 5' external transcribed spacer (5'ETS, a fragment

released during rRNA maturation), 5.8S rRNA precursors with 3' extensions, polyadenylated rRNA species and oligoadenylated box C/D snoRNAs (Allmang et al., 1999; Briggs et al., 1998; Grzechnik and Kufel, 2008; Kuai et al., 2004; Mitchell and Tollervey, 2003).

C. Composition and localization of exosome complexes in yeast and human

In yeast, cytoplasmic exosome complexes consist of EXO9 and Rrp44p bound to the bottom of the exosome barrel (EXO9+Rrp44p form EXO10) (Bonneau et al., 2009; Wang et al., 2007), whereas the nuclear exosome form contains a second exoribonuclease, Rrp6p, bound to its top (EXO9+Rrp44p+Rrp6p form EXO11) (Cristodero et al., 2008; Makino et al., 2013). Human exosome complexes are more diverse and exists in at least four variants. Since all human homologs of Rrp44p are excluded from nucleoli, exosome complexes in this compartment consist of EXO9 and hRRP6. By contrast, nucleoplasmic human exosomes contain both hDIS3 and hRRP6. Due to low cytoplasmic levels of hRRP6 (Lubas et al., 2011), cytoplasmic human exosomes are mostly represented by EXO9 associated with hDIS3L, although trace amounts of EXO9 with hRRP6 and hDIS3 also exist (Lubas et al., 2011; Tomecki et al., 2010).

D. Mode of action of Rrp44 and Rrp6

Several studies combining *in vitro* activity assays of reconstituted exosome complexes and structural data helped to understand the mode of action of yeast EXO10 and EXO11 (Bonneau et al., 2009; Makino et al., 2015; Wasmuth and Lima, 2012).

Bonneau and colleagues showed that RRP44 alone protects an RNA substrate fragment of 9-12 nt, while RRP44 associated to the EXO9 (EXO10) protects two fragments of 11-12 nt and 31-33 nt. This indicated that there are two routes to access the active site of Rrp44p: the RNA substrates are both threaded through the

central channel of EXO9 and can reach RRP44's active site directly, without going through the channel (Bonneau et al., 2009). However, even though these two pathways exist, a genome wide study using RNA-Protein Crosslinking (CRAC) suggested that most of the exosome's substrates are threaded through the central channel *in vivo* (Schneider et al., 2012).

Hence, although the exosome core is catalytically inert in yeast and humans, the mechanism of threading the RNA substrate through its central channel has been conserved from prokaryotes to eukaryotes. Supporting the idea that threading through the exosome's central channel is important, mutations occluding the central channel of yeast EXO9 have been shown to negatively affect the RNase activities of Rrp6p and Rrp44p in reconstituted EXO10 and EXO11 complexes (Wasmuth and Lima, 2012a). *In vivo,* partial channel occlusion leads to the accumulation of typical exosome substrates such as misprocessed RNA precursors (Drazkowska et al., 2013; Wasmuth and Lima, 2012), while complete occlusion of EXO9s central channel is lethal (Bonneau et al., 2009; Wasmuth and Lima, 2012). Moreover, the presence of EXO9 also alters RNA-binding and ribonucleolytic activities of Rrp44p and Rrp6p. For example, free Rrp44p degrades RNA substrates roughly ten times more efficiently than RRP44 associated with EXO10 complexes *in vitro* (Wasmuth and Lima, 2012). This finding may explain why expression of free Rrp44p was reported to have deleterious effects on cell viability (Schaeffer et al., 2009).

Interestingly, the exoribonucleolytic activities of Rrp44 and Rrp6 in EXO11 are also interconnected. Rrp6p stimulates RNA binding and activity of RRP44 in EXO11. Conversely, Rrp44p lacking its exoribonuclease activity (RRP44 exo-) severely inhibits Rrp6 activity in EXO11$^{44exo-/6}$, indicating that RNA binding by catalytically inactive Rrp44 blocks the access to the active site of Rrp6p. That can be explained by the processive mode of action of Rrp44p which binds the RNA substrate until its completely degraded, in contrast to distributive Rrp6p that releases its substrates after each catalytic cycle. Taken together, the activities of both

Rrp44p and Rrp6p are modulated by binding to EXO9 and influence each other in EXO11.

E. Rrp6 and Rrp44/Dis3 target distinct and overlapping exosome's substrates

Early studies on the degradation of model substrates suggested that Rrp6p is crucial for trimming 5.8S+30nt rRNA precursors and snoRNA precursors (Allmang et al., 1999a; Briggs et al., 1998; van Hoof et al., 2000), while Dis3p was implicated in 5'ETS elimination (Lebreton et al., 2008; Schneider et al., 2012). On a genome-wide level, the relative contributions of RRP6 and RRP44 were recently addressed by Schneider and colleagues in yeast, and by Gudipati et al. in human cell lines (Schneider et al., 2012; Gudipati et al., 2012). Gudipati at al. used genome-wide tiling arrays to map the RNA substrates that accumulate in human cell lines expressing catalytic mutants of hDIS3 and hRRP6 (Gudipati et al., 2012). Schneider and colleagues used *in vivo* RNA crosslinking combined with deep sequencing (crosslinking analysis of cDNAs, CRAC) with two subunits of the yeast exosome, Rrp41p and Csl4p, the two exosome-associated ribonucleases Rrp6p and Rrp44p, and the poly(A) polymerase Trf4 of the TRAMP complex (Trf4/5-Air1/2-Mtr4; further described in part IV of this introduction) (Schneider et al., 2012).

These experiments revealed that RRP44 and the exosome core subunits on one side, and RRP6 on the other side protected different fragments of the 5' ETS, confirming that the two exoribonucleases cooperate but make also distinct contributions to the degradation of this rRNA maturation by-product. In addition, RRP6 but neither RRP44 nor the exosome core subunits were precipitated with specific fragments mapping inside the 18S rRNA, indicating that RRP6 has a specific role in the elimination of misprocessed 18S species. By contrast, both RRP44 and RRP6 were crosslinked to 5.8S precursors. In fact, Rrp44p and Rrp6p, assisted by the TRAMP complex, were found to cooperate or act redundantly in processing or degradation of many exosome targets. For example, Rrp44p, Rrp6p and Trf4 were crosslinked to the Pol III transcripts 5S rRNA, U6 snoRNA or SRP RNA, and to Pol

II transcripts such as CUTs (cryptic unstable transcripts) and SUTs (stable unannotated transcripts). By contrast, highly structured tRNAs precursors were identified as specific targets of RRP44p, and other small structured RNA such as snRNAs and snoRNAs were preferentially crosslinked to RRP6. Interestingly, the exosome subunits Rrp4p and Csl4p were not crosslinked to these short structured RNAs. Therefore, it was proposed that such small highly structured RNA substrates may be degraded by RRP6 and RRP44 in pathways that are independent of the central channel of the core exosome (Schneider et al., 2012).

Both mRNAs and pre-mRNAs accumulated in cells expressing activity mutants of hRRP44 and hRRP6 (Gudipati et al., 2012), or were crosslinked to the exosome core subunits or Rrp6p and Rrp44p (Schneider et al., 2012). In yeast, Rrp6p was crosslinked to most intron-containing mRNAs, while RRP44 was preferentially bound to pre-mRNAs containing particular long introns. In human cells, hRRP44 seemed to be more important for the degradation of pre-mRNAs than hRRP6. However, both studies demonstrated that the exosome systematically degrades pre-mRNAs, possibly as part of a quality control pathway that constantly monitors mRNA processing (Gudipati et al., 2012; Schneider et al., 2012). Interestingly, tRNA precursors were also frequently crosslinked to yeast Rrp44p or detected in cells expressing mutant hDIS3. This suggested that RRP44/DIS3 has a specific role in the surveillance of tRNA production.

Taken together, these two genome-wide studies provided a transcriptome-wide map of exosome substrates and untraveled the relative contribution of the active exoribonucleases RRP6 and RRP44 in both human and yeast. This identified new roles of the exosome in pre-mRNA and tRNA surveillance and highlighted the specific and the redundant roles of RRP44 and RRP6.

F. Plant homologues of Rrp44p and Rrp6p

1) Three RNase II/R-like proteins are encoded by *Arabidopsis* genome

The *Arabidopsis* genome encodes three RNase II/R-like proteins, AtmtRNaseII/AtRNR1 (for RNase R homolog) (At5g02250), AtSOV (for suppressor of varicose) (AT1G77680) and AtRRP44 (AT2G17510). AtmtRNaseII/AtRNR1 resides in chloroplasts and mitochondria and was implicated in the maturation of 23S, 16S, 5S rRNAs and mRNAs (Bollenbach et al., 2005; Germain et al., 2012; Perrin et al., 2004). AtSOV, a non-essential cytoplasmic protein closely related to human hDIS3L2 (Astuti et al., 2012; Lubas et al., 2013), was shown to be involved in the degradation of selected mRNAs (Zhang et al., 2010). AtSOV lacks a PIN domain that was shown to promote the interaction of hDIS3L with the human exosome (Bonneau et al., 2009; Schneider et al., 2009; Tomecki et al., 2010). Therefore, SOV is unlikely to associate with the exosome core and probably acts independently of the exosome complex, similar to hDIS3L2 (Lubas et al. 2013; Tomecki et al. 2010). In all accessions of *Arabidopsis* but Col-0 AtSOV is catalytically active. In Col0, a single nucleotide polymorphism (SNP) (*A. thaliana* R705P) appears to alter AtSOV activity (Zhang et al., 2010).

AtRRP44 is an essential protein located both in the nucleus and cytoplasm (Zhang et al., 2010). Alike yeast Rpp44p/Dis3p or human hDIS3 and hDIS3L, AtRRP44 contains a N-terminal PIN domain that may promote its interaction with EXO9, and a C-terminal RNB domain endowed with exoribonucleolytic activity (Zhang et al., 2010). Whether AtRRP44 has also an endonucleolytic activity conferred by its PIN domain has not been investigated yet. AtRRP44 interacts with EXO9 *in vivo*, since it reproducibly co-purifies, albeit to low amounts, with *Arabidopsis* EXO9 ((Lange et al., 2014) this work). Down-regulation of RRP44 leads to an increase in the level of 5.8S rRNA processing intermediates with 3'end extensions (Kumakura et al., 2013). However, knock-down mutants of AtRRP44 displayed wild-type levels of mature 5.8S rRNA (Kumakura et al., 2013). This may

be explained by the fact that the remaining levels of AtRRP44 were sufficient to allow the processing of rRNA. Alternatively, when AtRRP44 is down-regulated both elimination of P-P' and processing of 5.8S rRNA precursors may be performed by compensating exoribonucleases. One possible candidate is one of the RRP6-like proteins in *Arabidopsis*, AtRRP6L2, that was shown to play a role in both of these processes (Lange et al., 2011, 2008). Another substrate of AtRRP44 is the P-P' fragment, a maturation by-product generated from the 5' External Transcribed Spacer (5'ETS) (Kumakura et al., 2013).

2) *Arabidopsis* genome encodes three RRP6-like proteins

The *Arabidopsis* genome encodes three Rrp6p homologues called RRP6-like, AtRRP6-like1 (AtRRP6L1, At1g54440), AtRRP6-like2 (AtRRP6L2, At5g35910) and AtRRP6-like3 (AtRRP6L3, At2g32415) (Chekanova et al., 2007; Lange et al., 2008). Phylogenetic analysis of RRP6-like proteins revealed that AtRRP6L1 and AtRRP6L2 cluster together with yeast and animal RRP6 proteins, whereas AtRRP6L3 homologues are only found in plants (Lange et al., 2008). All three AtRRP6-like proteins contain the IPR002562, 3'-5' exoribonuclease and the IPR002121 HDRC (for helicase/ RNase D C-terminal) motifs that are characteristic for RRP6 proteins. By contrast, the PMC2NT domain that is present in the N terminus of *S. cerevisiae* and *H. sapiens* Rrp6 proteins and promotes the interaction with the Rrp6p co-factor Rrp47p, is found only in AtRRP6L2 (Lange et al., 2008). Accordingly, only RRP6L2 but not RRP6L1 or RRP6L3 interact with the Arabidopsis RRP47 homologue (Sikorski et al., 2015). By now, none of the *Arabidopsis* RRP6-like proteins was shown to physically interact with EXO9 (Chekanova et al., 2007; Lange et al., 2014), suggesting that either such interactions are transient and therefore difficult to detect, or that the interaction of EXO9 and RRP6 is not conserved in *Arabidopsis*. Interestingly, each of the *Arabidopsis* RRP6-like proteins occupies a distinct intracellular compartment. While RRP6L3 is a cytosolic protein, RRP6L1 is found in

the nucleoplasm and the nucleolar vacuole. RRP6L2 is predominantly located in nucleoli.

The role of the cytoplasmic isoform AtRRP6L3 was not investigated so far and the *Arabidopsis* mutant down-regulated for the expression of AtRRP6L3 does not exhibit any morphological phenotype (Lange et al., 2008). AtRRP6L2 participates in the processing of 5.8S ribosomal RNA precursors and elimination of maturation by-products generated from the 5' external transcribed spacer (5'ETS) (Kumakura et al., 2013). In addition, AtRRP6L2 has also an exosome-independent function in the processing of 18S rRNA precursors (Sikorski et al., 2015). However, *rrp6l2* mutants have wild-type levels of mature rRNAs and no particular phenotype, indicating that the role of AtRRP6L2 in rRNA processing is not essential and can be compensated by other exoribonuclease such as AtRRP44 (see above).

In addition, AtRRPL2 and AtRRPL1 have overlapping roles in RNA degradation. AtRRP6L1 and AtRRP6l2 cooperate in the degradation of transcripts derived from loci silenced by RNA dependent DNA methylation (RdDM) pathways such as the SOLO LTR and SN1 loci (Shin et al., 2013). In addition, AtRRP6L1 and AtRRP6L2 are required for the processing or degradation of the ASL (for Antisense Long) transcript, and of the antisense RNA produced from the *FLC* locus (Shin and Chekanova, 2014). The antisense RNA produced from the FLC locus influences expression of the FLC mRNA, required for flowering (Shin and Chekanova, 2014). These findings explain the flowering phenotype of *rrp6l1/rrp6l2* double mutants observed under short day conditions (Hepworth and Dean, 2015). Likely, AtRRP6L1 and AtRRP6L2 have many more common RNA substrates that have not been identified yet.

However, AtRRP6L1 has also specific functions in RdDM that are not shared with AtRRP6L2. In a classical RdDM in *Arabidopsis*, the establishment of DNA methylation status of genes or transposable elements starts with the transcription of target loci by RNA polymerase IV (Pol IV) (reviewed in Du et al., 2015). Resulting

transcripts serve as a template for RNA-dependent polymerase 2 (RDR2) to make double stranded RNAs (dsRNAs) that are processed by Dicer-like 3 (DCL3) and loaded into Argonaute 4 (AGO4). Next, the AGO4/siRNA complexes are recruited to target loci, probably in a Pol V-dependent manner, to direct DRM2-catalyzed DNA methylation. Ye and colleagues reported that a distinct class of RdRM-directing siRNAs are generated via an alternative route that is independent of DCLs (named sidRNAs, for siRNAs DCL-independent) (Ye et al., 2016). They identify two 3'-5' exoribonucleases, Atrimmer2 and AtRRP6L1, named Atrimmer1 in their work. AtTrimmer 1 and 2 were found to be responsible for the trimming of several siRNAs required to initiate RdDM at specific loci. Whether AtRRP6L1 is processing these sidRNAs in an exosome-dependent or independent pathway was not investigated. Another role of AtRRP6L1 in RdDM was proposed by Zhang et al. (Zhang et al., 2014). This study showed that AtRRP6L1 positively regulates chromatin-associated long non-coding RNAs named scaffold lncRNAs and siRNAs in the RdDM pathway. AtRRP6L1 was demonstrated to associate with Pol V-dependent lncRNAs and maintain the levels of scaffold lncRNAs, and therefore proposed to mediate RdDM through retention of lncRNAs in the chromatin (Zhang et al., 2014). Interestingly, these functions of RRP6L1 in the RdDM pathway may be independent of the exosome (Zhang et al., 2014).

IV. Exosome cofactors

In vivo, exosome complexes are associated with a number of additional cofactors involved in exosome activation, substrate recognition and eventually transcription termination. In many cases, exosome cofactors form so-called activator/adaptor complexes containing an RNA helicase of the MTR4/SKI2 family, one or several RNA binding proteins (adaptors), proteins that mediate protein to protein interactions, and sometimes poly(A) polymerases.

RNA helicases of the MTR4/SKI2 DExH-box family are central to exosome activity. The crystal structure of Mtr4p and Ski2p revealed that besides the helicase domains RecA1 and RecA2, both helicases contain also a unique domain with a characteristic shape, called arch domain (Halbach et al., 2013, 2012; Jackson et al., 2010; Weir et al., 2010). The arch domain consists of two anti parallel coiled coils forming an arm ending in a globular structure, the so called KOW motif (Kyrpides-Ouzounis-Woese). The KOW motif is an RNA binding motif commonly found in ribosomal proteins (Thoms et al., 2015).

A. RNA helicase Ski2 and the SKI complex

Ski2p, the founding member of the family, is a cytoplasmic protein and a component of the SKI complex, comprising also the tetratricopeptide protein Ski3p and two copies of the WD4O proteins Ski8p (Brown et al. 2000). The "superkiller" genes (SKI) were originally identified in a genetic screen in yeast, where their depletion led to the accumulation of viral dsRNAs and the production of toxins (Toh-E et al., 1978). Ski2, Ski3 and Ski8 are conserved among eukaryotes (van Dijk et al., 2007; Dorcey et al., 2012). The SKI complex is required for all cytoplasmic functions of the exosome including the degradation of mRNAs via the nonsense-mediated or no-stop decay pathways (van Hoof et al., 2002; Mitchell and Tollervey, 2003). In plants, SKI2 is also required for the degradation of RISC-cleaved mRNAs (Branscheid et al., 2015). In yeast, the interaction of the SKI complex with the exosome is mediated by the GTPase Ski7p (Araki et al. 2001). A recently published structure of the yeast cytoplasmic exosome complex showed that Ski7p binds to the top of the exosome barrel, suggesting that Ski7 is constitutively bound to the cytoplasmic exosome complex in yeast (Kowalinski et al., 2016). The comparison of structures of the nuclear exosome containing Rrp6p (EXO11) and the cytoplasmic exosome containing Ski7 (EXO10+SKI7) suggests that Ski7p and Rrp6p evolved to

bind to the same surface of the exosome core (Kowalinski et al., 2016; Wasmuth et al., 2014).

Ski7 is crucial for the recognition of exosome substrates in the cytoplasm and mRNA quality-control since it was proposed to release transcripts from stalled ribosomes by binding to the A site (Van Hoof et al., 2002). Because Ski7p resembles translation-associated GTPases such as the eukaryotic elongation factor 1α eEF1α and the eukaryotic release factor 3 eRF3, it was suggested to mediate the interaction between the exosome/SKI complex and mRNA-associated ribosomes (Klauer and van Hoof, 2012). Notably, Ski7p has no sequence homologs in humans or plants. However, its function is probably fulfilled by isoforms of the ribosome recycling factor HBS1 (Saito et al., 2013). Both SKI7 and HBS1 proteins contain a GTPase domain (Kowalinski et al., 2016) and recognize and release transcripts from stalled ribosomes (Van Hoof et al., 2002).

B. RNA helicase MTR4

The central activator of the nuclear exosome is the RNA Helicase Mtr4. Its best studied role is to assist the exosome in the processing of 5.8S ribosomal rRNA and the degradation of rRNA maturation by-products such as the 5' external transcribed spacer (5'ETS). Both processing of the 5.8S 3' end and elimination of the 5' ETS require Mtr4's arch domain (Thoms et al., 2015). A recent study has shown that the arch domain serves as a binding site for the adapter proteins Nop53p and Utp18p, each containing a specific arch interaction motif (AIM) (Thoms et al., 2015). Nop53p and Utp18p are components of pre-ribosomal particles and specifically recognize 5.8S precursors and the yeast 5' ETS, respectively. Their interaction with the RNA Helicase Mtr4p recruits and activates the exosome for processing of the 5.8S rRNA and degradation of the 5' ETS (Thoms et al., 2015). Likely, additional adapters exist to recruit the exosome to other specific substrates. Such specific adapters are at least partially conserved among eukaryotes. Indeed,

homologs of both Nop53p (At2g40430) and Utp18p (At5g14050) were among the proteins that co-immunoprecipitaded with *Arabidopsis* AtMTR4 (Lange et al., 2014) suggesting that similar mechanism may take place in plants.

1) The TRAMP complex

In yeast, Mtr4p associates with the non-canonical poly(A) polymerases Trf4p or Trf5p and the Zn-knuckle RNA-binding proteins Air1p or Air2p in TRAMP complexes (LaCava et al., 2005; Vanácová et al., 2005; Wyers et al., 2005). Trf4p/Air2p/Mtr4p and Trf5p/Air1p/Mtr4p are largely but not fully redundant(Holub et al., 2012; Jia et al., 2012). The current data indicate that Trf5p is more important for nucleolar surveillance while Trf4p acts predominantly on nucleoplasmic substrates of the exosome exosome (San Paolo et al., 2009; Schmidt et al., 2012). Substrates of TRAMP complexes include sn(o)RNAs, rRNA precursors, aberrant tRNAs, mRNAs and ncRNAs like CUTs and antisense RNAs for degradation by the exosome domain (LaCava et al., 2005; Vanácová et al., 2005; Wyers et al., 2005).

Trf4p and Trf5p strongly interact with Rrp6p (Tudek et al., 2014). In addition, TRAMP binding to certain RNA substrates such as cryptic unstable transcripts recruits both the exosome and the Nad3-Nrb1-Sen1 transcription termination complex (Tudek et al., 2014). Furthermore, the TRAMP complex stimulates exosome activity by adding non-templated oligo(A) tails to the 3' ends of exosome substrates (LaCava et al., 2005; Vanácová et al., 2005; Wyers et al., 2005). As in the case of PNPase, polyadenylation promotes exoribonucleolytic degradation by the exosome complex that binds poly(A) with high affinity.

The TRAMP complex is conserved in fission yeast, *Drosophila* and humans (Bühler et al., 2008; Lubas et al., 2011; Nakamura et al., 2008). Human TRAMP comprising hMTR4, the non-canonical poly(A) polymerase hTRF4-2 (PAPD5), and the Zn-knuckle RNA-binding protein hZCCHC7 is restricted to nucleoli and required for

the degradation of the 5' ETS (Lubas et al., 2011). By contrast, processing of 5.8S precursors requires hMTR4 but is independent of TRAMP (Lubas et al., 2011). Plants posses a homologue of the non-canonical poly(A) polymerase Trf4p, namely AtTRL that is involved in the polyadenylation of ribosomal exosome substrates (Sikorski et al., 2015). However, a plant TRAMP-like complex was not identified yet and no poly(A) polymerases were detected in co-immunoprecipitations of AtMTR4. Instead, *Arabidopsis* MTR4 co-purifies with EXO9 and a large number of proteins involved in the biogenesis of ribosomal particles (Lange et al., 2014).

2) The NEXT complex

Interestingly, the nucleoplasmic fraction of hMTR4 is part of another trimeric complex located in the nucleoplasm, the so-called NEXT complex (for nuclear exosome targeting) (Lubas et al., 2011). The human NEXT complex comprises hMTR4, the strictly nucleoplasmic Zn-knuckle protein ZCCHC8 and the RNA-binding protein RBM7. The NEXT complex targets promoter upstream transcripts (PROMPTs) and other unstable transcripts for exosome-mediated degradation (Andersen et al., 2013; Lubas et al., 2015, 2011). Moreover, the NEXT complex physically interacts with the cap-binding complex (CBC) and the ARS2 protein (forming together the CBCA complex). CBCA suppresses read-through products by promoting transcription termination (Andersen et al., 2013).

NEXT-like complexes are also conserved in plants (Lange et al., 2014). Instead of MTR4, plant NEXT contains the plant-specific Mtr4 homologue AtHEN2, which shares 43% identity and 59-60% similarity with plant or yeast MTR4 proteins (Lange et al., 2014). Unlike *Arabidopsis* AtMTR4 that is a predominantly nucleolar protein, AtHEN2 resides in the nucleoplasm and in nucleoplasmic speckles, and promotes the degradation of non-ribosomal nuclear exosome targets, such as snoRNA precursors, miRNA precursors, lincRNAs, transcripts derived from intergenic regions or pseudogenes, excised introns and misprocessed mRNAs

(Lange et al., 2014). In addition to EXO9, AtHEN2 co-purifies with At4g10110, a homologue of the human NEXT component hRBM7, and with At5g38600 and At1g67210, both of which are related to ZCCHC8. AtHEN2 also co-purifies with two subunits of the cap binding complex (CBC), namely AtCBP80 (AT2G13540) and AtCBP20 (AT5G44200) and with MAGO NASHI (AT1G02140), which is a component of the exon junction complex (EJC) (Lange et al., 2014).

Another cofactor of the plant nuclear exosome is AtSOP1, a large Zn-finger protein that co-localizes with AtHEN2 in nucleoplasmic speckles (Hématy et al., 2016). A direct interaction of AtHEN2 and AtSOP1 was not demonstrated yet, however, AtSOP1 is required for the degradation of a subset of HEN2-dependent nuclear exosome targets, including mis-spliced mRNAs (Hématy et al., 2016). AtSOP1 appears to be a novel, plant-specific exosome cofactor, however, its Zn-finger domain shares limited sequence similarity with the zinc finger domain of *S. pombe* Red5. SpRed5 is part of the so-called NURS (for nuclear silencing) or MTREC (for Mtl1–Red1 core) complex that also contains second, exosome-associated helicase Mtl1 (for MTR4-like). MTREC mediates the association of the nuclear exosome with protein complexes involved in the recognition of various types of RNAs (Egan et al., 2014; Zhou et al., 2015). The precise composition of nuclear exosome activator/adaptor complexes varies between organisms and cellular compartments. Future studies should further characterize the composition and variety of exosome-associated proteins.

V. Functions of the exosome in ribosomal RNA processing

The surveillance of ribosome assembly by degrading both misprocessed and superfluous rRNA precursors is one of the best conserved roles of the eukaryotic exosome (Lafontaine, 2010). The prominent role of the *Arabidopsis* exosome in the quality control of ribosome assembly is illustrated by the stable association of the exosome cofactor AtMTR4 with components of 90S pre-ribosomal particles and the

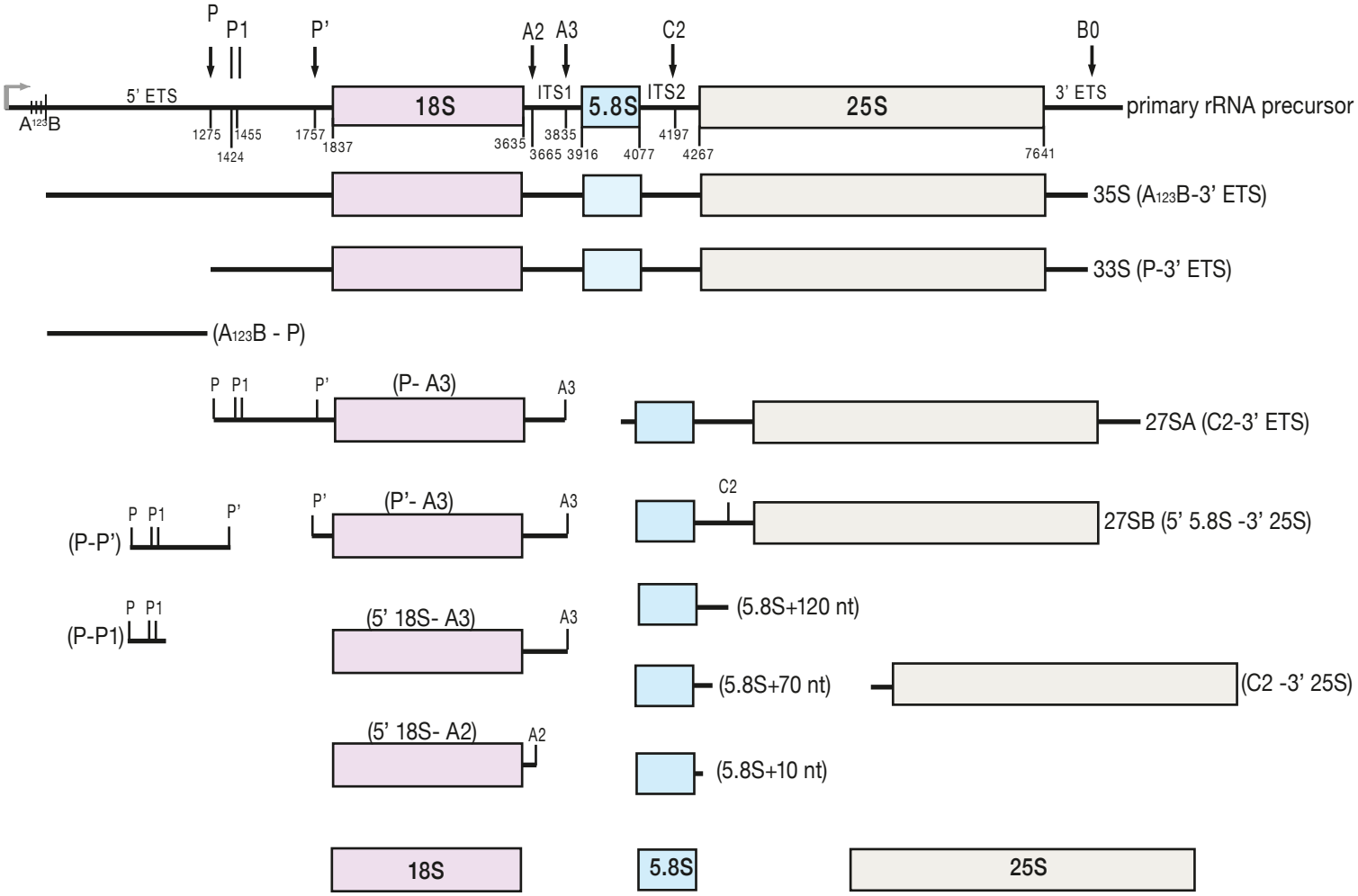

Figure 6. rRNA precursors detected in Arabidopsis.
The diagram is explained in the main text.

U3 Small subunit processome (Lange et al., 2014). 5S rRNA is transcribed by RNA Polymerase III (Pol III), whereas 18S, 5.8S and 25S rRNA (28S rRNA in human) are transcribed as a single polycistronic 35S precursor by RNA Polymerase I (Pol I). With about 60% of the cellular transcription, the 35S rRNA precursor is the most transcribed RNA (Kos and Tollervey, 2010). In this polycistronic transcript 18S, 5.8S and 25/28S rRNAs are separated by Internal Transcribed Spacers (ITS1 and ITS2) and flanked by External Transcribed Spacers (5'ETS and 3'ETS) which are eliminated during the maturation of pre-ribosomal particles to finally give rise to mature rRNAs.

In *Arabidopsis*, the 35S precursor has a size of about 7700 nt, 2500 nt of which are eliminated by both endo-and exoribonucleolytic processes. rRNA processing is by far best studied in *S. cerevisiae* and is believed to be largely conserved. However, mapping of the endonucleolytic cleavage sites revealed an additional processing site in the 5' ETS of both human and plant 35 precursors (Mullineux and Lafontaine, 2012; Turowski and Tollervey, 2015). A scheme of the cleavage sites within the *Arabidopsis* 35S precursor and the major processing intermediates are depicted in Figure 6. Only a few of the endo- and exonucleolytic activities involved in plant pre-rRNA processing have been identified so far. As determined in *Brassica oleracea*, a close relative of *Arabidopsis*, the cleavage at the P-site is mediated by a ribonucleoprotein complex containing U3 snRNA and nucleolin (U3 snoRNP) (Sáez-Vasquez et al., 2004). The endonucleolytic cleavage in the 3' ETS (at B0 site) is performed by AtRTL2, an orthologue of yeast Rnt1 (Comella et al., 2008; Kufel et al., 1999). An *Arabidopsis* homologue of the yeast endonuclease Nob1 generates the mature 3' end of the 18S rRNA (Missbach et al., 2013). The ribonucleases that cleave at A2, A3 and C2 or generate mature ends of 5.8S or 25S rRNAs have not been identified yet.

In addition to endonucleases, both 5'-3' and 3'-5' exoribonucleases are required for rRNA processing. Exoribonucleases also ensure the degradation of

misprocessed, misfolded or hypomodified rRNA precursors. In *Arabidopsis*, the nuclear 5'-3' exoribonucleases AtXRN2 and AtXRN3 are involved in the processing of the 5' extremities of 5.8S and 25S rRNA (Zakrzewska-Placzek et al., 2010). AtXRN2 and AtXRN3 have also redundant roles for the elimination of maturation by-products generated from the 5' ETS and the ITS1 (Zakrzewska-Placzek et al., 2010). In addition, AtXRN2 has a unique function in trimming the 5' extremity of the primary precursor transcript, which removes a sequence called the A123B cluster, a 123 nt region located in the 5'ETS, upstream of the P site. This trimming step is required to enable the endonucleolytic cleavage at the P site (Zakrzewska-Placzek et al., 2010). 3'-5' exoribonucleolytic degradation of rRNA precursors and fragments released by endonucleolytic cleavages is performed by the nuclear exosome. The two archetypical roles of the exosome in rRNA processing are 3' trimming of the 5.8 S rRNA and the elimination 5' ETS. In addition, 3'-5' exoribonucleolytic degradation contributes to the processing or quality control of 18S rRNA precursors (Lange et al., 2011; Preti et al., 2013; Rouquette et al., 2005; Sikorski et al., 2015; Tafforeau et al., 2013). However, some of the fragments that are excised from rRNA precursors do not accumulate upon down-regulation of either 5'-3' and 3'-5' or exoribonucleolytic pathways, suggesting that both pathways act also redundantly.

A. The exosome monitors early steps of rRNA processing

The largest precursor that can be detected in wild-type *Arabidopsis* plants is the P-3' ETS 33S precursor (Zakrzewska-Placzek et al., 2010; Lange et al., 2011; Missbach et al., 2013). The P-3' ETS 33S precursor accumulates in mutants lacking the RNA helicase AtMTR4 or upon down-regulation of the exosome subunits AtRRP4 or AtRRP41, indicating that it is a substrate of the nuclear exosome (Lange at al., 2011; Chekanova et al., 2007; Sikorski et al., 2015). However, no accumulation is observed upon loss of either AtRRP6L2 or down-regulation of

RRP44, suggesting that both exoribonucleolytic activities contribute to its degradation (Sikorski et al., 2015). The P-3' ETS precursors can be further processed at P' in the 5' ETS, the mature 5' end of the 18S rRNA, or the 3' end of the 25S rRNA. However, the P'-25S and 5' 18S-25S intermediates are barely detectable and accumulate only upon loss of AtMTR4 or down-regulation of *RRP4* or *RRP41*, indicating that they are low abundant side products rapidly degraded by the exosome, rather than intermediates of the main rRNA processing pathway (Sikorski et al., 2015). An alternative explanation for their low abundance in wild-type plants may be that they undergo rapid processing by cleavage at A2 in a pathway proposed as "5' ETS-first" by the group of E. Schleiff (Weis et al., 2015).

B. The exosome and AtRRP6 have different roles in the degradation of 18S precursors

In yeast, the precursors destined for the small and large ribosome subunits are separated by cleavage at the A2 site located 30 nt downstream of the mature 3' end of 18S rRNA. Cleavage at a site alike A2, 200 nt 3' downstream of the 18S 3' end, occurs also in *Arabidopsis* (Zakrzewska-Placzek et al., 2010). However, a substantial proportion of the P-25S precursors are cleaved at the A3 site, located 200nt downstream of the A2 site (Zakrzewska-Placzek et al., 2010; Lange et al., 2011; Sikorski et al., 2015). 5' processing of the resulting P-A3 intermediates generates P'-A3 and 18S-A3 18S precursors. P-A3, P'-A3 and 18S-A3 are substrates of the nuclear exosome, as they accumulate as polyadenylated species upon down-regulation of *RRP6L2, RRP44, MTR4* and components of EXO9 (Lange et al., 2011; Sikorski et al., 2015). Interestingly, intermediates alike P-A3 are also observed in yeast and human cells and are also substrates of exoribonucleolytic degradation by the exosome (Carron et al., 2011; Preti et al., 2013; Rouquette et al., 2005; Sloan et al., 2013; Tafforeau et al., 2013). Therefore, it was proposed that exoribonucleolytic trimming rather than endonucleolytic cleavage generates 18S-A2 intermediates in

humans. However, an alternative scenario is that 18S precursors that are produced by cleavage at A3 are dead-end products that cannot be further processed into mature 18S and are therefore removed by rRNA surveillance as it seems to be the case in yeast (Allmang et al., 2000; Carron et al., 2011; de la Cruz et al., 1998).

Since P-A2 or P'-A2 intermediates have never been detected in *Arabidopsis*, cleavage at A2 likely requires 18S-25S as a substrate. In addition, cleavage at A2 can probably occurs on 18S-A3 intermediates, since the existence of excised A2-A3 fragments has been proven (Sikorski et al., 2015; Zakrzewska-Placzek et al., 2010). A2-A3 fragments accumulate upon impairment of the 5'-3' exoribonucleolytic pathway, but not upon down-regulation of the exosome (Sikorski et al., 2015; Zakrzewska-Placzek et al., 2010).

Interestingly, 18S-A2 precursors do not accumulate upon down-regulation of AtMTR4, the exosome core complex or AtRRP44 (Sikorski et al., 2015). Instead, *Arabidopsis* 18S–A2 precursors are exclusively processed by AtRRP6L2 (Sikorski et al., 2015). Suggesting that the role of AtRRP6L2 in the degradation of these intermediates is an exosome-independent function of AtRRP6L2. Moreover, 18S-A2 substrates are frequently uridylated, whereas precursors cleaved at A3 undergo predominantly adenylation. The nucleotidyltransferase activity that is involved in the uridylation of 18S-A2 intermediates remains to be identified. It is also not clear whether AtRRP6L2 has an intrinsic specificity for uridylated substrates. Interestingly, human 18S-E precursors (equivalent to 18S-A2 in *Arabidopsis*) also undergo uridylation and exoribonucleolytic trimming (Preti et al., 2013). However, 18S-E intermediates do not accumulate upon down-regulation of hRRP6 or the exosome, indicating that they are trimmed by another activity. As in yeast, the mature 3' ends of human and plant 18S rRNA is generated in the cytoplasm by the endonuclease AtNOB1 hNOB1/AtNOB1 (Fatica et al., 2004; Lamanna and Karbstein, 2009; Pertschy et al., 2009; Missbach et al., 2013).

C. The exosome is required for the elimination of the 5' ETS

As briefly depicted above, the *Arabidopsis* 5' EST contains two cleavage sites named P and P'. Cleavage at the P site is an early event and the resulting 5' part of the 5' ETS is degraded by AtXRN2 and AtXRN3 (Zakrzewska-Placzek et al., 2010). Cleavage at P' generates a 482 nt P–P' fragment. Oligoadenylated P-P' fragments accumulate upon loss of AtMTR4, the exosome, AtRRP44 and to a lesser extent in AtRRP6L2 (Chekanova et al., 2007; Kumakura et al., 2013; Lange et al., 2011, 2008) demonstrating that the 5' ETS is eliminated by 3'-5' exoribonucleolytic degradation by both AtRRP44 and AtRRP6L2 activities.

In yeast and humans, the ETS is polyadenylated by the non-canonical poly(A) polymerases Trf4/5 and hTRF4-1/hTRF4-2, respectively (LaCava et al., 2005; Lubas et al., 2011). The *Arabidopsis* homologue AtTRL is a nuclear protein that is enriched in nucleoli (Sikorski et al., 2015). In *trl* mutants, oligo-A tails at the 3' ends of several rRNA precursors and the P-P' fragment are hardly detectable but not completely abolished. This demonstrates that AtTRL is the main activity for the adenylation of rRNA processing intermediates. However, other activities can adenylate rRNA processing intermediates and partially compensate for loss of AtTRL. *trl* mutants accumulate misprocessed 18S precursors that still contain the 5' ETS. In addition, *trl* mutants accumulate degradation intermediates of P-P' of about 278 and 330 nt (Sikorski et al., 2015). Interestingly, specific, 150-180 nt intermediates of P-P' degradation, so-called P-P1 fragments, are also detected in wild-type plants (Lange et al., 2011; Sikorski et al., 2015). The P-P1 region contains stem-loop structures that may impede exoribonucleolytic degradation, which may explain the relative abundance of these maturation by-products (Sáez-Vasquez et al., 2004; Sikorski et al., 2015; Zakrzewska-Placzek et al., 2010). Indeed, P-P1 fragments accumulate in several exosome mutants, demonstrating that they are substrates 3' exoribonucleolytic decay. Therefore, P-P1 fragments are an ideal model substrate to

study the relative contribution of the different activities associated with the nuclear exosome.

D. The exosome contributes to processing of 5.8S rRNA

Besides the 5' ETS, 5.8S rRNA precursors are the archetypical substrates of exosome-mediated RNA degradation in all eukaryotes that have been studied so far. 5.8S precursors are generated by cleavage at A3 and C2 in the ITS1 and ITS2, respectively (Henras et al., 2015; Weis et al., 2015).

In yeast, the mature 5' extremity of mature 5.8 is generated by the 5'-3' exoribonuclease Xrn1p (Henry et al. 1994). Similarly, plant AtXRN2 and AtXRN3 contribute to the maturation of 5.8S 5' ends, however, the relative mild accumulation of 5' misprocessed *Arabidopsis xrn2 xrn3* mutants may suggest the involvement of additional factors (Zakrzewska-Placzek et al., 2010). Maturation of the 3' end of 5.8S rRNA involves 3'-5' exoribonucleolytic degradation by the exosome (Allmang et al., 1999; Briggs et al., 1998; de la Cruz et al., 1998). The mechanism of 5.8S processing by the yeast exosome was recently elucidated by E. Conti's laboratory (Makino et al., 2015). They studied the relative contributions of Rrp44p and Rrp6p in the processing of 5.8S 3' extremities by a combination of enzymatic assays and structural data and proposed that both exosome-associated activities collaborate in a sequential manner during processing of 5.8S rRNA precursors. Larger 5.8S rRNA precursors are threaded through the exosome channel to reach the active site of the processive exoribonuclease Rrp44p that is bound to the bottom of the EXO9 core complex. When 5.8S precursors are degraded to a size of 5.8S+30nt they are too short to span the central channel of EXO9 and become a substrate of Rrp6p, which further trims them to 5.8S+6nt (Makino et al., 2015).

In yeast, the final step of 5.8S processing, removal of the last nucleotides, is performed by Ngl2p in the cytoplasm (Thomson and Tollervey, 2010). Interestingly, Ngl2p is not essential for viability indicating that ribosomes that contain 5.8S rRNA

with short 3' extensions are (at least partially) functional (Thomson and Tollervey, 2010).

In *Arabidopsis*, processing of the 5.8S rRNA involves the RNA helicase AtMTR4, the exosome core complex and the exoribonucleases AtRRP6L2 and AtRRP44 (Chekanova et al., 2007; Kumakura et al., 2013; Lange et al., 2011). Three types of 5.8S precursors are easily detected in plant exosome mutants: 5.8S+120 nt, +70 nt and +10 nt. The 5.8S+120 nt precursor is generated by cleavage at C2 site. 5.8S+70nt species are predominantly observed in *mtr4* mutants. Finally, 5.8S+10 nt precursors accumulate in both *mtr4* and *rrp6L2* mutants, although to different levels (Lange et al., 2011). However, the relative contributions of the two exoribonucleases AtRRP6L2 and AtRRP44 to processing of plant 5.8S precursors have not been studied in directly comparable experiments so far. An additional challenge is to unravel the contribution of the unique phosphorolytic activity of plant EXO9 to individual steps of 5.8S processing.

Aims of the thesis

In all eukaryotes studied to date, the EXO9 core complex of the RNA exosome is catalytic inert, and catalytic activity is provided solely by associated exoribonucleases of the RRP44 and RRP6 families. Importantly, the sequence analysis of the plant exosome subunit AtRRP41 suggested that this protein possesses residues shown to be essential for phosphorolytic exoribonuclease activity in the related enzymes PNPase and archaeal EXO9. This suggested that plant EXO9 could have an intrinsic phosphorolytic activity, which would be unique among eukaryotic exosomes.

Therefore, the first goal of this study is to investigate the catalytic activity of the exosome core complex (EXO9) in *Arabidopsis*. I used *rrp41* mutants complemented either with wild-type ($RRP41^{WT}$) or mutated ($RRP41^{Pi-}$, $RRP41^{Pi\text{-}Cat\text{-}}$) versions of AtRRP41 to purify EXO9 complexes and perform *in vitro* activity assays. These experiments show that AtRRP41 is indeed the active subunit of EXO9. In this manuscript I demonstrate that EXO9's activity meets the three criteria for phosphorolytic catalysis, namely phosphate dependency, release of nucleoside diphosphates and reversibility of the reaction. I also investigate some basic requirements of this activity and address the question whether EXO9 has a distributive or processive activity.

Ribosomal RNA processing is one of the most conserved roles of the eukaryotic exosome, and the relative contributions of both Rrp6p and Rrp44p to this process have been intensively studied in yeast. As plant EXO9 has a third catalytic activity conferred by the exosome core complex, the second task of my study is to understand the contribution of this unique phosphorolytic activity to the degradation of the archetypical exosome substrates 5' ETS and 5.8S rRNA precursors *in vivo*. In this context, I also analyze the relative contribution of

AtRRP44, AtRRP6L2 and EXO9 in plant rRNA processing. I demonstrated that EXO9 has a specific, non redundant role in the elimination of a specific degradation intermediate of the 5'ETS and show that AtRRP44, AtRRP6L2 and EXO9 sequentially cooperate in processing of 5.8S rRNA precursors.

In the time frame of my PhD I generated a large number of plants lines that express active or inactive versions of EXO9 in backgrounds otherwise compromised in RNA metabolism. This work provides the genetic material for future studies of exosome-mediated RNA degradation in *Arabidopsis* to unravel the relative contributions of exosome-associated activities in plants and to better understand their biological roles. The long term goal of this future work is to understand why the phosphorolytic activity of the EXO9 complex has been retained and is conserved in the entire green lineage.

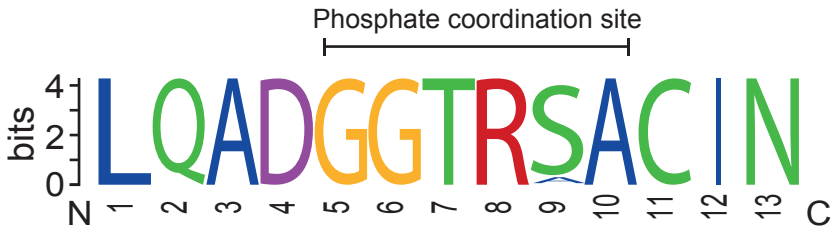

Figure 7. Residues essential for phosphate coordination in RRP41 are conserved in all land plants (Embryophyte). Logo illustrating the conservation of the phosphate coordination site among plant RRP41 proteins. Sequences of RRP41 proteins from 27 plant species including mosses, mono- and dicotyledons were aligned with ClustalX. The 13 amino acid sequences including the GGTRSA phosphate coordination site were used to calculate a sequence logo illustrating sequence conservation using the weblogo.berkeley.edu/logo.cgi site. The overall height of each stack indicates the sequence conservation at that position (measured in bits), whereas the height of symbols within the stack reflects the relative frequency of the corresponding amino acid at that position. The maximum sequence conservation per site is $\log_2 20 \approx 4.32$ bits for proteins.

Sequences from following plants were used to calculate the logo: *Physcomitrella patens, Selaginella moellendorffii, Populus trichocarpa, Vitis vinifera, Aquilegia caerulea, Camellia sinensis, Citrus clementina, Crocus sativus, Setaria italica, Thellungiella halophila, Capsella rubella, Arabidopsis thaliana, Arabidopsis lyrata, Brassica rapa, Mimulus guttatus, Sorghum bicolor, Oryza sativa, Zea mays, Brachypodium distachyon, Glycine max, Phaseolus vulgaris, Prunus persica, Carica papaya, Manihot esculenta, Ricinus communis, Medicago truncatula, Eucalyptus grandis.*

Results

Chapter 1. Transgenic lines to study the catalytic activity of EXO9 and its function in *Arabidopsis thaliana*

I. The phosphate coordination site is conserved in all land plant RRP41 proteins

The residues essential for phosphorolytic activity of RNase PH or the RNase PH-like proteins like bacterial PNPase and archaeal Rrp41 comprise residues responsible for RNA binding, phosphate binding and cleavage (Lorentzen et al., 2005). While yeast and human Rrp41p/hRRP41 proteins do contain the residues required for RNA binding and cleavage, the positively charged arginine residue essential for phosphate coordination is absent (Dziembowski et al., 2007). By contrast, a putative phosphate coordination site is conserved in *Arabidopsis* and rice RRP41 proteins (Dziembowski et al., 2007). Based on this observation it was suggested that *Arabidopsis* and rice RRP41 may have retained a phosphorolytic activity similar to archaeal enzymes (Dziembowski et al., 2007). To further investigate whether the presence of a potentially functional phosphate coordination site is present in RRP41 proteins from other plant species, we performed a sequence alignment of RRP41 proteins from 27 plant species including mosses, mono- and dicotyledons (listed in the legend of Figure 7). The sequences of the phosphate coordination sites GGTRSA with surrounding aminoacids were used to create a sequence logo (Crooks et al., 2004) illustrating the conservation of this sequence in plants. All residues reach the highest possible conservation (4.32 bits), except serine which has slightly lower conservation and in rare cases is replaced by alanine (Figure 7, position 9 in the logo). This results show that the residues essential for

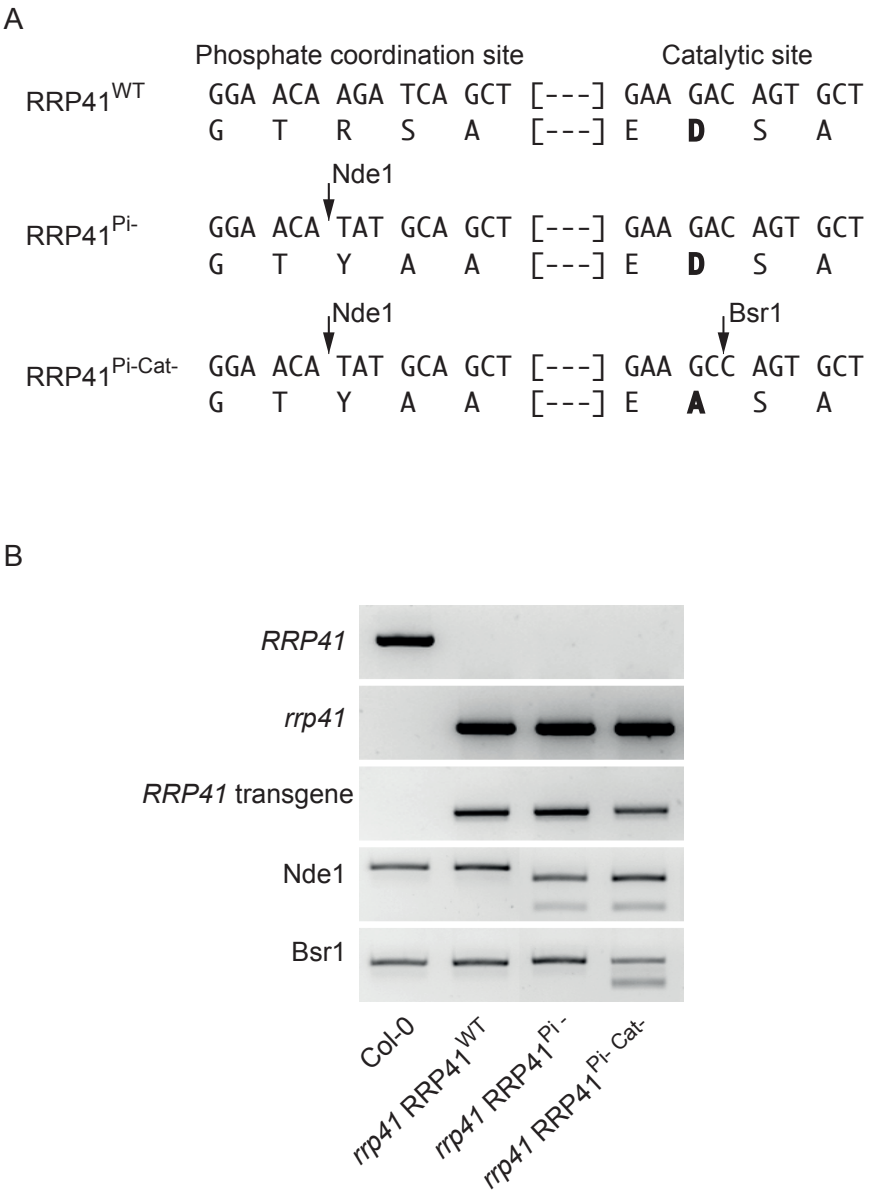

Figure 8. Expression of wild-type and mutated AtRRP41 in *Arabidopsis*.
A. Scheme depicting mutations introduced in phosphate coordination site and cleavage site in RRP41^{Pi-} (mutated only in phosphate coordination site) or RRP41^{Pi-Cat} (mutated in phosphate coordination site and cleavage site) compared to wild-type AtRRP41. B. All versions of *RRP41* were cloned as genomic constructs to produce fusion proteins with C-terminal myc- or GFP-tags and expressed under the control of the endogenous *RRP41* promoter in the *rrp41* mutant background. All PCRs were carried out with the same forward primer in the *RRP41* coding sequence. The reverse primer for *RRP41* PCR products is complementary to the 3' UTR that is only present in the endogenous *RRP41* gene. *rrp41* PCR products are amplified with a reverse primer complementary to the T-DNA insertion present in Salk_112819 rrp41 mutants. RRP41 transgenes are detected with a reverse primer complementary to the sequence encoding the myc-tag, which replaces the natural 3' UTR in RRP41^{WT}, RRP41^{Pi-} and RRP41$^{Pi-Cat-}$ plants. For Nde1 and Bsr1 digestions, PCR products were amplified with a reverse primer complementary to both endogenous and transgenic RRP41 genes.

phosphate coordination are strictly conserved and suggest that all land plant RRP41 proteins have a functional phosphate coordination site.

II. Characterization of plant lines expressing wild-type and mutated versions of AtRRP41

A. Expression of wild-type and catalytic inactive RRP41 proteins in *Arabidopsis thaliana*

The strict conservation of aminoacid residues essential for phosphate binding further supported the idea that plant EXO9 might be catalytically active. Therefore, we decided to experimentally study the catalytic activity of plant EXO9 using *Arabidopsis thaliana* as a model. To this end, three constructs were designed by Heike Lange to express tagged versions of wild-type and catalytic inactive RRP41 in stable *Arabidopsis* transformants.

In RRP41^{Pi-}, the phosphate binding site was mutated by changing R131 and S132 to Y and A, respectively, in order to mimic the respective residues of the catalytically inactive human hRRP41 (R131Y, S132A) (Figure 8 A). In RRP41$^{Pi-Cat-}$ both the phosphate binding residues and the D174 residue required for cleavage of the phosphodiester bond were mutated (R131Y, S132A and D174A). All versions of RRP41 were expressed under the control of the endogenous *RRP41* promoter and contained a C-terminal GFP or myc tag. In order to replace the essential endogenous RRP41 protein with the tagged versions of RRP41, the constructs encoding wild-type and mutated versions of RRP41 were transformed into heterozygous RRP41/rrp41 (Salk_112819) plants. Homozygous *rrp41* mutants expressing either myc- or GFP-tagged RRP41^{WT}, RRP41^{Pi-} and RRP41$^{Pi-Cat-}$ proteins were identified from the selfed progeny of primary transformants using PCR and restriction analysis, since the mutations in the phosphate coordination site and in the cleavage

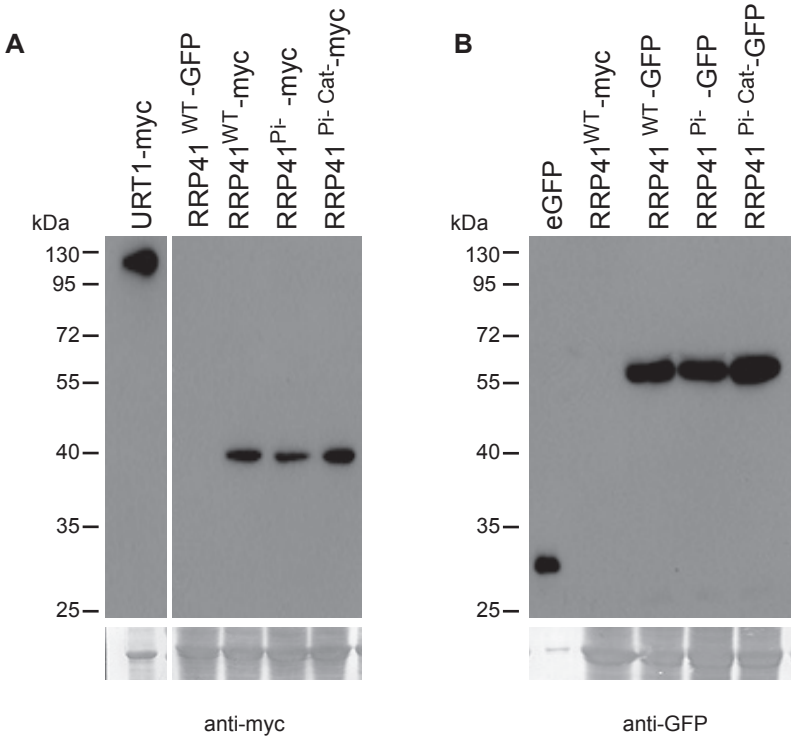

Figure 9. Expression of myc or GFP-tagged RRP41 proteins in stable *Arabidopsis* transformants. Protein extracts from *Arabidopsis thaliana rrp41* lines complemented with myc or GFP-tagged wild-type (RRP41^{WT}) and mutated (RRP41^{Pi-} or RRP41$^{Pi-Cat-}$) versions of AtRRP41 were analysed by western blot. Proteins were separated by SDS PAGE and transferred to a PVDF membrane. Fusion proteins were detected using anti-myc (panel A) and anti-GFP (panel B) antibodies. Middle lane containing size marker was removed from panel A. URT1-myc and eGFP plants were used as controls. Membrane stained with Coomassie blue is shown as loading control.

site introduced NdeI and BsrI restriction sites, respectively. An example illustrating the genotyping of *rrp41* mutants expressing either myc-tagged RRP41^{WT}, RRP41^{Pi-} and RRP41$^{Pi-Cat-}$ is provided in Figure 8B. The fact that it was possible to obtain homozygous *rrp41* mutants suggests that the putative activity of EXO9 is not essential for viability since both wild-type and mutated versions of AtRRP41 rescued lethality of *rrp41*.

To test the expression of the RRP41 transgenes at the protein level and to determine whether wild-type and mutated AtRRP41 are expressed to similar levels, a western blot analysis was performed. As can be seen in Figure 9A, a signal at 40 kDa was detected in all three samples from plants expressing myc-tagged versions of AtRRP41. The observed size fits approximately to the calculated size of RRP41-myc of about 35 kDa. Moreover, comparable expression levels are observed for both wild-type (RRP41^{WT}) and mutated versions (RRP41^{Pi-}, RRP41$^{Pi-Cat-}$). All GFP-tagged versions of RRP41 migrated slightly above 55 kDa (Figure 9B), closely to their calculated size of 54 kDa. As for myc-tagged RRP41, also GFP-tagged versions accumulated to similar levels. However, even if the endogenous *RRP41* promoter was used to control the expression of the transgene, it would be interesting to compare the expression level of the transgenic AtRRP41 proteins with that of the endogenous AtRRP41 in wild-type plants. This additional control would require an antibody against AtRRP41 and ideally, a second antibody against another subunit of the core exosome. Both antibodies are being produced in the host laboratory.

B. Wild-type and mutated RRP41 proteins show similar intracellular distributions

The intracellular localization of GFP tagged wild-type (RRP41^{WT}) and mutated (RRP41^{Pi-} and RRP41$^{Pi-Cat-}$) versions of RRP41 protein was analyzed by confocal microscopy (Figure 10). The subcellular localization of GFP-tagged

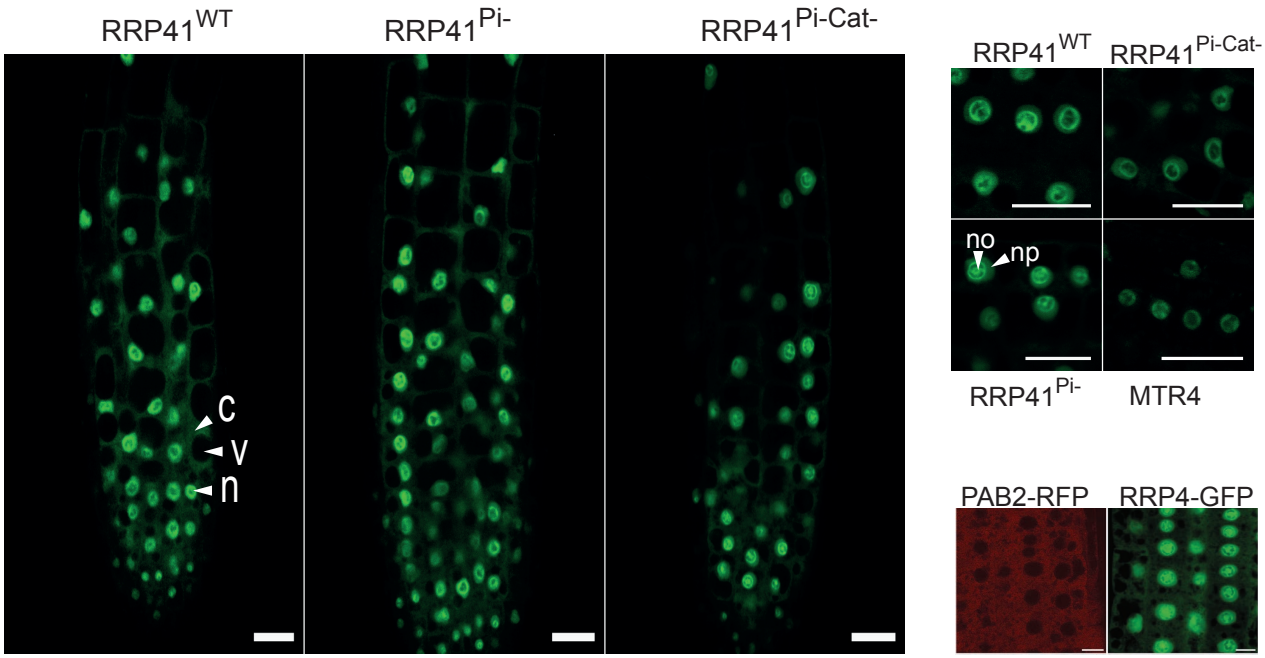

Figure 10. All three versions of AtRRP41 protein show similar intracellular localization (nucleus and cytoplasm). The intracellular localization of GFP tagged wild-type and mutated versions of AtRRP41 protein was analysed by confocal microscopy. *Arabidopsis thaliana rrp41* plants complemented with RRP41^{WT}, RRP41^{Pi-} or RRP41^{Pi-Cat} were grown on MS agar plates supplemented with 0.5 % sucrose. Samples prepared from the root tips of 10-day old seedlings were analysed with a ZEISS LSM 700 confocal microscope using a 510nm laser. MTR4-GFP is shown as nucleolar marker. PAB2-RFP is shown as cytoplasmic marker. RRP4-GFP (subunit of EXO9's cap) is used as a marker for dual localization (nucleus and cytoplasm). c: cytoplasm, n: nucleus, no: nucleolus, np: nucleoplasm, v: vacuole. The scale bars are 20μm except panel with PAB2 and RRP4 where scale bars are 10 μm.

AtRRP41 versions was compared to the localization of another subunit of plant EXO9, namely AtRRP4-GFP expressed under the control of the 35S promoter, the nucleolar exosome cofactor AtMTR4-GFP, or a RFP-tagged version of the cytoplasmic protein PAB2. As expected, PAB2-RFP localized only in the cytosol and AtMTR4-GFP was detected only in nucleoli. By contrast AtRRP4 was detected both in cytoplasm and nuclei. Similarly, all three versions of GFP-tagged AtRRP41, wild-type and mutated ones, were detected in cytoplasm and nuclei, and enriched in nucleoli.

This localization pattern of RRP41 is in agreement with the expected localization of exosome complexes (Allmang et al., 1999; Huh et al., 2003; Tomecki et al., 2010; Schilders et al., 2007; Staals et al., 2010) and shows that both wild type and mutated versions of RRP41 have identical intracellular distributions. Moreover, all three RRP41 transgenic lines displayed similar intensity of GFP signal in agreement with the results of the Western blot analysis and confirm that the three versions of RRP41 are expressed to similar levels.

C. Both RRP41^{WT} and RRP41$^{Pi\text{-}Cat\text{-}}$ are incorporated into high molecular weight complexes

The calculated size of an *Arabidopsis* EXO9 exosome complex is 274 kDa (Chekanova et al., 2007; Lange et al., 2014). The size of myc-tagged AtRRP41 is 35 kDa. Due to the substantial size difference between RRP41 monomer and EXO9 complex, tagged AtRRP41 assembled into EXO9 can be discriminated from unincorporated RRP41 subunits by gel filtration analysis. Previously gel filtration experiments using Tap-tagged RRP41 determined a complex size of 210-443 kDa (Chekanova et al., 2007).

To test whether active and inactive versions of AtRRP41 are incorporated into exosome complexes, proteins from RRP41^{WT} and RRP41$^{Pi\text{-}Cat\text{-}}$ plants were extracted under native conditions and analyzed by gel filtration chromatography followed by

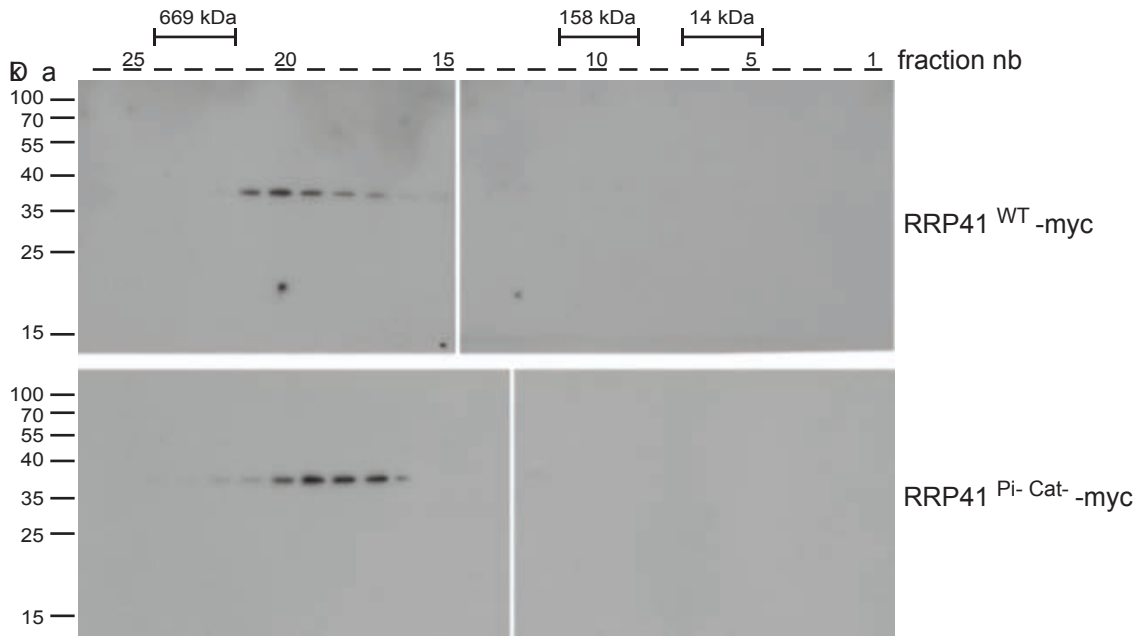

Figure 11. Both active and inactive versions of AtRRP41 protein are incorporated into high molecular weight complexes. Proteins were extracted under native conditions from *rrp41* plants complemented with myc-tagged RRP41^{WT} or RRP41$^{Pi\text{-}Cat\text{-}}$. Total plant extracts were clarified by centrifugation and were then analysed by gel filtration using a Superose 6 20 10/300 column (GE Healthcare Life Sciences). The column was calibrated using Thyroglobulin (669 kDa), Aldolase (158 kDa) and RNaseA (14 kDa) markers (GE Healthcare Life Sciences). Elution fractions were collected and fractions containing myc-tagged AtRRP41 subunits were identified by western blot analysis using an anti-myc monoclonal antibody (Roche).

western blot analysis. As can be seen in Figure 11, both versions of myc-tagged AtRRP41 migrated at a size of > 400 kDa corresponding to a large molecular weight complex. The small difference in the migration pattern of proteins extracted from $RRP41^{WT}$ or $RRP41^{Pi\text{-}Cat\text{-}}$ may be explained by experimental variations. The size of >400 kDa is larger than the calculated size for EXO9 of 270 kDa. This discrepancy between calculated and determined complex size may be due to the inherent imprecision of such experiments, but could also reflect the association of additional co-factors to EXO9. However, the important point is that no signals corresponding to AtRRP41 monomers were detected and that both wild-type and mutated versions of AtRRP41 were incorporated in complexes of comparable sizes.

These results indicate that both wild-type and mutated AtRRP41 proteins are fully incorporated in high molecular weight complexes, which indeed corresponded to EXO9 complexes as detailed below.

D. All versions of AtRRP41 are incorporated into EXO9 complexes

Next, I performed co-immunoprecipitation using myc-tagged $RRP41^{WT}$, $RRP41^{Pi\text{-}}$ or $RRP41^{Pi\text{-}Cat\text{-}}$ as baits. Col-0 (wild-type plants from Colombia ecotype) plants were used for mock-IP. Samples were extracted from inflorescences, purified with anti-myc antibodies coupled to magnetic MicroBeads and eluted with SDS-PAGE loading buffer. SDS-PAGE followed by silver stain revealed a similar pattern of bands in all RRP41 samples, different from the pattern in Col-0 (Figure 12.A). Mass-spectrometric analysis identified all nine subunits of EXO9, namely RRP41, RRP42, RRP43, both isoforms of RRP45 (RRP45A and RRP45B), RRP46, MTR3, CSL4, RRP4 and RRP40A with high Mascot scores and high number of spectra (Figure 12.B, all subunits of EXO9 are marked in green). This result demonstrated that both wild-type and mutated versions of RRP41 are incorporated into EXO9. Additionally, I identified low amounts of the helicases AtHEN2 or AtMTR4 and

A

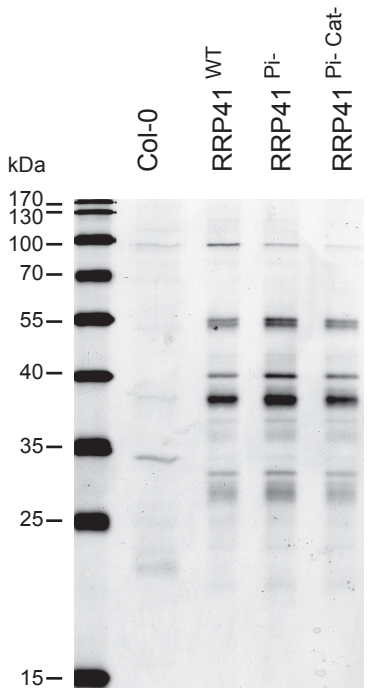

B

		RRP41^{WT}		RRP41^{Pi-}		RRP41$^{Pi-Cat-}$	
Accession	Name	Mascot score	#Spectra	Mascot score	#Spectra	Mascot score	#Spectra
At1g03360	AtRRP4	1586	713	1793	750	1519	745
At1g60080	AtRRP43	2172	279	2444	310	2247	296
At2g25355	AtRRP40A	1804	183	1974	198	1769	208
At3g07750	AtRRP42	1677	363	1653	431	1705	369
At3g46210	AtRRP46	780	74	875	97	695	81
At3g60500	AtRRP46B/ CER7	2394	273	2484	317	2264	299
At3g61620	AtRRP41	1765	354	1444	265	1257	251
At4g27490	AtMTR3	1741	211	1753	235	1729	235
At5g38890	AtCSL4	1542	283	1672	311	1432	299
At1g59760	AtMTR4	910	27	916	28	215	6
At2g17510	AtRRP44	779	26	767	25	697	19
At2g06990	AtHEN2	274	6	289	8	215	6

Figure 12. All versions of AtRRP41 are incorporated into exosome complexes.
A. Silver stain analysis of eluates from co-immunopreciptation of RRP41-myc revealed similar pattern of bands in RRP41^{WT}, RRP41^{Pi-} or RRP41$^{Pi-Cat-}$ but different from the Col-0 sample. Co-immunoprecipitation was performed on *rrp41* mutants complemented with myc-tagged RRP41^{WT}, RRP41^{Pi-} or RRP41$^{Pi-Cat-}$ as baits. Col-0 plants were used for mock-IP. Eluates were subjected to LC-MS/MS analysis to identify proteins co-purifying with AtRRP41. Briefly, proteins were extracted under native conditions by grinding, followed by extract clarification by ultracentrifugation at 150 000 x g. Next, protein extracts were incubated with anti-myc antibodies coupled to magnetic MicroBeads (Miltenyi Biotec), washed and eluted with SDS-PAGE loading buffer, resolved by 10 % SDS-PAGE and visualized by silver stain. B. All nine canonical subunits of exosome are detected with a high Mascot score and high number of spectra in IP on *rrp41* mutants complemented with myc-tagged RRP41^{WT}, RRP41^{Pi-} or RRP41$^{Pi-Cat-}$. Mass-spectrometric analysis was carried out as previously described (Lange et al., 2014). Nine subunits of the exosome core are marked in green.

Figure 13. Both the wild-type (RRP41^{WT}) and mutated (RRP41^{Pi-} or RRP41$^{Pi-Cat-}$) AtRRP41 versions complement the lethal *rrp41* mutation and grew similar to wild-type. *rrp41* plants complemented with wild-type and mutated versions of AtRRP41 protein were grown in soil in 16h light/ 8h darkness. Photo was taken 30 days post germination (30 dpg).

exoribonuclease AtRRP44, in agreement with previously published data (Lange et al., 2014).

Therefore, these data confirm that the high molecular complex AtRRP41 versions are incorporated in is the exosome and also demonstrate that I can purify intact exosome complexes from plants.

III. Conclusions and brief discussion

Interestingly, both wild-type and mutated RRP41 versions complement the otherwise lethal *rrp41* mutation and grew similar to wild-type, suggesting that the putative phosphorolytic activity of RRP41 is not essential at least under standard laboratory conditions (Figure 13). However, it cannot be excluded at this stage that EXO9's phosphorolytic activity may become essential under specific biotic or abiotic stress. The impact of certain stress conditions on *rrp41* complemented lines was tested, like viral infection, however with negative results. Another explanation for the wild-type growth of $RRP41^{Pi-}$ and $RRP41^{Pi\text{-}Cat-}$ plants is that the lack of phosphorolytic activity can be compensated by other exoribonucleolytic activity. This second possibility is further explored in Chapter 3.

All versions of AtRRP41 showed a similar intracellular localization pattern in both cytoplasm and nuclei, with enrichment in nucleoli. This is in agreement with predicted exosome localization (Allmang et al., 1999; Huh et al., 2003; Tomecki et al., 2010; Schilders et al., 2007; Staals et al., 2010) and previously published data (Chekanova et al., 2007; Lange et al., 2014). However, a different localization was reported for AtRRP45B and AtRRP45A which were both detected in cytoplasm and nuclei but excluded from the nucleoli (Hooker et al., 2007). However, this localization was determined using transient expression of fusion proteins in *Nicotiana benthamiana*. The disadvantage of transient expression experiments is that overexpression of proteins may alter their subcellular localization. Therefore, another type of localization studies should be used for confirmation. Localization

studies using GFP tag, especially in the case of such small protein as AtRRP41 (27kDa) may lead to some artefacts too. However, the fact that all AtRRP41 versions rescue the lethality of *rrp41* mutation shows that mutations introduced in AtRRP41 do not affect plant viability and therefore very likely localize to their correct compartments. Moreover, the very same localization pattern as for AtRRP41 was shown for another subunit of plant EXO9, AtRRP4, supporting dual localization pattern with enrichment in nuclei (Lange et al., 2014).

Both wild-type and mutated version of AtRRP41 are incorporated into high molecular weight complexes with an apparent size of more than 400 kDa. Gel filtration due to its imprecision does not allow for exact estimation of the size of the protein complex. Importantly, no signal corresponding to AtRRP41 monomer was detected, showing that both wild-type and mutated version of AtRRP41 are fully incorporated into high molecular weight complex.

The mass spectrometric analysis of proteins co-purified with AtRRP41 identified all nine subunits of EXO9 proving that both wild-type ($RRP41^{WT}$) and mutated ($RRP41^{Pi-}$, $RRP41^{Pi-Cat-}$) versions of AtRRP41 are incorporated into exosome complexes. This result also shows that I am able to purify intact exosome complexes from *Arabidopsis*. Interestingly also additional associated factors co-purified with EXO9, such as helicases AtHEN2 and AtMTR4 and exoribonuclease AtRRP44, although in low amounts. This may reflect the dynamic character of interactions between those EXO9-associated factors and core exosome in plants. By contrast, we did not detect a single spectrum corresponding to any of the three RRP6-like proteins, similar to previous results (Chekanova et al., 2007; Lange et al., 2014). Because of the negative nature of this observation, one must remain cautious in its interpretation. It is possible that, unlike their homologues in yeast and humans, AtRRP6-like proteins do not associate with EXO9 in plants or that this interaction is weak.

As demonstrated in this chapter, *rrp41* plants complemented with wild-type ($RRP41^{WT}$) or mutated ($RRP41^{Pi-}$, $RRP41^{Pi\text{-}Cat-}$) versions of AtRRP41 can be used as a source material for studying catalytic properties of EXO9 *in vitro* and as tools for addressing EXO9's functions *in vivo*.

Chapter 2. Catalytic activity of EXO9 in *Arabidopsis*

The key question of this work is whether the plant EXO9 is catalytically active. As detailed in the introduction plant EXO9 adopts a ring-shaped structure that resembles bacterial phosphorolytic enzymes such as PNPase or the archaeal exosome. However, while bacterial PNPase and archaeal exosomes contain three phosphorolytically active subunits, plant EXO9 contains only one subunit, AtRRP41, that possesses all amino acid residues required for phosphorolytic activity. Phosphorolytic enzymes use inorganic phosphate (Pi) to attack the phosphodiester bond of RNA substrate, releasing nucleoside diphosphates (NDPs). Moreover, when NDPs are present in excess, phosphorolytic enzymes have polymerizing activity and synthesize RNA tails. In this chapter I studied the catalytic properties of plant EXO9. First, I tested whether RRP41 is enzymatically active and investigate some basic requirements of this activity (Mg^{2+}-dependency, inhibition by Ca^{2+} and ATP). Next, I tested whether EXO9s activity fulfils the three requirements of phosphorolysis that are phosphate-dependency, release of nucleoside diphosphates (NDPs) and reversibility (synthesis of RNA tails). Finally, I tested some catalytic properties of EXO9.

I. The plant exosome is catalytically active

A. AtRRP41 is the catalytically active subunit of plant core exosome

To test whether AtRRP41 is the active subunit of plant exosome I performed *in vitro* activity assays using EXO9's purified from plant lines expressing wild-type ($RRP41^{WT}$) or mutated ($RRP41^{Pi-}$ and $RRP41^{Pi\text{-}Cat-}$) versions of AtRRP41 proteins. Mock-purified proteins from plants not expressing any myc-tagged protein served as an additional control (mock-IP). Samples obtained by Mock-IP, immunopurified EXO9 complexes containing wild-type or mutated versions of AtRRP41, or buffer

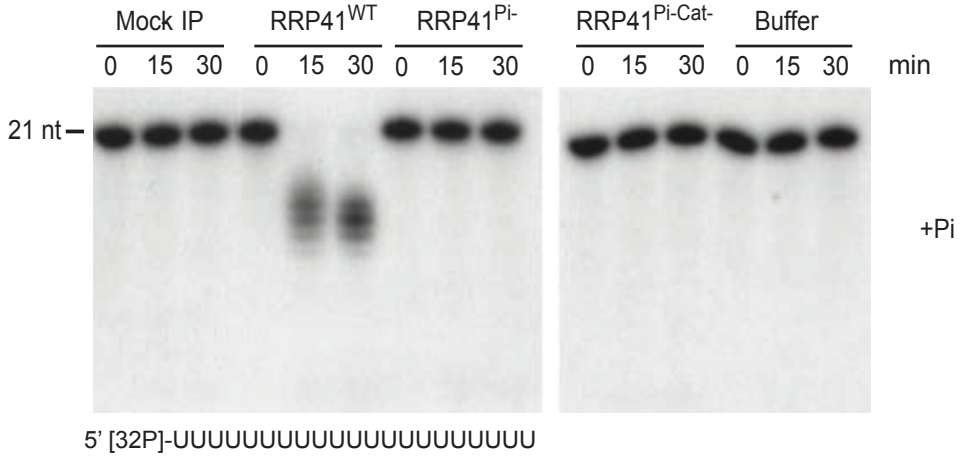

Figure 14. Plant EXO9 activity is conferred by RRP41. Exosome complexes purified from Col-0, RRP41^{WT}, RRP41^{Pi-} and RRP41$^{Pi-Cat-}$ plants and IP eluate buffer were incubated with 5'- labeled oligo(U)$_{21}$ RNA substrate in presence of 3.5 mM inorganic phosphate. Samples were collected at the indicated time points and analysed by denaturing 17% PAGE and autoradiography. Each reaction contained 1.4 nM of EXO9 and 25 nM of RNA substrate. Mock-IP: IP on Col-0 plants, RRP41^{WT}, RRP41^{Pi-} and RRP41$^{Pi-Cat-}$: *rrp41* mutants complemented with myc-tagged RRP41^{WT}, RRP41^{Pi-} or RRP41$^{Pi-Cat-}$ respectively, Pi: phosphate.

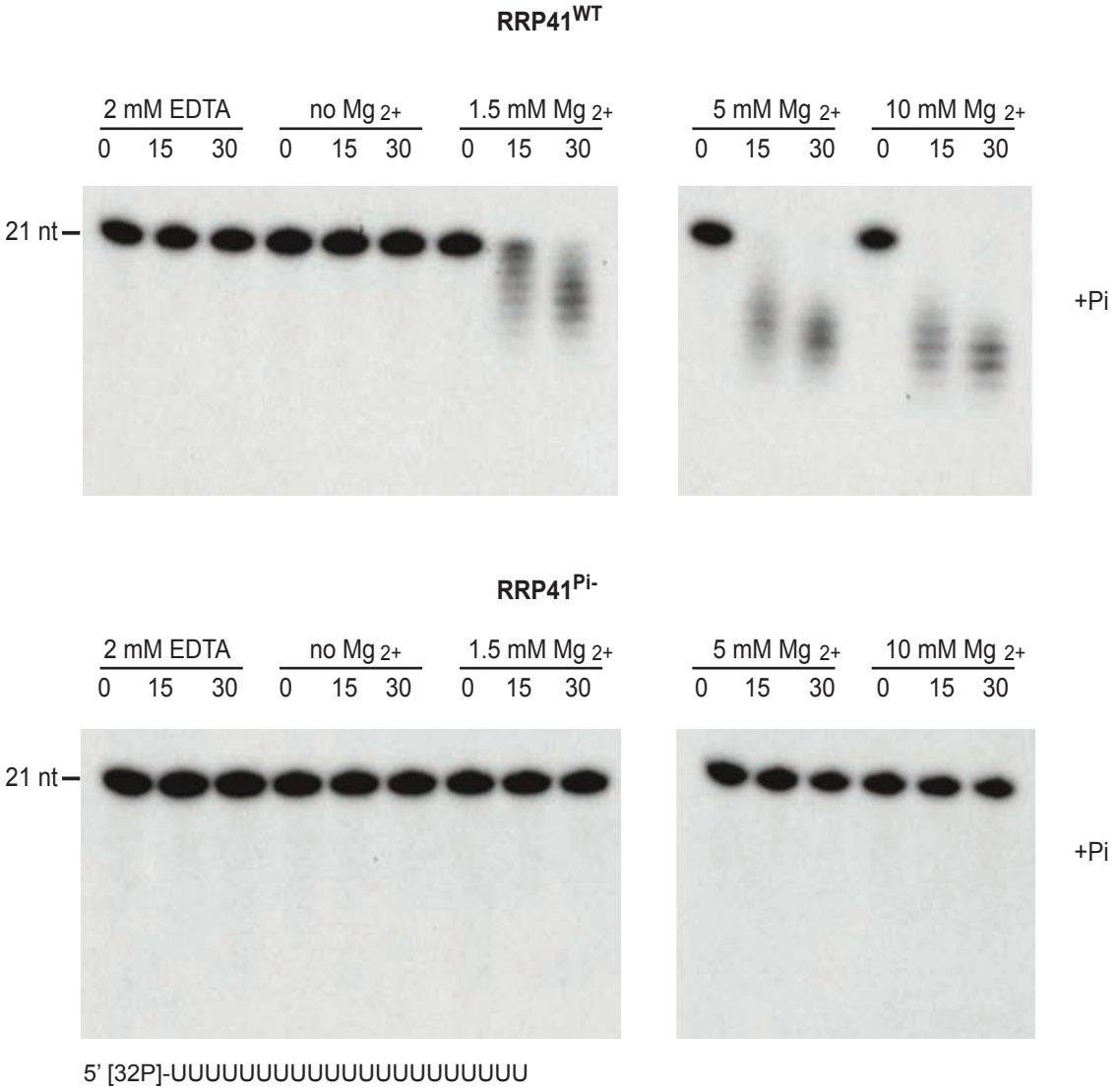

Figure 15. Activity of plant EXO9 is Mg^{2+}-dependent. EXO9 purified from $RRP41^{WT}$and $RRP41^{Pi-}$ plants were incubated with 5'- labeled oligo$(U)_{21}$ in the presence of inorganic phosphate. Reactions were carried out in the presence of EDTA (2 mM) or 0, 1.5, 5 or 10 mM $MgCl_2$. Samples were collected at the indicated time points (minutes), stopped by adding 1 volume of RNA loading buffer and analysed by denaturing 17% PAGE and autoradiography. Each reaction contained 1.4 nM of exosome complexes and 25 nM of RNA substrate.$RRP41^{WT}$ and $RRP41^{Pi-}$: *rrp41* mutants complemented with myc-tagged $RRP41^{WT}$or $RRP41^{Pi-}$ respectively, Pi: phosphate.

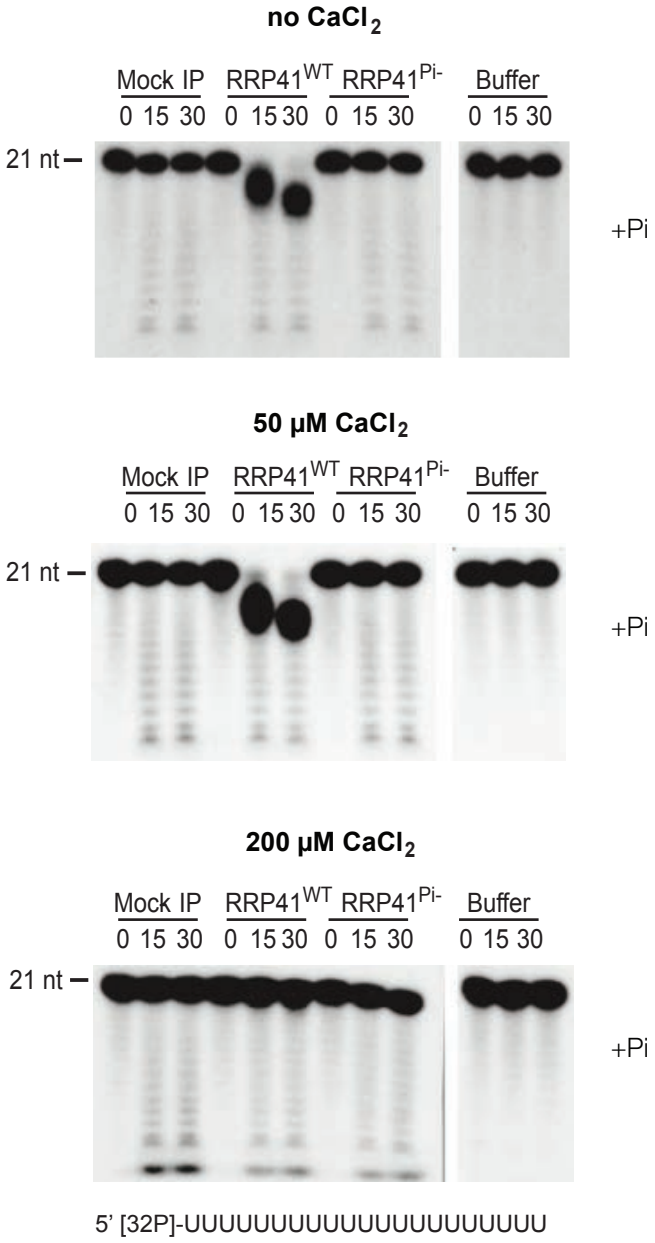

Figure 16. Activity of plant EXO9 is inhibited by Ca^{2+}. EXO9 purified from Col-0, $RRP41^{WT}$ and $RRP41^{Pi-}$ plants and IP wash buffer were incubated with 5'- labeled oligo$(U)_{21}$ in the presence of inorganic phosphate. Three sets of reactions with 0, 50 or 200 µM $CaCl_2$ were performed. Samples were collected at the indicated time points (minutes), stopped by adding 1 volume of RNA loading buffer and analysed by denaturing 17% PAGE and autoradiography. Each reaction contained 1.4 nM of exosome complexes and 25 nM of RNA substrate. Mock-IP: IP on Col-0 plants, $RRP41^{WT}$ or $RRP41^{Pi-}$: *rrp41* mutants complemented with myc-tagged $RRP41^{WT}$ or $RRP41^{Pi-}$ respectively, Pi: phosphate.

(comprising 100 mM NaCl, 20 mM MOPS pH 7.5, 0.1% Triton X100) only were incubated with the RNA substrate in the presence of 3.5 mM inorganic phosphate (Pi). The RNA substrate was 5'[^{32}P]-labeled oligo(U)$_{21}$. Samples were collected after 0, 15, and 30 minutes, resolved by denaturing PAGE and analyzed by autoradiography. No degradation of the radiolabeled RNA substrate was observed in buffer, in mock-IP, or when substrates were incubated with EXO9 containing mutated RRP41 (RRP41^{Pi-} or RRP41$^{Pi-Cat-}$) (Figure 14). By contrast, the RNA substrate was degraded in the presence of EXO9 containing the wild-type RRP41 (RRP41^{WT}). Degradation products of up to 6 nucleotides smaller than the undigested RNA substrate were observed after 30 minutes of the time course.

This result shows that EXO9 has a catalytic activity conferred by the RRP41 subunit and trims a RNA substrate *in vitro*.

B. Activity of RRP41 is Mg^{2+}-dependent

Phosphorolytic enzymes such as the archaeal exosome require Mg^{2+} ions for activity (Evguenieva-Hackenberg et al., 2014). Mg^{2+} is the most abundant divalent cation in eukaryotic cells, with concentrations ranging from 1-25 mM Mg^{2+} in plant cells, depending on the tissue (Moomaw and Maguire, 2008). However, the concentration of free Mg^{2+} in the cytosol is considerably less with only 0.4 to 0.5 mM, since Mg^{2+} is bound to many proteins and metabolites such as ATP (Karley and White, 2009; Maathuis, 2009).

To test EXO9's Mg^{2+} requirements I performed activity assays in the presence of inorganic phosphate (Pi) and either EDTA or $MgCl_2$. 5'[^{32}P]-labeled oligo(U)$_{21}$ was used as a substrate. Time course and sample analysis were performed as described in the paragraph above. As in the previous experiment, RNA degradation was only observed in reactions containing EXO9 purified from RRP41^{WT} plants, and no degradation was observed in control reactions (Figure 15). No degradation was

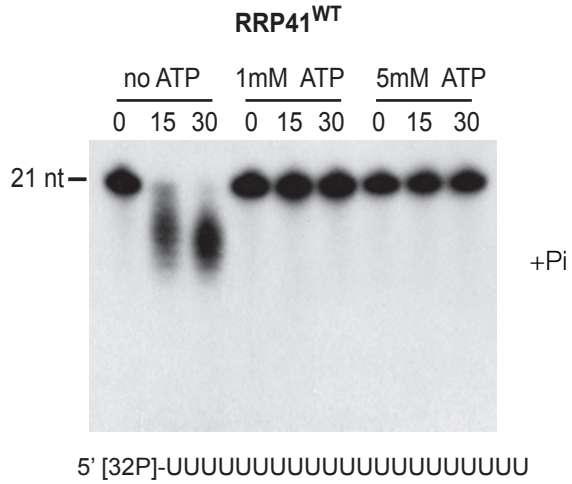

Figure 17. Activity of plant EXO9 is inhibited by ATP. EXO9 purified from RRP41^{WT}and RRP41^{Pi-} plants was incubated with 5'- labeled oligo(U)21 in the presence of inorganic phosphate(Pi) and 0, 1 or 5 mM ATP. Samples were collected at the indicated time points (minutes), stopped by adding 1 volume of RNA loading buffer and analysed by denaturing 17% PAGE and autoradiography.Each reaction contained 1.4 nM of exosome complexes and 25 nM of RNA substrate. RRP41^{WT}: *rrp41* mutants complemented with myc-tagged RRP41^{WT}, Pi: phosphate.

observed when Mg^{2+} was omitted or in the presence of EDTA. As can be seen in Figure 15, the activity of EXO9 was stimulated by increasing concentrations of Mg^{2+}. These results confirm that the activity of plant EXO9 is Mg^{2+}-dependent. Even though I observed a slightly higher activity in the presence of 5 and 10 mM Mg^{2+}, I decided to work with 1.5 mM Mg^{2+} since these rather low concentrations are more similar to the magnesium concentrations in living plant cells.

C. Activity of RRP41 is inhibited by Ca^{2+}

The replacement of Mg^{2+} by other divalent cations such as Ca^{2+} usually results in the complete loss of the activity of Mg^{2+}-dependent enzymes. To test whether the activity of EXO9 is inhibited by Ca^{2+}, I performed activity assays with different concentrations of $CaCl_2$. EXO9 purified from $RRP41^{WT}$ and $RRP41^{Pi-}$ plants and control from mock IP were incubated with 5'[^{32}P]-labeled oligo$(U)_{21}$ in the presence of phosphate (Pi) and either 0, 50 or 200 μM $CaCl_2$. The samples collected during the time course were analyzed by denaturing PAGE and autoradiography. In all samples except buffer a contaminating processive activity was observed, however, this did not severely compromise the experiment. As seen in Figure 16, RRP41-dependend degradation of the RNA substrate was most efficient in presence of phosphate but in absence of Ca^{2+}. While the presence of 50 μM $CaCl_2$ did not affect the activity of EXO9, the addition of 200 μM $CaCl_2$ abolished it. Hence, as many Mg^{2+}-dependent enzymes, plant EXO9 is indeed inhibited by Ca^{2+}.

D. Activity of RRP41 is inhibited by ATP

It has been reported that ATP binds to and inhibits the bacterial phosphorolytic enzyme PNPase (Del Favero et al., 2008). To test whether ATP has also an inhibitory effect on EXO9 activity I performed in vitro activity assays with

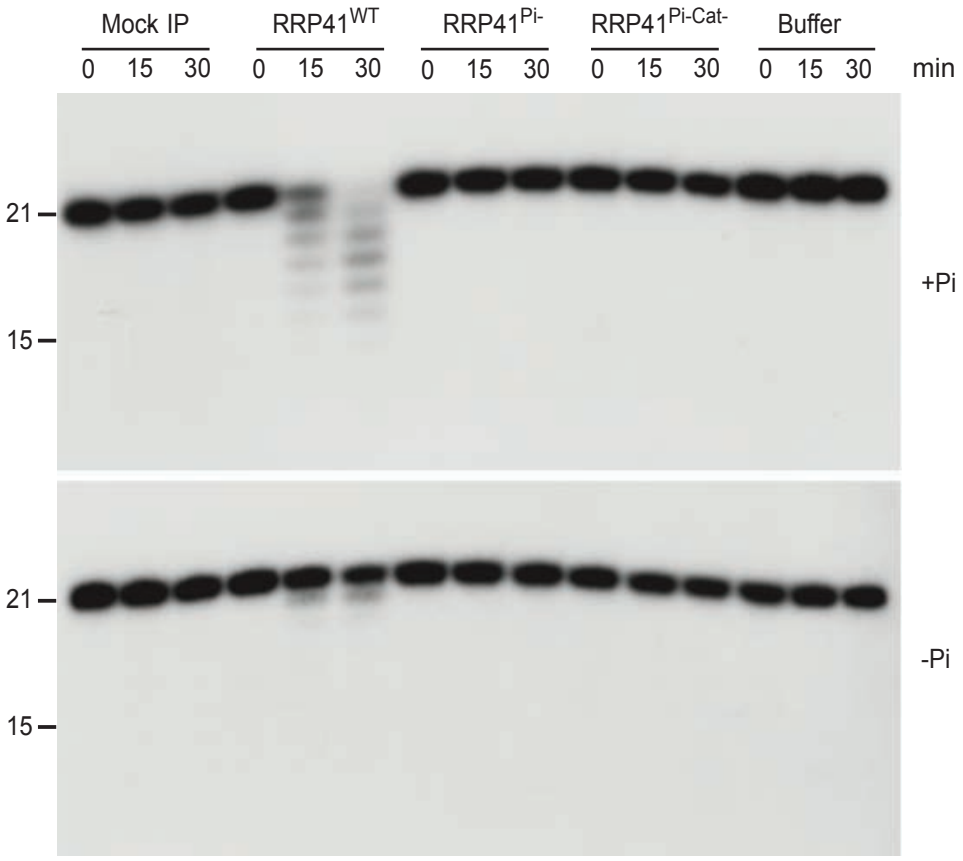

Figure 18. Plant EXO9 activity is stimulated by phosphate. Exosome complexes purified from Col-0, RRP41^{WT}, RRP41^{Pi-} and RRP41$^{Pi-Cat-}$ plants and IP wash buffer were incubated with 5'-labeled oligo(U)$_{21}$ RNA substrate in the presence (+Pi) or absence (-Pi) of inorganic phosphate. Reactions in +Pi assay contained 3.5 mM phosphate. Samples were collected at the indicated time points and analysed by denaturing 17% PAGE and autoradiography. Each reaction contained 0.4 nM of Exo9 and 6 nM of RNA substrate. Mock-IP: IP on Col-0 plants, RRP41^{WT}, RRP41^{Pi-} and RRP41$^{Pi-Cat-}$: *rrp41* mutants complemented with myc-tagged RRP41^{WT}, RRP41^{Pi-} or RRP41$^{Pi-Cat-}$ respectively, Pi: phosphate.

EXO9 containing either wild-type or mutated RRP41 proteins in the presence of inorganic phosphate and 0, 1 or 5 mM ATP. 5'[^{32}P]-labeled oligo(U)$_{21}$ served as a RNA substrate. As seen in Figure 17 no degradation was observed when the substrate was incubated with mutated RRP41 (RRP41^{Pi-}), while RNA degradation was observed in presence of EXO9 purified from RRP41^{WT} plants. In absence of exogenously added ATP, EXO9 removed several nt from the RNA substrate. By contrast, no trimming was observed in presence of 1 or 5 mM ATP. This shows that ATP inhibits the activity of EXO9.

Taken together, my results show that plant EXO9 has an RNA-trimming activity conferred by AtRRP41, and that this activity is Mg2+-dependent and inhibited by Ca2+ and ATP.

II. EXO9 has a phosphorolytic activity

To investigate whether EXO9s activity is phosphorolytic I tested three characteristic properties of phosphorolysis: phosphate-dependency, release of nucleoside diphosphates (NDPs) and reversibility (synthesis of RNA tails).

A. EXO9s activity is phosphate-dependent

To test whether EXO9's activity is phosphate-dependent I performed an *in vitro* activity assay with exosome complexes containing either active (RRP41^{WT}) or inactive (RRP41^{Pi-} and RRP41$^{Pi-Cat-}$) versions of RRP41, alongside with mock-IP and buffer controls. All assays were performed either in the presence of 3.5 mM inorganic phosphate (Pi) or in the absence of Pi. A 5'[^{32}P]-labeled oligo(U)$_{21}$ was used as substrate. As seen in Figure 18 degradation performed by RRP41^{WT} is strongly stimulated by inorganic phosphate. In the absence of phosphate (Pi-), the activity observed in the sample containing wild-type EXO9 was substantially

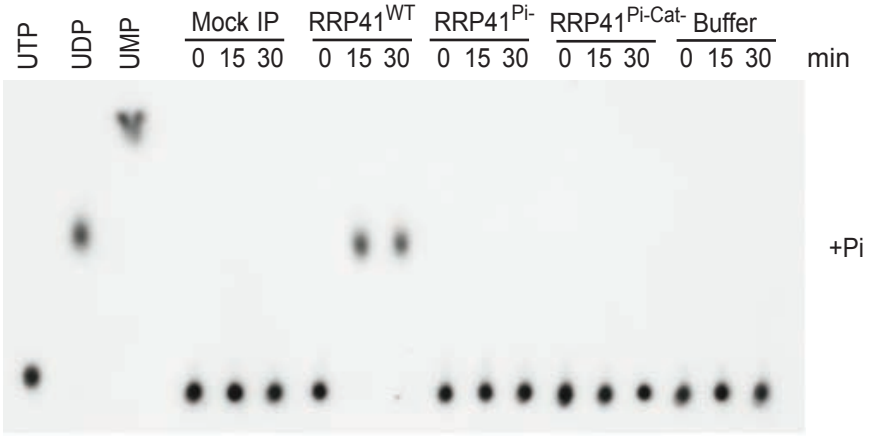

Figure 19. Activity of plant EXO9 releases NDPs. Exosome complexes purified from Col-0, $RRP41^{WT}$, $RRP41^{Pi-}$ and $RRP41^{Pi-Cat-}$ plants and IP wash buffer were incubated with 3'[^{32}P]-labeled oligo$(U)_{22-23}$ RNA substrate (oligo$(U)_{21}$ RNA was 3' labeled with [^{32}P] αUTP using Cid1 poly(U) polymeras**e**. Aliquots were taken at indicated time points, stopped by addition of EDTA, separated on thin-layer chromatography (TLC) plate (polyetyleneimine-cellulose) and analysed by autoradiography. UTP, UDP and UMP seen on the left side of each panel were used as references. Each reaction contained 1.4 nM of EXO9 and 25 nM of RNA substrate.Mock-IP: IP on Col-0 plants, $RRP41^{WT}$, $RRP41^{Pi-}$ and $RRP41^{Pi-Cat-}$: *rrp41* mutants complemented with myc-tagged $RRP41^{WT}$, $RRP41^{Pi-}$ or $RRP41^{Pi-Cat-}$ respectively, Pi: phosphate.

decreased compared to the activity observed in presence of phosphate. This shows that the activity is stimulated by inorganic phosphate, as expected for a phosphorolytic reaction. The remaining activity in absence of added Pi can be explained by residual inorganic phosphate present in the buffers used during the EXO9s purification or during the activity assay.

B. RNA degradation by EXO9 releases nucleoside diphosphates (NDPs)

In order to determine the reaction product released by the degradation by EXO9 I incubated exosome complexes containing either active ($RRP41^{WT}$) or inactive ($RRP41^{Pi-}$ and $RRP41^{Pi-Cat-}$) versions of RRP41, alongside with mock-IP and a IP elution buffer samples, with 3'[^{32}P]-labeled $oligo(U)_{22-23}$ RNA as a substrate in the presence of inorganic phosphate (Pi). To prepare the substrate used in this assay, $oligo(U)_{21}$ RNA was 3' labeled with α[^{32}P]-UTP using Cid1 poly(U) polymerase. The time course was performed as previously described. The products of the reaction were separated by thin layer chromatography using polyethylenimine-cellulose plates and analyzed by autoradiography. α[^{32}P]-UTP, α[^{32}P]-UDP and α[^{32}P]-UMP were loaded as references on the left side of the plate (Figure 19). UDP and UMP would be released as products of phosphorolytic and hydrolytic activity, respectively. When the PEI-TLC is developed with 0.5 M lithium chloride 1M formic acid, UTP stays at the loading origin while UDP and UMP migrate to the middle and the top of the TLC plate respectively. No release of nucleotides was observed in control reactions. In the presence of EXO9 containing wild-type RRP41, the reaction released nucleoside diphosphates (NDPs) as products of degradation, the typical product of phosphorolytic exoribonucleases. These results are key to the demonstration that RRP41's activity is phosphorolytic.

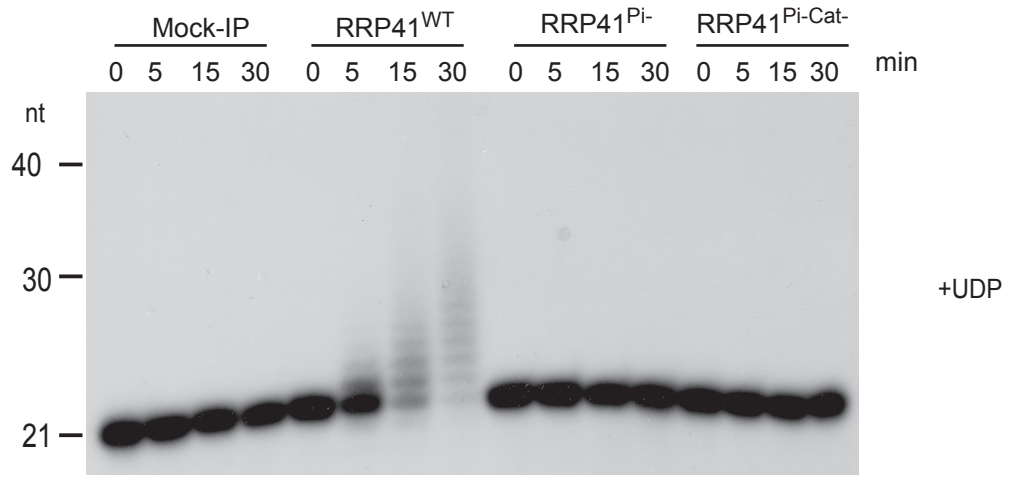

Figure 20. Plant EXO9 can synthesize RNA tails. EXO9 purified from Col-0, RRP41^{WT}and RRP41^{Pi-} plants and IP wash buffer were incubated with 5'- labeled oligo$(U)_{21}$ in the presence of 1 mM UDP. Samples were collected at the indicated time points, reactions were stopped by adding 1 volume of RNA loading buffer and analysed by denaturing 17% PAGE and autoradiography.Each reaction contained 1.4 nM of Exo9 and 25 nM of RNA substrate. Mock-IP: IP on Col-0 plants, RRP41^{WT}, RRP41^{Pi-} and RRP41$^{Pi-Cat-}$: *rrp41* mutants complemented with myc-tagged RRP41^{WT}, RRP41^{Pi-} or RRP41$^{Pi-Cat-}$ respectively, UDP- uridine diphosphate.

C. Plant exosome has an intrinsic capacity to synthesize RNA tails

Finally, to test if plant EXO9 has polymerizing activity I performed an *in vitro* synthesis assay with exosome complexes containing either active ($RRP41^{WT}$) or inactive ($RRP41^{Pi-}$ and $RRP41^{Pi-Cat-}$) versions of AtRRP41, this time in the presence of 1 mM UDP but in absence of inorganic phosphate. As seen in Figure 20, no addition of uridines was observed in buffer, in mock-IP, or when substrates were incubated with EXO9 containing mutated AtRRP41 ($RRP41^{Pi-}$ and $RRP41^{Pi-Cat-}$). In the presence of EXO9 containing wild-type version of RRP41 ($RRP41^{WT}$) I observed the synthesis of oligo(U) tails. This result demonstrates that the reaction is reversible, showing that plant EXO9 has another characteristic feature of a phosphorolytic enzyme.

Taken together my results show that the activity of *Arabidopsis* EXO9 is indeed stimulated by inorganic phosphate, releases nucleotide diphosphates and is reversible, hence shows all three characteristic features of phosphorolytic activities. Therefore, EXO9 is a phosphorolytic enzyme.

III. Plant EXO9's substrate specificity

A. Plant exosome can synthesize RNA tails using any of four nucleoside diphosphates

To further investigate the specificity of EXO9's synthesizing activity, I incubated EXO9 containing the wild-type version of RRP41 ($RRP41^{WT}$) with 5'[^{32}P]-labeled oligo$(U)_{21}$ RNA substrate and 1 mM of each ADP, CDP, GDP or UDP, respectively (Figure 21). Samples collected after 0, 5, 15 or 30 minutes were analyzed by denaturing PAGE and autoradiography.

I observed synthesis of tails in each of the assays (Figure 21), showing that plant EXO9 can add A-, C-, G- or U-tails to RNA substrates. In all cases, except in the

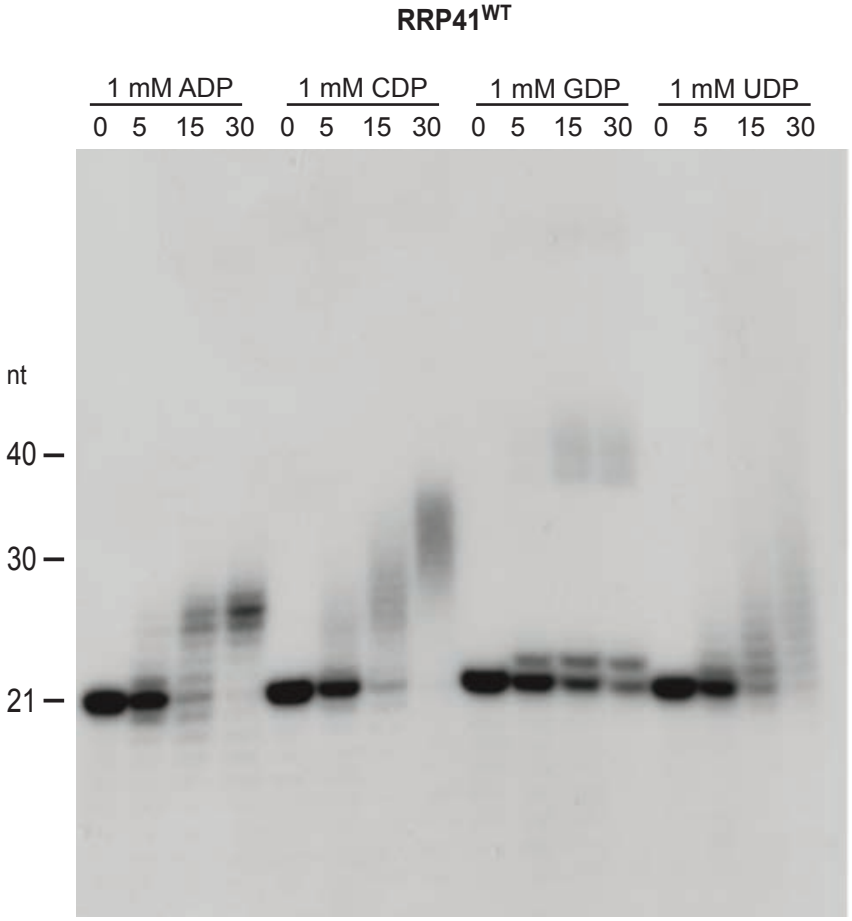

Figure 21. Different patterns of RNA tails synthesised by plant EXO9 depending of the nature of NDPs. EXO9 purified from RRP41^{WT} plants were incubated with 5'- labeled oligo$(U)_{21}$ in the presence of 1 mM ADP, CDP, GDP or UDP. Samples were collected at the indicated time points, reactions were stopped by adding 1 volume of RNA loading buffer and analysed by denaturing 17% PAGE and autoradiography. Each reaction contained 1.4 nM of Exo9 and 25 nM of RNA substrate. RRP41^{WT}: *rrp41* mutants complemented with myc-tagged RRP41^{WT}, ADP- adenosine diphosphate, CDP-cytidine diphosphate, GDP- guanosine diphosphate, UDP- uridine diphosphate.

presence of GDP, I could observe both, synthesis and to some extent degradation. Interestingly, the length of the synthesized tails differed. This differences may reflect intrinsic affinity properties of EXO9 in respect of each nucleoside diphosphate. In the presence of GDP, I observed a distinct reaction product of 22 nt. This showed that the RNA substrates was extended by a single nucleotide. In addition, signals of 40 nt and longer products were detected, but no synthesis intermediates between them. This suggested that the first nucleotide was added in a distributive reaction, whereas 40 nt and longer products of synthesis were created in a processive reaction. To formally show that A-, C- and G- tails are indeed synthesized by EXO9 these *in vitro* synthesis assays should also be performed with catalytic inactive EXO9. However, no synthesis was detected in the presence of EXO9 with abolished activity (Figure 20), strongly suggesting that EXO9 and not a contaminating polymerase is responsible for the synthesis of these tails.

The fact that EXO9 has a polymerizing activity *in vitro* opens the possibility that EXO9 can also synthesize tails *in vivo*. Indeed, both bacterial PNPase and archaeal exosome have been shown to add heteropolymeric poly(A)-rich tails to 3' end of RNAs (Mohanty and Kushner, 2000; Portnoy et al., 2005). Such Poly(A)-rich tails are added to truncated coding and to non-coding RNA molecules in bacteria, the majority of archaea and chloroplasts. These tails serve as landing pads for several exoribonucleases and therefore stimulate RNA degradation (Lange et al., 2009; Norbury, 2013; Slomovic et al., 2008). Therefore, it is interesting to investigate whether plant EXO9 does synthesize specific tails *in vivo*. In a recent study, Li and colleagues detected viral RNAs with non-templated heteropolymeric and poly(A)-rich tails in infected *Arabidopsis* plants (Li et al., 2014). Interestingly, these poly(A)-rich tails resemble the tails added by bacterial and chloroplastic PNPases or the archaeal exosome (Slomovic et al., 2008), suggesting that they may have been also synthesized by a phosphorolytic activity. However, in my preliminary results I did

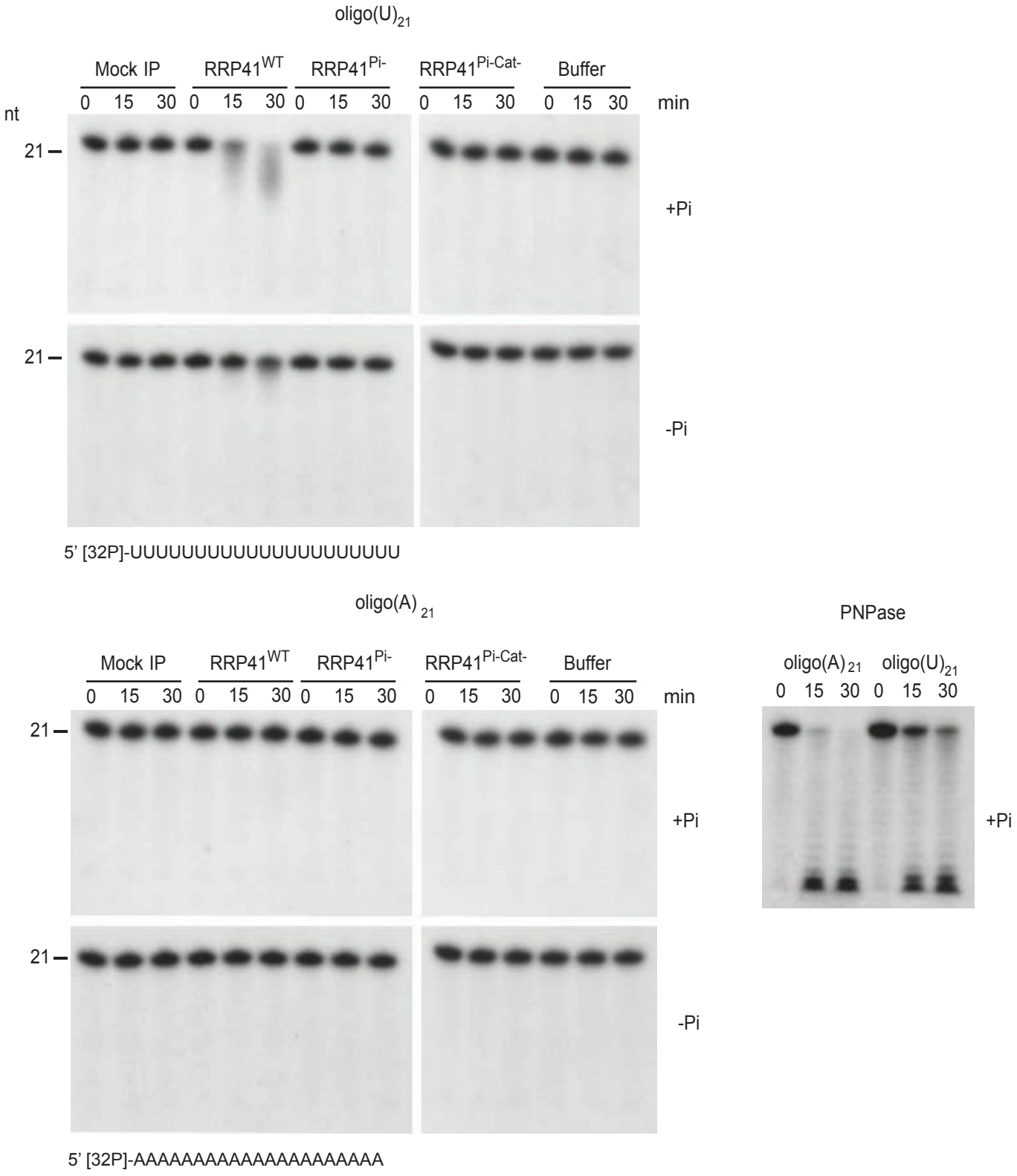

Figure 22. Plant EXO9 trims oligo(U)$_{21}$ and does not degrade oligo(A)$_{21}$ substrate. Exosome complexes purified from Col-0 (mock-IP), RRP41^{WT}, RRP41^{Pi-} and RRP41$^{Pi-Cat-}$ plants and IP wash buffer were incubated with 5'- labeled oligo(U)$_{21}$ or 5'- labeled oligo(A)$_{21}$ RNA substrate in the presence or absence of inorganic phosphate (Pi). PNPase was used as a control. Samples were collected at the indicated time points, reactions were stopped by adding 1 volume of RNA loading buffer and analysed by denaturing 17% PAGE and autoradiography. Each 20 µl reaction contained 0.4 nM of Exo9 and 25 nM ofRNA substrate. Mock-IP: IP on Col-0 plants, RRP41^{WT}, RRP41^{Pi-} and RRP41$^{Pi-Cat-}$: *rrp41* mutants complemented with myc-tagged RRP41^{WT}, RRP41^{Pi-} or RRP41$^{Pi-Cat-}$ respectively, Pi: phosphate.

not detect heteropolymeric tails (more details in discussion, D. Does plant EXO9 synthesize tails *in vivo*?)

B. Plant EXO9 preferentially degrades oligouridylated substrates

To test the specificity of plant EXO9's degradation *in vitro*, I performed degradation assays with substrates that differed in composition (homo- or heteropolymeric sequences) or length (21 or 31 nucleotides). Homopolymeric substrates like oligo(A) or oligo(U) RNAs are routinely used in *in vitro* assays to determine properties of ribonucleases. Based on data available for archaeal and yeast exosomes (Audin et al., 2016; Makino et al., 2015; Lorentzen et al., 2005), both 21-nt and 31-nt RNA substrates are long enough to reach the AtRRP41 active site.
To test whether EXO9 can degrades s differentially oligo$(U)_{21}$ and oligo$(A)_{21}$ RNA substrates I incubated EXO9 complexes containing active and inactive versions of AtRRP41 or mock-IP with 5'[^{32}P]-labeled homopolymeric oligo$(U)_{21}$ or oligo$(A)_{21}$ RNA substrates. Unexpectedly, EXO9 degraded the 5'[^{32}P]-labeled oligo$(U)_{21}$, but not the 5'[^{32}P]-labeled oligo$(A)_{21}$ substrate, indicating that EXO9 has a stronger preference for oligo(U) RNA *in vitro* (Figure 22). This preference of oligo(U) over oligo(A) *in vitro* was surprising since substrates of the plant exosome are often polyadenylated *in vivo* (Chekanova et al., 2007; Lange et al., 2014, 2011, 2008). For comparison, I performed a control reaction with bacterial PNPase. As shown in Figure 22, PNPase degraded both oligo(U) and oligo(A) substrates in a similar manner. In both cases, short oligonucleotides, appeared after 15 minutes.

To further investigate whether EXO9 has an intrinsic preference for uridylated sequences, I tested the degradation of three different substrates. Each substrate had a similar core sequence, however, the first substrates terminated with two uridines (5'FAM-CCCCACCACCAUCACUUCACCACCAUCACUU, 5'-FAM-$(H)_{29}(U)_2$), the second terminated with 14 adenosines (5'FAM-

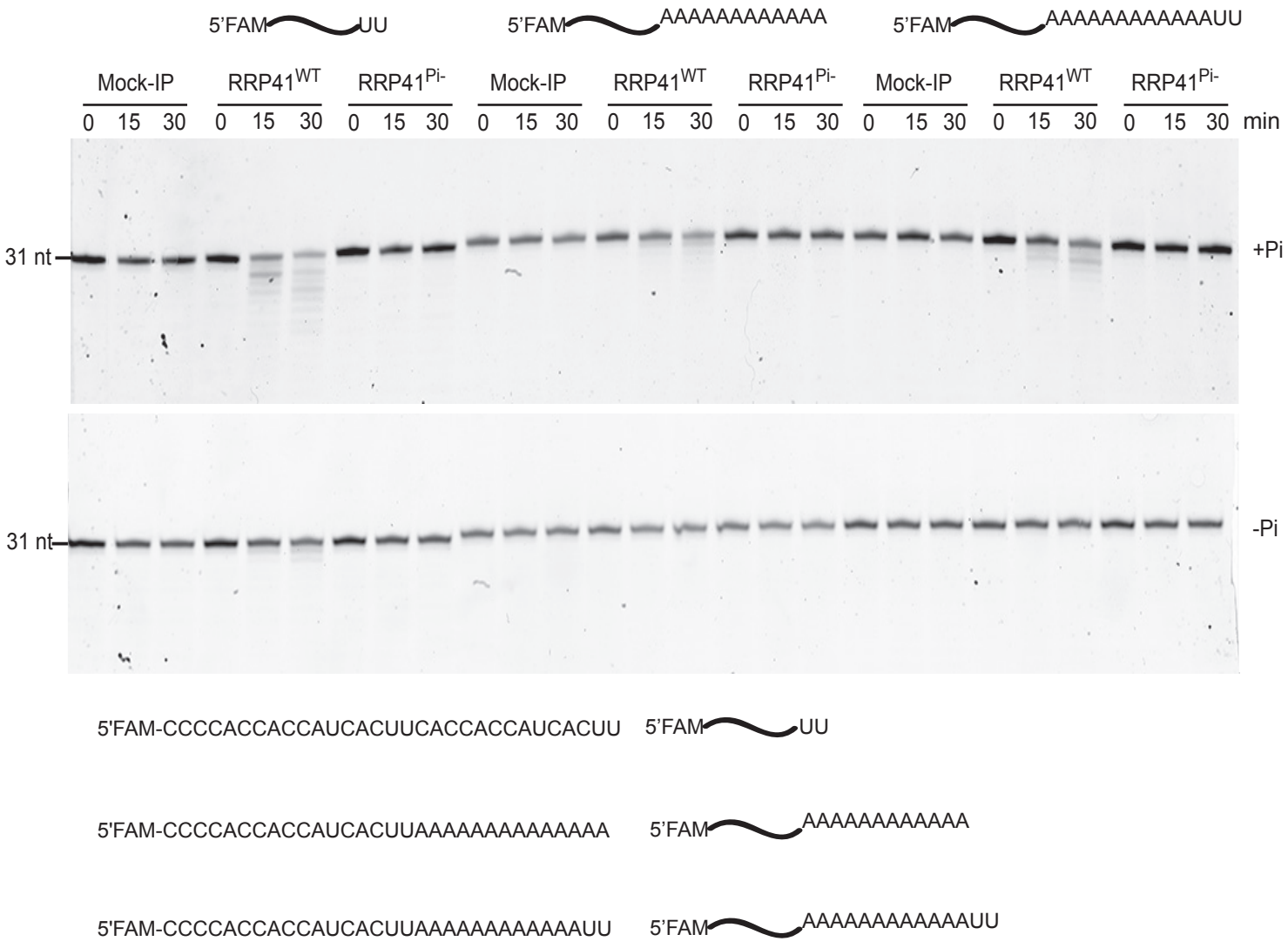

Figure 23. Plant EXO9 preferentially degrades uridylated substrates *in vitro*. EXO9 purified from Col-0 (mock-IP), RRP41^{WT}and RRP41^{Pi-} plants was incubated with three different 31nt 5'FAM-labeled heteropolymeric RNA substrates. The sequences of the substrates are indicated on the bottom part of the figure. Samples were collected at the indicated time points (minutes), stopped by adding 1 volume of RNA loading buffer and analysed by denaturing 17% PAGE and autoradiography. Each reaction contained 1.4 nM of exosome complexes and 35 nM of RNA substrate. Mock-IP: IP on Col-0 plants, RRP41^{WT}, RRP41^{Pi-}: *rrp41* mutants complemented with myc-tagged RRP41^{WT} or RRP41^{Pi-} respectively, Pi: phosphate.

CCCCACCACCAUCACUUAAAAAAAAAAAA-AA, 5‘-FAM-$(H)_{17}(A)_{14}$), and the third substrate terminated with 12 adenosines and two uridines (5'FAM-CCCCACCACCAUCACUUAAAAAAAAAAAAAAUU, 5‘-FAM-$(H)_{17}(A)_{12}(U)_2$). All three substrates were 5’FAM-labelled 31-nt heteropolymers. Each of the substrates was incubated with EXO9 complexes purified from $RRP41^{WT}$ and $RRP41^{Pi-}$ plants in the presence or absence of inorganic phosphate (Pi). As observed previously no degradation was observed in control reactions and degradation of the substrates occurred only with EXO9 containing wild-type RRP41, and was stimulated by the presence of inorganic phosphate (Pi) (Figure 23). Interestingly, this preliminary experiment showed that the three RNA substrates were not degraded to the same extent. Both substrates containing two uridines at the 3’ end, namely 5‘-FAM-$(H)_{29}(U)_2$ and 5‘-FAM-$(H)_{17}(A)_{12}(U)_2$were trimmed to larger extent as compared with the 5‘-FAM-$(H)_{17}(A)_{14}$ substrate. (Figure 23). However, the experiment was done only once and must be regarded as preliminary. To further support the hypothesis that plant EXO9 has an intrinsic preference for uridylated substrates, more experiments with additional substrates should be performed. However, this experiment also demonstrates that plant EXO9 can degrade a substrate containing a homopolymeric tail of 14As. The fact that plant EXO9 can degrade adenylated substrates *in vitro* is in line with *in vivo* data (Chekanova et al., 2007; Schneider et al., 2012; West et al., 2006). Hence, the intriguing observation is that plant EXO9 did not degrade the 21-nt oligo(A) RNA. One possible explanation may be that the efficient recognition or degradation of short oligo(A) RNA substrates requires additional factors, such as RNA helicases or RNA binding proteins that may be absent from immunopurified EXO9 complexes. For example, tight binding of the RNA substrate to the exosome cap may impair its degradation *in vitro*, while RNA helicases may release such substrates from the cap and allow feeding in the central channel *in vivo*. Alternatively, a 21-nt substrate bound to the poly(A) binding sites of

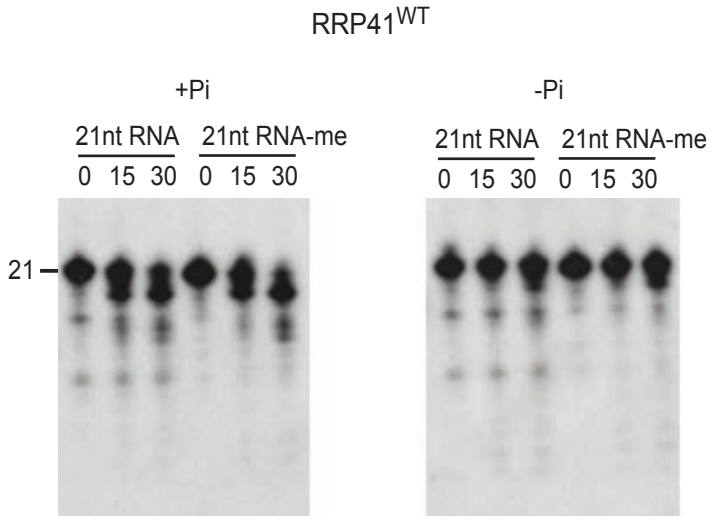

Figure 24. Plant EXO9 is trimming 21 nt heteropolymeric substrate (both non-methylated and methylated at 3' ribose). Exosome complexes containing active RRP41 were incubated with 5'- labeled heteropolymeric oligo RNA (miR168) with or without methyl group at the 3' ribose in the presence or absence of inorganic phosphate (Pi). Samples collected at indicated time points were analysed by 17% denaturing PAGE and autoradiography. Each 20 µl reaction contained 1.4 nM of Exo9 and 25 nM of RNA substrate.RRP41^{WT}: *rrp41* mutants complemented with myc-tagged RRP41^{WT}, Pi: phosphate.

the cap may be simply too short to reach some RNA-binding sites in EXO9, while 31-nt adenylated substrate is long enough to be efficiently bound.

As described above, I observed that plant EXO9 can nibble oligo$(U)_{21}$ but not oligo$(A)_{21}$ suggesting that the nucleotide composition of short RNA substrates can influence EXO9's activity. This raised the question whether EXO9 can also degrade a heteropolymeric substrate of 21 nt. For this purpose, I incubated EXO9 complexes containing active AtRRP41 with 5'[^{32}P]-labeled 21-nt miRNA168. Samples were collected at indicated time points and analyzed by PAGE and autoradiography. As seen in Figure 24, EXO9 removed several nucleotides from miRNA168. This result shows that EXO9 can bind and trim a 21-nt heteropolymeric miRNA substrate. In plants, miRNAs are 3' methylated by the methyltransferase HEN1. In absence of HEN1, unmethylated miRNAs become 3' uridylated by the uridyltransferase AtHESO1, and are degraded by yet unknown exoribonucleases (Chen et al., 2002; Zhao et al., 2012). As my result show that EXO9 can degrade an unmethylated miRNA, I next tested whether 2´-0-methylation of the 3´ribose will protect a miRNA substrate against degradation by EXO9 in vitro. As seen in Figure 24 (RNA-me) the methylated miRNA substrate was trimmed to the same extent as the non methylated substrate. This result showed that 2' O-methylation does not protect a 21-nt oligo RNA from degradation by EXO9 *in vitro*.

IV. Plant EXO9 has a distributive activity

Bacterial phosphorylases like RNase PH and PNPase and the archaeal exosome are processive ribonucleases, i.e. they degrade their RNA substrates completely without releasing degradation intermediates. With processive enzymes, both full-length substrates and the end-products of the degradation reaction are observed at the same time. By contrast, distributive enzymes release their substrates after the removal of one or few nucleotides, and then rebind to perform the next

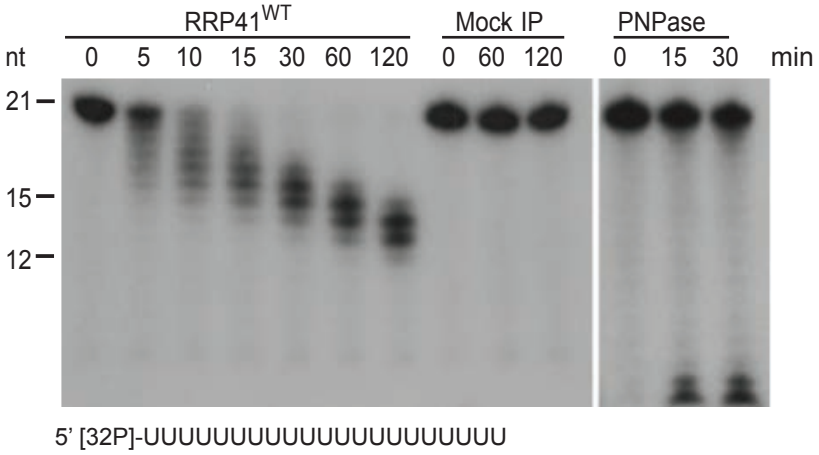

Figure 25. Activity of plant EXO9 unlike bacterial PNPase is distributive. Exosome complexes purified from Col-0 (mock-IP) or RRP41^{WT} plants were incubated with 5'- labeled oligo(U)$_{21}$ RNA substrate in the presence of inorganic phosphate (Pi). PNPase was used as a control. Samples were collected at the indicated time points, reactions were stopped by adding 1 volume of RNA loading buffer and analysed by denaturing 17% PAGE and autoradiography. Each reaction contained 1.4 nM of Exo9 and 25 nM of RNA substrate. Mock-IP: IP on Col-0 plants, RRP41^{WT}: *rrp41* mutants complemented with myc-tagged RRP41^{WT}, Pi: phosphate.

catalytic step. Therefore, the pool of substrates is degraded step by step, and degradation intermediates can be observed.

Interestingly, the degradation of 5' labelled RNA substrates by EXO9 produced distinct degradation intermediates (Figure 14), suggesting a rather distributive mode of action. To further investigate this possibility, I performed a degradation experiment during a longer time course, and compared EXO9s activity to the activity of bacterial PNPase as a reference for a processive phosphorylase. A time course with PNPase was performed separately. Briefly, EXO9 or a sample from mock-IP were incubated with 5'[^{32}P]-labeled oligo(U)$_{21}$ RNA substrate in the presence of inorganic phosphate (Pi). Samples were collected at 0, 5, 10, 15, 30, 60 and 120 minutes and analyzed by denaturing PAGE and autoradiography. Upon incubation of RNA substrates with PNPase for 15 and 30 min, I observed both non-degraded substrates and the short oligonucleotides that are the end-product of the reaction. These results are in line with published data (Del Favero et al., 2008) and are typically observed with processive enzymes, because the substrate molecule is bound and not released until the degradation is accomplished. By contrast, intermediate products of the degradation process were observed when the substrate was incubated with EXO9. This suggests that EXO9 releases degradation intermediates after removal of each single nucleotide. This experiment strongly indicates that the phosphorolytic activity of plant EXO9 is indeed distributive.

To sum up, I showed here that *Arabidopsis* EXO9 has an exoribonucleolytic activity that is abolished by mutations in the phosphate coordination site of AtRRP41. EXO9 activity is stimulated by inorganic phosphate, releases nucleoside diphosphates and is reversible. Taken together, these data demonstrate that EXO9 has a phosphorolytic activity conferred by the AtRRP41 subunit.

Moreover, EXO9 is rather trimming than completely degrading its substrates in vitro. While bacterial PNPase and exosome complexes from archaea to eukaryotes are known to degrade polyadenylated RNAs *in vivo*, plant EXO9 did not degrade homopolymeric oligo$(A)_{21}$ substrates in my *in vitro* experiments, and trimmed adenylated substrates less efficient than uridylated ones.

Another interesting feature of plant EXO9 is that, unlike bacterial PNPase, EXO9 has a distributive activity. Together with the fact that EXO9 removed only several nucleotides from all substrates that I tested *in vitro*, this raises the interesting possibility that EXO9 could be involved in trimming RNA substrates *in vivo*. However, the presence of EXO9's co-factors may also modulate the intrinsic properties of EXO9 *in vivo*.

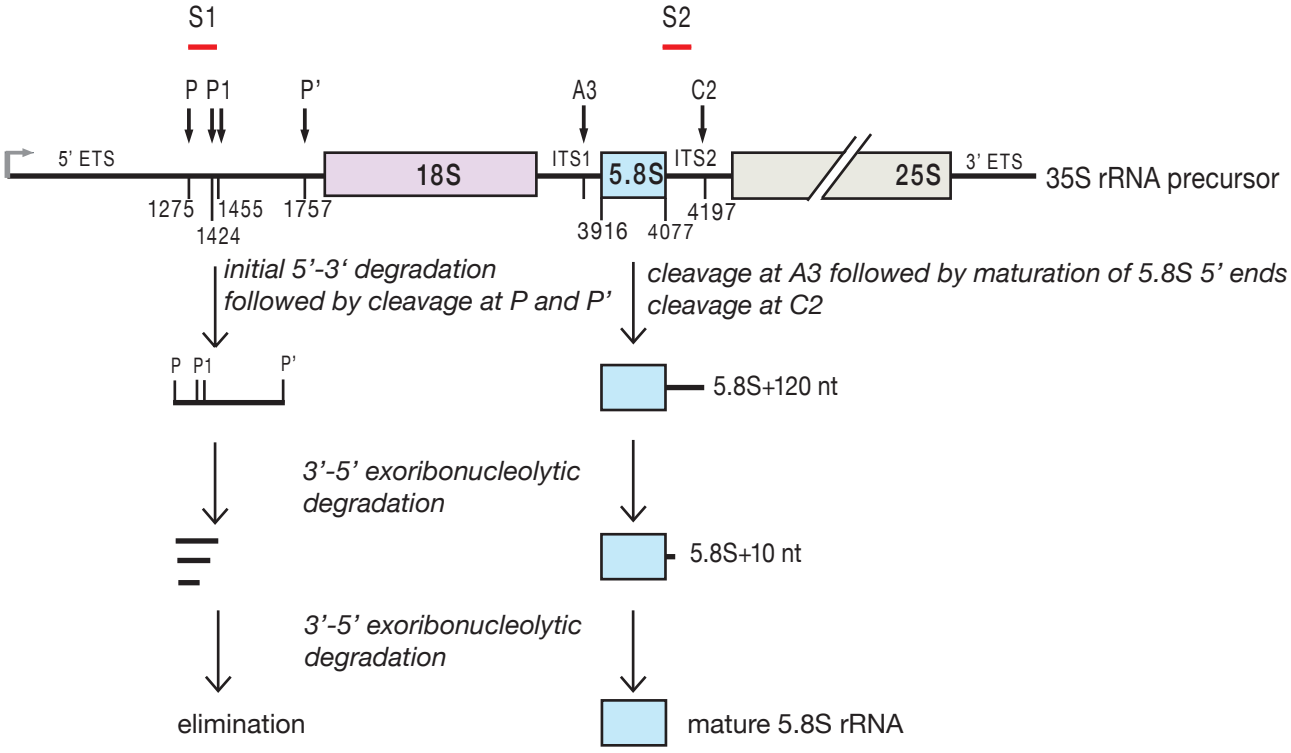

Figure 26. Diagram illustrating the rRNA maturation by-products generated from the 5′ ETS (P-P′ and P-P1) and the 5.8S rRNA processing intermediates. Description in the main text. Red bars show location of S1 and S2 probes used for detection P-P' maturation by-product and 5.8S rRNA precursors respectively.

Chapter 3. Arabidopsis EXO9s activity participates in the elimination of rRNA maturation by-products (5'ETS) and in the processing of rRNA precursors (pre-5.8S)

My *in vitro* activity assays revealed that plant EXO9 has a distributive phosphorolytic activity. Furthermore, EXO9 was rather trimming than completely degrading its RNA substrates *in vitro*. However, due to presence of cofactors *in vivo*, EXO9 may both trim and completely degrade its endogenous RNA substrates. In all organisms studied so far, both the 5' ETS and 5.8S rRNA precursors are archetypical substrates of 3' -5' exoribonucleolytic activity of the exosome. To decipher whether the activity of plant EXO9 degrades or trims endogenous RNAs, I therefore analyzed the processing of 5'ETS and 5.8S rRNA in plants expressing either wild-type or mutated versions of RRP41.

In *Arabidopsis*, the 5'ETS is eliminated in a stepwise manner involving both 5'-3' and 3'-5' degradation pathways. First the 5' extremity of the polycistronic 35S rRNA precursor is shortened by the 5'- 3' exoribonuclease XRN2 to expose the P site for the endonucleolytic cleavage carried out by the U3 snoRNP (Sáez-Vasquez et al., 2004; Zakrzewska-Placzek et al., 2010). Cleavage at P site generates a 33S precursor. Next, cleavage at the P' site releases a 482 nt P-P' fragment from the 5'ETS (Figure 26). The further degradation of the P-P' intermediate involves the exosome core complex, the RNA helicase AtMTR4, the exoribonucleases AtRRP44 and AtRRP6L2, and the terminal nucleotidyltransferase AtTRL (Chekanova et al., 2007, Lange et al., 2008; Kumakura et al., 2013; Lange et al., 2011, Sikorski et al., 2015). Exoribonucleolytic degradation by the exosome and its cofactors generates several smaller intermediates of about 200-150 nt in size, named P-P1 fragments (Figure 26). Initially, P-P1 intermediates were thought to be a product of another endonucleolytic cleavage event (Zakrzewska-Placzek et al., 2010). However, putative cleavage products such as P1-P' were not detected to date and in fact, P-P1

intermediates are likely generated by 3' exoribonucleolytic degradation of P-P' fragments. Since the 5' part of the P-P1 fragment contains a stem-loop structure of approximately 120 nt (Sáez-Vasquez et al., 2004) that could be a potential obstacle for exoribonucleases, P-P1 fragments are quite abundant and easily detected in wild-type plants (Lange et al., 2011; Kumakura et al., 2013;Sikorski et al., 2015; Zakrzewska-Placzek et al., 2010).

A second potential target of EXO9's activity is 5.8S rRNA precursors (Figure 26). The 3' maturation of 5.8S rRNA starts with a cleavage within the ITS2 at the C2 site, which produces a 284 nt 5.8S precursor harboring a 3' extension of 120 nt. Cleavage at C2 is followed by exoribonucleolytic degradation involving AtMTR4, AtRRP44 and AtRRP6L2 (Kumakura et al. 2013; Lange et al. 2011; Lange et al. 2008). This generates two main populations of 5.8S precursors with heterogeneous 3' extensions of approximately 70 and 10 nt and sizes of 230 and 170 nt, respectively (Lange et al., 2011; Sikorski et al., 2015). The largest (+120) and smallest (+10) precursors are readily detected in wild type plants. All three populations of precursors accumulate in the *mtr4* and to lower extent in *rrp6L2* mutants, showing that both MTR4 and RRP6L2 contribute to 5.8S processing (Lange et al., 2011; Sikorski et al., 2015). *RRP44KD* mutants also show a mild accumulation of 5.8S precursors (Kumakura et al., 2013). However, none of the individual mutants show diminished steady-state levels of mature 5.8 rRNA, indicating a high level of redundancy between these different activities.

I. Arabidopsis mutant lines to study impact of the activity of RRP41 on ribosomal RNA processing

To test if EXO9's activity contributes to rRNA processing I examined the degradation of the 5'ETS and the processing of 5.8S precursors rRNA in *rrp41* mutants complemented with either wild-type version of AtRRP41 ($RRP41^{WT}$) or

catalytically inactive (RRP41^{Pi-} or RRP41$^{Pi-Cat-}$). In addition, I used a number of established plant lines for the generation of double mutants or as controls.

The impact of the exosome in its role as a protein complex can be estimated in *rrp41*^{iRNAi} plants, where an estradiol-inducible RNAi construct triggers the down-regulation of the *RRP41* mRNA (Chekanova et al., 2007). As probably all EXO9s subunits except AtCSL4 are required for the integrity of EXO9, the down-regulation of *RRP41* results in the down-regulation of the entire exosome complex. Growing of *rrp41*^{iRNAi} plants in the presence of estradiol leads to silencing of the *RRP41* mRNA, which results in growth arrest and subsequent death of seedlings. Down-regulation of the exosome via *RRP41* silencing leads to accumulation of P-P' and P-P1 maturation by-products generated from 5'ETS and 3'-extended 5.8S rRNA species (7S rRNA) (Chekanova et al., 2007).

MTR4 encodes a conserved RNA helicase, that is reported to be a crucial exosome cofactor involved in the processing and degradation of P-P' and the processing or degradation of both 18S and 5.8S rRNA precursors (Lange et al., 2011; Sikorski et al., 2015). In this study, I used the *mtr4-1* T-DNA insertion line (GK_048G02) (Lange et al., 2011). *mtr4* plants exhibit a phenotype typical for ribosomal protein mutants and for plants lacking factors involved in rRNA processing (Byrne, 2009), such as triple or fused cotyledons and pointed first leaves. On the molecular level, loss of MTR4 results in the accumulation of the P–P' fragment and of 5.8S rRNA precursors (Lange et al., 2011; Sikorski et al., 2015).

RRP44 is an essential gene that encodes the conserved exosome-associated exoribonuclease RRP44 present in the nucleus and cytoplasm (Zhang et al., 2010). As in other eukaryotes, *Arabidopsis* RRP44 is required for rRNA processing (Kumakura et al., 2013; Sikorski et al., 2015). In this study, I used *RRP44KD* knock down lines in which the down-regulation of *RRP44* is achieved by the expression of artificial miRNAs under the control of a mesophyll-specific promoter (Kumakura et al., 2015). Therefore, knock-down of *RRP44* occurs only in mature leaves and does

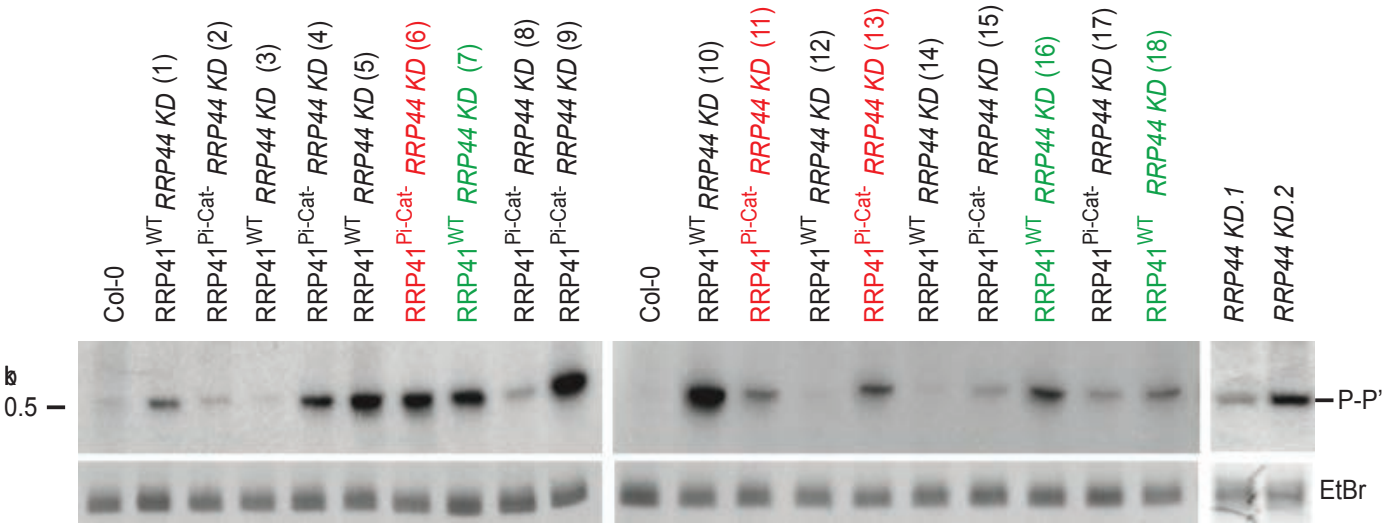

Figure 27. Assessment of *RRP44 KD* efficiency in RRP41^{WT} and RRP41$^{PI\text{-}Cat\text{-}}$ backgrounds.
Northern blot showing the accumulation of the P-P' fragment in Col-0 and primary transformants of RRP41^{WT}*RRP44KD* and RRP41$^{PI\text{-}Cat\text{-}}$*RRP44KD*. Established *RRP44KD-1* and *RRP44KD-2* lines (Kumakura et al., 2013) are shown on the right.
Total RNA extracted 35 days post-germination (dpg) from rosette leaves was separated on 6% denaturing PAGE, transferred to membranes and hybridized using probe S1 located between P and P' processing sites in the 5' ETS (see Figure 26). Ethidium bromide (EtBr) staining of the 5S rRNA was used as a loading control. The migration of the 0.5 kb RNA marker (kb) is indicated on the left.

not affect overall growth or fertility. *RRP44KD* plants show a mild phenotype manifested in slightly curly leaves. On the molecular level, down-regulation of *RRP44* leads to the accumulation of P-P' and several pre-5.8S rRNAs (Kumakura et al., 2013; Sikorski et al., 2015).

RRP6-like2 (RRP6L2) encodes one of the three RRP6-like proteins expressed in *Arabidopsis*. It resides mainly in the nucleolus. *rrp6L2* is a T-DNA insertion mutant line (*rrp6l2-1*, Gabi_825G09) showing mild accumulation of polyadenylated P-P' fragments and mild accumulation of 5.8S rRNA precursors (Lange et al., 2011, 2008).

Importantly, single mutants lacking *MTR4* and *RRP6L2* or plants with down-regulated *RRP44* expression show wild-type levels of mature 5.8S rRNA, probably because they have partially redundant functions. Possibly, both exoribonucleases could also act partially redundantly with the activity of the core exosome, which could mask the effects of the compromised activity in RRP41$^{Pi\text{-}Cat\text{-}}$ lines. Therefore, I generated *rrp41* plants complemented with RRP41^{WT} or RRP41$^{Pi\text{-}Cat\text{-}}$ in *mtr4*, *rrp6L2* and *RRP44 KD* mutant backgrounds, either by crosses or by introducing the artificial microRNA targeting the *RRP44* mRNA (Kumakura et al., 2013) into *rrp41* RRP41^{WT} and RRP41$^{Pi\text{-}Cat\text{-}}$ plants.

To assess the silencing of *RRP44* mRNA in individual transformants I analyzed the levels of P-P', a key substrate of AtRRP44 by northern blots. The hybridization probe was complementary to positions 1275-1297 of the 35S precursor located in the 5' region of the P-P' fragment (Figure 26, probe S1). As expected, the level of P-P' accumulation varied between transformants (Figure 27) indicating that the efficiency of silencing was different in individual plants. However, accumulation of P-P' was detected in 11 of the 18 lines tested, indicating that these 11 lines were indeed plants with a sufficient down-regulation of RRP44. For further analysis, I selected transformants showing comparable levels of P-P' accumulation, namely the transformants 7, 16 and 18 for RRP41^{WT} *RRP44KD*, and

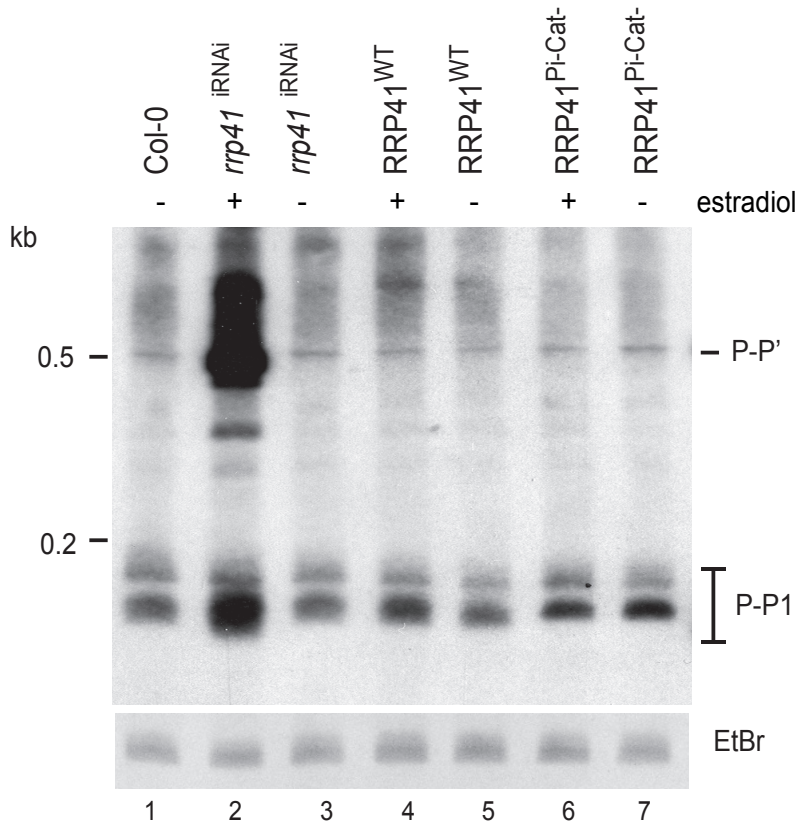

Figure 28. Down-regulation of *RRP41* led to a pronounced accumulation of P-P', P-P1 and additional intermediates generated from the 5'ETS. Total RNAs were isolated from 11 day-old seedlings of Col-0, *rrp41*^{iRNAi}, RRP41^{WT} and RRP41$^{Pi-Cat-}$ grown in the presence (+) or absence (-) of estradiol. RNAs were separated on 6% denaturing PAGE, transferred and hybridized using probe S1. Equal loading is indicated by the image of part of the gel with 5S rRNA stained with ethidium bromide (EtBr). Sizes of the RNA markers (kb) are given of the left. Labels indicating intermediates derived from 5'ETS (P-P' and P-P1) are shown on the right.

transformants 6, 11 and 13 for RRP41$^{Pi\text{-}Cat\text{-}}$ *RRP44KD* (Figure 27, chosen transformants are indicated in color, green for RRP41^{WT} *RRP44 KD* and red for RRP41$^{Pi\text{-}Cat\text{-}}$ *RRP44KD*).

II. The activity of plant EXO9 contributes to the elimination of 5'ETS

A. EXO9 activity generates the smallest P-P1 fragment

In order to test whether the activity of plant EXO9 plays a role in the elimination of the 5'ETS I analyzed the accumulation of P-P' fragments by northern blot. Alongside the plants expressing either RRP41^{WT} (active) or RRP41$^{Pi\text{-}}$ or RRP41$^{Pi\text{-}Cat\text{-}}$ (inactive), I included Col-0 and *rrp41*^{iRNAi} lines as controls. All plants were grown either in presence or absence of estradiol. Total RNA was resolved by denaturing PAGE, transferred to nylon membranes and hybridized with probe S1. As can be seen in Figure 28, I detected a fragment of approximately 500 nt corresponding to P-P', and three fragments of around 150-200 nt corresponding to P-P1 in wild-type plants. Similar levels of both P-P' and P-P1 fragments were detected in *rrp41*^{iRNAi} samples grown in the absence of estradiol and wild-type Col-0 plants. By contrast, estradiol-induced down-regulation of *RRP41* led to a pronounced accumulation of P-P', P-P1 and additional intermediates generated from the 5'ETS, as previously reported by Chekanova and colleagues (Chekanova et al., 2007). No accumulation of P-P' nor the additional intermediates were observed in RRP41^{WT} or RRP41$^{Pi\text{-}Cat}$.

However, the patterns of P-P1 seemed to be slightly different between RRP41^{WT} and RRP41$^{Pi\text{-}Cat}$. To explore this initial finding, I analyzed RNA isolated from Col-0, RRP41^{WT}, RRP41$^{Pi\text{-}}$ and RRP41$^{Pi\text{-}Cat\text{-}}$ with a higher resolution denaturing PAGE, and performed a northern blot with the same probe as before. In Col-0 and in the presence of active exosome, three distinct intermediates of about

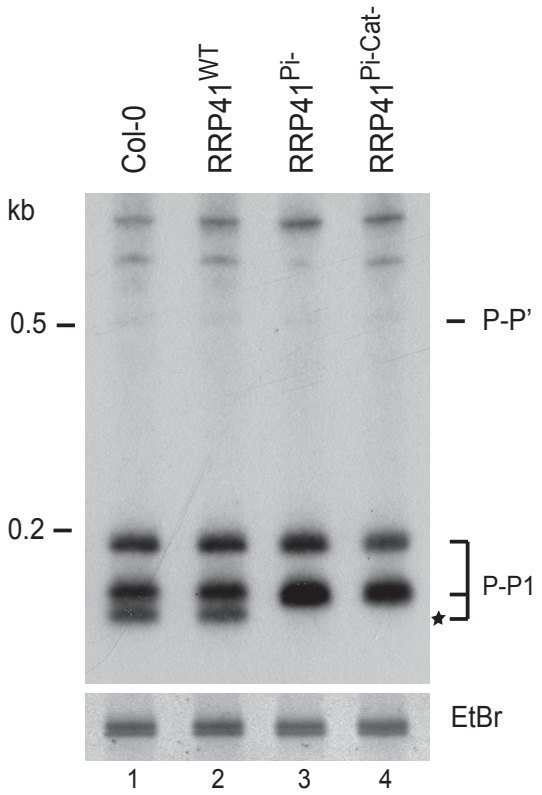

Figure 29. EXO9 activity generates the smallest P-P1 fragment. Total RNAs were isolated from inflorescences of Col-0, RRP41^{WT}, RRP41^{Pi-} and RRP41$^{Pi-Cat-}$. RNAs were separated on 6% denaturing PAGE, transferred and hybridized using probe S1. 5S rRNA stained with ethidium bromide (EtBr) is shown as loading control. Sizes of the RNA markers (kb) are given of the left. P-P' and P-P1 intermediates are indicated on the right. The intermediate generated by activity of EXO9 is marked with asterisk.

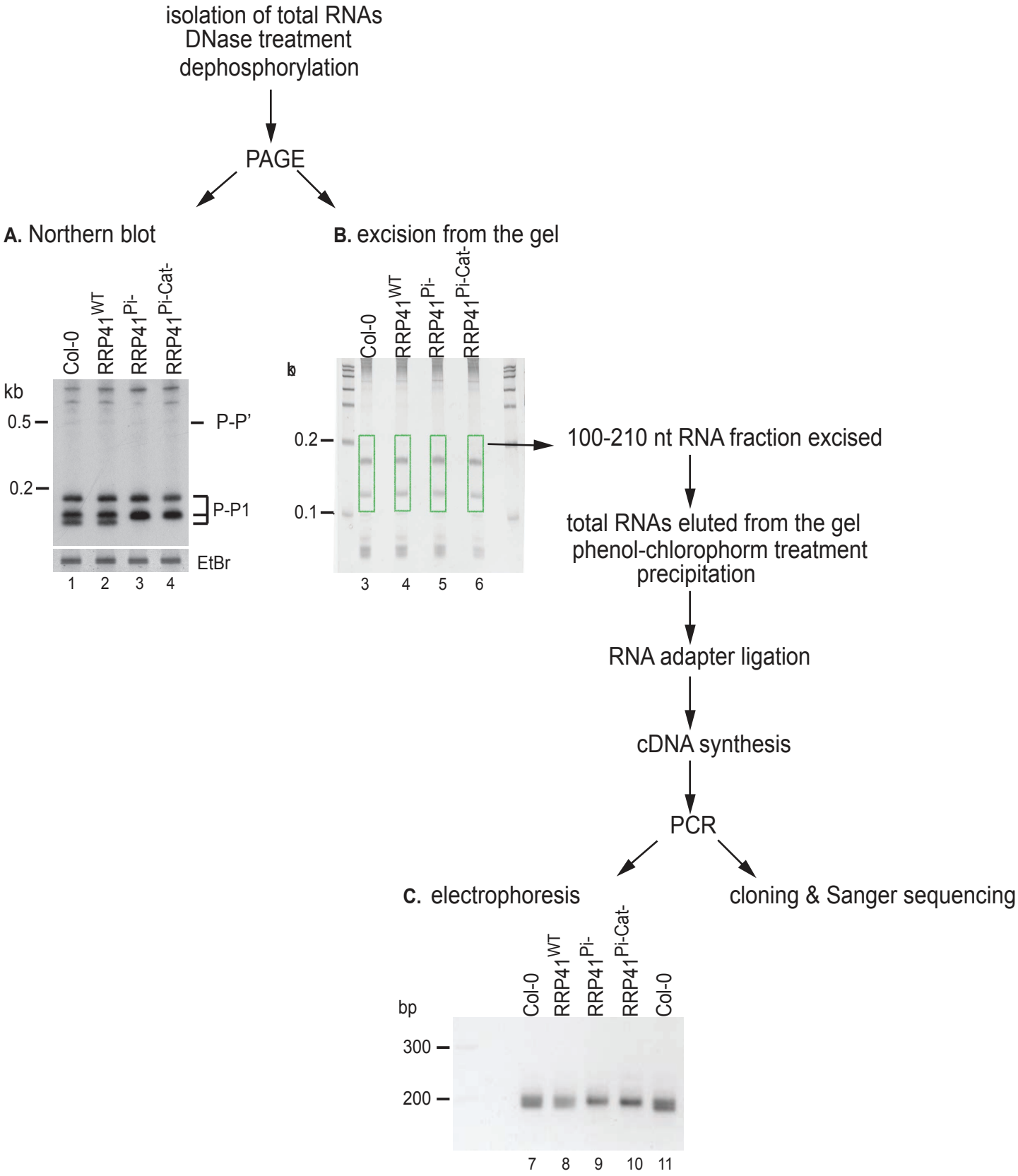

Figure 30. Diagram illustrating the experimental procedure of mapping P-P1 degradation intermediates in Col0, RRP41^{WT}, RRP41^{Pi-} and RRP41$^{Pi-Cat-}$ by 3'RACE PCR. Total RNAs were DNase treated, dephosphorylated and separated on 6% denaturing PAGE. Two gels were prepared in parallel, one for mapping and one for Northern as a control (panel A, Northern blot performed as in Figure 28). RNAs of about 100-210 nt were excised from the gel (panel B), eluted, treated with phenol-chloroform and precipitated. Next a RNA adapter was ligated to the 3'ends of obtained RNAs and the cDNA synthesis was performed by using a primer complementary to the adapter sequence. Then P-P1 fragments were amplified using primers binding to the 5' of P-P1 and to the 3' adapter sequence. An aliquot of PCR products was resolved on agarose gel (panel C) and the rest was treated with PCR clean-up kit and then cloned and sequenced (results illustrated in Figure 31).

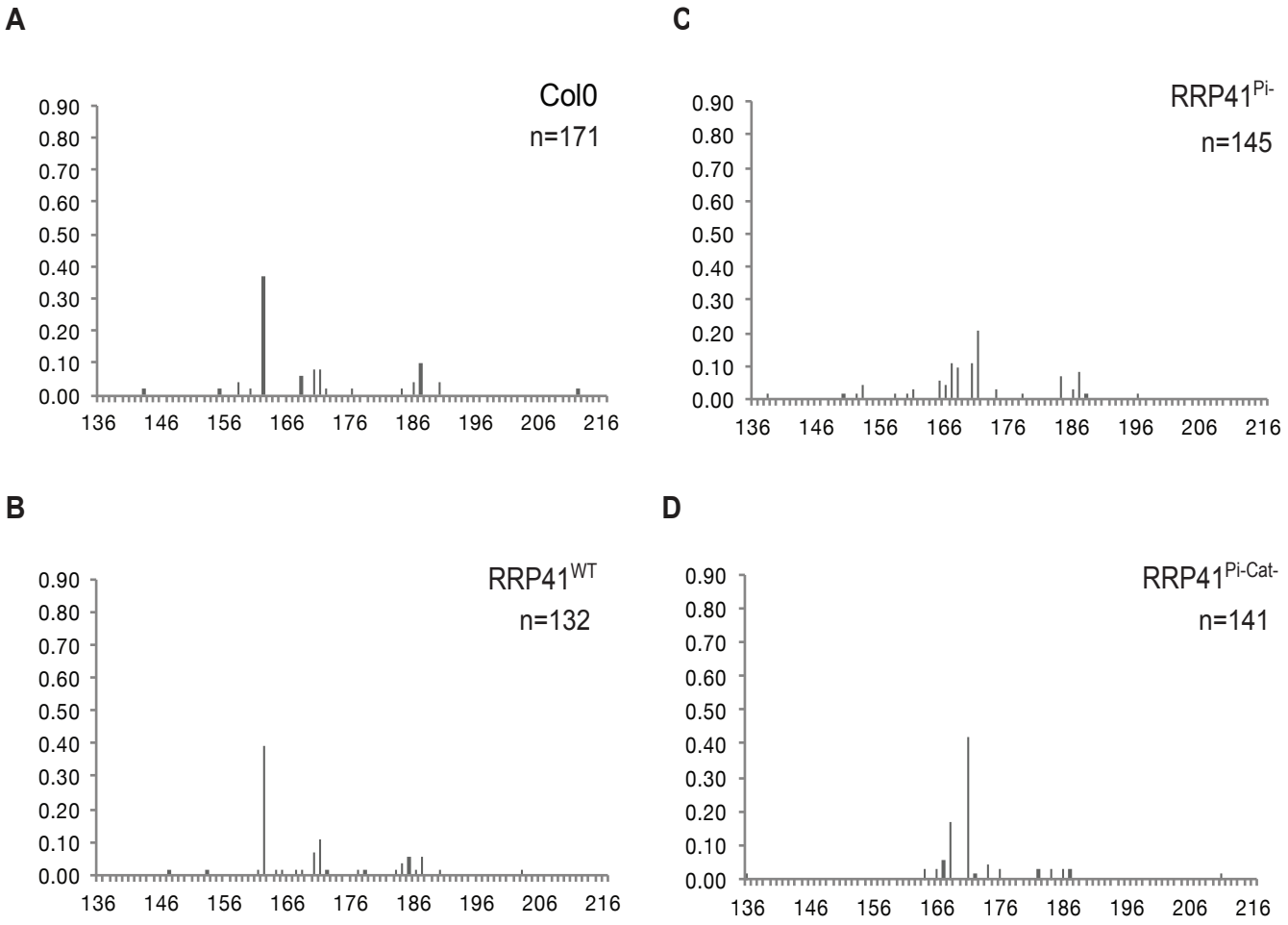

Figure 31. Graph illustrating the frequencies of P-P1 intermediates in Col0, RRP41^{WT}, RRP41^{Pi-} and RRP41$^{Pi-Cat-}$. The 3' extremities of P-P1 fragments were determined by 3' RACE PCR followed by cloning and sequencing. Bars represent P-P1 fragments with a defined length, their frequency is indicated by the bar size. The sequences obtained from two independent experiments (using seedlings or flowers as a starting material) were analysed together.

200-150 nt were detected (Figure 29). Interestingly, I detected only the two larger intermediates in catalytically inactive mutants, RRP41^{Pi-} and RRP41$^{Pi-Cat-}$ (Figure 29). This suggested that the smallest intermediate was generated by the EXO9 activity (Figure 29, the intermediate generated by EXO9 activity is marked by an asterisk).

In order to better understand the contribution of EXO9's activity to 5'ETS degradation I mapped the 3' ends of P-P1 intermediates by 3'RACE-PCR followed by cloning and sequencing. The experimental scheme is illustrated in Figure 30. Briefly, total RNA was extracted from flowers of Col-0, RRP41^{WT}, RRP41^{Pi-} and RRP41$^{Pi-Cat-}$ resolved on 6% denaturing PAGE and stained with ethidium bromide. The fractions corresponding to 100-210 nt were excised from the gel, and RNAs were eluted and precipitated. Next, an RNA adapter was ligated to the 3' extremities of the size-selected RNAs and cDNA synthesis was initiated using a primer complementary to the adapter sequence. Finally, P-P1 fragments were amplified using a forward primer in the 5' region of P-P1 and a reverse primer complementary to the 3' adapter sequence. Aliquots of the PCR products were analyzed by electrophoresis.

In Col-0 and RRP41^{WT} samples, I observed two main bands of around 200 and 180 bp (Figure 30, panel C, lanes 7 and 8). By contrast, in RRP41^{Pi-} and RRP41$^{Pi-Cat-}$ samples I observed only one prominent band of around 200 bp, while the smallest band was missing (Figure 30, panel C, lanes 9 and 10). This was in agreement with the pattern of RNA fragments observed by northern blot (Figure 30, panel A). Next, the 3' RACE PCR products were cloned and analyzed by Sanger sequencing. The experiment was repeated using seedlings as a starting material. Since the results obtained with both tissues were similar, the sequences obtained in both experiments were analyzed together. 171, 132, 145 and 141 sequences corresponded to P-P1 in Col-0, RRP41^{WT}, RRP41^{Pi-} and RRP41$^{Pi-Cat-}$, respectively. The frequency of fragments with identical 3' extremities was plotted against their length (Figure 31). Three main populations of P-P1 fragments of 162, 171 and 186 nt respectively,

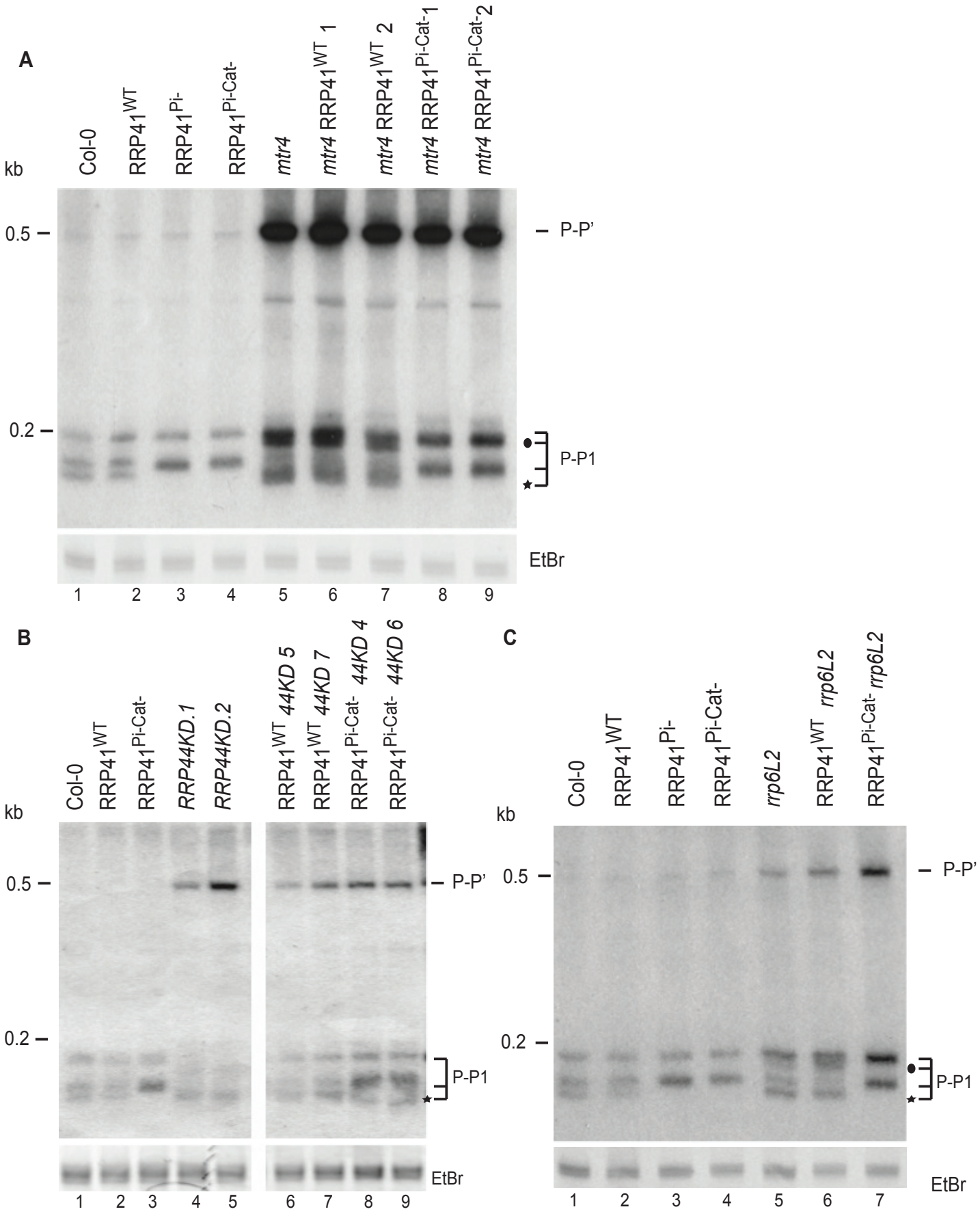

Figure 32. AtMTR4, AtRRP44, AtRRP6L2 and EXO9 cooperate for the degradation of 5'ETS. Total RNAs were extracted from 11-days seedlings (panel A) or 35 dpg (days post germination) rosette leaves (panels B and C), separated on 6% denaturing PAGE, transferred and hybridized with probe S1. Samples are indicated above the panels. Ethidium bromide (EtBr) staining of 5S rRNA was shown as a loading control. Panel A: single and double mutants of AtRRP41 and *mtr4*, panel B: single and double mutants of AtRRP41 and AtRRP44KD, panel C: single and double mutants of AtRRP41 and *rrp6L2*. Sizes of RNA markers (kb) are indicated on the left. P-P' and P-P1 intermediates are indicated on the right. Intermediate generated exclusively by EXO9 activity is marked with asterisk. Additional intermediate observed in the *mtr4* or *rrp6L2* background is marked with a dot.

were obtained from both wild type and RRP41^{WT} samples (Figure 31, panels A and B). By contrast, only the two larger populations of intermediates with 171 and 186 nt length were obtained from RRP41^{Pi-} and RRP41$^{Pi-Cat-}$ (Figure 31, panels C and D). These data show that the enzymatic activity of EXO9 removes about 9-10 nucleotides from the medium-sized 171 nt intermediate, thereby generating the smallest 162 nt P-P1 fragment.

In conclusion, EXO9's activity contributes to the degradation of the 5' ETS by trimming P-P1 fragments.

B. AtMTR4, AtRRP44, AtRRP6L2 and EXO9 cooperate for the degradation of 5'ETS

To test whether a potential effect of mutated EXO9 activity on the accumulation of P-P' could be masked by other factors, I also analyzed the accumulation of the 5'ETS in Col-0, RRP41^{WT}, RRP41$^{Pi-Cat-}$ and *mtr4* single mutants and in plants expressing only tagged versions of active or inactive RRP41 in the *mtr4* background. As compared to Col-0, RRP41^{WT}, RRP41$^{Pi-Cat-}$, all plants lacking MTR4 (*mtr4*, RRP41^{WT} *mtr4* and RRP41$^{Pi-Cat-}$ *mtr4*) showed a marked accumulation of both P-P' and P-P1 fragments (Figure 32A, lanes 5-9). In addition, the pattern of bands corresponding to P-P1 fragments was different in *mtr4* samples as compared to Col-0, RRP41^{WT}, RRP41$^{Pi-Cat-}$, as an additional fragment slightly smaller than the largest P-P1 fragment was detected (Figure 32A, lanes 1 vs lane 5, marked by a dot). This additional band was also detected in RRP41^{WT} *mtr4*, but not in RRP41$^{Pi-Cat-}$ *mtr4* (Figure 32A, lanes 6,7 vs 8,9). These results suggest that this additional P-P1 fragment is generated by EXO9. The fact that this fragment is only detected in *mtr4* background may indicate that this fragment is rapidly degraded by an MTR4-dependent process in wild-type. Alternatively, it is possible that in the absence of

MTR4, that usually sits the top of the EXO9, the substrates can reach deeper into the central channel of exosome to be further trimmed by EXO9's activity.

Next, I analyzed by northern blots the accumulation of 5' ETS-derived intermediates in plants down-regulated for the exoribonuclease AtRRP44 with samples of Col-0, RRP41^{WT}, RRP41$^{Pi\text{-}Cat\text{-}}$ and *RRP44KD* single mutants and plants expressing only active or inactive RRP41 in an *RRP44KD* background (RRP41^{WT}*RRP44KD* and RRP41$^{Pi\text{-}Cat\text{-}}$*RRP44KD*). As compared to Col-0, *RRP44 KD* plants had elevated levels of P-P'. However, similar amounts of P-P' were detected in RRP41^{WT}*RRP44KD* and RRP41$^{Pi\text{-}Cat\text{-}}$*RRP44KD* (Figure 32B, lanes 6 and 7 vs 8 and 9). As observed before, three P-P1 fragments were observed in Col-0 and RRP41^{WT} while only two P-P1 fragments were detected in RRP41$^{Pi\text{-}Cat\text{-}}$ samples. By contrast, a smear without discrete bands suggesting intermediates of heterogeneous sizes were present in two independent *RRP44KD* samples. RRP41^{WT}*RRP44KD* samples accumulated three fragments similar to Col-0 and RRP41^{WT}. By contrast, RRP41$^{Pi\text{-}Cat\text{-}}$*RRP44KD* samples showed a clear accumulation of the mid-size P-P1 fragment. This result suggests that AtRRP44 generates the mid-size P-P1 fragment, that is subsequently trimmed by EXO9's activity.

Next, I analyzed 5' ETS-derived fragments in mutants lacking both AtRRP6L2 and EXO9 activity. In this experiment, I analyzed Col-0, RRP41^{WT}, RRP41$^{Pi\text{-}Cat\text{-}}$ and *rrp6L2* alongside with RRP41^{WT} *rrp6L2* and RRP41$^{Pi\text{-}Cat\text{-}}$ *rrp6L2* double mutants. In agreement with previous data (Lange et al., 2008), I noticed a slight accumulation of P-P' in *rrp6l2* single mutant (Figure 32C, lane 5). A similar accumulation of P-P' was observed in RRP41^{WT}*rrp6l2* samples. By contrast, a more pronounced accumulation of P-P' was observed in RRP41$^{Pi\text{-}Cat\text{-}}$*rrp6L2* samples (Figure 32C, lane 7). This suggested that both RRP6L2's and EXO9's activities act redundantly in the degradation of the P-P' fragment. However, as compared to AtMTR4, the impact of

AtRRP6L2 and EXO9s activity seems to be rather minor. Interestingly, the additional P-P1 intermediate that we detected in *mtr4* mutants (Figure 32A) was also detected in the *rrp6L2* background (Figure 32C, lanes 5 and 6, marked by a dot). Again, this additional fragment is detected in RRP41^{WT}*rrp6L2* but not in RRP41$^{Pi\text{-}Cat\text{-}}$ *rrp6l2* samples. This indicates that this fragment is generated by EXO9's activity, and subsequently efficiently degraded by AtRRP6L2. Alternatively, as seen in *mtr4* mutant background, this fragment may be further trimmed by EXO9's activity in the absence of AtRRP6L2.

Taken together, my results show that the activity of the core exosome contributes to the elimination of the 5' ETS. The data shown here reveal that at least three exoribonucleolytic activities cooperate for the degradation of the 5' ETS. Apparently, AtRRP44 is responsible for the bulk degradation of the P-P' fragments and generation of the largest P-P1 fragment, while both AtRRP6L2 and EXO9 activities contribute to the degradation of P-P1 intermediates but play rather minor roles for the overall elimination of the 5' ETS. My data suggest that AtRRP6L2 and EXO9 take over the P-P1 intermediate after initial trimming by AtRRP44. A possible explanation is that the processive enzyme AtRRP44 is stalled at the secondary structure in P-P1. My data show that in this process, EXO9 has a specific role that is not redundant with the activities of AtRRP6L2 and AtRRP44: EXO9 is responsible for the generation of the smallest of the three P-P1 fragments that can be detected in Col-0. An additional contribution of EXO9's activity is revealed in *rrp6L2* or *mtr4* backgrounds, where EXO9 generates another intermediate fragment from the largest P-P1 fragment. This additional fragment may be a common substrate for EXO9 and AtRR6L2. However, the strong accumulation of P-P1 fragments in r*rp41*^{iRNAi} lines and *mtr4* mutants as compared to the mild accumulation in single mutants indicates that three activities of

AtRRP44, AtRRP6L2 and EXO9 cooperate and act largely redundant for the elimination of P-P fragments.

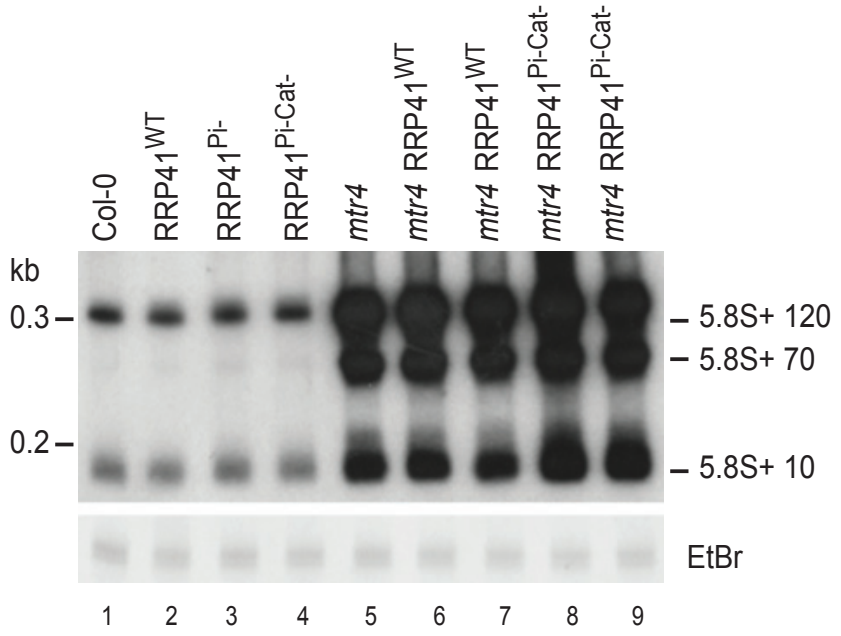

Figure 33. The impact of RNA helicase AtMTR4 on the processing of 5.8S rRNA may mask the effect of other activities involved in this process. Total RNAs were isolated from 11-days seedlings of plants indicated on top of the panel, separated on 6% denaturing PAGE, transferred and hybridized with probe S2. Ethidium bromide (EtBr) staining of 5S rRNA shows equal loading. Sizes of the RNA markers (kb) are given of the left. 5.8S rRNA precursors are indicated on the right.

III. The activity of plant EXO9 contributes to the processing of 5.8S rRNA precursors

A. RNA helicase AtMTR4 is crucial for efficient processing of 5.8S rRNA precursors

Since the activity of EXO9 is involved in trimming of the P-P1 intermediates generated during degradation of the the 5'ETS, I hypothesized that it could also be involved in the trimming of another common substrate of AtMTR4, AtRR6L2 and AtRRP44, namely 5.8S rRNA precursors. To address the question whether EXO9 activity contributes to 5.8S rRNA processing, I first analyzed the accumulation of 5.8S rRNA precursors in Col-0, RRP41^{WT}, RRP41^{Pi-} and RRP41$^{Pi-Cat-}$ plants by northern blot. In the same time, I also analyzed *mtr4* mutants and plants expressing either wild-type or mutated RRP41 in the *mtr4* mutant background. The probe hybridized to the region in the very beginning of the ITS2 and 3' of mature 5.8S and therefore, detected only precursors of 5.8S rRNA (Figure 26, probe S2). In agreement with published data, I detected two pronounced bands corresponding to 5.8S+120 and 5.8S+10 precursors, and a faint band corresponding to 5.8S+70 precursors in Col-0 samples (Figure 33, lane 1). All three precursors accumulated to similar levels in RRP41^{WT}, RRP41^{Pi-} and RRP41$^{Pi-Cat-}$ samples (Figure 33, lanes 2-4). One possible explanation could be that EXO9's activity is not involved in 5.8S processing. Alternatively, redundant activities may compensate for loss of EXO9 activity in RRP41^{Pi-} and RRP41$^{Pi-Cat-}$ plants. Indeed, the results obtained in *mtr4* mutant background may argue for the second possibility. As described previously, loss of AtMTR4 alone resulted in a massive accumulation of all three forms of 5.8S precursors, namely 5.8S+120nt, +70nt and +10nt (Figure 33, lane 5). But despite the overall high accumulation in all samples lacking AtMTR4, I could repetitively observe a stronger accumulation of the smallest band corresponding to 5.8S+10

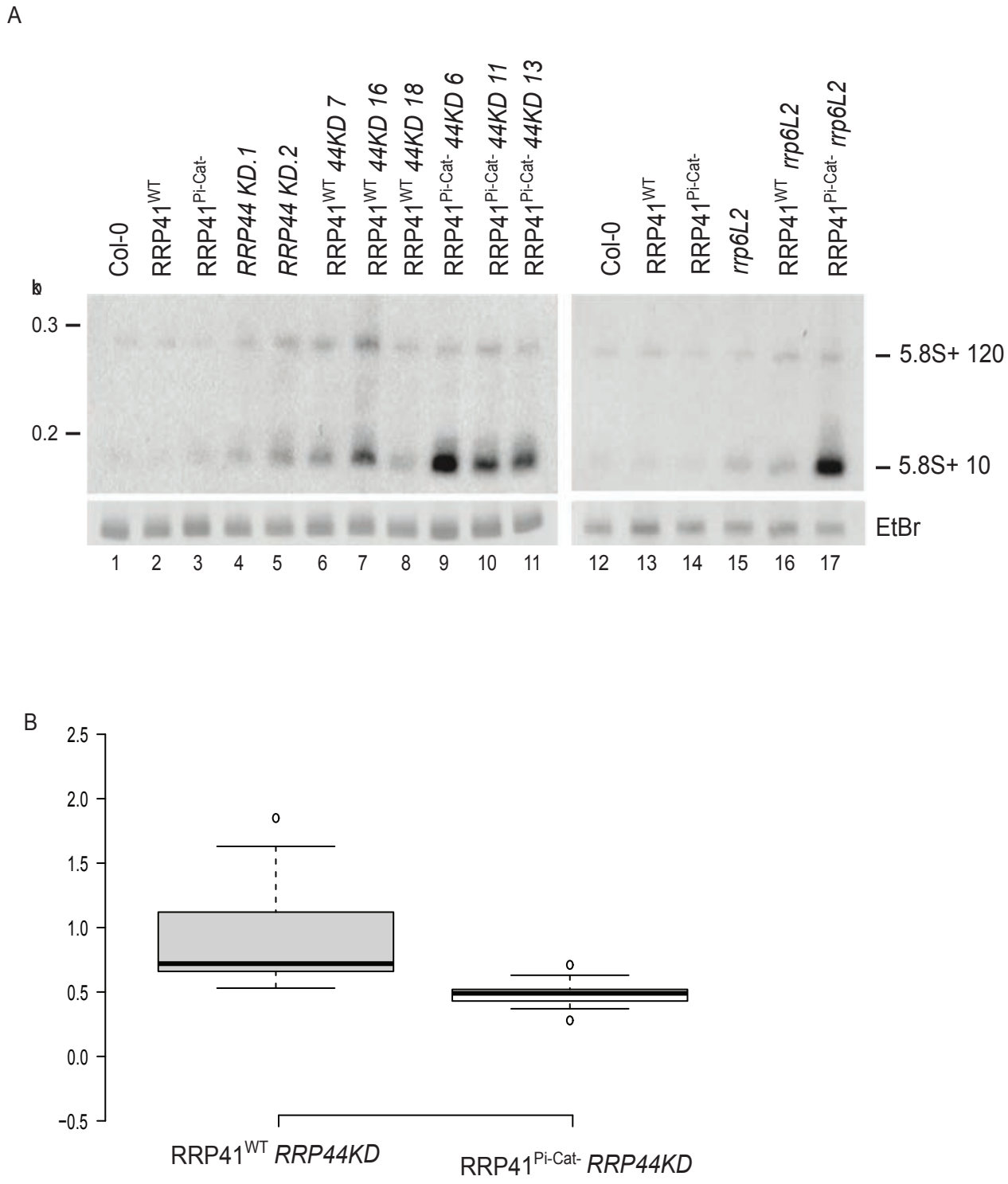

Figure 34. AtRRP44, AtRRP6L2 and EXO9 cooperate for trimming of 5.8S precursors
A. Total RNAs isolated from 35dpg rosette leaves were separated on 6% denaturing PAGE, transferred and hybridized with a probe S2 complementary to ITS2 (Figure 26). Samples names are indicated on top of the panel. 5S rRNA stained with ethidium bromide (EtBr) is shown as a loading control. Sizes of RNA markers (kb) are indicated on the left. **B)** The levels of pre-5.8S rRNA were analysed in 21 independent plant lines of RRP41^{WT} RRP44KD and 16 of RRP41$^{Pi\text{-}Cat\text{-}}$ RRP44KD by northern blot (as described in A), quantified by Fhosphorimager and ImageJ, and the ratio between the larger and the smaller precursor is presented as a box-plot. Sizes of the RNA markers (kb) are given of the left. 5.8S rRNA precursors are indicated on the right.

precursors in plants lacking both EXO9 activity and AtMTR4 (Figure 33, lanes 8 and 9 vs. 6 and 7).

This suggested that EXO9 activity may indeed contribute to the processing of a population of smaller 5.8S precursors. However, the relative small differences between RRP41^{WT}*mtr4* and RRP41$^{Pi\text{-}Cat\text{-}}$*mtr4* may indicate that the contribution of EXO9's activity is masked by a compensating exoribonucleolytic activity.

B. EXO9 contributes to trimming of 5.8S rRNA precursors

One prominent candidate for such a compensating activity is the exosome-associated exoribonuclease AtRRP44. To test whether AtRRP44 acts together with EXO9 in the processing of 5.8S rRNA precursors I compared the accumulation of 5.8S rRNA precursors in the Col-0, RRP41^{WT}, RRP41$^{Pi\text{-}Cat\text{-}}$, *RRP44KD*, RRP41^{WT}*RRP44KD* and RRP41$^{Pi\text{-}Cat\text{-}}$*RRP44KD* plants by northern blot. In agreement with previously published data (Kumakura et al., 2013) both longer (5.8S+120) and shorter (5.8S+10) precursors slightly accumulated already upon down-regulation of *RRP44* alone (Figure 34A, lanes 4 and 5). Interestingly, simultaneous down-regulation of *RRP44* and loss of RRP41 activity resulted in increased accumulation of the shortest 5.8S rRNA precursors, while accumulation of the longer precursor was similar in *RRP44 KD*, RRP41^{WT}*RRP44KD* and RRP41$^{Pi\text{-}Cat\text{-}}$*RRP44KD* (Figure 34, lanes 9-11). These data indicated that the enzymatic activity of AtRRP44 is required for the processing or degradation of the 5.8S+120 precursor, while the activities of both EXO9 and AtRRP44 are involved in trimming 5.8S precursors. To confirm this observation, I quantified the accumulation of 5.8S rRNA precursors in all RRP41^{WT}*RRP44KD* and RRP41$^{Pi\text{-}Cat\text{-}}$*RRP44KD* lines that were confirmed to silence *RRP44* efficiently. RNA from 21 independent lines of RRP41^{WT}*RRP44KD* and 16 of RRP41$^{Pi\text{-}Cat\text{-}}$*RRP44KD* lines was analyzed by northern blots, visualized using a FUJI PhosphorImager, and quantified using ImageJ software. The results are presented as

a box-plot (Figure 34B). The quantitative analysis confirmed that the shorter 5.8S+10 precursors accumulate in the double mutant lacking both EXO9 and RRP44 activities.

Another RNase that may compensate for the lack of EXO9 activity is AtRRP6L2. To address the potential redundancy between EXO9 and AtRRP6 activities for the processing of 5.8S rRNA precursors, I analyzed the levels of 5.8S precursors in Col-0, RRP41^{WT}, RRP41$^{Pi\text{-}Cat\text{-}}$, *rrp6l2*, RRP41^{WT} *rrp6L2* and RRP41$^{Pi\text{-}Cat\text{-}}$*rrp6L2* plants. As in previous experiments, similar levels of both larger and smaller 5.8S precursors were detected in Col-0, RRP41^{WT}, RRP41$^{Pi\text{-}Cat\text{-}}$(Figure 34A, lanes 12-14). In agreement with published data (Lange et al., 2011), the smaller 5.8+10 precursors were slightly accumulated in *rrp6L2* (Figure 34A, lane 15). Similar slightly accumulated levels of 5.8S+10 precursors were also detected in RRP41^{WT} *rrp6L2*. By contrast, the double mutant devoid of both EXO9 and RRP6L2 activities showed a clearly increased accumulation of the 5.8S+10 precursors (Figure 34A, lane 17).

This result shows that activity of EXO9's contributes, together with the activity of AtRRP6L2, to processing of small 5.8S precursors.

C. EXO9, AtRRP44 and AtRRP6L2 cooperate for trimming of 5.8S rRNA precursors

To better understand the relative contributions of EXO9's and RRP6L2's activities to 5.8S processing I mapped the 3' extremities of the smallest 5.8S precursors by 3'RACE PCR. The experimental procedure was similar to the procedure to map the extremities of P-P1 fragments described above. To substantially enrich the pool of 5.8S precursors, RNA of about 170 nt to about 350 nt was size-selected prior to adapter ligation and cDNA synthesis. In agreement with the poor detection of small 5.8S precursors in Col-0, RRP41^{WT}, RRP41$^{Pi\text{-}Cat\text{-}}$,

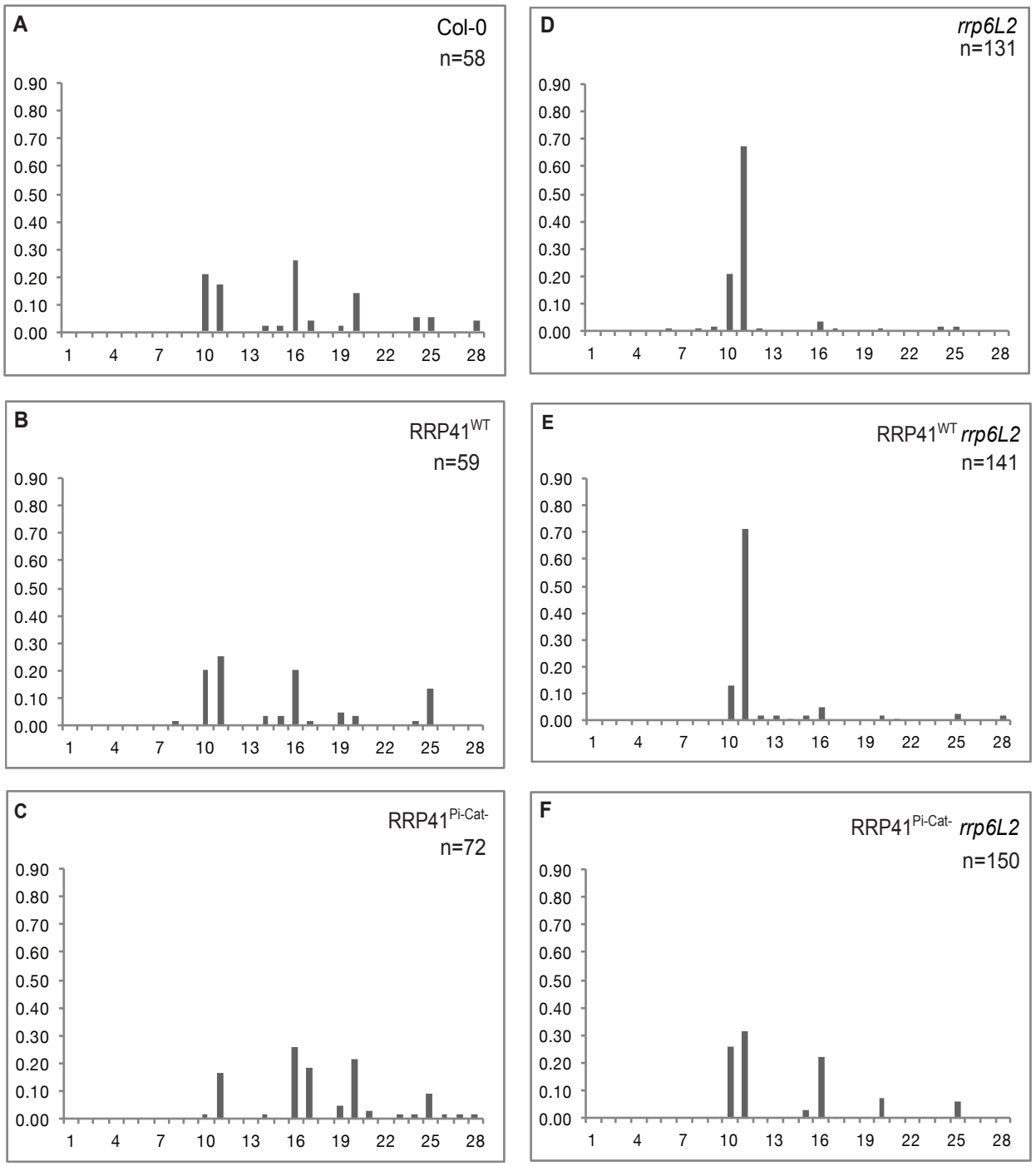

Figure 35. Graph illustrating the frequencies of 5.8S RNA precursors in Col0, RRP41^{WT}, RRP41$^{Pi\text{-}Cat\text{-}}$, *rrp6L2*, RRP41^{WT}*rrp6L2* and RRP41$^{Pi\text{-}Cat\text{-}}$*rrp6L2*. The 3' extensions of 5.8S rRNA were determined by 3' RACE PCR followed by cloning and sequencing. Bars represent P-P1 fragments with a defined length, their frequency is indicated by the bar size. The sequences obtained from two independent experiments (using seedlings or flowers) were analysed together. The number of obtained clones for each genotype is indicated in the top right corner of each panel. A: Col0, B: RRP41^{WT}, C: RRP41$^{Pi\text{-}Cat\text{-}}$, D: *rrp6L2*, E: RRP41^{WT}*rrp6L2*, F: RRP41$^{Pi\text{-}Cat\text{-}}$*rrp6L2*.

only 37-47% of the cloned sequences mapped to the 5.8S precursors in these samples. By contrast, 85-98% of the sequences corresponded to 5.8S precursors in *rrp6l2*, RRP41^{WT}*rrp6l2* or RRP41$^{Pi\text{-}Cat\text{-}}$*rrp6l2*. The frequency of each precursor was calculated for each sample. In the wild-type and RRP41^{WT} samples the 5.8S precursors had extensions of 10, 11, 16, 20, 24 and 28 nt (Figure 35A and B). A population of +11 nt was also detected in RRP41$^{Pi\text{-}Cat\text{-}}$ samples, while the frequency of +10 nt precursors was decreased (Figure 35C). By contrast, precursors with an extension of 16 and 20 nt were more frequent as compared to Col-0 and RRP41^{WT}. In *rrp6l2* and RRP41^{WT} *rrp6l2*, the +11 precursors were clearly more frequent as compared to Col-0 and RRP41^{WT} alone, while precursors with 16 nt or larger extensions were virtually absent (Figure 35D and E). By contrast in RRP41$^{Pi\text{-}Cat\text{-}}$ *rrp6l2* plants the majority of precursors were extended by 10-11 nt, although +16 up to +25 nt species are also detected (Figure 35F).

Mapping the 3' ends of 5.8S precursors provided molecular details about the heterogenic nature of the population of short 5.8S precursors that were detected by northern blots and confirmed that the activity of EXO9 contributes to 5.8S processing in *Arabidopsis*. The higher frequency of precursors with extension of more than 11 nt in plants with inactive EXO9 suggests that these intermediates are substrates of EXO9's activity in the wild-type situation. *Vice versa*, the lower frequency of 5.8S +10/+11 in these plants suggests that EXO9's activity makes an important contribution to the production of these smaller precursors. However, as 5.8S +10 precursors are still detected in RRP41$^{Pi\text{-}Cat\text{-}}$ plants, other activities can also generate 5.8S+10 and +11 precursors in plants. One activity capable of producing 5.8S +10/+11 may be RRP6L2. But since 5.8S +10/+11 precursors are still detected in RRP41$^{Pi\text{-}Cat\text{-}}$ *rrp6L2* samples, another yet unknown activity can also generate these precursors, at least in this genetic background. Based on my *in vitro* studies, an extension of 10 nt is too short to reach the active site of plant EXO9.

Hence, 5.8S +10 precursors are likely the substrate of RRP6L2, as revealed by their accumulation in *rrp6l2* mutants. This explanation would be in line with recent structural data demonstrating that yeast 5.8S precursors are sequentially processed by the activities of Rrp44p and Rrp6p of EXO11 (Makino et al., 2015).

Taken together, my results show that the three activities of AtRRP44, EXO9 and AtRRP6L2 contribute to 5.8S rRNA processing in plants. The larger form of 5.8S precursors (5.8S +120nt) is mainly a substrate of AtRRP44 and to some extent of AtRRP6L2. Efficient processing of larger precursors requires the action of the RNA helicase AtMTR4, as illustrated by the pronounced accumulation of larger precursors with 70 and 120 nt extensions in *mtr4* mutants. Prominent accumulation of a population of small precursors in the absence of EXO9's and AtRRP6L2's activities suggests that both activities cooperate in processing small 5.8S precursors.

Discussion and perspectives

A. Plant EXO9 has a phosphorolytic activity conferred by AtRRP41

Eukaryotic exosome complexes are structurally related to bacterial phosphorolytic enzymes such as RNase PH and PNPase or archaeal exosomes. They share with a common ancestry enzyme the ring-shaped structure with a prominent central channel. Since in the bacterial phosphorolytic exoribonucleases and in the archaeal exosome complex the active sites are buried within the central channel, the RNA substrates are threaded through it in order to be processed or degraded. Threading of RNA through the central channel also applies to eukaryotic exosomes. However, the exosome of yeast and human are catalytically inert and rely on the enzymatic activity of two associated hydrolytic ribonucleases bound at each side of the exosome's channel: Rrp6p/hRRP6 sitting at the top and Rrp44p/hRRP44 curled up on the bottom (Dziembowski et al., 2007; Makino et al., 2013; Schneider et al., 2009; Wasmuth and Lima, 2014).

In this work I demonstrated that the plant exosome possesses a single active site within the central channel. The active site is provided by AtRRP41, since the enzymatic activity was abolished when the phosphate coordination site of AtRRP41 was mutated. The catalytic activity of EXO9 is strongly stimulated by inorganic phosphate (Pi), releases nucleoside diphosphates (NDPs) and is reversible, and therefore, meets all three criteria of a phosphorolytic activity.

The presence of a phosphorolytic activity within the exosome core complex is is an outstanding feature of the plant exosome and makes it unique among eukaryotic exosomes.

B. No detectable activity of AtRRP44 in EXO9 preparations

AtRRP44 was identified as one of EXO9's interactants by mass spectrometry analysis of proteins co-purifying with EXO9 (this study; (Lange et al., 2014)). Hence, plant exosome complexes are associated with AtRRP44 *in vivo*, and therefore have, in all likelihood also the hydrolytic activity conferred by this enzyme. An obvious explanation for the fact that I do not observe a hydrolytic activity in my *in vitro* assays with purified exosome complexes is that my preparations contained only trace amounts of AtRRP44. This suggests that the interaction between EXO9 and At44P44 in plants is less stable than in yeast and humans. Another possible explanation for the lack of detection of AtRRP44's activity could be the related to the biochemical conditions used in my assays. Yeast and human Rrp44 contains two catalytic domains, RNB and PIN, which provide exoribonucleolytic and endoribonucleolytic activities, respectively (Drazkowska et al., 2013; Lebreton et al., 2008; Schaeffer et al., 2009; Tomecki et al., 2010). Since both RNB and PIN domains are conserved in AtRRP44, it very likely possesses exo- and endoribonucleolytic activities as well (Lange and Gagliardi, 2012). However, even if the trace amounts of AtRRP44 would be enough to detect both activities, the experimental conditions used in the degradation assays *in vitro* are likely not compatible with the conditions required for AtRRP44 endo and exoribonucleolytic activities (Dziembowski et al., 2007). The exoribonucleolytic activity of AtRRP44 may be inhibited by the 1.5 mM magnesium ions present in the reaction buffer, since it was reported that yeast Rrp44p is active at submillimolar concentrations of magnesium ions but strongly inhibited by concentrations higher than 1mM (Dziembowski et al., 2007). The endoribonucleolytic activity of Rrp44p requires non-physiological concentrations (5 mM) of manganese ions, which were absent from the reaction buffer I used.

In addition to the minute amount of AtRRP44 and the inadequate biochemical conditions, another reason for not detecting AtRRP44 activity is probably linked to the nature of the RNA substrates used in most experiments.

According to structural and biochemical data obtained with yeast and human EXO10 complexes, the minimal size of RNA substrates must be 31-33 nt to reach the Rrp44p exoribonucleolytic active site *via* the central channel (Bonneau et al., 2009). In most experiments I used 21 nt long RNA substrates, that are long enough to reach AtRRP41's catalytic site but not AtRRP44's one *via* the central channel. However, a direct access to Rrp44p is possible and requires RNA substrates of only 9-12 nt. Despite the existence of this direct route, mutations occluding the central channel of EXO9 impair the RNase activities of Rrp44p in the context of EXO10 and are lethal (Bonneau et al., 2009; Wasmuth and Lima, 2012). Hence, albeit direct access to the RRP44's active site is possible, it is more likely that the substrates are threaded through the exosome central channel to reach the AtRRP44 active site. In addition, the direct path to the active site of Rrp44p is likely used only by a small subset of substrates *in vivo,* such as incorrectly folded tRNAs (Mitchell, 2014; Schneider et al., 2012). Hence, the 21 nt substrates used in my study may not fulfil the requirements for direct access to AtRRP44.

Taken together, both the biochemical conditions of the assays, the length and nature of the RNA substrates used and the extremely low level of co-purifying AtRRP44 protein explain why neither the endo- nor the exoribonucleolytic activity of AtRRP44 were detected in my *in vitro* assays.

C. Are AtRRP44, AtRRP6 and EXO9 activities interconnected?

Since AtRRP44 physically interacts with EXO9 *in vivo*, it should provide EXO9 with the hydrolytic activity *in planta*. In addition, AtRRP6L2 (and possibly AtRRP6L1 and AtRRP6L3) may also interact with the plant exosome *in vivo*, although this has not been demonstrated yet. It is interesting to speculate how EXO9's phosphorolytic activity is influenced by the binding of AtRRP44 and possibly AtRRP6L2. It was shown that the activity of yeast Rrp44p is diminished when bound to the exosome core (Wasmuth and Lima, 2012). By contrast, binding

of Rrp6p, independent of its activity, stimulated the catalytic activity of Rrp44p (Wasmuth and Lima, 2012). Do EXO9's and AtRRP44's activities influence each other in plants? Is AtRRP6L2 binding to the exosome core and modulates the activity of both RRP44 and EXO9? These questions could be addressed by reconstituting plant exosome complexes of EXO9, AtRRP44 and RRP6L2 *in vitro*. I attempted to reconstitute an EXO10 complex by combining purified EXO9 with recombinant AtRRP44 but without success. The main reason for this negative results may be that the amount of EXO9 purified from *Arabidopsis* is very low (approximately 100ng per one purification). The reconstitution of EXO9 with AtRRP44 *in vitro* requires testing multiple conditions for protein-complex binding and for catalytic activity, such as testing a range of magnesium concentrations suitable for both EXO9 and AtRRP44. Therefore, this approach is severely limited by the minute amounts of available EXO9. In theory, this could be solved by optimizing the EXO9 purification conditions in order to obtain more EXO9. However, the affinity purification of endogenously expressed EXO9 is unlikely to allow the purification of massive amounts of EXO9. This strategy was extremely successful to demonstrate the intrinsic phosphorolytic activity of EXO9 in *Arabidopsis*, but is limited for an extensive biochemical study of the plant EXO9. Alternatively, the reconstitution of plant EXO9 from individual recombinant subunits should provide large amounts for biochemical experiments. Unfortunately, such a reconstitution by a collaborating laboratory was so far unsuccessful and is yet to be set up.

Table 1. Examples of heteropolymeric tails.
(Adapted from Slomovic et al., 2008)

Organism	Polymerase	Example of a representative tail
B. subtilis (Campos-Guillen et al., 2005)	PNPase	$GA_3UA_6CUA_4CACA_{18}UA_8CAACA_3UACGA_4CA_3U_2A_{17}CA_3GA_9U_2A_8$ (23S rRNA)
S. coelicolor (Bralley and Jones, 2002)	PNPase	$A_3UA_2U_2A_3UA_5UA_4U_2A_4GA_5UA_{17}$ (23S rRNA)
E. coli (Mohanty and Kusher, 2000)	PNPase	$A_6GCUACAUGA_{12}GCUGACGUGA_6GAGACUAU_2CGA_4CAG_2A_3GUA_8U_{21}$ (lpp)
Synechocystis (Rott et al., 2003	PNPase	$G_2UGACAGA2G_3A_5UAUACAGAGA_2GAUGA_3GUA_2GUA_2GAGAGAUCUGAGCGA_4CU_2A_5GA_5CUA_6$-$CAAG_2A_2GA_3GA_2U_2GA_4G_3CA_9U_2AGACACA_6$ (rbcL)
Spinach chloroplast (Lisitsky et al, 1996)	PNPase	$A_2GAGAG_2AG_2CA_6G_2A_2GA_5GAGA_3G_2A_2GUA_3GA_2GCA_4GA_6G_2CAGAGA_5G_2A_3GA_3GA_4GAGAGA_3$-$G_2ACA_7UA_8GAGA_3G_2A_4G_2AG_2ACAG_2A_4GAG_2A_3CA_5GAGC_2AGA_5G_2AG_2A_4G_2CGAG_2AGA_5GAGA$-$GAUA2C_4A_{13}GAG_2AG2A_3C_3A_3G_2A_3UA_9G_2A_3GUG_2A_{14}$ (psbA)
Archaea (*Sulfolobus*) Portnoy et al., 2005	Archaeal exosome	$AGAUA_3CUGA_2GACAGA_7G_2A_4GA_2UA_4GAUAGAGAUA_4UAGUAGAG_3AUGA_3GACUA_{12}G_2AUA_{17}$ (16S rRNA)
Human (Slomovic et al., 2006)	?	$A_5GA_4GA_7GA_3GA_3GA_3GAG_2A_2GA_2GAG_2AGA_5G_2AGA_2G_2AGA_6G_3AG_2A_4GAG_2AG\ A_3GA_2GUA_5GA_{19}$ (28S rRNA)

lpp- lipoprotein; rbcL- the large subunit of Rubisco; psbA- one of the catalytic proteins of photosystem II

D. Does EXO9 synthesize tails *in vivo*?

The stimulation of RNA degradation by oligoadenylation was first described in bacteria, then in chloroplast and plant mitochondria (Lange et al., 2009; Norbury, 2013; Slomovic et al., 2008). Later on, it was shown that oligoadenylation also stimulates the degradation of most nuclear non-coding RNAs by the exosome in all eukaryotes (Chekanova et al., 2007; LaCava et al., 2005; Vanácová et al., 2005; Wyers et al., 2005). Those non-coding RNAs include snRNAs, snoRNAs, miRNA precursors, antisense RNAs, spliced introns, rRNAs, tRNAs as well as cryptic unstable transcripts (CUTs) in yeast or promoter upstream transcripts (PROMPTs) in humans. Non-coding RNAs are adenylated by members of the Terminal Nucleotidyl Transferases (TNTases) family, also called non-canonical poly(A)polymerases (ncPAPs). This type of TNTases is typified by *S. cerevisiae* Trf4p and Trf5p, and their homologues in mammals POLS and PAPD5 (Norbury, 2013). Recently, AtTRL, a homologue of Trf4 and one of the 15 ncPAPs encoded by the *Arabidopsis* genome, was shown to adenylate 3' ends of 5.8S and 18S precursors and rRNA maturation by-products such as P-P' (Sikorski et al., 2015). Polyadenylation-induced RNA degradation is not restricted to nuclear non-coding RNAs and it is also suspected to operate in the cytosol (Harnisch et al. 2016; Slomovic et al. 2008).

In addition to *bona fide* ncPAPs, PNPases can also synthesize poly(A)-rich tails in chloroplasts and bacteria (Slomovic et al., 2008). In archaea, poly(A)-rich tails are synthesized by the exosome (Evguenieva-Hackenberg et al., 2014). Therefore, phosphorolytic enzymes such as bacterial PNPase or archaeal exosome provide two activities, namely RNA degradation and tailing (Mohanty and Kushner, 2000; Portnoy et al., 2005; Slomovic et al., 2008). A characteristic signature of the tails synthesized by these phosphorolytic enzymes is their heteropolymeric nature. Examples of heteropolymeric tails are presented in Table 1. These heteropolymeric poly(A)-rich stretches found on transcripts in bacteria, chloroplasts and archaea attract 3'-5' exoribonucleases and stimulate degradation (Schuster and Stern, 2009;

Slomovic et al., 2008, 2006, 2005). Therefore, the poly(A)-rich tails added by the phosphorolytic PNPases or the archaeal exosome play the same role in stimulating RNA degradation as the short homopolymeric poly(A) tails added by TNTases.

My previous results have shown that plant EXO9 can not only degrade RNA but also add untemplated ribonucleotides to the RNA substrate. Although this tailing is irrefutable when performed in a test tube, it remains to be determined whether EXO9 could tail RNAs *in vivo*. Plant EXO9 has the potential to synthesize heteropolymeric tails because the four ribonucleotides can be substrates of EXO9 *in vitro*. The exact composition of hypothetical heteropolymers synthesized by EXO9 both in vitro and *in vivo* will depend on the respective amounts of each ribonucleotide and on their respective affinity for EXO9 and remains to be determined.

To date no endogenous RNA with heteropolymeric tails was detected in the cytosol or nucleus of plants. One possibility is that such tails were not detected due to technical limitations of the method used for detection and characterization of RNA tails, such as oligo(dT)-primed RT-PCR combined with Sanger sequencing. Interestingly, the recently established technique TAIL-seq may help to better characterize 3' tails of various endogenous and exogenous (e.g. viral) tails. TAIL-seq was set up in mammalian cells (Chang et al. 2014), but soon after was adapted for *Arabidopsis* (Zuber et al., 2016).

The first heteropolymeric tails detected in the plant cytosol were reported in a recent study. Those tails were not detected on endogenous RNAs but on viral RNAs. Addition of non-templated poly(A)-rich and heteropolymeric tails added to the 3' extremities and to degradation fragments of viral RNAs was reported for seven positive strand plant viruses *Tobacco mosaic virus* (TMV), *Cucumber mosaic virus* (CMV), *Odontoglossum ring-spot virus* (ORSV), *Cucumber green mottle mosaic virus* (CGMMV), *Tobacco rattle virus* (TRV), *Turnip crinkle virus* (TCV) and *Tobacco necrosis virus* (TNV), suggesting that tailing of viral RNAs is a common process in infected plants (Li et

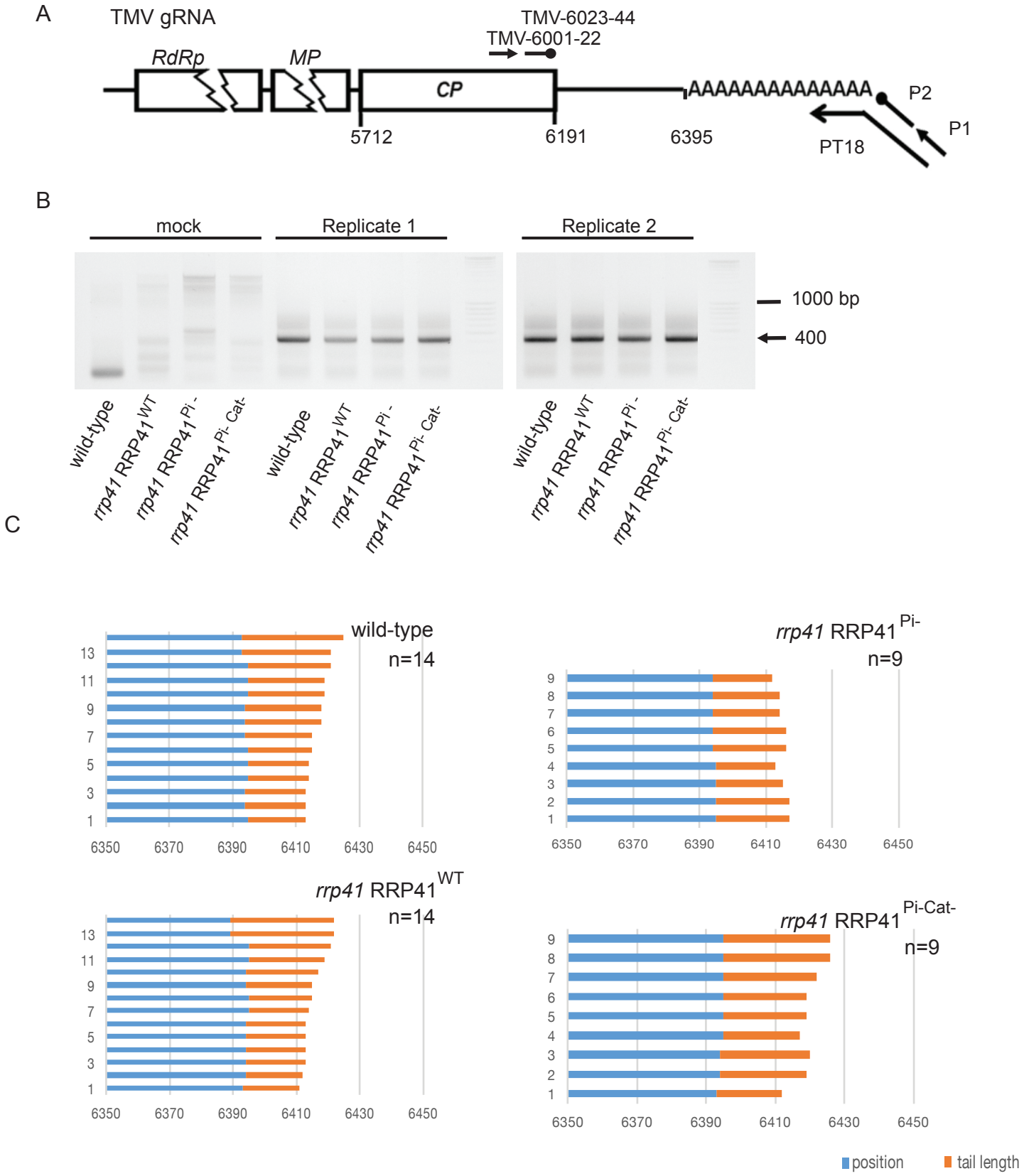

Fig.36. Oligo dT-primed RT-PCR detection of the polyadenylated TMV gRNA in *Arabidopsis*. RRP41WT, RRP41Pi- and RRP41Pi-Cat- infected with TMV. A. Schematic diagram of TMV gRNA with three open reading frames encoding viral components of polymerase (RdRp), movement protein (MP) and coat protein (CP). Primers used for oligo dT-primed RT PCR are marked as bars with arrows (oligo dT P18 and first PCR) or circles (nested PCR). B. PCR products obtained from mock and infected wild-type and RRP41 lines by oligo dT-primed RT-PCR. Total RNAs were isolated from TMV-inoculated or mock treated leaves of Col-0, RRP41WT, RRP41Pi- and RRP41Pi-Cat- 4days post inoculation (4dpi). Next, oligo dT-primed cDNA synthesis was performed using primer P18. cDNA served as a template for the first PCR (TMV-6001-22/ P1) and obtained products were used as a template in the nested PCR (TMV-6023-44/P2) and separated on 1% agarose gel. C. Individual clones obtained from Col-0, RRP41WT, RRP41Pi- and RRP41Pi-Cat- are shown on separate panels. The 3'end of TMV gRNA is shown in blue and nontemplated nucleotides (tails) are shown in orange. The position of 3'end is marked on axis x and the clone number on axis y. TMV-Tobacco mosaic virus, WT-wild-type.

al., 2014; He et al. 2015). Such heteropolymeric tails are characteristic signatures of phosphorolytic enzymes, three of which are present in plants: chloroplastic PNPase, mitochondrial PNPase and, as I discovered during my thesis, EXO9. Li and al already tested whether the tails detected on TMV-derived RNAs were synthesized by chloroplastic PNPase (cpPNPase), by analyzing viral tails in infected *N. benthamiana* transformed with a construct that triggered the down-regulation of cpPNPase. Since down-regulation of cpPNPase had no effect on tailing viral RNAs Li et al. did not identify the responsible enzyme. Therefore, I explored the possibility whether EXO9 activity could be responsible for the tailing of viral RNAs.

To test whether EXO9 is involved in the tailing of viral RNAs, I infected *Arabidopsis* plants expressing active or catalytically inactive RRP41 with *Tobacco mosaic virus* (TMV) or *Oilseed Rape Mosaic Virus* (ORMV). A subset of plants of each genotype was mechanically treated without the virus (mock infection). I did not observe any phenotypical differences between wild-type, $RRP41^{WT}$ and $RRP41^{Pi-}$, $RRP41^{Pi-Cat-}$ plants upon infection. To characterize the tails added to viral RNAs I used the same approach as Li and colleagues. Briefly, 4 days post inoculation (4dpi), total RNA was extracted and reverse transcribed using an oligo d(T) primer containing 18 Ts and an adapter sequence. In the first PCR step, I used forward primers situated in the 3' end of the sequence encoding the coat protein and a reverse primer complementary to the adapter sequence added during cDNA synthesis (Figure 36A and Figure 37A for TMV and ORMV, respectively). The obtained PCR products served as a template for the second, nested PCR. In both cases the amplified products had the expected size of about 400bp, corresponding to 372nt of the 3' end plus the non-templated tail and the primer for TMV, or about 300bp, corresponding to 266nt plus tail and primers for ORMV. I did not observe obvious differences between the PCR products amplified from wild-type, $RRP41^{WT}$, $RRP41^{Pi-}$ and $RRP41^{Pi-Cat-}$ (Fig. 36B and 37B). Nevertheless, we decided to clone and sequence the PCR products to precisely analyze the polyadenylation sites as well as

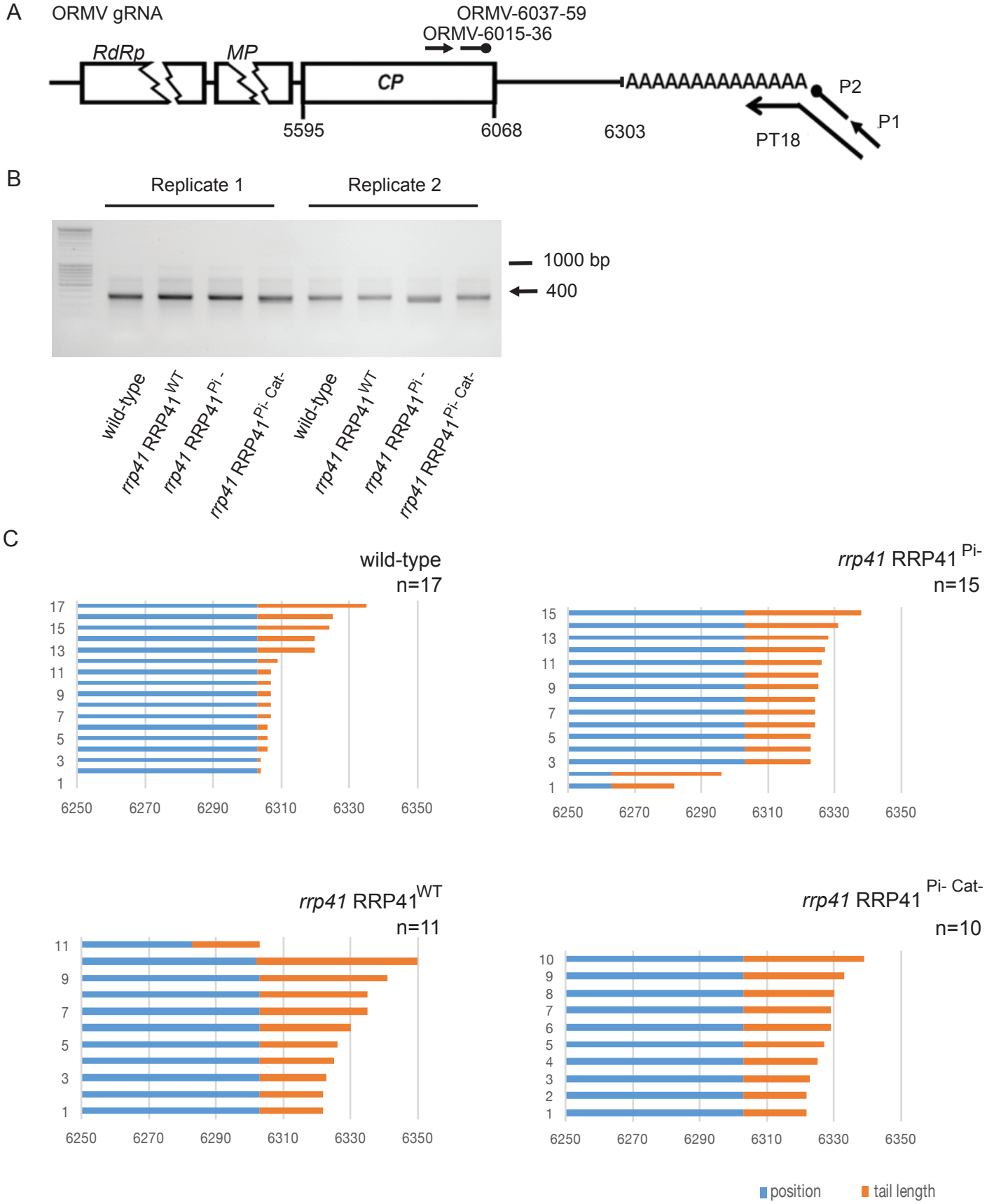

Fig.37. Oligo dT-primed RT-PCR detection of the polyadenylated ORMV gRNA in *Arabidopsis*. RRP41WT, RRP41Pi- and RRP41Pi-Cat- infected with ORMV. A. Schematic diagram of the oligo dT-primed RT-PCR in ORMV gRNA. Primers used for oligo dT-primed RT PCR are marked as bars with arrows (oligo dT P18 and first PCR) or circles (nested PCR). B. PCR products obtained from ORMV infected wild-type and RRP41 lines by oligo dT-primed RT-PCR. Total RNAs were isolated from ORMV-inoculated leaves of Col-0, RRP41WT, RRP41Pi- and RRP41Pi-Cat- 4days post inoculation (4dpi). Then, oligo dT-primed cDNA synthesis was performed using primer P18. cDNA served as a template for the first PCR (ORMV-6015-36/ P1) and obtained products were used as a template in the second nested PCR (ORMV-6037-59/P2) and separated on 1% agarose gel. C. Individual clones obtained from Col-0, RRP41WT, RRP41Pi- and RRP41Pi-Cat- are shown on separate panels. The 3'end of ORMV gRNA is shown in blue and nontemplated nucleotides (tails) are shown in orange. The position of 3'end is marked on axis x and the clone number on axis y. ORMV-Oilseed rape mosaic virus, WT-wild-type.

length and composition of non-encoded tails. If the exosome would be solely responsible for tailing viral RNAs we would not expect any non-templated tails in RRP41^{Pi-} and RRP41$^{Pi-Cat-}$ samples. In addition, differences in tail composition could hint to the involvement of compensating activities.

The analyzed sequences of tails obtained from TMV-infected plants containing active (wild-type and RRP41^{WT}) and inactive exosome (RRP41^{Pi-} and RRP41$^{Pi-Cat-}$) were very similar in length and composition. The maximal size *TMV* gRNA tails detected in plants containing active or inactive exosome was 34 or 28 As respectively (including 18As of the primer used for cDNA synthesis). Similarly, the maximal size of tails added to *ORMV* gRNA detected in plants containing active or inactive was exosome 35 or 36 As respectively. However, the majority of tails added to viral gRNAs were of size barely exceeding the size of 18 As, corresponding to the 18Ts of the primer used for initiating reverse transcription. These results show that viral RNAs are indeed tailed in *Arabidopsis*. However, I detected only short polyA tails. Therefore, we cannot conclude whether or not EXO9 is involved in synthesis of heteropolymeric tails.

It was unexpected that I did not detect heteropolymeric viral tails although I used the same experimental approach and the same virus (TMV) as Li and colleagues. This could be due to technical issues. Another technical approach that allows the detection of untemplated nucleotides with no preconceived idea of their nature should be tested. One possibility to avoid preselection of templates by oligo(dT) priming would be 3'RACE-PCR after ligation of an adapter to the RNA 3' ends. This approach would allow the analysis of the nucleotide composition of tails in an unbiased way to reveal a hypothetical involvement of EXO9. However, the outcome of such an experiment depends on the proportion of tailed versus unmodified viral RNAs. Of note, the presence of heteropolymeric tails on viral RNAs awaits independent confirmation by another laboratory. However, if these

heteropolymeric tails indeed exist, EXO9 stands as a very interesting candidate for their synthesis, provided that the detection method is optimized.

E. *Arabidopsis* EXO9 preferentially degrades oligo$(U)_{21}$ over oligo$(A)_{21}$ RNA substrate *in vitro*

Another interesting feature of plant EXO9's activity that I observed in my *in vitro* degradation assays was its preference for oligo$(U)_{21}$ RNA substrates, while oligo$(A)_{21}$ was not degraded. In addition, I observed that plant EXO9 is trimming heteropolymeric substrates containing an oligo(A) tail less efficiently than a substrate of the very same sequence containing uridines at the 3' end. This was an unexpected observation since exosome substrates are often polyadenylated *in vivo*. However, the observed *in vitro* substrate specificity of purified EXO9 likely reflects intrinsic binding properties of the plant core exosome. By contrast, the *in vivo* binding specificity of the plant exosome complex is likely modulated by associated cofactors, such as AtMTR4, AtHEN2, or the SKI complex. Purified EXO9 is likely to lack some cofactors that confer the binding of oligo(A) RNA substrates *in vivo*. In archaeal exosomes, the Csl4 or Rrp4 subunits of the exosome cap confer the substrate specificity to the exosome complex (Roppelt et al., 2010). Csl4 binds poly(A)-poor RNAs, whereas Rrp4 confers binding to poly(A)-rich RNA substrates. However, this is not the case for the yeast exosome. Wasmuth and Lima showed that reconstituted exosome complexes containing both Rrp44p and Rrp6p degrade poly(A) RNA substrate 28-fold more efficiently than exosome complexes containing only Rrp44p (Wasmuth and Lima, 2012), suggesting that Rrp6p participates in conferring the preference for poly(A) RNA in yeast. Since the association of any of RRP6-like proteins with plant EXO9 was not demonstrated so far, is not known whether RRP6-like proteins or other factors would mediate the recognition of adenylated substrates. An alternative possibility is that EXO9 may indeed preferentially degrade uridylated RNA substrates in *Arabidopsis*.

Interestingly, exosome substrates can be also uridylated. Ibrahim et al. showed that the *C. reinhardtii* terminal nucleotidyltransferase MUT68 uridylates small RNAs *in vivo*, and that the presence of uridines stimulated the degradation by RRP6 *in vitro* (Ibrahim et al., 2010). Lim and colleagues showed in mammalian cell lines that uridylation of miRNA precursors by the two terminal uridylyltransferases TUT7 and TUT4 facilitated their degradation by exosome complex (Lim et al., 2014). They also showed how the substrate specificity of two catalytic subunits of the human exosome complex, hDIS3 and hRRP6, helps to distinguish productive from aberrant pre-miRNAs. By performing a transcriptome-wide analysis of 3' mRNAs tails, Lim and colleagues demonstrated that TUT7 and TUT4 also uridylate mRNAs and that this oligo-uridylation marks them for subsequent degradation by several RNases including the exosome (Lim et al., 2014). Finally, a collaborative work between our group and Joanna Kufel's laboratory revealed that distinct rRNA processing intermediates, in particular 5' 18S-A2 and 5.8S+70nt precursors, can have short U tails (Sikorski et al., 2015). The accumulation of uridylated 5' 18S-A2 and 5.8S+70 precursors in *Arabidopsis rrp6L2* mutants supported the idea that these uridylated rRNA precursors may be substrates of AtRRP6L2. Alternatively, 18S-A2 precursors may be exported to the cytoplasm and uridylated there, similarly to the situation in human. However, we did not yet investigate whether the presence of U-tails facilities the degradation by AtRRP6L2 or EXO9 *in vivo*. To understand how uridylation affects the stability and degradation of rRNA processing intermediates we first need to identify the responsible uridylation activity. In order to determine the respective impact of adenylation vs uridylation on EXO9's activity *in vivo*, we also need to identify more substrates of EXO9's activity as discussed at the end of this thesis.

F. EXO9 has a distributive activity

The catalytic activity of the plant core exosome has some similarities with the activity of archaeal exosome complexes or bacterial phosphorolytic enzymes such as RNase PH or PNPase: all are phosphorolytic enzymes. But in contrast to PNPase or the archaeal exosome which are processive, plant EXO9 has a distributive activity *in vitro*. Whether an exoribonuclease possesses a distributive or a processive activity can be influenced by the number, the binding force and the spatial distribution of RNA binding sites. Audin and colleagues recently showed that the processivity of archaeal exosome is influenced by the RNA binding sites in the neck-region of the exosome's central channel (Audin et al., 2016). They demonstrated that a point mutation (R67G) in each of the three Rrp41 subunits of the S. *sulfolobus* exosome reduced the affinity between the exosome and the RNA substrate by three orders of magnitude. Moreover, exosome complexes bearing these mutations produced degradation intermediates, indicating that the processivity of the enzyme was compromised. Similarly, the processivity of bacterial PNPase was affected upon deletion of the KH/S1 RNA binding domains or upon mutation of RNA binding sites within the central channel (Shi et al., 2008). Whether and how the activity of plant EXO9 is influenced by RNA binding to the channel is not known. Since no structural data are available for plant EXO9, the residues that could be responsible for RNA binding within the central channel have not been formally identified. However, point mutations at the entry and exit of the central channel of yeast exosome (*S. cerevisiae* Rrp41 K62E, S63D and R95E, R96E respectively) impacts channeling through the catalytically inert EXO9 complex towards the active site of Rrp44p. This demonstrates that the neck region is definitively also important in eukaryotic exosomes (Bonneau et al., 2009).

Another prominent difference between archaeal and plant EXO9 is the number of catalytic active sites. While archaeal exosomes possess three active sites, plant EXO9 has only one (Lorentzen et al. 2005, this work). Audin et al. analyzed in detail

the mechanism of degradation by the archaeal exosome. By using a specific NMR technique they demonstrated that all three active sites of the archaeal exosome are used during the degradation reaction. They showed that the RNA substrate jumps from one active site to another and that all three active sites are exploited during catalysis. Upon reduction of the number of active sites, the activity of the exosome was markedly reduced from 15 to 10 cleavages per second. Unfortunately, they did not report yet the effect of a reduced number of active sites on the processivity of the exosome. The archaeal exosome with its three catalytic active sites is a perfect model to test the impact of the number of active sites on the processivity of the complex. Hence, to date we do not understand whether the reason for the distributive character of plant EXO9's activity is linked to the fact that it has only a single catalytic active site, or, similar to what has been shown for the PNPase and the archaeal exosome, related to the number, the binding force and the distribution of its internal RNA-binding sites.

It is interesting to compare the activities of plant, yeast and human exosomes. Exosome complexes in yeast and humans possess the processive activity of Rrp44p/hDIS3 and the distributive activity of Rrp6p/hRRP6. A similar combination of activities is achieved in plant exosome complexes comprising EXO9 and AtRRP44. Hence, it is tempting to speculate that the combination of a processive and a distributive activity within a single protein complex is important for exosome function in eukaryotes. Maybe the activity of EXO9 was evolutionary conserved in all land plants to compensate for the absent or weak interaction with AtRRP6-like proteins?

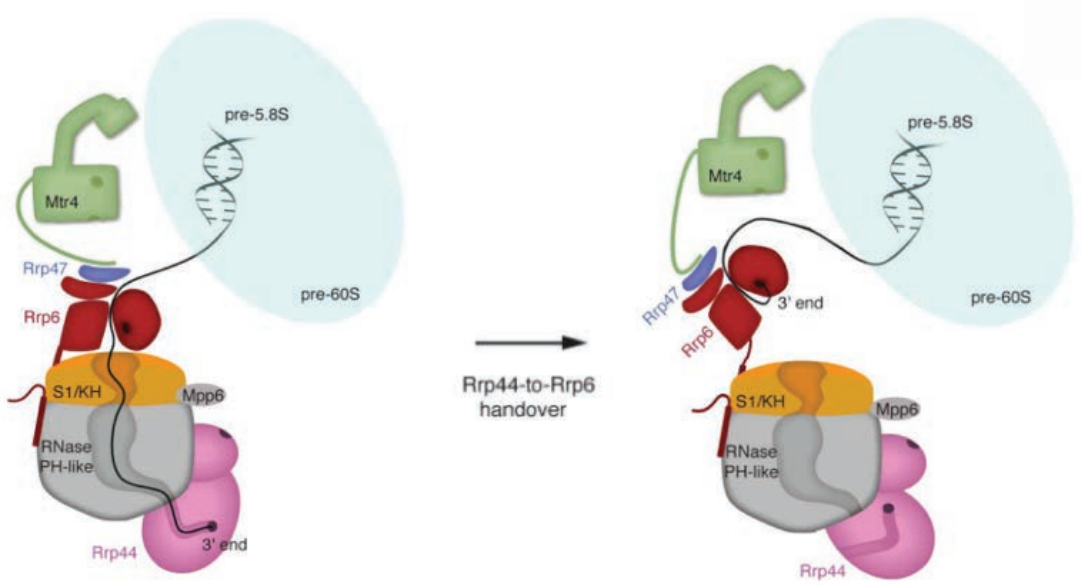

Figure 38. Processing of 5.8S rRNA precursor requires cooperation of processive Rrp44p and distributive Rrp6p activities. A model of pre-5.8S rRNA processing in yeast, proposed by Makino et al. The large 5.8S rRNA precursor is threaded through the exosome channel to reach the active site of the processive RRP44 bound to the bottom of EXO9 (catalytically inert in yeast). When 5.8S precursors are degraded to a size of 5.8S+30nt they are too short to span the central channel of EXO9 and are handed over to distributive RRP6 bound to the top of EXO9. (Adapted from Makino et al., 2016)

G. AtRRP44, EXO9 and AtRRP6L2 may act sequentially in the processing of 5.8S rRNA precursors

Recent work by Makino et al. has solved an important aspect of the mechanism of 5.8S rRNA processing in yeast (Makino et al., 2015). They postulate that exosome-bound ribonucleases Rrp44p and Rrp6p cooperate in a sequential manner for processing of the 5.8S rRNA (Makino et al., 2015). By combining structural data and enzymatic assays they showed that the large 5.8S rRNA precursor is threaded through the exosome channel to reach the active site of the Rrp44p, that is bound to the bottom of the catalytically inert yeast EXO9. When 5.8S precursors are degraded to a size of 5.8S+30nt they are too short to span the central channel of EXO9 and to reach RRP44's active site, and become a substrate of Rrp6p bound to the top of yeast EXO9. The "handing over" of the RNA substrate to Rrp6 involves a conformational change, i.e. the EXO11 complex adopts an open configuration (Figure 38), probably required to retract the substrate out of the channel and allow degradation by Rrp6p. Yeast Rrp6p further processes the precursor to a size of 5.8S+6nt.

As compared with yeast, the three main populations of plant 5.8S precursors are 5.8S+120, +70 and +10 nt. I have shown here that all three exoribonucleolytic activities, AtRRP44, EXO9 and AtRRP6L2 contribute to 5.8S rRNA processing. My analysis showed that the longest precursors are predominantly processed by AtRRP44, albeit RRP6L2 can clearly contribute. 5.8S +70 intermediates are predominantly observed upon loss of MTR4 or down-regulation of exosome core subunits, but accumulate also upon down-regulation of the exoribonucleases RRP44 and RRP6L2. Why the intermediate plant 5.8S precursor is 40 nt longer than its yeast counterpart? One possible explanation is that the plant ITS1 contains binding sites for ribosome biogenesis factors or harbors secondary structures that are an obstacle for exoribonucleolytic degradation, similar to what is thought for the semi-stable P-P1 fragments derived from the 5'ETS. Another possibility is that the 70 nt

correspond to the footprint of a particular plant exosome complex. The minimal length of an RNA substrate to reach through the central channel of plant EXO9 to the active site of AtRRP44 is probably similar to the minimal length of yeast exosome's substrates of 30-33nt. Hence, a footprint of 70nt implies the binding of additional factors to the top of the EXO9 – RRP44 complex. However, this remains speculative until all factors involved in this process will be identified and more biochemical and structural data become available for the plant exosome.

Northern blot analysis combined with mapping 3' ends of 5.8S rRNA precursors using 3'RACE clearly showed that EXO9's activity is involved in the processing of 5.8S precursors. Indeed, the absence of both activities, EXO9 and AtRRP6L2, lead to pronounced accumulation of small 5.8S precursors. This pronounced accumulation of +10 and larger species shows that EXO9's activity, alongside AtRRP6L2, plays a role in the processing of 5.8S rRNA precursors (Figure 34).

Mapping the 3' ends of 5.8S precursors provided molecular details about the heterogenic nature of the population of short 5.8S precursors that were detected by northern blots and confirmed that the activity of EXO9 contributes to 5.8S processing in *Arabidopsis*. Briefly, in a wild-type situation, precursors of +10/+11, +16, + 20 and +25 nt were detected. When EXO9 was inactive, the majority of precursors was extended by 16-25 nt and the +10 precursors were less frequent. By contrast, in the absence of AtRRP6L2 the most frequent precursors were the ones extended by 10-11 nt, and the other species observed in the wild type situation (extended by 16-25 nt) were barely detected. In plants devoid of both activities, EXO9 and AtRRP6L2, the majority of precursors were extended by 10-11 nt, although +16 up to +25 nt species are also detected. It is tempting to speculate what are respective contributions of each activity in generating these precursors. The shift in precursor's size towards longer forms (16-25 nt) in plants with inactive EXO9 suggest that these longer precursors are substrates of EXO9 in a wild-type

situation. Lower frequency of +10 species suggests that EXO9's activity contributes to generating them. However, since +10 precursors are still detected in plants with inactive EXO9, another activity/activities can generate these precursors as well. Since in the absence of AtRRP6L2 the +10/+11 precursors are still detected it suggests that yet another activity is involved in generating them. A possible explanation for accumulation of +10/+11 precursors may be that the putative additional activity can trim longer precursors only until these are extended by 10-11 nt. Yet +10/+11 precursors are likely substrates of AtRRP6L2. Sequence analysis showed that the +10/+11 precursors are most frequent in the absence of AtRRP6L2. However, by Northern blot we do not observe accumulation. The only possible explanation is that these precursors are removed by a compensating activity.

The results presented in this work show that the catalytic activity residing inside the channel of plant EXO9 contributes to the processing of 5.8S precursors. This is in line with the idea that 5.8S precursors that are too short to reach the catalytic site of RRP44, i.e in all likelihood 5.8S precursors with extensions of less than 33nt, are further trimmed by the phosphorolytic activity conferred by the RRP41 subunit of the exosome core complex. The results obtained by cloning of 3' RACE products suggest that EXO9 trims precursors extended for 16-25nt. This is in line with *in vitro* data showing that EXO9 trims its RNA substrates to a final size of 15 nt. Smaller than 15 nt substrates are probably too short to reach the active site of AtRRP41. Therefore, the 5.8S precursors with extensions of 10 and 11 nt are probably generated by a yet unknown activity. Hence, another ribonucleolytic activity yet to be identified contributes to 5.8S processing in *Arabidopsis*. However, similar to the situation in yeast, further processing of 5.8S+10 precursors requires AtRRP6L2. Hence, our current working model is that AtRRP44, EXO9 and a yet unidentified activity, and lastly AtRRP6L2 act sequentially to trim 5.8S rRNAs. The

final maturation of 5.8S rRNA may require additional ribonucleases alike the situation in yeast.

Testing this model will require further experiments. One interesting experiment that could be done immediately is to experimentally measure the distance between the entry of the exosome to the AtRRP41's active site. Substrates composed of double stranded RNAs with single stranded 3' extensions of different length should be tested in *in vitro* activity assays. If the reconstitution of an EXO9 +RRP44 complex *in vitro* would be successful, similar experiments could be performed to determine the length required to reach AtRRP44's active site. Of course, the minimal size to reach the active site of AtRRP44 or EXO9 might be different *in vivo*, due to the binding of exosome co-factors to the top of the plant exosome complex.

H. Does AtRRP6L2 interact with plant EX09?

Yeast and humans RRP6 homologs are systematically co-purified with exosome complexes, suggesting that they are tightly bound (Allmang et al., 1999; Mitchell et al., 1997; Tomecki et al., 2010). By contrast, the physical association of plant EXO9 with any of the homologues of Rrp6p (AtRRP6L1-3) was not shown to date (Chekanova et al., 2007; Lange et al., 2014). One possible explanation is that the association of AtRRP6L2 (or any other AtRRP6-like protein) is transient and is therefore not maintained during co-immunoprecipitation of the core exosome, under experimental conditions optimized to obtain mainly intact EXO9. Another technical reason may be that AtRRP6L2 could be difficult to detect by mass spectrometry, for instance because it is degraded during the experimental procedure. To further investigate whether AtRRP6L2 binds to the exosome complex or not we plan to perform co-immunoprecipitation experiments with tagged version of AtRRP6L2. Knowing that in yeast and humans the C-terminal part of RRP6 contacts exosome core, this experiment should be performed with N-terminal tagged version

of RRP6. Furthermore, formaldehyde crosslinking should be considered to stabilize transient interactions. To this end, I produced suitable *Arabidopsis* transgenic lines expressing tagged RRP6L2 in the *rrp6l2* background which could be used to perform these experiments. However only a positive outcome of the crosslinking experiment would allow final conclusions about a possible interaction of AtRRP6L2 with the core exosome.

Another scenario would be that AtRRP6-like proteins do indeed not interact with exosome core in plants. In fact, exosome core-independent functions were reported for RRP6-like proteins in plants: AtRRP6L1 was shown play an exosome-independent role in an RNA dependent DNA methylation (RdDM) pathway (Zhang et al., 2014). RRP6L2, was shown to specifically degrade a specific 18S rRNA precursor that is not a substrate of the exosome (Sikorski et al., 2015). In this context it is interesting to note that AtMTR4 is readily detected in plant exosome preparations. In yeast, the interaction of Mtr4 with the exosome is actually mediated by Rrp6 and Rrp47 (Schuch et al., 2014). The interaction of RR6L2 and RRP47 is conserved in plants (Sikorski et al., 2015), however, former work in the laboratory indicates that none of the plant RRP6-like proteins binds to AtMTR4, at least in yeast two-hybrid assays (unpublished data of Lucas Philippe). Hence, we can also not rule out that plant RRP6 homologs have lost the capacity to interact with the exosome core complex, and may even speculate that AtMTR4 can bind to EXO9 independently of AtRRP6L2. Maybe the activity that was retained within the core of the plant exosome has enabled the evolution of three AtRRP6-like proteins that do not bind or bind only transiently to the exosome core.

I. Other endogenous substrates of plant EXO9?

The most challenging task for future work is to identify further endogenous substrates of the plant EXO9's activity. Possibly, the activity of EXO9 may generally contribute to many if not all degradation functions of the exosome. However, it may

also have unique roles alike the trimming of particular rRNA precursors. An unbiased way to detect the substrates of EXO9's activity would be a genome-wide approach on *rrp41* plants complemented with catalytically active or inactive versions of AtRRP41. However, if the defects due to EXO9 lack of activity correspond only to extensions of few nucleotides, their genome-wide detection is technically challenging. In addition, as redundancy is a general problem in analyzing RNA degradation pathways, we cannot expect a pronounced accumulation of EXO9's substrates. Hence, approaches that are based on substrate accumulation as standard RNA-seq are not very promising. In fact, such an experiment was performed in collaboration with A. Dziembowski's laboratory but failed to identify new substrates of EXO9.

Applying a method like CRAC (in vivo RNA crosslinking) (Schneider et al., 2012), successfully used to identify the substrates of Rrp6p or Rrp44p in yeast, would be technically difficult to apply for EXO9 for several reasons. First, it would not allow to discriminate between the substrates of AtRRP41 and AtRRP44, since in both cases the substrates are threaded through the central channel. Second, reliable procedures to perform CRAC in plants have not been established yet.

Hence, targeted approaches to investigate the contribution of EXO9's activity to selected processes may be more straightforward. An obvious and interesting question to address is whether plant EXO9's contributes to the trimming of microRNA. In fact, my *in vitro* activity tests have shown that plant EXO9 degrades 21-nucleotide oligo(U) substrates, and that the substrate is only nibbled and not completely degraded. These findings are reminiscent of plant microRNAs that can be uridylated (tailed) and trimmed when the methyltransferase AtHEN1 is absent (Li et al., 2005). *hen1* mutants exhibit a pleiotropic phenotype comprising reduced organ size, altered rosette leaf shape and increased number of inflorescences (Ibrahim et al., 2010). Activities responsible for miRNA uridylation have been assigned to the nucleotidyltransferases AtHESO1 and AtURT1 (Chen et al., 2002).

By contrast, the exoribonuclease responsible for trimming uridylated miRNAs remains unknown. To check whether EXO9 activity is involved in microRNA trimming I crossed heterozygous HEN1/*hen1* plants with homozygous *rrp41* lines expressing either wild-type or mutated AtRRP41 protein. If miRNAs are degraded by EXO9 we would have expected to observe a partial rescue of the *hen1* phenotype by inactivation of EXO9. Intriguingly, genotyping of the progeny revealed that the *rrp41* mutation complemented with the transgenes did not segregate in a regular Mendelian manner. We would have expected to re-isolate plant carrying the RRP41 transgenes in a ration of 1:4. However, in average, only 1-5 out of one hundred F2 plants were homozygous *rrp41* plants. Even more intriguingly, this effect was similar for both $RRP41^{WT}$ and $RRP41^{Pi\text{-}Cat\text{-}}$ transgenes. For now, we cannot explain this observation although it seems that the abnormal segregation is not linked to Exo9's activity. By now I obtained plants heterozygous for *HEN1* allele, but homozygous for *rrp41* complemented with $AtRRP41^{WT}$ or $AtRRP41^{Pi\text{-}Cat\text{-}}$. In the progeny of obtained heterozygous plants we expect to obtain plants that are homozygous for both *hen1 rrp41,* complemented with AtRRP41. In the meantime, another strategy to elucidate the possible role of EXO9 in miRNA trimming must be developed.

The potential involvement of EXO9 in small RNA trimming is only one out of many possible functions that remain to be tested. The identification of novel endogenous substrates of plant EXO9's activity, though technically challenging, is critical to understanding its function.

General conclusion

Taken together, my work demonstrated that plant EXO9 has a phosphorolytic activity that is unique among eukaryotic exosomes. This activity contributes to ribosomal rRNA processing and may well be involved in other processes that remain to be identified.

My results are well in line with current models of 5.8S rRNA processing. However, further work will be required to better understand the precise contributions of each of the three activities that are associated with the plant exosome.

In particular, we should experimentally address the interaction of the plant exosome core complex and AtRRP6L2, and exploit *in vitro* approaches to better define the minimal length of the RNA substrates required to reach the active sites of plant EXO9 and EXO10.

Another interesting issue is to investigate the respective preferences for oligoadenylated and oligouridylated RNA substrates both *in vitro* and *in vivo*.

The identification of the endogenous substrates of the plant EXO's activity is a technical challenge, but could be crucial to finally understand why this unique activity is conserved in all land plants.

Materials and methods

Materials

Bacterial strains

Escherichia coli strain used for plasmid amplification was TOP10F' (Invitrogen), of genotype F- *mcrA* Δ(*mrr-hsd*RMS-*mcr*BC) Φ80*lac*ZΔM15 Δ *lac*X74 *rec*A1 *ara*D139 Δ(*ara leu*)7697 *gal*U *gal*K *rps*L (StrR) *end*A1 *nup*G.

Agrobacterium tumefaciens strain used for *Arabidopsis* transformation was GV3101 (pMP90), carrying the resistance to gentamycin on its chromosome and rifampicin resistance on Ti plasmid. Ti plasmid is disarmed, it possesses the *vir* genes needed for T-DNA transfer, but has no functional T-DNA region of its own.

Plant material and growth conditions

All *Arabidopsis thaliana* plants are in the Columbia-0 (Col-0) genetic background. All plant lines used or generated in this study are presented in Table 2. Plants were grown at 20-24 °C with 16h day/8h darkness cycles, either on soil or *in vitro* on MS agar plates supplemented with 0.5 % sucrose.

Vectors

pGEM-T® easy (Promega)

The pGEM-T® easy vector allows direct cloning of PCR products using TA cloning technique. This technique relies on the ability of adenine (A) and thymidine (T) on different DNA fragments to hybridize and become ligated in the presence of ligase. This linearized vector contains a single 3'-terminal thymidine at both ends. PCR products are generated by thermostable Taq DNA polymerase, which preferentially adds an adenine to the 3' end of the product. The cloning region is located within the region coding for β-galactosidase (under IPTG-inducible lac promoter), therefore successful cloning of an insert into this vector interrupts the coding sequence of β-

galactosidase and the recombinant clones can be identified by color screening on indicator plates (containing ampicillin for vector selection, and IPTG and X-Gal for vectors containing inserts selection).

Methods

Transformation of E. coli by heat shock

Competent *E. coli* cells stored at -80°C were thawn on ice for approximately 20 minutes. DNA (10 ng of plasmid DNA or 5 µL of the pGEM-Teasy® (Promega) ligation reaction) was added to each tube. The content of each tube was mixed by swirling gently. The tubes were stored on ice for 30 minutes. The tubes were transferred to a rack placed in a preheated 42 °C circulating water bath. The tubes were incubated at 42 °C for exactly 90 seconds. Samples were transferred to ice and chilled for about 1 minute. 1 mL of LB medium (10 g/L bacto-tryptone, 5 g/L yeast extract, 5 g/L NaCl, pH 7.2) was added to each tube. The cultures were incubated for 45 minutes at 37 °C to allow the bacteria to recover and to express the antibiotic resistance marker encoded by the plasmid. Cells were collected by centrifugation 5000 x g, resuspended in 100 µL of LB media and plated onto LB plates supplemented with appropriate antibiotics. Plates were incubated at 37 °C for 12-16 hours.

Plasmid isolation

Plasmids were isolated from transformed *E. coli* cells using the NucleoSpin® Plasmid kit according to the manufacturer's protocol. Cells were collected by centrifugation (30 seconds at 11,000 x g). The pellet was resuspended in 200 µL buffer A1 (50 mM Tris HCl pH 8, 10 mM EDTA, 5.5 µg/ml RNase A). Cells were lysed with 150 µL of buffer A2 (200 mM NaOH, 1 %(w/v) SDS). Lysates were neutralized with 150 µL Buffer A3 (3 M potassium acetate pH 5.3). Cell debris were removed by centrifugation for 1 min at 11,000 x g. Next, the supernatant was applied to a

NucleoSpin® Plasmid column. The column was washed with 500 µL of AW Buffer (50 % guanidine hydrochloride, 50 % isopropanol) and centrifuged at 11,000 x g for 1 minute. 600 µL of Buffer A4 (70 % EtOH, 10 mM Tris HCL pH 8) was added and samples were centrifuged for 1 minute at 11,000 x g. The columns were dried by centrifugation for 2 minutes at 11,000 x g. The plasmid DNA was eluted with 50 µL of Buffer AE (10 mM Tris HCl, 0.5 mM EDTA, pH 8.5). The DNA concentration was estimated by measuring UV absorption at 260nm with a Nanodrop 2000 Spectrophotometer (Thermo Scientific).

Transformation of Agrobacterium tumefaciens by heat shock

100 ng of DNA was added to 200 µL chemically competent *Agrobacterium tumefaciens* cells (strain GV3101). Samples were incubated for 30 minutes on ice. Samples were frozen in liquid Nitrogen and heat-shocked for 5 minutes at 37°C. Cells were incubated for 2 hours at 28 °C in 1 ml of LB medium before spreading on LB plates supplemented with rifampicin (34 µg/mL) and gentamycin (15 µg/mL) (to select for the strain and the helper plasmid present in the GV3101 strain) and a third antibiotic specific for transformed construct. Transformed colonies appeared after 3 days at 28 °C. For each construct, a single colony was transferred to 1 ml LB supplemented with rifampicin, gentamicin and a construct-specific antibiotic. Cultures were incubated at 28°C overnight.

Plant methods

DNA extraction from *Arabidopsis*

Genomic DNA was isolated from *Arabidopsis* leaf tissue (8mm^2) of Col-0 or mutant plants. The plant material was homogenized with glass beads in a Precellys grinder (6,500 rpm x 30 seconds x 2 x 5 second pause) in DNA extraction buffer (200 mM Tris HCl pH 7.5, 250 mM NaCl, 25 mM EDTA). Cell debris were removed by centrifugation (12,000 x g, 5 minutes, 4 °C). 0.7 vol isopropanol were added to the

supernatant, and after 5 minute incubation at room temperature, the precipitated DNA was collected by centrifugation for 10 minutes at 12000 x g. The pellet was washed with 70 % ethanol and collected by centrifugation for 10 minutes at 12000 x g. The pellet was dissolved in 40 µL of water and the DNA concentration was estimated by measuring UV absorption at 260 nm with a Nanodrop 2000 Spectrophotometer (Thermo Scientific). For high-throughput genotyping, 96-well plates were used. Plant material was homogenized with metal beads using TissueLyserII (Retch, force 30/s x 2) in DNA extraction buffer. Cell debris were removed by centrifugation (3700 x g, 10 minutes, 4 °C). 0.7 vol isopropanol were added to the supernatant, and after 5 minute incubation at room temperature, the precipitated DNA was collected by centrifugation for 10 minutes at 3700 x g. The pellet was washed with 70 % ethanol and collected by centrifugation for 10 minutes at 3700 x g. The pellet was dissolved in 40 µL of water and the DNA concentration was measured by Nanodrop.

Genotyping

The presence or absence of T-DNA insertions was determined by PCR amplification. Two gene-specific primers were used for the amplification of wild-type alleles. A gene-specific primer and a primer complementary to the left border of the T-DNA insertion were used for the detection of mutant alleles (primers used in this study are listed in Table 3).

Each PCR reaction of 20 µL contained 1x GoTaq Buffer (Promega), 1.5 mM MgCl2, 0.2 mM of each of dNTPs, 0.2 µM of each forward and reverse primers, 0.2 U (5 U/µL) GoTaq® DNA Polymerase and 100 ng of extracted DNA. PCR settings were 29 cycles of 30 s denaturation at 94°C, 30 s annealing at 50-54°C (depending on the primers used), and 1 minute elongation at 72 °C. PCR amplification products were separated by electrophoresis (135 mV, 20 minutes) in 1.5 % agarose in TBE 0.5x

(89 mM Tris; 89 mM Boric Acid; 2 mM EDTA), and visualized with ethidium bromide (0.7 µg/ml).

Agrobacterium -mediated transformation of *Arabidopsis thaliana*

Arabidopsis plants were transformed by the flower-dip method adapted from Clough and Bent (Clough and Bent, 1998). Three days prior to plant transformation, 5-ml liquid cultures (pre-cultures) of *Agrobacterium* carrying the binary vector of interest were inoculated and incubated at 28°C with vigorous agitation in LB medium containing suitable antibiotics. After 2 days, 200 ml of LB medium was inoculated with 1 ml of the pre-culture and incubated again with vigorous agitation for an additional 24 hours at 28°C. *Agrobacterium* cells were collected by centrifuging at 3000 x g for 10 minutes, at room temperature. The cell pellet was resuspended in 400 ml of infiltration medium (0.5x Murashige and Skoog salts supplemented with Gamborg's B5 vitamins (Duchefa), 5% sucrose (w/v), 50 µL/liter Silwet L-77). The *Agrobacterium* suspension was transferred the to a convenient vessel for dipping plants. Pot of plants were inverted and inflorescences were dipped the into the suspension and allowed to soak for 30 seconds. After dipping, the pots were layed on their sides for 15 minutes to remove excess of infiltration medium with *Agrobacterium*. After infiltration plants were placed under a plastic dome and protected by a non-transparent cover for the 48 hours before plants were returned to their normal growing conditions. After about 3 weeks, seeds were collected. In some experiments the T-DNA contained a GFP-tagged OLE0 protein expressed in the seed coat, allowing the selection of transformants with an epifluorescence microscope (Zeiss, Axio Zoom). In other experiments the T-DNA conferred resistance to the herbicide Bialophos.

Arabidopsis infection with TMV or ORMV

Virion preparation

Virions used in this study were a kind gift from Dr Khalid Amari and were prepared from infected *N. benthamiana* leaves. Leaves were homogenized to fine powder in liquid nitrogen. 1 ml 0.5 M sodium phosphate buffer pH 7.4 and 0.1 % 2-mercaptoethanol was added for each gram of leaf material. After addition of 1 vol butanol/chloroform 1:1 (v/v), phases were separated by centrifugation (2x 15 min at 12000 x g) and virions in the aqueous phase were precipitated with 4 % polyethylene glycol 8000 at 20000 x g. The pellet was resuspended in 10 mM sodium-phosphate buffer pH 7.4 and cleared by centrifugation at 5000 x g for 10 min. The supernatant was precipitated again with 4 % polyethylene glycol 8000 and 1 % NaCl and resuspended in 10 mM sodium phosphate buffer pH 7.4. Virion concentration was estimated from absorbance values at 260 nm.

Arabidopsis infection

Arabidopsis plants infected with *Tobacco mosaic virus* (TMV) or *Oilseed Rape Mosaic Virus* (ORMV) by rubbing the surface of the third true rosette leaf with carborundum (silicon carbide) covered with virion suspension or with 50 mM phosphate buffer (Mock). Upon systemic infection 4th day post inoculation (dpi) leaves 8 and 6 were harvested, snap-cooled in liquid nitrogen and stored at -80°C. Nine independent plants for each treatment were used.

Analysis of TMV or ORMV-infected plants

Four days post inoculation, total RNA for tails composition analysis was extracted using TRI Reagent® (MRC) according to the manufacturer's instructions, and then quantified with a Nanodrop 2000 (Thermo Scientific). RNA was reverse transcribed into cDNA using SuperScript II Reverse Transcriptase (Invitrogen). For cDNA synthesis 5 µg of total RNA was added to 4 µM oligo(dT) primer comprising a 3' adapter sequence and 18Ts, 0.5 mM dNTPs and water in a final volume of 15 µL.

After 2 minute denaturation at 60 °C samples were chilled on ice and the cDNA synthesis was performed in 25 µL reactions comprising 200 U SuperScript II Reverse Transcriptase (Invitrogen), 1 x reaction buffer provided by the manufacturer, 10 mM DTT and 1 U of RNaseOUT (Invitrogen). Samples were incubated 1 h at 50°C before the reaction was stopped by incubation for 15 minutes at 70°C. cDNAs were stored at -20°C.

To amplify tails added to 3' extremity of viral RNAs two PCR were performed. In the first PCR step, the viral tails were amplified using primers binding to the 3' end of the sequence encoding the coat protein and complementary to the adapter sequence added by the cDNA synthesis primer. Obtained PCR products served as a template for the second, nested PCR. Next, 3' RACE PCR products were cloned in pGEM®-T Easy (Promega) and analyzed by sequencing.

Subcellular localization of fluorescent proteins

The intracellular localization of GFP tagged wild-type and mutated versions of AtRRP41 proteins was analyzed by confocal microscopy. Plants expressing AtPAB2-RFP, AtMTR4-GFP and AtRRP4-GFP were used as controls for cytoplasmic, nucleolar and dual (cytoplasm and nuclei) localization. Plants were grown on MS agar plates supplemented with 0.5 % sucrose. Samples prepared from the root tips of 10-day old seedlings were analyzed with a ZEISS LSM 700 confocal microscope using a 510nm laser.

Gel filtration

200 mg of *Arabidopsis thaliana* flowers from myc-RRP41^{WT} or myc-RRP41$^{Pi\text{-}Cat\text{-}}$ transgenic lines were ground in 1 ml of 20 mM Tris HCl pH 7.6, 150 mM NaCl, 0.5% Tween20, EDTA-free cOmplete™protease inhibitors (Sigma Aldrich) at 4°C. Crude extracts were clarified by centrifugation at 16 000 x g and 150 000 x g for 5 and 15 min, respectively. 250 μl of the ultracentrifugation supernatant were

analyzed by gel filtration using a Superose 6 20 10/300 column (GE Healthcare Life Sciences) equilibrated in 20 mM Tris HCl pH 7.6, 150 mM NaCl, 0.1% Tween20 and run at 0.25 ml/min. Elution fractions containing myc-tagged RRP41 subunits were identified by western blot analysis using an anti-myc monoclonal antibody (Roche). The Superose 6 column was calibrated using Thyroglobulin (669 kDa), Aldolase (158 kDa) and RNaseA (14 kDa) markers (GE Healthcare Life Sciences). Elution fractions were collected and samples were separated by SDS-PAGE and analyzed by western blot using an anti-myc monoclonal antibody (Roche).

EXO9 purification from *Arabidopsis thaliana*

All procedures were performed at 4°C. 200 mg of frozen *Arabidopsis thaliana* flowers from Col-0, $RRP41^{WT}$, $RRP41^{Pi-}$, $RRP41^{Pi-Cat-}$ were ground in liquid nitrogen in ice-cold lysis buffer comprising 150 mM NaCl, 50 mM Tris HCl (pH 8.0), 1% Triton X100, and protease inhibitors cocktail (EDTA-free, cOmplete™, Sigma Aldrich). The lysate was clarified by centrifugation at 16 000 g for 5 min. The clarified lysate was centrifuged at 150 000 g for 15 min and the supernatant was incubated with anti-myc tagged magnetic MicroBeads (MACS Tech by Miltenyi Biotec) by rotating for 30 minutes. MACS Separation columns (M Columns, MACS Tech by Miltenyi Biotec) were placed in the magnetic field of the μMACS separator and equilibrated with lysis buffer. The lysates were applied onto the columns. Columns were rinsed four times with lysis buffer, two times washed with high salt buffer consisting of 250 mM NaCl, 20 mM MOPS, 0.1 % Triton X100. The two final washing steps were performed with elution buffer comprising 100 mM NaCl, 20 mM MOPS pH 7.5, 0.1% Triton X100. Proteins were eluted with 100 μL elution buffer (to be further used in in vitro activity assays) or with 100 μL Laemmli buffer (60 mM Tris-Cl pH 6.8, 2 % SDS, 10 % glycerol, 5 % β-mercaptoethanol, 0.01 % bromophenol blue) to be analyzed by SDS-PAGE and silver stain or by mass spectrometry. Mass-

spectrometric analysis was carried out by the Proteomic Platform at the Institut de Biologie Moléculaire et Cellulaire (IBMC) in Strasbourg.

In vitro activity assays of plant EXO9

Degradation and synthesis in vitro

Each 20 μL reaction contained 0.4 or 1.4 nM EXO9 complexes bound to anti-myc beads and 6.25, 25 or 35 nM of RNA substrate (EXO9 and RNA substrates concentrations are indicated in each figure). Activity assays were carried out at 20°C in reaction buffer comprising 50 mM NaCl, 20 mM MOPS pH 7.5, 1.5 mM MgCl2, 1.5 mM DTT, 1 U/µL RNase inhibitor, 0.05 % Triton X100. "+Pi" assays contained 3.5 mM potassium phosphate. Synthesis assays contained 1 mM of the indicated NDPs. 5 μL aliquots were taken at indicated time points and the enzymatic reaction was stopped by adding 5 μL formamide supplemented with 10 mM EDTA, 0.1 % bromophenol blue, and 0.1 % xylene cyanol FF. Samples were separated on 16% polyacrylamide, 7 M Urea and TBE and visualized by autoradiography. For TLC analysis, reactions were stopped with EDTA before samples were loaded on PEI-Cellulose F plates (Merck Millipore), resolved in 0.5 M LiCl 1 M formic acid, and visualized by autoradiography.

3' end labelling of RNA substrates

To obtain 3' labelled substrates for the in in vitro activity assays analyzed by thin layer chromatography, 10 pmol of RNA oligo were dissolved in 14.7 µL of water, heated at 70°C for 3 minutes and quenched on ice for 1 minute. 2 µL NEB buffer 2 (10x), 1 µL of Cid1 polyU polymerase (New England Biolabs) (2U/ µL) and 25 pmol of [α-^{32}P] UTP was added to the sample. The labelling was performed at room temperature for 15 minutes. Because of the respective concentrations of the RNA oligo and the labeled UTP, only 1 to 2 uridines were added to the 3' end of the RNA substrate. The reaction products were purified using G-50 columns.

5' end labelling of RNA substrates and probes

5 pmol of RNA (used as a substrate for EXO9 in *in vitro* activity assays)/DNA oligo (reverse complement of the RNA to be detected, used for northern blot) was resuspended in 9.5 μL water and heated at 70°C for 3 minutes and quenched on ice for 1 minute. 2 µL buffer A (10X, provided with T4 Polynucleotide Kinase (PNK), Thermo Scientific), 1 µL of T4 PNK (10U/ µL; Thermo Scientific) and 25 pmol of [γ-32P] ATP was added to the sample. Reaction was mixed by tapping the tube gently. Labelling was performed in a water bath at 37°C for 30 minutes. The reaction products were purified using G-50 columns. Table 4 lists sequences of RNA oligos used in *in vitro* activity assays (Figures 14-25). Table 3 lists probes used to detect RNA species by northern blot (Figures 27-34).

RNA analysis

RNA extraction

RNA from seedlings or leaves or flowers of Col-0 and mutant plants was extracted using the TRI Reagent® (MRC). Plant tissue was ground to a fine powder in liquid nitrogen using a mortar and pestle. 1 mL of TRIzol® Reagent was added per 100 mg of tissue. When samples were thawed, the suspension was transferred to a 1.5 mL tube, supplemented with 0.2 mL chloroform per each mL of TRIzol added. Samples were vortexed and incubated at room temperature for 5 minutes. Samples were centrifuged at 16,000 x g, for 15 minutes at room temperature. The aqueous phase was transferred to a fresh 1.5 ml tube. 0.5 volumes of isopropanol were added and samples were incubated for another 5 minutes at room temperature. Precipitated RNA was collected by centrifugation at 16,000 x g for 5 minutes at 4 °C. The supernatant was removed and pellets were washed with 1 ml of ice cold 70 % ethanol and then dissolved in 50 µL of water. samples were subjected into a second round of purification. Samples were further purified by adding 1 volume of a 25:24:1 mix of acid-phenol: chloroform: isoamyl alcohol, vortexed and incubated for 5

minutes at room temperature. Next, samples were centrifuged at 16,000 x g for 15 minutes at 4 °C. The upper aqueous phase was transferred to a fresh 1.5 mL tube, and supplemented with 1/10 volumes of 3 M NaAc pH 5.2, 2.5 volumes of 100 % ethanol, and 0,05-1µg/µL glycogen (Thermo Scientific) as a carrier when working with small amounts of RNA. RNA precipitation was carried out overnight at -20°C or for 2 hours at -80 °C.

RNA was collected by centrifugation at 16,000 x g for 15 minutes at 4 °C. The supernatant was removed, and the RNA pellet was washed with ice cold 70 % ethanol and centrifuged at 16,000 x g for 15 minutes at 4 °C. The ethanol was removed and the pellet was dissolved in 20 µL of water. RNA was quantified by measuring the absorption at 260 and 280 nm with a Nanodrop 2000 (Thermo Scientific). RNA samples were stored at -80°C.

Detection of endogenous RNA substrates of EXO9's phosphorolytic activity

RNA sample preparation and PAGE

For mapping of 3' extremities of EXO's endogenous substrates 20 μg of total RNA extracted from seedlings or flowers of Col-0, RRP41^{WT}, RRP41^{Pi-}, RRP41$^{Pi-Cat-}$ plants were treated with 10 µL of DNase I (50-375U/ µL, Invitrogen) in 1x DNase I buffer for 1 hour at room temperature. DNase was removed phenol/chloroform/isoamyl alcohol extraction before the RNA was precipitated and dissolved in water. Next, samples were dephosphorylated using 20 µL alkaline phosphatase FastAP (1U/ µL, Thermo Scientific) in 1x Fast AP buffer for 30 minutes at 37 °C.

Isolation of RNA fragments from polyacrylamide gels and mapping 3' ends of endogenous EXO9's substrates

Approximately 5 μg of total DNase-treated and dephosphorylated RNAs were separated on 6 % polyacrylamide, 7 M Urea and TBE and stained with ethidium bromide.

For mapping of 3’ extremities, RNA of 100 to 210 nt or 170-350 nt (for mapping 5’ETS or 5.8S rRNA precursors, respectively) were excised from the gel. Gel slices were frozen on dry ice, fragmented using a sterile 1 mL tip and eluted overnight in Maxam and Gilbert buffer (0.5 M ammonium acetate, 10 mM magnesium acetate, 1 mM EDTA and 0.1 % SDS) at 24°C. Size-selected RNAs were treated with 1 volume of 25:24:1 mix of acid-phenol: chloroform: isoamyl alcohol, precipitated and dissolved in water. Next, size-selected RNA was ligated to an RNA primer R1(5’P-CUAGAUGAGACCGUCGACAUGAAUUC-3’NH2) using T4 RNA ligase (Thermo Scientific). cDNA synthesis was initiated using a primer complementary to the ligated adapter (primers are listed in Table 3). 3’ ends were amplified by PCR using Dream Taq polymerase (30 cycles of 30 s denaturation at 94°C, 30 s annealing at 52°C and 10 s elongation at 72°C). 3' RACE PCR products were cloned in pGEM®-T Easy (Promega) and analyzed by sequencing.

Northern blot

Denaturing PAGE

Stock solution for 16% polyacrylamide urea gels was prepared as follows: 14.8 g urea, 16 mL 40% acrylamide (19:1) solution and 8 mL of 5X TBE were combined in a 50 mL falcon tube for a final volume of ~40 mL. The solution was incubated in water bath at 37°C and stirred until the urea dissolved completely. Then, 40 µL TEMED and 400 µL 10% APS were quickly added (a fresh APS aliquot was used for each gel). The mixture was quickly vortexed and the gels were poured using 10 mL pipet. Before loading the samples, the gel was pre-run in 1x TBE for 15 minutes at 15W. 5 μg of total RNA were ethanol-precipitated and dissolved in RNA loading buffer (95% (v/v) formamide, 0.025% (w/v) bromophenol blue, 0.025% (w/v) xylene cyanol FF, 5 mM EDTA, 0.025% (w/v) SDS, pH 8.5) and pre-heated at 65°C prior to loading onto the gel. Electrophoresis was performed in 1x TBE buffer at 15

W. Quality of electrophoresis and the equal loading of samples was assessed by staining the gel with ethidium bromide.

Transfer

Once separated by denaturing electrophoresis RNAs were transferred to HybondN+ (Amersham) nylon membranes using semi-dry horizontal transfer system (Bio-Rad). A nylon membrane and two identically-sized pieces of Whatmann paper were cut to fit the gel. All blot components were briefly soaked in 1x TBE. All components were placed in the transfer system, on the anode, as follows, first Whatmann paper, nylon membrane, gel and the second Whatmann paper. Bubbles were removed and top electrode (cathode) was assembled. Transfer was performed for 45 minutes at 20V. Immediately after transfer was completed the membrane was UV crosslinked with an energy of 120 mJ (Hoefer).

Membranes were placed into a hybridization tube with the RNA-side facing to the interior, and 10-15 mL of 0.5 M sodium phosphate pH 7.2, 7 % SDS buffer were added. Pre-hybridization was carried out 30 minutes at 45-50°C (depending on the melting temperature of the primer used as a probe). 5' labeled probe was added to hybridization buffer and hybridization was performed at 42°C for 10-18 h.

Membranes were washed three times with 2x SSC, 0.5% SDS for 30 minutes at 35°C. The last washing step was performed using 2x SSC. Finally, membranes were exposed to X-ray film (Kodak) with an enhancer screen at -80°C for 5-24 h depending on the strength of the signal.

For reprobing, membranes were stripped with 0.1% SDS pre-heated to 85°C. The solution was allowed to cool down at room temperature, and the procedure was repeated with pre-heated 0.1% SDS. Efficiency of stripping was checked by exposing the membrane to a X-ray film. After stripping, membranes were rinsed for 5 minutes with 2x SSC at RT to remove the excess SDS, transferred to a hybridization tube and hybridized with a new probe.

Protein analysis

Protein extraction using SDS Urea buffer

Arabidopsis thaliana inflorescences (2-3 flower buds) were homogenized in 1.5 mL tubes in 150-300 µL of SDS Urea extraction buffer (80 mM Tris HCl pH 6.8, 0.1 M DTT, 4 M Urea, 2 % (w/v) SDS, 10 % (v/v) Glycerol) using a pestle. Samples were heated for 3 minutes at 80 °C and cell debris were removed by centrifugation at 16,000 x g for 5 minutes at room temperature. The supernatant was transferred to a fresh 1.5 ml tube and stored at -20°C.

Protein extraction using phenol buffer

100 mg of frozen *Arabidopsis thaliana* inflorescences were ground in a mortar in the presence of liquid nitrogen and extracted with 600 µL of extraction buffer (0.7 M sucrose, 0.5 M Tris-Cl pH 8.0, 0.1 M NaCl, 5 mM EDTA pH 8.0, 2% β-mercaptoethanol) and vortexed. 600 µL of Tris buffered phenol were added and the mixture was vortexed for 5 minutes at RT. Samples were centrifuged at 13,000 x g for 10 min at 4°C. The phenolic phase was collected and precipitated overnight with 5 volumes of 0.1 M ammonium acetate in methanol at −20°C. Protein precipitates were collected by centrifugation at 13,000 x g for 15 min at 4°C, and washed twice with ice cold 0.1 M ammonium acetate in methanol. The pellet was dried and resuspended in 50-100 µL of resuspension buffer (10% glycerol, 3% SDS, 60 mM Tris HCL pH 8.0).

SDS-PAGE

The Bio-Rad MiniProtean Tetra System was used for SDS-PAGE. The separating gel contained 10 % (w/v) Acrylamide/Bisacrylamide 29:1, 100 mM Tris HCl pH 8.8, 0.1 % (w/v) SDS, 0.1 % (w/v) APS, 0.05 % (v/v) TEMED). The stacking gel contained 4 % (w/v) Acrylamide/Bisacrylamide 29:1, 100 mM Tris HCl pH 6.8, 0.1 % (w/v) SDS, 0.05 % (w/v) APS, 0.1 % (v/v) TEMED. Protein samples in 1x Laemmli buffer (60 mM Tris-Cl pH 6.8, 2 % SDS, 10 % glycerol, 5% β-mercaptoethanol, 0.01 % bromophenol blue) were pre-heated for 5 minutes at 95 °C prior to loading onto gel. Electrophoresis was performed at 25 mA/gel for 90 minutes in 2.5 mM Tris pH 8.3, 19.2 mM Glycine, 0.01 % SDS (w/v).

Western blot

After electrophoresis, proteins were transferred to a PVDF membrane (Immobilon P, Millipore) activated with 100 % methanol prior to transfer.

All blot components were briefly soaked in transfer buffer (25 mM Tris 192 mM Glycine pH 8.3, 15% methanol). The gel and the methanol-activated PVDF membrane were placed between two pieces of filter paper and two sponges and assembled in a Bio-Rad Trans-Blot SD system. The transfer was performed in transfer buffer for 45 minutes with 250 mA at 4 °C. After transfer the membranes were incubated in 50 ml TBS-T with 5 % milk powder (50 mM Tris HCl, pH 7.6, 150 mM NaCl, 0.1% Tween 20, 5 % milk) to avoid unspecific adsorption of the antibody.

To detect myc-tagged proteins, membranes were incubated for 1 hour at room temperature with 1/10000 α-myc antibody (Roche) in TBS-T supplemented with 5% milk. Membranes were rinsed 3 times with TBS-T and incubated with 1/10000 goat anti-mouse secondary antibody in TBS-T with 5% milk. To detect GFP-tagged proteins, membranes were incubated with HRP-coupled anti-GFP antibodies (Milteyi) (1:5000 in TBS-T, 2 % milk) for 1 hour at RT. Membranes were washed

three times in TBS-T for 5 minutes. After washing, membranes were revealed with Lumi LightPlus (Roche). Luminescence was detected with a Fusion FX camera system.

Protein staining

Coomassie staining of the SDS-PAGE gel

SDS-PAGE gels were rinsed with water and incubated with Coomassie staining solution (0.0025% Coomassie Brilliant Blue R-250, 90% methanol, 10% acetic acid) for 30 min – 16h before the the staining solution was removed incubation with destaining solution (90% methanol, 10% acetic acid) for 30-60 minutes.

Silver staining

SDS-PAGE gels were fixed in 50% methanol, 12% trichloric acid, 2% CuCl2 for 25 minutes, washed in 10% ethanol, 5% acetic acid for 20 minutes, sensitized in 0.01 % KMnO4 for three minutes, and washed for 10 minutes in 10% ethanol, 5% acetic acid, for 10 min in 10% ethanol, and for 10 min in water. Gels were incubated in 0.2 % silver nitrate (AgNO3) for 20 minutes. The excess of silver nitrate was removed by brief rinsing the gel with water. Gels were incubated with 10% potassium carbonate (K2CO3) for 1 minute and developed with 3% potassium carbonate and 0.05% formaldehyde solution until protein bands were visualized. The developing reaction was stopped by incubating the gel with 1% acetic acid for 5-10 minutes.

Table 2. Plant material used and generated in this study.

mutant name	gene	AGI	coordinates	additional information
rrp41 RRP41^{WT}	*RRP41*	At3g61620	Salk_112819	Heike Lange; rrp41 complemented with myc-tagged AtRRP41WT
rrp41 RRP41^{Pi-}	*RRP41*	At3g61620	Salk_112819	Heike Lange; rrp41 complemented with myc-tagged AtRRP41Pi-
rrp41 RRP41$^{Pi-Cat-}$	*RRP41*	At3g61620	Salk_112819	Heike Lange; rrp41 complemented with myc-tagged AtRRP41Pi-Cat-
rrp6L1 (A3)	*RRP6L1*	At1g54440 (A=L1)	GABI_344G09 (A3)	Lange et al., 2008
rrp6L2 (B4)	*RRP6L2*	At5g35910 (B = L2)	GABI_825G09 (B4)	Lange et al., 2008
rrp6L3 (C3)	*RRP6L3*	At2g32415 (C= L3)	GABI_691C02 (C3)	Lange et al., 2008
RRP44KD1	*RRP44A*	At2g17510	Col-0	Kumakura et al., 2013; Col-0 background plants expressing artificial RNAs (amiR_RRP44A-2) RRP44A
RRP44KD2	*RRP44A*	At2g17510	Col-0	Kumakura et al., 2013; Col-0 background plants expressing artificial RNAs (amiR_RRP44A-2) *RRP44A*
mtr4-1	*MTR4*	At1g59760	GABI_048G02	

hen2-1	*HEN2*	At2g06990	GABI_774H07	
hen1-6	*HEN1*	At4g20910	Salk_090960	
rrp41 RRP41^{WT} rrp6 L1	*RRP41, RRP6L1*			this study
rrp41 RRP41$^{Pi\text{-}Cat\text{-}}$ rrp6L1	*RRP41, RRP6L1*			this study
rrp41 RRP41^{WT} rrp6L2	*RRP41, RRP6L2*			this study
rrp41 RRP41$^{Pi\text{-}Cat\text{-}}$ rrp6L2	*RRP41, RRP6L2*			this study
rrp41 RRP41^{WT} rrp6L1 rrp6L2	*RRP41, RRP6L1, RRP6L2*			this study
rrp41 RRP41$^{Pi\text{-}Cat\text{-}}$ rrp6L1 rrp6L2	*RRP41, RRP6L1, RRP6L2*			this study
rrp41 RRP41^{WT} rrp6L1 rrp6L2 rrp6L3	*RRP41, RRP6L1, RRP6L2, RRP6L3*			this study
rrp41 RRP41$^{Pi\text{-}Cat\text{-}}$ rrp6L1 rrp6L2 rrp6L3	*RRP41, RRP6L1, RRP6L2, RRP6L3*			this study
rrp41 RRP41^{WT} rrp6 L3	*RRP41, RRP6L3*			this study
rrp41 RRP41$^{Pi\text{-}Cat\text{-}}$ rrp6L3	*RRP41, RRP6L3*			this study
rrp41 RRP41^{WT} mtr4	*RRP41, MTR4*			this study
rrp41 RRP41$^{Pi\text{-}Cat\text{-}}$ mtr4	*RRP41, MTR4*			this study
rrp41 RRP41^{WT} hen2	*RRP41, HEN2*			this study
rrp41 RRP41$^{Pi\text{-}Cat\text{-}}$ hen2	*RRP41, HEN2*			this study

rrp41 RRP41^{WT} RRP44KD1	*RRP41, RRP44A*			7 independent lines; this study
rrp41 RRP41^{WT} RRP44KD2	*RRP41, RRP44A*			11 independent lines; this study
rrp41 RRP41$^{Pi\text{-}Cat\text{-}}$ RRP44KD1	*RRP41, RRP44A*			4 independent lines; this study
rrp41 RRP41$^{Pi\text{-}Cat\text{-}}$ RRP44KD2	*RRP41, RRP44A*			11 independent lines; this study
rrp41 RRP41^{WT} rrp6L2 RRP44KD2	*RRP41, RRP6L2, RRP44A*			15 independent lines, this study
rrp41 RRP41$^{Pi\text{-}Cat\text{-}}$ rrp6L2 RRP44KD2	*RRP41, RRP6L2, RRP44A*			15 independent lines, this study
rrp41 RRP41^{WT} mtr4 RRP44KD2	*RRP41, MTR4, RRP44A*			15 independent lines, this study
rrp41 RRP41$^{Pi\text{-}Cat\text{-}}$ mtr4 RRP44KD2	*RRP41, MTR4, RRP44A*			15 independent lines, this study
hen1-6/HEN1 rrp41 RRP41^{WT}	*RRP41, HEN1*			this study
hen1-6/HEN1 rrp41 RRP41$^{Pi\text{-}Cat\text{-}}$	*RRP41, HEN1*			this study
hen1-6 RRP4KD	*RRP41, HEN1*			this study; homozygous *hen1-6* plants expressing artificial miRNAs (amiRRRP4-3) against *RRP4*
hen1-6 RRP41KD	*RRP41, HEN1*			this study; homozygous *hen1-6* plants expressing artificial miRNAs (amiR_RRP41-1) against *RRP41*

hen1-6 RRP44KD	*RRP41, HEN1*			this study; homozygous *hen1-6* plants expressing artificial miRNAs (amiR44P44A-2) against *RRP44*
rrp6L1 RRP6L1-GFP	*RRP6L1*	At1g54440 (A=L1)		this study; RRP6L1-GFP expression to be tested
rrp6L1 RRP6L1-myc	*RRP6L1*	At1g54440 (A=L1)		this study; RRP6L1-myc expression to be tested
rrp6L2 RRP6L2-GFP	*RRP6L2*	At5g35910 (B = L2)		this study; *rrp6L2* line expressing RRP6L2-GFP
rrp6L2 RRP6L2-myc	*RRP6L2*	At5g35910 (B = L2)		this study; *rrp6L2* line expressing RRP6L2-myc

Table 3. DNA oligonucleotides used in this study

Gene	description	Sequence 5'-3'	Application
At3g61620	RRP41-Fw	TTCCTTCAGGTTCTACAAGCTG	genotyping
At3g61620	RRP41-wt-Rev	CCTCAACTTCCACAAACAACAG	genotyping
technical	Salk-left border	ATTTTGCCGATTTCGGAAC	genotyping
technical	RRP41-myc-Rev	TAGCTTTTGTTCACCGTTAATTAAC	genotyping
technical	RRP41-WT-or-PiCAt-Rev	CCTTGCAACCTTCAGAAGC	NdeI digestion site introduced; to distinguish between WT and Pi-Cat-RRP41
At1g54440	RRP6L1-Fw	GAGCTTCAGCGTCTTCTCTG	genotyping
At1g54440	RRP6L1-wt-Rev	TCTGTGCCTGTTTTCTCAATC	genotyping
technical	Sail-left border	GCTTCCTATTATATCTTCCCAAATTACCAATACA	genotyping
At5g35910	RRP6L2-Fw	GTGGTTACTGGCTCGGCA	genotyping
At5g35910	RRP6L2-wt-Rev	ATACTGACAGCCAAAACATAACCC	genotyping
technical	Gabi-left border	GGGCTACACTGAATTGGTAGCTC	genotyping
At2g32415	RRP6L3-Fw	TGTGGGTTGAGACAGAGTCG	genotyping
At2g32415	RRP6L3-wt-Rev	GCACATAGAAATTTGGGGGAC	genotyping
At1g59760	MTR4-Fw	CCGTAGATGTGTTGACTAGATG	genotyping
At1g59760	MTR4-wt-Rev	CTAGCCTTCGTAAAACACGC	genotyping
At2g06690	HEN2-Fw	CAGAAACCGTAAATGTTTTGGAAT	genotyping
At2g06690	HEN2-Rev	ATTGTCCTTCGGCACGACTC	genotyping
At4g20910	HEN1-Fw	ACTCAACAACTTCCTCATCG	genotyping
At4g20910	HEN1-wt-Rev	TACTCCTACTCCAAAGGCG	genotyping
nuclear rRNA	S1	ACGCCGAACGTTCAATTAACTC	Northern blot
nuclear rRNA	S2	AGGATGGTGAGGGACGACGATTT	Northern blot
nuclear 5.8S	5.8S-Fw	TCTGCCTGGGTGTCACAAATC	3'RACE
nuclear 18S	5'ETS-Fw	ATCTCGCGCTTGTACGGCTTTG	3'RACE
technical	Adapter-Rev	GAATTCATGTCGACGGTCTCA	3'RACE
technical	PT18	GCTGTCAACGATACGCTACGTAACGGCATGAC AGTGT18	cDNA synthesis
technical	P1 (Rev)	GCTGTCAACGATACGCTACGT	3'RACE
technical	P2 (Rev)	CTACGTAACGGCATGACAGTG	3'RACE

TMV gRNA	TMV-5372-94 (Outer) (Fw)	TGGAGTTTGTGTCGGTGTGTATT	3’RACE
TMV gRNA	TMV-6023-44 (Inner) (Fw)	GACTGCCGAAACGTTAGATGCT	3’RACE
ORMV gRNA	ORMV-6015-34	TATTACCTTGGGCTACTGCG	3’RACE
ORMV gRNA	ORMV-6037-56	AACAGGGCAGAGTTCGAGGT	3’RACE

Table 4. RNA oligonucleotides used in this study.

Name	Sequence 5’ -3’	Length	Application
R1	[pC]UAGAUGAGACCGUCGACAUGAAUU[C-NH2]	26	Adapter for 3’RACE
miR168	UCGCUUGGUGCAGGUCGGGAA	21	*in vitro* activity assay
miR168Meth	UCGCUUGGUGCAGGUCGGGA[mA]	21	*in vitro* activity assay
$(U)_{21}$	UUUUUUUUUUUUUUUUUUUUU	21	*in vitro* activity assay
$(A)_{21}$	AAAAAAAAAAAAAAAAAAAAA	21	*in vitro* activity assay
5‘-FAM-$(H)_{29}(U)_2$	5'FAM-CCCCACCACCAUCACUUCACCACCAUCACUU	31	*in vitro* activity assay
5‘-FAM-$(H)_{17}(A)_{14}$	5'FAM-CCCCACCACCAUCACUUAAAAAAAAAAAAAA	31	*in vitro* activity assay
5‘-FAM-$(H)_{17}(A)_{12}(U)_2$	5'FAM-CCCCACCACCAUCACUUAAAAAAAAAAAAUU	31	*in vitro* activity assay

Contexte biologique

La dégradation des ARN est un processus finement contrôlé jouant un rôle primordial dans le traitement et le renouvellement des ARN codants et non codants. Parmi les acteurs de la dégradation, l'**exosome** constitue un complexe exoribonucléolytique ayant une activité majeure dans la régulation d'un panel varié de substrats ARN. L'exosome a été découvert comme l'activité 3'-5' exoribonucléolytique responsable de la maturation de l'extrémité 3' de l'ARN ribosomal (ARNr) 5.8S chez la levure Saccharomyce cerevisiae (Mitchell et al., 1997, 1996). Depuis, plusieurs études transcriptomiques globales réalisées chez les plantes, les levures, les insectes ou chez l'homme ont révélé l'exosome comme un facteur primordial impliqué dans la maturation ou la dégradation de virtuellement toutes les classes d'ARN codants et non-codants (Chekanova et al. 2007, Kiss and Andrulis, 2010, Gudipati et al., 2012, Schneider et al. 2012, Szczepinska et al., 2015).

Dans le noyau, les fonctions principales de l'exosome sont la maturation de précurseurs d'ARN non-codants, ainsi que la détection et l'élimination d'ARN aberrants et de sous-produits de maturation. L'exosome nucléaire est notamment impliqué dans la maturation des ARNr, des petits ARN nucléaires ou snRNA et des petits ARN nucléolaires ou snoRNA (Allmang et al., 1999a, 1999b; van Hoof et al., 2000). Parmi les substrats de l'exosome nucléaire figurent également les précurseurs des sn(o)RNA, des ARNm et les ARN de transfert (ARNt) présentant des défauts de maturation. L'exosome est aussi crucial pour l'élimination d'ARN non-codants issus de la transcription de régions intergéniques comme les CUTs (cryptic unstable transcripts) chez la levure ou les PROMPTs (PROMoter uPstream Transcripts) chez l'homme (LaCava et al., 2005; Neil et al., 2009; Orban and Izaurralde, 2005; Preker et al., 2008; Schneider et al., 2012; Vanácová et al., 2005; Wyers et al., 2005). Enfin, l'exosome est responsable de l'élimination des sous-produits de la maturation de transcrits primaires. Ces sous-produits de maturation incluent les introns épissés ou les espaceurs internes et externes excisés au cours de la maturation des ARNr.

Dans le cytoplasme, l'exosome contribue à la dégradation générale des ARNm et est impliqué dans l'élimination d'ARNm défectueux ou dont la traduction est bloquée. Ces différents ARNm sont pris en charge par des voies spécialisées de contrôle de qualité des

ARNm (nonsense-mediated decay, nonstop decay or no-go decay pathways) (Anderson and Parker, 1998; Bousquet-Antonelli et al., 2000; Doma and Parker, 2007; Gudipati et al., 2012; van Hoof et al., 2000; Houseley and Tollervey, 2009; Schneider et al., 2012).

L'exosome cible une très grande variété de substrats grâce à de nombreuses protéines adaptatrices qui fournissent une spécificité de reconnaissance permettant d'identifier les substrats de l'exosome et de discriminer entre les ARN destinés à la dégradation ou à la maturation. Ainsi, l'exosome interagit dans le noyau et le cytosol avec des hélicases ARN de type MTR4/SKI2. Ces hélicases participent à la reconnaissance des RNPs dont l'ARN devient substrat de l'exosome. Elles déstabilisent les structures secondaires des ARN et les interactions de protéines associées à l'ARN. Enfin, elles orientent l'extrémité 3' des ARN substrats au travers du canal central de l'exosome afin de les présenter au site actif, siège de la dégradation ribonucléolytique de 3' en 5'. L'hélicases nucléaire MTR4 s'associe à des facteurs accessoires comme des poly(A) polymérases et des protéines de liaison à l'ARN (Schneider and Tollervey, 2013; Lubas et al., 2012). Chez la levure, Mtr4 est en complexe avec une poly(A) polymérase non-canonique (Trf4 ou Trf5) et une protéine de liaison à l'ARN (Air1 ou Air2) formant le complexe TRAMP (pour Trf4/5-Air1/2-Mtr4 polyadenylation complex). Chez l'homme, MTR4 est partie intégrante de deux complexes distincts, dans le nucléole et le nucléoplasme. Dans le nucléole, MTR4 forme un complexe de type TRAMP, alors que dans le nucléoplasme, elle s'associe avec d'autres types de protéines de liaison à l'ARN formant le complexe NEXT (pour nuclear exosome-targeting complex) qui est notamment impliqué dans l'élimination de transcrits PROMPTs ou d'ARN défectueux (Lubas et al., 2011; Lubas et al., 2015). De manière intéressante, chez *Schizosaccharomyces pombe* et les plantes, il existe un deuxième type d'hélicase nucléaire de type MTR4, appelées Mtl1 (pour MTR4-like) et HEN2, respectivement. Ces hélicases s'associent avec différents facteurs pour assister l'exosome dans la dégradation de transcrits cryptiques ou défectueux comme des ARNm non-épissés (Lange et al., 2014; Zhou et al., 2015).

En raison de son implication dans la maturation, le contrôle de qualité et la dégradation de virtuellement toutes les classes d'ARN, l'exosome représente un acteur clé du métabolisme des ARN dans la cellule eucaryotique.

Bien que le nombre de sous-unités varie, l'organisation structurale de l'exosome est globalement conservée entre les eucaryotes et les archées (Dziembowski et al., 2007; Chlebowski et al., 2011, Schneider et al., 2012). Chez les eucaryotes, l'exosome est composé de 9 sous-unités (**EXO9**) qui forment une structure en tonneau dont le centre renferme un canal assurant le passage des macromolécules d'ARN. Cette architecture est similaire à celle observée pour la RNase PH et la polynucléotide phosphorylase (PNPase), deux enzymes phosphorolytiques bactériennes. Chez les archées, l'exosome possède une activité phosphorolytique processive assurée par ses 3 sites catalytiques situés dans le canal central. *A contrario*, chez l'homme et la levure, la présence d'une mutation au sein du site de coordination du phosphate rend EXO9 catalytiquement inactif. De ce fait l'activité de l'exosome chez l'homme et la levure est assurée par l'activité hydrolytique de RNases qui lui sont physiquement associées. Ces enzymes comprennent Rrp6, Rrp44/Dis3 et, uniquement chez l'homme, Dis3L (Chlebowski et al., 2011). Bien qu'il existe des voies par lesquelles les substrats de l'exosome peuvent être dégradés indépendamment de l'utilisation de son canal central (Schneider et al., 2012; Liu et al., 2014), la majorité des ARN passent à travers ce dernier pour atteindre soit le site actif de Rrp41 (dans le cas des archées) ou Rrp44 (chez l'homme et la levure) (Schneider et al, 2012; Wasmuth and Lima, 2012; Drazkowska et al., 2013).

L'interaction entre EXO9 et RRP44 est conservée chez ***Arabidopsis*** (Lange et al., 2014). En revanche si trois homologues de RRP6 (RRP6-Like) sont bien présents chez les plantes, aucune étude d'interaction entre ces derniers et l'exosome n'a jusqu'alors permis de valider un quelconque lien physique. De manière intéressante, la protéine **RRP41**, une des sous-unités du cœur de l'exosome, semble avoir retenu son **activité phosphorolytique** chez la plante. Des alignements de séquences suggèrent que les résidus requis pour cette dernière sont conservés dans toute la lignée verte bien qu'absent chez ses homologues eucaryotes dont le cœur de l'exosome est catalytiquement inactif. L'exosome rencontré chez les plantes pourrait alors être le seul, parmi l'ensemble de ceux présents chez les eucaryotes, à avoir maintenu une activité phosphorolytique au sein de son canal central.

Les objectifs de ma thèse ont été les suivants :

i. Tester l'existence de l'activité catalytique du cœur de l'exosome chez les plantes
ii. Comprendre quelle est la contribution apportée par l'activité phosphorolytique de EXO9 par rapport à l'activité hydrolytique des protéines RRP44 et RRP6-Like dans les processus de dégradation des ARN *in vivo*.

L'ensemble des résultats obtenus permet de mieux appréhender le rôle joué par l'activité phosphorolytique de l'EXO9 et les raisons évolutives de sa conservation dans toute la lignée verte.

RESULTATS

A. L'EXO9 d'Arabidopsis possède une activité phosphorolytique

Afin de déterminer expérimentalement si EXO9 de plante a maintenu une activité phosphorolytique, j'ai effectué des tests d'activité *in vitro* en présence d'exosome purifié de plantes d'*Arabidopsis*. La purification de complexes d'exosomes a été réalisée à partir de lignées mutantes *rrp41* complémentées avec une version sauvage de RRP41 ($RRP41^{WT}$), ou des versions mutées de ce dernier ($RRP41^{PI-}$, $RRP41^{PI-CAT-}$), fusionnée à une étiquette à leur extrémité C-terminale. Les versions mutées de RRP41 correspondent à des mutants catalytiques qui ont été soit mutés dans le site de coordination du phosphate ($RRP41^{PI-}$) ou doublement mutés dans le site de coordination du phosphate et le site catalytique ($RRP41^{PI-CAT-}$). L'expression des protéines recombinantes $RRP41^{WT}$, $RRP41^{PI-}$ et $RRP41^{PI-CAT-}$ se fait sous la dépendance du promoteur endogène de RRP41. Plusieurs expériences tendent à démontrer d'une intégrité et d'une fonctionnalité préservées des différentes versions de RRP41 *in vivo*. Tout d'abord, une analyse en western blot a montré que les versions sauvage et mutées de RRP41 étiquetées soit par myc soit par la GFP sont exprimées à des niveaux comparables (Figure 1A). De plus, l'ensemble des versions de RRP41 ($RRP41^{WT}$, $RRP41^{PI-}$ et $RRP41^{PI-CAT-}$) présentent une double localisation nucléaire et cytoplasmique (Figure 1B). Des analyses de gel filtration révèlent aussi que les différentes versions de RRP41 sont incorporées dans des complexes protéiques de haut poids moléculaire (Figure 1C). Enfin, des analyses en spectrométries de masse, montrent que toutes les sous-unités de l'EXO9

sont copurifiées avec les différentes versions de RRP41, qu'elles soient sauvage ($RRP41^{WT}$) ou catalytiquement inactives ($RRP41^{PI-}$ ou $RRP41^{PI-CAT}$) (Figure 2A and B).

Chez la plante, la conservation des acides aminés du site de coordination du phosphate présent au sein de la sous-unité RRP41 suggère que l'exosome a retenu une activité phosphorolytique. Une telle activité phosphorolytique implique que l'**activité des fractions d'EXO9** purifiées soit dépendante de la présence de phosphate inorganique (**Pi**), conduise à la libération de nucléosides diphosphates (**NDP**) et soit **réversible** (c'est à dire que EXO9 ayant incorporé RRP41 actif soit capable de synthétiser de l'ARN en présence d'excès de nucléosides diphosphates). En vue de tester l'activité enzymatique de ces fractions, j'ai réalisé des expériences de cinétiques enzymatiques à partir de fractions d'exosomes purifiées contenant la version de RRP41 sauvage ($RRP41^{WT}$) ou catalytiquement inactives ($RRP41^{PI-}$, $RRP41^{PI-CAT-}$) ainsi que d'un substrat ARN radiomarqué.

J'ai dans un premier temps incubé les différentes versions purifiées de l'EXO9 avec de l'ARN radiomarqué avec ou sans ajout de phosphate inorganique. J'ai observé une dégradation d'un substrat ARN en présence d'exosome contenant la version sauvage de RRP41 mais pas en présence de celles contenant les versions catalytiquement inactives. Cette activité, c.-à-d. la dégradation des substrats ARN par l'exosome, est de surcroît stimulée par l'addition de Pi dans le milieu réactionnel (Figure 3A). Dans un second temps j'ai analysé le produit de cette réaction par chromatographie sur couche mince (TLC pour Thin Layer Chromatography). Cette expérience a révélé que la réaction produit bien des nucléosides diphosphates (Figure 3B). J'ai finalement procédé à un dernier type de test d'activité dans lequel j'ai ajouté un excès de NDP sans ajout de Pi. J'ai observé, dans ces conditions, que l'EXO9 est capable de synthétiser de l'ARN et donc que la réaction est réversible (Figure 3C). La stimulation de l'activité de l'exosome suite à l'ajout de phosphate inorganique, le relargage de NDP et la réversibilité de la réaction ont démontré que **l'EXO9 *d'Arabidopsis* a bel et bien une activité phosphorolytique conférée par la sous-unité RRP41**.

En sus, l'ensemble de ces expériences m'a permis de révéler des caractéristiques inattendues concernant l'activité catalytique de l'exosome. J'ai montré que, de façon surprenante, l'EXO9 dégrade préférentiellement des substrats oligo(U) plutôt qu'oligo(A).

De plus, et en opposition avec l'activité processive observée pour les enzymes phosphorolytiques procaryotes (l'exosome des archées ou les PNPase bactériennes), la dégradation par l'exosome chez la plante est une activité distributive (Figure 3D). Ces deux observations pourraient avoir un rôle fondamental pour la compréhension des fonctions liées à l'activité phosphorolytique de l'exosome chez les plantes.

B. L'EXO9 contribue à la dégradation des ARN ribosomiques

Mes tests d'activité *in vitro* ont révélé que l'EXO9 *d'Arabidopsis* a une activité phosphorolytique distributive. De plus, EXO9 est capable de rogner plutôt que de complètement dégrader ses substrats *in vitro*. Il est important de noter que la présence de co-facteurs *in vivo* pourrait modifier ces propriétés, et il est possible que l'activité de EXO9 puisse à la fois rogner et complètement dégrader ses substrats *in vivo*. Afin de rechercher des substrats d'EXO9 *in vivo*, j'ai décidé de tester l'influence potentielle de l'activité intrinsèque de EXO9 sur deux substrats archétypiques de l'exosome : la partie 5' du précurseur des ARNr ou 5'ETS (pour External Transcribed Spacer) et les précurseurs des ARNr 5.8S, tous deux connus comme étant des substrats de l'exosome chez tous les eucaryotes (Schneider et al., 2012; Gudipati et al., 2012; Lange et al., 2011, Kumakura et al. 2013, Sikorski et al. 2015).

Pour ce faire, j'ai dans un premier temps analysé par northern blot l'accumulation des **fragments P-P1**, sous-produits de maturation dérivant de la 5'ETS. De manière intéressante, j'ai observé des profils particuliers de ces fragments dans les plantes exprimant la version sauvage ou inactive de RRP41. Tandis que trois fragments de tailles différentes sont observés dans des plantes sauvages et des plantes de la lignées mutante *rrp41* complémentées avec RRP41^{WT}, seulement deux des fragments les plus larges sont observés dans les lignées mutantes complémentées avec les versions catalytiquement inactives de RRP41 (Figure 4A). Cette observation indique que la production des intermédiaires P-P1 de plus petite taille est exclusivement permise par l'activité catalytique de RRP41. Ceci a été confirmé après analyse des fragments P-P1 par 3' RACE PCR (Figure 4B) et m'a permis d'obtenir les premières évidences quant à un rôle *in vivo* de l'activité phosphorolytique de l'exosome chez les plantes.

Il existe plusieurs RNases pouvant avoir des fonctions partiellement redondantes dans la maturation des ARNr. La présence de ces RNases pourrait rendre difficile la mise en évidence et l'étude des fonctions additionnelles de l'EXO9. Afin de palier ce problème, et d'analyser plus en détails le rôle joué par l'activité de l'EXO9 dans la maturation des ARNr, j'ai produit différentes lignées d'intérêts :

- Deux lignées résultantes du croisement de plantes transgéniques RRP41^{WT} et RRP41$^{PI\text{-}CAT}$ avec des plantes mutantes homozygotes pour l'exoribonucléase RRP6L2 (*rrp6l2*). Ces lignées ont été nommées *rrp6l2* RRP41^{WT} et *rrp6l2* RRP41$^{PI\text{-}CAT\text{-}}$ respectivement.
- Trois lignées résultantes de la transformation des plantes transgéniques RRP41^{WT}, RRP41$^{PI\text{-}}$ ou RRP41$^{PI\text{-}CAT}$ avec des microARN artificiels (amiRNA) permettant une inactivation partielle de l'expression de l'exoribonucléase RRP44 (Kumakura et al., 2013). Lesdites lignées ont été nommées RRP41^{WT} 44KD, RRP41$^{PI\text{-}}$ 44KD et RRP41$^{PI\text{-}CAT\text{-}}$ 44KD respectivement.

L'analyse par northern blot de l'accumulation des précurseurs d'ARNr 5,8S (pré-ARNr 5,8S), dans ces différents fonds génétiques, m'a permis de mettre en évidence la contribution de RRP44, RRP6L2 et de l'EXO9 dans la maturation des ARN 5,8S. J'ai en effet observé que la perte simultanée de l'activité de l'exosome et de l'expression de RRP44 ou RRP6L2 entraîne une accumulation différentielle des précurseurs des ARNr 5,8 (pré-ARNr 5,8S). En effet, les plantes dont l'expression de RRP44 est réduite mais qui expriment la version catalytiquement active de RRP41 (RRP41^{WT} 44KD) accumulent des pré-ARNr 5,8S ayant une extension de 120 nucléotides (pré-ARNr +120nt). *A contrario* lorsque les versions catalytiquement inactives de RRP41 sont exprimées, c'est à dire dans un fond génétique RRP41$^{PI\text{-}}$ 44K ou RRP41$^{PI\text{-}CAT\text{-}}$ 44K, on observe une accumulation des pré-ARNr 5,8S avec des extensions de petite taille. Un tel phénomène est également observé dans les lignées dans lesquelles à la fois l'expression de RRP6L2 et l'activité de l'exosome sont abolies (lignées *rrp6l2* RRP41$^{PI\text{-}CAT\text{-}}$) (Figure 4C). Afin de caractériser plus en détails la contribution de l'activité de l'EXO9 dans la maturation de ARNr 5,8S j'ai analysé et comparé par 3' RACE le profil des extrémités 3' des pré-ARN 5,8S dans les fonds génétiques suivants : Col0, RRP41^{WT}, RRP41$^{PI\text{-}}$, RRP41$^{PI\text{-}CAT}$, *rrp6l2*, *rrp6l2* RRP41^{WT}, *rrp6l2* RRP41$^{PI\text{-}CAT\text{-}}$. La

cartographie précise des extrémités des précurseurs des ARNr 5,8S a fourni des indications détaillées quant à la nature hétérogène de la population de précurseurs 5,8S détectés par northern blot. Ces résultats ont surtout confirmé que l'activité intrinsèque de EXO9 contribue à la maturation des ARNr chez *Arabidopsis* (Figure 4D). Brièvement, dans une plante *Arabidopsis* non-mutée, des précurseurs de l'ARN 5,8S +10/+11, +16, + 20 and +25 nt sont détectés. Dans le cas où EXO9 est inactif, la majorité des précurseurs comprend des extensions de 16-25 nt et le précurseur +10 est moins fréquent. Le décalage de taille vers des précurseurs plus longs suggère que ces précurseurs plus longs sont des substrats de EXO9 dans une situation sauvage. La plus faible fréquence d'espèces à +10 nt suggère que l'activité de EXO9 contribue à leur production. Cependant, la présence de ces précurseurs dans des plantes exprimant une version inactive de EXO9 indique que d'autre(s) activité(s) puisse(nt) produire ces intermédiaires. La situation est plus contrastée en absence de l'exoribonucléase RRP6L2. Dans des mutants *rrp6L2*, les précurseurs 5,8S les plus fréquents possèdent une extension de 10-11 nt, et les autres espèces observées en situation sauvage (étendues par 16-25 nt) sont à peine détectables. Ces observations suggèrent que les précurseurs +10/11 nt sont probablement des substrats de RRP6L2. En absence des activités de RRP6L2 et EXO9, la majorité des précurseurs ont des extensions de +10/11 nt, bien que des extensions de 16 à 25 nt sont aussi détectées. Ces résultats indiquent que les activités de RRP6L2 et EXO9 agissent de manière séquentielle sur les précurseurs des ARNr 5,8S. Le précurseur ARNr 5,8S + 120 nt est un substrat de RRP44, les précurseurs avec des extensions de 16 à 25 nt sont des substrats de EXO9 qui rogne les extensions jusqu'à une taille de +10 nt. Enfin, les précurseurs ARNr 5,8S + 10/11 nt sont pris en charge par RRP6L2.

Conclusion

Au cours de ma thèse, j'ai pu montrer que l'EXO9 d'*Arabidopsis* possède une activité exoribonucléolytique et que cette activité est abolie par des mutations dans le site de coordination des phosphates et dans le site catalytique présents au sein de la sous-unité RRP41. De plus, l'activité de l'EXO9 est stimulée en présence de phosphate inorganique, libère des nucléosides diphosphates et est réversible. Ces résultats prouvent que **l'EXO9 a une activité phosphorolytique qui est apportée par la sous-unité RRP41**. J'ai également

pu montrer que **l'activité d'EXO9, de RRP44 et de RRP6L2 contribue à l'élimination des 5' ETS et à la maturation des ARNr 5.8S chez *Arabidopsis***. Mes résultats montrent également que l'EXO9, RRP44 et RRP6L2 agissent séquentiellement sur les intermédiaires de dégradation P-P1 des 5'ETS et sur les précurseurs 5.8S : les intermédiaires les plus longs sont initialement dégradés par RRP44, et deviennent ensuite substrats de l'EXO9, puis de RRP6L2. Ces observations sont en accord avec le modèle récent proposant une action séquentielle similaire de RRP44 et RRP6 dans la maturation des ARNr 5.8S de levure. Par une combinaison de tests enzymatiques et de données structurales, Makino *et al.* ont pu montrer que dans la levure, le précurseur 5.8S est introduit dans le canal de l'exosome jusqu'à atteindre le site actif de la protéine processive RRP44 qui se trouve a la base de EXO9 (dans la levure, le cœur de l'exosome est catalytiquement inactif) (Makino et al., 2015). Quand le précurseur 5.8S est dégradé jusqu'à atteindre une taille de 5.8S+30nt, sa taille ne lui permet plus d'atteindre RRP44 via le canal central, il devient dès lors substrat de RRP6 puisque cette dernière est située au sommet de l'EXO9.

Contrairement à la levure, un lien physique entre l'EXO9 de plantes et les homologues de RRP6 (RRP6L1 à 3 chez la plante) n'a jamais pu être démontré. Cependant, la voie de maturation de l'ARN ribosomique pré-ARNr 5.8S chez la plante semble être similaire à la voie de maturation des ARNr 5.8S chez la levure. En outre, mes résultats sur la dégradation des fragments P-P1 et des 5'ETS suggèrent que l'action successive de différents facteurs est un mode d'action général aux différentes voies dégradation des ARN par l'exosome. Alors que la fonction de l'exosome de la levure et de l'homme repose sur l'activité hydrolytique des exoribonucléases RRP44 et RRP6, l'exosome de plantes a une activité phosphorolytique additionnelle, située à l'intérieur du canal central de EXO9.

Perspectives

Un des perspectives les plus intéressantes de ce travail consistera à identifier d'autres ARN substrats de l'activité de EXO9 chez les plantes. Il est possible que cette activité soit impliquée dans la plupart des fonctions de l'exosome, si ce n'est dans toutes. Les données actuelles *in vitro* et *in vivo* indiquent que EXO9 rogne plutôt que dégrade complètement ses substrats. Afin d'identifier la totalité des substrats de EXO9, il serait intéressant d'employer une méthode globale de détermination des extrémités 3' comme le TAIL-seq (Chang et al.

2014). Le TAIL-seq a été développé pour analyser la taille des queues poly(A) des ARNm et a récemment été utilisé par notre équipe chez *Arabidopsis* (Zuber et al., 2016). En théorie, cette technique n'est pas spécifique des ARNm mais peut être utilisée pour comparer les extrémités de tous les ARN d'une taille supérieure à 200 nt. Le TAIL-seq semble donc être une technique prometteuse pour identifier d'autres substrats de EXO9 chez *Arabidopsis*. En sachant que les activités de EXO9, RRP6L2 et RRP44 peuvent agir de manière redondante, comme dans le cas des ARNr, la recherche des substrats supplémentaires de EXO9 devrait être conduite dans les doubles ou triple mutants établis dans cette étude.

Une autre problématique intéressante à aborder serait de déterminer si EXO9, comme les activités phosphorolytiques des PNPases bactériennes ou de l'exosome des Archées, est capable de synthétiser des extensions nucléotidiques *in vivo*. En effet, les PNPases et l'exosome des Archées ont été montré comme étant responsables de l'ajout d'extensions hétéropolymériques riches en A *in vivo* (Mohanty and Kushner, 2000; Portnoy et al., 2005; Slomovic et al., 2008). Mes résultats indiquent que EXO9 *d'Arabidopsis* est capable d'ajouter des extensions nucléotiques *in vitro* (Figure 3C) mais aucune extension hétéropolymérique n'a pour l'instant été détectée pour des ARN endogènes chez les plantes. De manière intéressante, de telles extensions viennent d'être rapportées pour plusieurs virus à ARN dans des plantes *Arabidopsis* infectées (Li et al., 2014; He et al., 2015). La composition de ces extensions est compatible avec l'implication d'une activité phosphorolytique. Il existe trois enzymes présentant une telle activité chez les plantes : la PNPase chloroplastique (dont l'implication a déjà été écartée dans les études susnommées), la PNPase mitochondriale et comme je le montre dans cette étude, EXO9. Pour tester si l'activité de EXO9 est impliquée dans la modification des extrémités 3' d'ARN viraux, la présence et la composition des extensions pourraient être comparées entre les plantes infectées exprimant EXO9 actif (plantes $RRP41^{WT}$) ou inactif ($RRP41^{Pi-}$, $RRP41^{Pi-Cat-}$).

L'identification d'autres substrats endogènes de l'activité de EXO9 chez les plantes et la découverte d'autres rôles biologiques de cette activité seront des éléments essentiels pour mieux comprendre pourquoi l'activité phosphorolytique de l'exosome a été conservé chez les plantes terrestres.

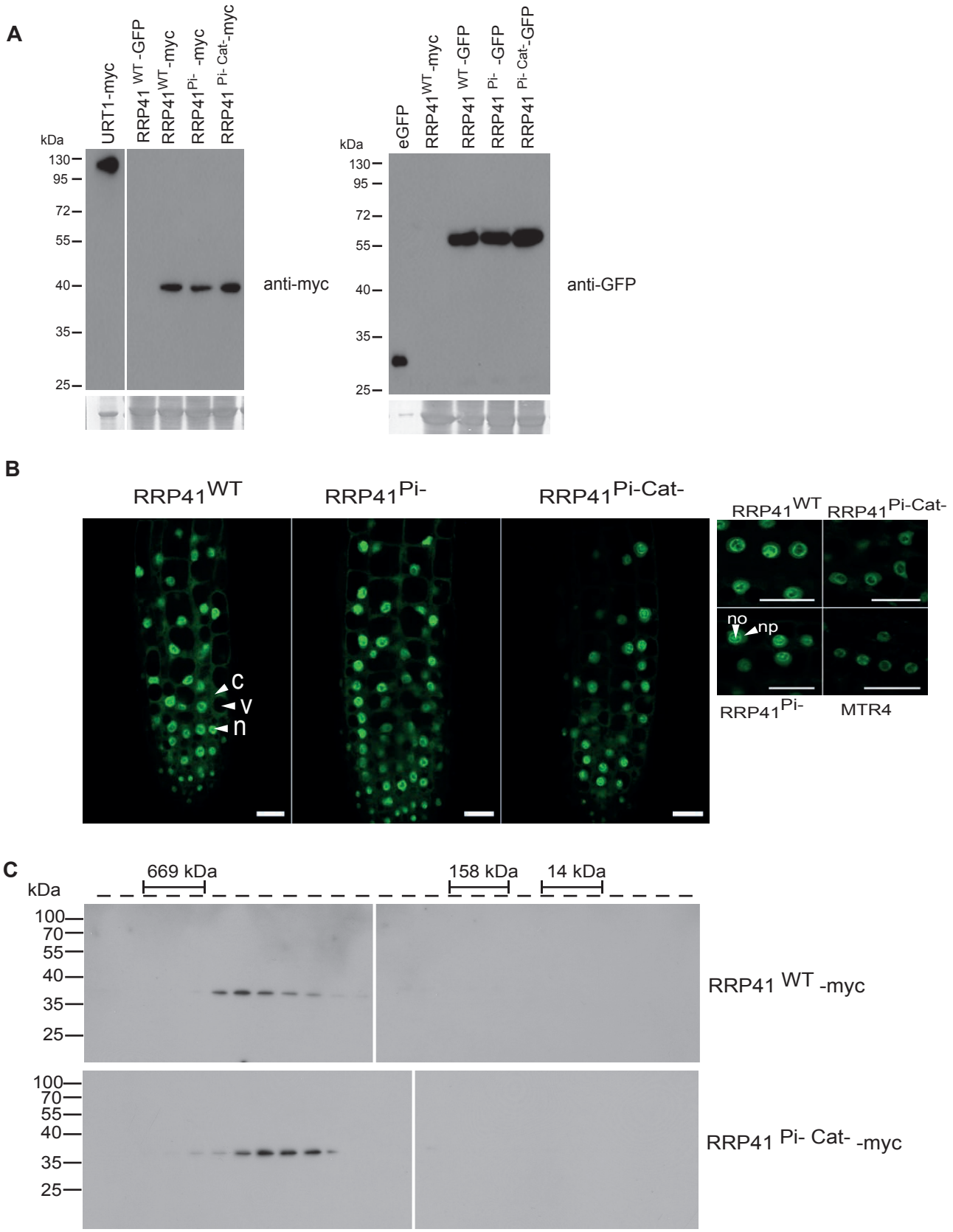

Figure 1. Caractérisation des protéines RRP41 sauvage et mutées exprimées dans des lignées stables *d'Arabidopsis.* A. Les protéines RRP41 sauvage et mutées sont exprimées à des niveaux comparables. Des extraits protéiques totaux issus de plantes *rrp41* complémentées par expression de versions active ou inactives de RRP41 ont été analysés par western blots. B. Localisation de $RRP41^{WT}$, $RRP41^{PI-}$ et $RRP41^{PI-Cat-}$ fusionnées à la GFP dans des racines de lignées transgéniques *d'Arabidopsis*. Toutes les protéines de fusion sont détectées avec une intensité de fluorescence comparable. La fluorescence est présente dans le noyau et le cytoplasme. La fusion MTR4-GFP est utilisée comme marqueur nucléolaire. n, noyau ; c, cytosol; v, vacuole; no, nucléole; np, nucléoplasme. La barre d'échelle représente 20 µm. C. Les protéines RRP41 sauvage et mutées sont incorporées dans des complexes de haut poids moléculaire. Des extraits protéiques totaux issus de plantes *rrp41* complémentées par expression de versions active ou inactives de RRP41 ont été analysés par filtration sur gel, suivie d'analyses en western blots utilisant un anticorps dirigé contre l'étiquette myc. Le profil d'élution de marqueurs de taille est indiqué au dessus des fractions. La migration de marqueurs de poids moléculaires est indiquée à gauche des gels.

A

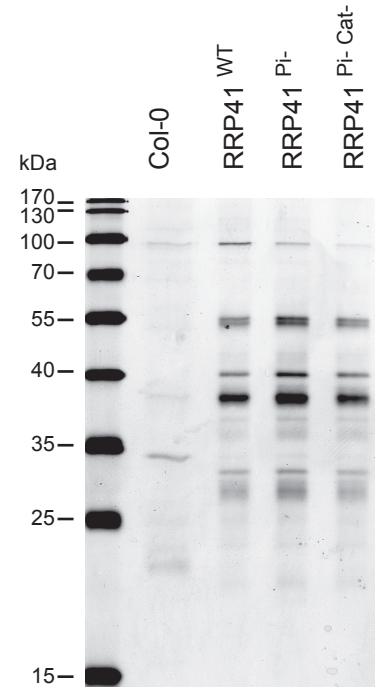

B

		RRP41^{WT}		RRP41^{Pi-}		RRP41$^{Pi-Cat-}$	
Accession	Name	Mascot score	#Spectra	Mascot score	#Spectra	Mascot score	#Spectra
At1g03360	AtRRP4	1586	713	1793	750	1519	745
At1g60080	AtRRP43	2172	279	2444	310	2247	296
At2g25355	AtRRP40A	1804	183	1974	198	1769	208
At3g07750	AtRRP42	1677	363	1653	431	1705	369
At3g46210	AtRRP46	780	74	875	97	695	81
At3g60500	AtRRP46B/ CER7	2394	273	2484	317	2264	299
At3g61620	AtRRP41	1765	354	1444	265	1257	251
At4g27490	AtMTR3	1741	211	1753	235	1729	235
At5g38890	AtCSL4	1542	283	1672	311	1432	299
At1g59760	AtMTR4	910	27	916	28	215	6
At2g17510	AtRRP44	779	26	767	25	697	19
At2g06990	AtHEN2	274	6	289	8	215	6

Figure 2. Toutes les versions de AtRRP41 sont incorporées dans des complexes de l'exosome. A. Des extraits protéiques de plantes Col-0, RRP41^{WT}, RRP41^{PI-} and RRP41$^{Pi-Cat-}$ ont été soumis à une immunopurification à l'aide d'anticorps anti-myc, séparés par SDS-PAGE et colorés à l'argent. La taille des marqueurs de poids moléculaires est indiquée en kDa.

B. Analyse par spectrométrie de masse des complexes EXO9 immunopurifiés de plantes RRP41^{WT}, RRP41^{PI-} and RRP41$^{PI-Cat-}$. Les neuf sous-unités du cœur de l'exosome sont indiquées en vert.

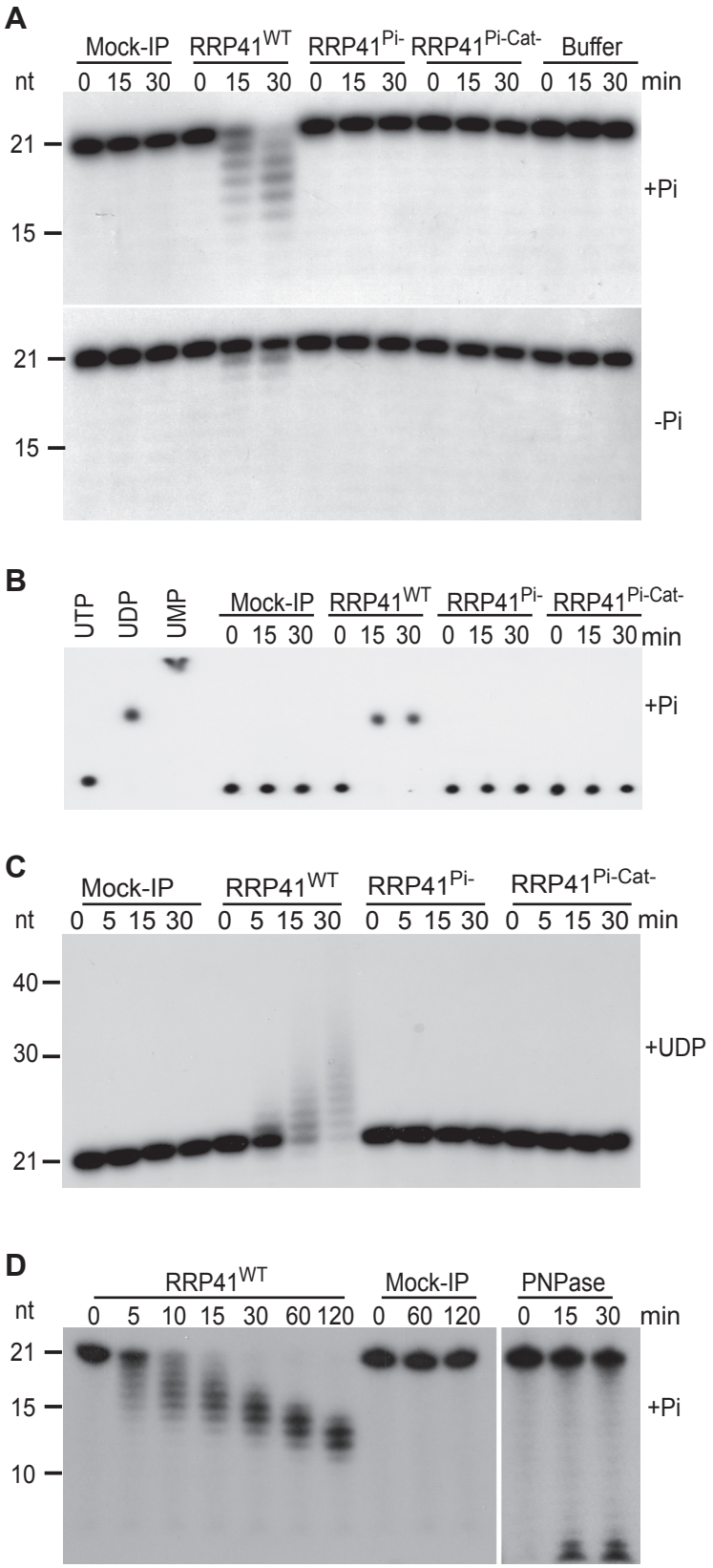

Figure 3. EXO9 d'Arabidopsis possède une activité phosphorolytique distributive conférée par la sous-unité RRP41.
Tests d'activité in vitro avec des exosomes immunopurifiés de plantes Col-0 (mock-IP), RRP41^{WT}, RRP41^{PI-} and RRP41$^{PI-Cat-}$.
A. Dégradation en présence et absence de phosphate inorganique (Pi) d'un substrat ARN de 21 Us marqué en 5' par ^{32}P. B. Analyse par chromatographie en couche mince montrant la production de nucléosides diphosphates à partir d'un substrat ARN de 21 Us marqué en 3' par ^{32}P.
C. Synthèse d'extensions nucléotidiques en présence d'1 mM UDP.
D. Le profil de détection de produits de dégradation intermédiaire à partir d'un substrat ARN de 21 Us marqué en 5' par ^{32}P indique la nature distributive de l'activité de EXO9 *d'Arabidopsis*. Pour comparaison, l'activité processive d'une PNPase bactérienne est montrée à droite.

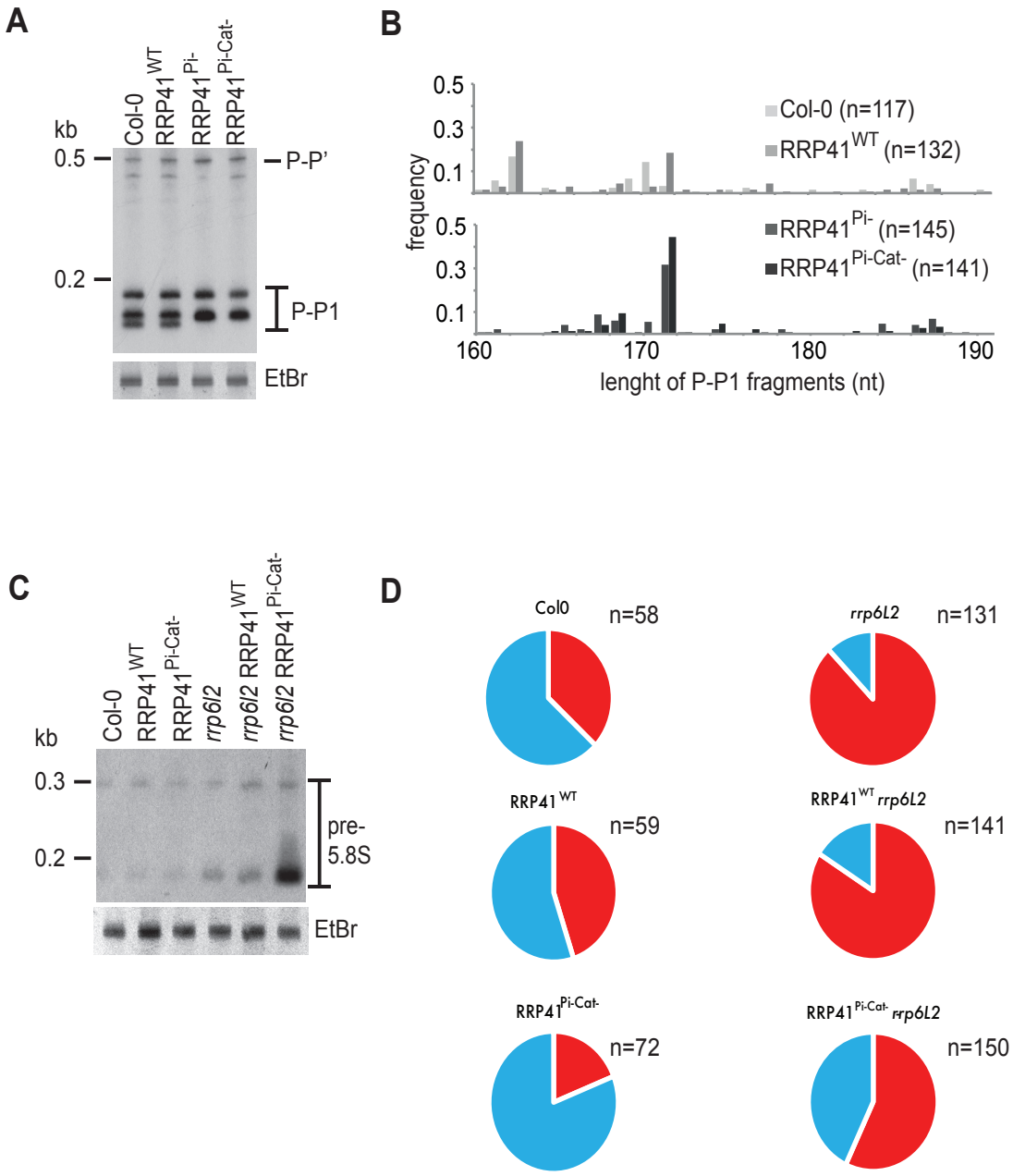

Figure 4. L'activité de EXO9 contribue au processus de maturation des ARNr.

Analyse par northern blots et cartographie des extrémités 3' du fragment P-P1, un sous-produit de maturation des ARNr (A, B) et des précurseurs de l'ARNr 5.8S (C, D) dans des plantes exprimant soit la version sauvage ou une version mutée de RRP41 dans des mutants simples ou doubles pour RRP41 et RRP6L2. EtBr, bromure d'éthidium. n, nombre de clones 3' RACE obtenus pour chaque échantillon.

Sources bibliographiques :

Allmang, C., Kufel, J., Chanfreau, G., Mitchell, P., Petfalski, E., Tollervey, D., 1999a. Functions of the exosome in rRNA, snoRNA and snRNA synthesis. EMBO J. 18, 5399–410.

Allmang, C., Petfalski, E., Podtelejnikov, A., Mann, M., Tollervey, D., Mitchell, P., 1999b. The yeast exosome and human PM-Scl are related complexes of 3' --> 5' exonucleases. Genes Dev. 13, 2148–58.

Anderson, J.S., Parker, R.P., 1998. The 3'-5' degradation of yeast mRNAs is a general mechanism for mRNA turnover that requires the SKI2 DEVH box protein and 3'-5' exonucleases of the exosome complex. EMBO J. 17, 1497–506.

Bousquet-Antonelli, C., Presutti, C., Tollervey, D., 2000. Identification of a regulated pathway for nuclear pre-mRNA turnover. Cell 102, 765–75.

Chang, H., Lim, J., Ha, M., Kim, V.N., 2014. TAIL-seq: genome-wide determination of poly(A) tail length and 3' end modifications. Mol. Cell 53, 1044–52.

Chekanova, J.A., Gregory, B.D., Reverdatto, S.V., Chen, H., Kumar, R., Hooker, T., Yazaki, J., Li, P., Skiba, N., Peng, Q., Alonso, J., Brukhin, V., Grossniklaus, U., Ecker, J.R., Belostotsky, D.A., 2007. Genome-wide high-resolution mapping of exosome substrates reveals hidden features in the Arabidopsis transcriptome. Cell 131, 1340–53.

Chlebowski, A., et al., Catalytic properties of the eukaryotic exosome. Adv Exp Med Biol, 2011. 702: p. 63-78.

Doma, M.K., Parker, R., 2007. RNA quality control in eukaryotes. Cell 131, 660–8.

Drazkowska, K., Tomecki, R., Stodus, K., Kowalska, K., Czarnocki-Cieciura, M., Dziembowski, A., 2013. The RNA exosome complex central channel controls both exonuclease and endonuclease Dis3 activities in vivo and in vitro. Nucleic Acids Res. 41, 3845–58.

Gudipati, R.K., Xu, Z., Lebreton, A., Séraphin, B., Steinmetz, L.M., Jacquier, A., Libri, D., 2012. Extensive degradation of RNA precursors by the exosome in wild-type cells. Mol. Cell 48, 409– 21.

He, M., Jiang, Z., Li, S., He, P., 2015. Presence of poly(A) tails at the 3'-termini of some mRNAs of a double-stranded RNA virus, southern rice black-streaked dwarf virus. Viruses 7, 1642–50.

Houseley, J., Tollervey, D., 2009. The many pathways of RNA degradation. Cell 136, 763–76. Hu, W., Sweet, T.J., Chamnongpol, S., Baker, K.E., Coller, J., 2009. Co-translational mRNA decay in Saccharomyces cerevisiae. Nature 461, 225–9.

Kiss, DL., Andrulis, ED., 2010. Genome-wide analysis reveals distinct substrate specificities of Rrp6, Dis3, and core exosome subunits. RNA, 16(4):781-91.

Kumakura, N., Otsuki, H., Tsuzuki, M., Takeda, A., Watanabe, Y., 2013. Arabidopsis AtRRP44A is the functional homolog of Rrp44/Dis3, an exosome component, is essential for viability and is required for RNA processing and degradation. PLoS ONE 8, e79219.

LaCava, J., Houseley, J., Saveanu, C., Petfalski, E., Thompson, E., Jacquier, A., Tollervey, D., 2005. RNA degradation by the exosome is promoted by a nuclear polyadenylation complex. Cell 121, 713–24.

Lange, H., Sement, F.M.M., Gagliardi, D., 2011. MTR4, a putative RNA helicase and exosome co-factor, is required for proper rRNA biogenesis and development in Arabidopsis thaliana. Plant J. 68, 51–63.

Lange, H., Zuber, H., Sement, F.M.M., Chicher, J., Kuhn, L., Hammann, P., Brunaud, V., Bérard, C., Bouteiller, N., Balzergue, S., Aubourg, S., Martin-Magniette, M.-L.L., Vaucheret, H., Gagliardi, D., 2014. The RNA helicases AtMTR4 and HEN2 target specific subsets of nuclear transcripts for degradation by the nuclear exosome in Arabidopsis thaliana. PLoS Genet. 10, e1004564.

Liu, Q., Greimann, J.C., Lima, C.D., 2006. Reconstitution, activities, and structure of the eukaryotic RNA exosome. Cell 127, 1223–37. Dziembowski et al 2007.

Liu, J.J., et al., Visualization of distinct substrate-recruitment pathways in the yeast exosome by EM. Nat Struct Mol Biol, 2014. 21(1): p. 95-102.

Li, W., Zhang, Y., Zhang, C., Pei, X., Wang, Z., Jia, S., 2014. Presence of poly(A) and poly(A)-rich tails in a positive-strand RNA virus known to lack 3′ poly(A) tails. Virology 454-455, 1–10.

Lorentzen, E., et al., RNA channelling by the archaeal exosome. EMBO Rep, 2007. 8(5): p. 470-6.

Lorentzen, E., Conti, E., 2005. Structural basis of 3′ end RNA recognition and exoribonucleolytic cleavage by an exosome RNase PH core. Mol. Cell 20, 473–81.

Lubas, M., Christensen, M.S., Kristiansen, M.S., Domanski, M., Falkenby, L.G., Lykke-Andersen, S., Andersen, J.S., Dziembowski, A., Jensen, T.H., 2011. Interaction profiling identifies the human nuclear exosome targeting complex. Mol. Cell 43, 624–37.

Lubas, M., Chlebowski, A., Dziembowski, A., Jensen, T.H., 2012. Biochemistry and Function of RNA Exosomes. Enzymes 31, 1–30.

Lubas, M., Andersen, P.R., Schein, A., Dziembowski, A., Kudla, G., Jensen, T.H., 2015. The human nuclear exosome targeting complex is loaded onto newly synthesized RNA to direct early ribonucleolysis. Cell Rep 10, 178–92.

Makino, D.L., et al., RNA degradation paths in a 12-subunit nuclear exosome complex. Nature, 2015. 524(7563): p. 54-8.

Mitchell, P., Petfalski, E., Tollervey, D., 1996. The 3′ end of yeast 5.8S rRNA is generated by an exonuclease processing mechanism. Genes Dev. 10, 502–13.

Mitchell, P., Petfalski, E., Shevchenko, A., Mann, M., Tollervey, D., 1997. The exosome: a conserved eukaryotic RNA processing complex containing multiple 3′-->5' exoribonucleases. Cell 91, 457–66.

Mohanty, B.K., Kushner, S.R., 2000. Polynucleotide phosphorylase functions both as a 3′ right- arrow 5' exonuclease and a poly(A) polymerase in Escherichia coli. Proc. Natl. Acad. Sci. U.S.A. 97, 11966–71.

Neil, H., Malabat, C., Aubenton-Carafa, Y. d', Xu, Z., Steinmetz, L.M., Jacquier, A., 2009. Widespread bidirectional promoters are the major source of cryptic transcripts in yeast. Nature 457, 1038–42.

Orban, T.I., Izaurralde, E., 2005. Decay of mRNAs targeted by RISC requires XRN1, the Ski complex, and the exosome. RNA 11, 459–69

Portnoy, V., Evguenieva-Hackenberg, E., Klein, F., Walter, P., Lorentzen, E., Klug, G., Schuster, G., 2005. RNA polyadenylation in Archaea: not observed in Haloferax while the exosome polynucleotidylates RNA in Sulfolobus. EMBO Rep. 6, 1188–93.

Preker P., Nielsen J., Kammler S., Lykke-Andersen S., Christensen M.S., Mapendano C.K., Schierup M.H., Jensen T.H., 2008. RNA exosome depletion reveals transcription upstream of active human promoters. Science, 322(5909):1851-4

Schneider, C., Kudla, G., Wlotzka, W., Tuck, A., Tollervey, D., 2012. Transcriptome-wide analysis of exosome targets. Mol. Cell 48, 422–33.
Schneider, C., Tollervey, D., 2013. Threading the barrel of the RNA exosome. Trends Biochem. Sci. 38, 485–93.

Sikorski, P.J., Zuber, H., Philippe, L., Sement, F.M.M., Canaday, J., Kufel, J., Gagliardi, D., Lange, H., 2015. Distinct 18S rRNA precursors are targets of the exosome complex, the exoribonuclease RRP6L2 and the terminal nucleotidyltransferase TRL in Arabidopsis thaliana. Plant J. 83, 991–1004.

Slomovic, S., Portnoy, V., Yehudai-Resheff, S., Bronshtein, E., Schuster, G., 2008. Polynucleotide phosphorylase and the archaeal exosome as poly(A)-polymerases. Biochim. Biophys. Acta 1779, 247–55.

Szczepinska, T., Kalisiak, K., Tomecki, R., Labno, A., Borowski., LS., Kulinski, TM., Adamska, D., Kosinska J., Dziembowski, A., 2015. DIS3 shapes the RNA polymerase II transcriptome in humans by degrading a variety of unwanted transcripts. Genome Res. 25, 1622–1633.

Vanácová, S., Wolf, J., Martin, G., Blank, D., Dettwiler, S., Friedlein, A., Langen, H., Keith, G., Keller, W., 2005. A new yeast poly(A) polymerase complex involved in RNA quality control. PLoS Biol. 3, e189.

Wasmuth, E.V., Lima, C.D., 2012a. Exo- and endoribonucleolytic activities of yeast cytoplasmic and nuclear RNA exosomes are dependent on the noncatalytic core and central channel. Mol. Cell 48, 133–44.

Wyers, F., Rougemaille, M., Badis, G., Rousselle, J.-C.C., Dufour, M.-E.E., Boulay, J., Régnault, B., Devaux, F., Namane, A., Séraphin, B., Libri, D., Jacquier, A., 2005. Cryptic pol II transcripts are degraded by a nuclear quality control pathway involving a new poly(A) polymerase. Cell 121, 725–37.

Zhou, Y., Zhu, J., Schermann, G., Ohle, C., Bendrin, K., Sugioka-Sugiyama, R., Sugiyama, T., Fischer, T., 2015. The fission yeast MTREC complex targets CUTs and unspliced pre-mRNAs to the nuclear exosome. Nat Commun 6, 7050.

Zuber, H., Scheer, H., Ferrier, E., Sement, F.M.M., Mercier, P., Stupfler, B., Gagliardi, D., 2016. Uridylation and PABP Cooperate to Repair mRNA Deadenylated Ends in Arabidopsis. Cell Rep 14, 2707–17.

Communications

Posters

Sikorska N., Lange H., Gagliardi D. 'The plant exosome core complex is active'
EMBO/EMBL Symposia: The Complex Life of mRNA. Heidelberg. October 5-8, 2014, Heidelberg (Germany)

Sikorska N., Lange H., Gagliardi D. 'The phosphorolytic activity of the core exosome contributes to rRNA maturation in *Arabidopsis*'
SifrARN. 8-10 of March 2016. Toulouse (France)

Orale

Sikorska N., Lange H., Gagliardi D. 'Catalytic activity of the exosome core complex'
Post-transcriptional Gene Regulation in Plants.
July 10-11, 2015, Paris (France)

Publication en préparation

Natalia Sikorska, Hélène Zuber, Heike Lange and Dominique Gagliardi. The phosphorolytic activity of the plant core exosome contributes to 5.8S rRNA maturation.

Bibliography

Allmang, C., Kufel, J., Chanfreau, G., Mitchell, P., Petfalski, E., Tollervey, D., 1999a. Functions of the exosome in rRNA, snoRNA and snRNA synthesis. EMBO J. 18, 5399–410.

Allmang, C., Mitchell, P., Petfalski, E., Tollervey, D., 2000. Degradation of ribosomal RNA precursors by the exosome. Nucleic Acids Res. 28, 1684–91.

Allmang, C., Petfalski, E., Podtelejnikov, A., Mann, M., Tollervey, D., Mitchell, P., 1999b. The yeast exosome and human PM-Scl are related complexes of 3' --> 5' exonucleases. Genes Dev. 13, 2148–58.

Andersen, P.R., Domanski, M., Kristiansen, M.S., Storvall, H., Ntini, E., Verheggen, C., Schein, A., Bunkenborg, J., Poser, I., Hallais, M., Sandberg, R., Hyman, A., LaCava, J., Rout, M.P., Andersen, J.S., Bertrand, E., Jensen, T.H., 2013. The human cap-binding complex is functionally connected to the nuclear RNA exosome. Nat. Struct. Mol. Biol. 20, 1367–76.

Anderson, J.S., Parker, R.P., 1998. The 3'-5' degradation of yeast mRNAs is a general mechanism for mRNA turnover that requires the SKI2 DEVH box protein and 3'-5' exonucleases of the exosome complex. EMBO J. 17, 1497–506.

Aït-Bara, S., Carpousis, A.J., 2015. RNA degradosomes in bacteria and chloroplasts: classification, distribution and evolution of RNase E homologs. Mol. Microbiol. 97, 1021–135.

Araki, Y., Takahashi, S., Kobayashi, T., Kajiho, H., Hoshino, S., Katada, T., 2001. Ski7p G protein interacts with the exosome and the Ski complex for 3'-to-5' mRNA decay in yeast. EMBO J. 20, 4684–93.

Assenholt, J., Mouaikel, J., Andersen, K.R., Brodersen, D.E., Libri, D., Jensen, T.H., 2008. Exonucleolysis is required for nuclear mRNA quality control in yeast THO mutants. RNA 14, 2305–13.

Astuti, D., Morris, M.R., Cooper, W.N., Staals, R.H., Wake, N.C., Fews, G.A., Gill, H., Gentle, D., Shuib, S., Ricketts, C.J., Cole, T., Essen, A.J. van, Lingen, R.A. van, Neri, G., Opitz, J.M., Rump, P., Stolte-Dijkstra, I., Müller, F., Pruijn, G.J., Latif, F., Maher, E.R., 2012. Germline mutations in DIS3L2 cause the Perlman syndrome of overgrowth and Wilms tumor susceptibility. Nat. Genet. 44, 277–84.

Audin, M.J., Wurm, J.P., Cvetkovic, M.A., Sprangers, R., 2016. The oligomeric architecture of the archaeal exosome is important for processive and efficient RNA degradation. Nucleic Acids Res. 44, 2962–73.

Bollenbach, T.J., Lange, H., Gutierrez, R., Erhardt, M., Stern, D.B., Gagliardi, D., 2005. RNR1, a 3'-5' exoribonuclease belonging to the RNR superfamily, catalyzes 3' maturation of chloroplast ribosomal RNAs in Arabidopsis thaliana. Nucleic Acids Res. 33, 2751–63.

Bonneau, F., Basquin, J., Ebert, J., Lorentzen, E., Conti, E., 2009. The yeast exosome functions as a macromolecular cage to channel RNA substrates for degradation. Cell 139, 547–59.

Bousquet-Antonelli, C., Presutti, C., Tollervey, D., 2000. Identification of a regulated pathway for nuclear pre-mRNA turnover. Cell 102, 765–75.

Branscheid, A., Marchais, A., Schott, G., Lange, H., Gagliardi, D., Andersen, S.U., Voinnet, O., Brodersen, P., 2015. SKI2 mediates degradation of RISC 5'-cleavage fragments and prevents secondary siRNA production from miRNA targets in Arabidopsis. Nucleic Acids Res. 43, 10975–88.

Briggs, M.W., Burkard, K.T., Butler, J.S., 1998. Rrp6p, the yeast homologue of the human PM-Scl 100-kDa autoantigen, is essential for efficient 5.8 S rRNA 3' end formation. J. Biol. Chem. 273, 13255–63.

Bühler, M., Spies, N., Bartel, D.P., Moazed, D., 2008. TRAMP-mediated RNA surveillance prevents spurious entry of RNAs into the Schizosaccharomyces pombe siRNA pathway. Nat. Struct. Mol. Biol. 15, 1015–23.

Brown, J.T., Bai, X., Johnson, A.W., 2000. The yeast antiviral proteins Ski2p, Ski3p, and Ski8p exist as a complex in vivo. RNA 6, 449–57.

Byrne, M.E., 2009. A role for the ribosome in development. Trends Plant Sci. 14, 512–9.

Callahan, K.P., Butler, J.S., 2010. TRAMP complex enhances RNA degradation by the nuclear exosome component Rrp6. J. Biol. Chem. 285, 3540–7.

Carpousis, A.J., Houwe, G. Van, Ehretsmann, C., Krisch, H.M., 1994. Copurification of E. coli RNAase E and PNPase: evidence for a specific association between two enzymes important in RNA processing and degradation. Cell 76, 889–900.

Carron, C., O'Donohue, M.-F.F., Choesmel, V., Faubladier, M., Gleizes, P.-E.E., 2011. Analysis of two human pre-ribosomal factors, bystin and hTsr1, highlights differences in evolution of ribosome biogenesis between yeast and mammals. Nucleic Acids Res. 39, 280–91.

Chang, H., Lim, J., Ha, M., Kim, V.N., 2014. TAIL-seq: genome-wide determination of poly(A) tail length and 3' end modifications. Mol. Cell 53, 1044–52.

Chekanova, J.A., Gregory, B.D., Reverdatto, S.V., Chen, H., Kumar, R., Hooker, T., Yazaki, J., Li, P., Skiba, N., Peng, Q., Alonso, J., Brukhin, V., Grossniklaus, U., Ecker, J.R., Belostotsky, D.A., 2007. Genome-wide high-resolution mapping of exosome substrates reveals hidden features in the Arabidopsis transcriptome. Cell 131, 1340–53.

Chekanova, J.A., Shaw, R.J., Wills, M.A., Belostotsky, D.A., 2000. Poly(A) tail-dependent exonuclease AtRrp41p from Arabidopsis thaliana rescues 5.8 S rRNA processing and mRNA decay defects of the yeast ski6 mutant and is found in an exosome-sized complex in plant and

yeast cells. J. Biol. Chem. 275, 33158–66.

Chen, X., Liu, J., Cheng, Y., Jia, D., 2002. HEN1 functions pleiotropically in Arabidopsis development and acts in C function in the flower. Development 129, 1085–94.

Chernyakov, I., Whipple, J.M., Kotelawala, L., Grayhack, E.J., Phizicky, E.M., 2008. Degradation of several hypomodified mature tRNA species in Saccharomyces cerevisiae is mediated by Met22 and the 5'-3' exonucleases Rat1 and Xrn1. Genes Dev. 22, 1369–80.

Chlebowski, A., Tomecki, R., Gas López, M.E.E., Séraphin, B., Dziembowski, A., 2011. Catalytic properties of the eukaryotic exosome. Adv. Exp. Med. Biol. 702, 63–78.

Choi, J.M., Park, E.Y., Kim, J.H., Chang, S.K., Cho, Y., 2004. Probing the functional importance of the hexameric ring structure of RNase PH. J. Biol. Chem. 279, 755–64.

Clough S.J., Bent A.F., 1998. Floral dip: a simplified method for Agrobacterium-mediated transformation of Arabidopsis thaliana. Plant J.,16(6):735-43.

Coburn, G.A., Mackie, G.A., 1999. Degradation of mRNA in Escherichia coli: an old problem with some new twists. Prog. Nucleic Acid Res. Mol. Biol. 62, 55–108.

Comella, P., Pontvianne, F., Lahmy, S., Vignols, F., Barbezier, N., Debures, A., Jobet, E., Brugidou, E., Echeverria, M., Sáez-Vásquez, J., 2008. Characterization of a ribonuclease III-like protein required for cleavage of the pre-rRNA in the 3'ETS in Arabidopsis. Nucleic Acids Res. 36, 1163–75.

Crooks, G.E., Hon, G., Chandonia, J.-M.M., Brenner, S.E., 2004. WebLogo: a sequence logo generator. Genome Res. 14, 1188–90.

Cruz, J. de la, Kressler, D., Tollervey, D., Linder, P., 1998. Dob1p (Mtr4p) is a putative ATP-dependent RNA helicase required for the 3' end formation of 5.8S rRNA in Saccharomyces cerevisiae. EMBO J. 17, 1128–40.

Dijk, E.L. van, Schilders, G., Pruijn, G.J., 2007. Human cell growth requires a functional cytoplasmic exosome, which is involved in various mRNA decay pathways. RNA 13, 1027–35.

Doma, M.K., Parker, R., 2007. RNA quality control in eukaryotes. Cell 131, 660–8.

Dorcey, E., Rodriguez-Villalon, A., Salinas, P., Santuari, L., Pradervand, S., Harshman, K., Hardtke, C.S., 2012. Context-dependent dual role of SKI8 homologs in mRNA synthesis and turnover. PLoS Genet. 8, e1002652.

Drazkowska, K., Tomecki, R., Stodus, K., Kowalska, K., Czarnocki-Cieciura, M., Dziembowski, A., 2013. The RNA exosome complex central channel controls both exonuclease and endonuclease Dis3 activities in vivo and in vitro. Nucleic Acids Res. 41, 3845–58.

Du, J., Johnson, L.M., Jacobsen, S.E., Patel, D.J., 2015. DNA methylation pathways and their

crosstalk with histone methylation. Nat. Rev. Mol. Cell Biol. 16, 519–32.

Dziembowski, A., Lorentzen, E., Conti, E., Séraphin, B., 2007. A single subunit, Dis3, is essentially responsible for yeast exosome core activity. Nat. Struct. Mol. Biol. 14, 15–22.

Egan, E.D., Braun, C.R., Gygi, S.P., Moazed, D., 2014. Post-transcriptional regulation of meiotic genes by a nuclear RNA silencing complex. RNA 20, 867–81.

El Hage, A., Koper, M., Kufel, J., Tollervey, D., 2008. Efficient termination of transcription by RNA polymerase I requires the 5' exonuclease Rat1 in yeast. Genes Dev. 22, 1069–81.

Evguenieva-Hackenberg, E., Hou, L., Glaeser, S., Klug, G., 2014. Structure and function of the archaeal exosome. Wiley Interdiscip Rev RNA 5, 623–35.

Fatica, A., Tollervey, D., Dlakić, M., 2004. PIN domain of Nob1p is required for D-site cleavage in 20S pre-rRNA. RNA 10, 1698–701.

Favero, M. Del, Mazzantini, E., Briani, F., Zangrossi, S., Tortora, P., Dehò, G., 2008. Regulation of Escherichia coli polynucleotide phosphorylase by ATP. J. Biol. Chem. 283, 27355–9.

Gazzani, S., Lawrenson, T., Woodward, C., Headon, D., Sablowski, R., 2004. A link between mRNA turnover and RNA interference in Arabidopsis. Science 306, 1046–8.

Germain, A., Kim, S.H., Gutierrez, R., Stern, D.B., 2012. Ribonuclease II preserves chloroplast RNA homeostasis by increasing mRNA decay rates, and cooperates with polynucleotide phosphorylase in 3' end maturation. Plant J. 72, 960–71.

Greimann, J.C., Liu, Q., Lima C.D., 2007. Erratum. Cell. 131(1), 188-9

Grzechnik, P., Kufel, J., 2008. Polyadenylation linked to transcription termination directs the processing of snoRNA precursors in yeast. Mol. Cell 32, 247–58.

Gudipati, R.K., Xu, Z., Lebreton, A., Séraphin, B., Steinmetz, L.M., Jacquier, A., Libri, D., 2012. Extensive degradation of RNA precursors by the exosome in wild-type cells. Mol. Cell 48, 409–21.

Gy, I., Gasciolli, V., Lauressergues, D., Morel, J.-B.B., Gombert, J., Proux, F., Proux, C., Vaucheret, H., Mallory, A.C., 2007. Arabidopsis FIERY1, XRN2, and XRN3 are endogenous RNA silencing suppressors. Plant Cell 19, 3451–61.

Haile, S., Estevez, A.M., Clayton, C., 2003. A role for the exosome in the in vivo degradation of unstable mRNAs. RNA 9, 1491–501.

Hajnsdorf, E., Braun, F., Haugel-Nielsen, J., Régnier, P., 1995. Polyadenylylation destabilizes the rpsO mRNA of Escherichia coli. Proc. Natl. Acad. Sci. U.S.A. 92, 3973–7.

Halbach, F., Reichelt, P., Rode, M., Conti, E., 2013. The yeast ski complex: crystal structure and

RNA channeling to the exosome complex. Cell 154, 814–26.

Halbach, F., Rode, M., Conti, E., 2012. The crystal structure of S. cerevisiae Ski2, a DExH helicase associated with the cytoplasmic functions of the exosome. RNA 18, 124–34.

Harlow, L.S., Kadziola, A., Jensen, K.F., Larsen, S., 2004. Crystal structure of the phosphorolytic exoribonuclease RNase PH from Bacillus subtilis and implications for its quaternary structure and tRNA binding. Protein Sci. 13, 668–77.

Harnisch, C., Cuzic-Feltens, S., Dohm, J.C., Götze, M., Himmelbauer, H., Wahle, E., 2016. Oligoadenylation of 3' decay intermediates promotes cytoplasmic mRNA degradation in Drosophila cells. RNA 22, 428–42.

Haugel-Nielsen, J., Hajnsdorf, E., Regnier, P., 1996. The rpsO mRNA of Escherichia coli is polyadenylated at multiple sites resulting from endonucleolytic processing and exonucleolytic degradation. EMBO J. 15, 3144–52.

He, F., Li, X., Spatrick, P., Casillo, R., Dong, S., Jacobson, A., 2003. Genome-wide analysis of mRNAs regulated by the nonsense-mediated and 5'-3' mRNA decay pathways in yeast. Mol. Cell 12, 1439–52.

He, M., Jiang, Z., Li, S., He, P., 2015. Presence of poly(A) tails at the 3'-termini of some mRNAs of a double-stranded RNA virus, southern rice black-streaked dwarf virus. Viruses 7, 1642–50.

Hématy, K., Bellec, Y., Podicheti, R., Bouteiller, N., Anne, P., Morineau, C., Haslam, R.P., Beaudoin, F., Napier, J.A., Mockaitis, K., Gagliardi, D., Vaucheret, H., Lange, H., Faure, J.-D.D., 2016. The Zinc-Finger Protein SOP1 Is Required for a Subset of the Nuclear Exosome Functions in Arabidopsis. PLoS Genet. 12, e1005817.

Henras, A., Plisson-Chastang, C., O'Donohue, M., Chakraborty, A., Gleizes, P., 2015. An overview of pre-ribosomal RNA processing in eukaryotes. Wiley Interdisciplinary Reviews: RNA 6, 225–242.

Henry, Y., Wood, H., Morrissey, J.P., Petfalski, E., Kearsey, S., Tollervey, D., 1994. The 5' end of yeast 5.8S rRNA is generated by exonucleases from an upstream cleavage site. EMBO J. 13, 2452–63.

Hepworth, J., Dean, C., 2015. Flowering Locus C's Lessons: Conserved Chromatin Switches Underpinning Developmental Timing and Adaptation. Plant Physiol. 168, 1237–45.

Holub, P., Lalakova, J., Cerna, H., Pasulka, J., Sarazova, M., Hrazdilova, K., Arce, M.S., Hobor, F., Stefl, R., Vanacova, S., 2012. Air2p is critical for the assembly and RNA-binding of the TRAMP complex and the KOW domain of Mtr4p is crucial for exosome activation. Nucleic Acids Res. 40, 5679–93.

Holub, P., Vanacova, S., 2012. TRAMP Stimulation of Exosome. Enzymes 31, 77–95.

Hooker, T.S., Lam, P., Zheng, H., Kunst, L., 2007. A core subunit of the RNA-processing/degrading exosome specifically influences cuticular wax biosynthesis in Arabidopsis. Plant Cell 19, 904–13.

Houseley, J., Tollervey, D., 2009. The many pathways of RNA degradation. Cell 136, 763–76.
Hu, W., Sweet, T.J., Chamnongpol, S., Baker, K.E., Coller, J., 2009. Co-translational mRNA decay in Saccharomyces cerevisiae. Nature 461, 225–9.

Hu, W., Sweet, T.J., Chamnongpol, S., Baker, K.E., Coller, J., 2009. Co-translational mRNA decay in Saccharomyces cerevisiae. Nature 461, 225–9.

Huh, W.-K.K., Falvo, J.V., Gerke, L.C., Carroll, A.S., Howson, R.W., Weissman, J.S., O'Shea, E.K., 2003. Global analysis of protein localization in budding yeast. Nature 425, 686–91.

Ibrahim, F., Rymarquis, L.A., Kim, E.-J.J., Becker, J., Balassa, E., Green, P.J., Cerutti, H., 2010. Uridylation of mature miRNAs and siRNAs by the MUT68 nucleotidyltransferase promotes their degradation in Chlamydomonas. Proc. Natl. Acad. Sci. U.S.A. 107, 3906–11.

Jackson, R.N., Klauer, A.A., Hintze, B.J., Robinson, H., Hoof, A. van, Johnson, S.J., 2010. The crystal structure of Mtr4 reveals a novel arch domain required for rRNA processing. EMBO J. 29, 2205–16.

Januszyk, K., Lima, C.D., 2014. The eukaryotic RNA exosome. Curr. Opin. Struct. Biol. 24, 132–40.

Januszyk, K., Liu, Q., Lima, C.D., 2011. Activities of human RRP6 and structure of the human RRP6 catalytic domain. RNA 17, 1566–77.

Jia H., Wang X., Anderson J.T., Jankowsky E., 2012. RNA unwinding by the Trf4/Air2/Mtr4 polyadenylation (TRAMP) complex. Proc Natl Acad Sci U S A, 109(19):7292-7.

Jones, C.I., Zabolotskaya, M.V., Newbury, S.F., 2012. The 5' → 3' exoribonuclease XRN1/Pacman and its functions in cellular processes and development. Wiley Interdiscip Rev RNA 3, 455–68.

Karbstein, K., 2013. Quality control mechanisms during ribosome maturation. Trends Cell Biol. 23, 242–50.

Karley, A.J., White, P.J., 2009. Moving cationic minerals to edible tissues: potassium, magnesium, calcium. Curr. Opin. Plant Biol. 12, 291–8.

Kastenmayer, J.P., Johnson, M.A., Green, P.J., 2001. Analysis of XRN orthologs by complementation of yeast mutants and localization of XRN-GFP fusion proteins. Meth. Enzymol. 342, 269–82.

Kim, M., Krogan, N.J., Vasiljeva, L., Rando, O.J., Nedea, E., Greenblatt, J.F., Buratowski, S., 2004. The yeast Rat1 exonuclease promotes transcription termination by RNA polymerase II.

Nature 432, 517–22.

Klauer, A.A., van Hoof, A., 2012. Degradation of mRNAs that lack a stop codon: a decade of nonstop progress. Wiley Interdiscip Rev RNA. 3(5):649-60

Kilchert C., Wittmann S., Passoni M., Shah S., Granneman S., Vasiljeva L., 2015. Regulation of mRNA Levels by Decay-Promoting Introns that Recruit the Exosome Specificity Factor Mmi1. Cell Rep.,13(11):2504-15.

Kos, M., Tollervey, D., 2010. Yeast pre-rRNA processing and modification occur cotranscriptionally. Mol. Cell 37, 809–20.

Kowalinski, E., Kögel, A., Ebert, J., Reichelt, P., Stegmann, E., Habermann, B., Conti, E., 2016. Structure of a Cytoplasmic 11-Subunit RNA Exosome Complex. Mol. Cell 63, 125–34.

Kuai, L., Fang, F., Butler, J.S., Sherman, F., 2004. Polyadenylation of rRNA in Saccharomyces cerevisiae. Proc. Natl. Acad. Sci. U.S.A. 101, 8581–6.

Kufel, J., Dichtl, B., Tollervey, D., 1999. Yeast Rnt1p is required for cleavage of the pre-ribosomal RNA in the 3’ ETS but not the 5' ETS. RNA 5, 909–17.

Kumakura, N., Otsuki, H., Tsuzuki, M., Takeda, A., Watanabe, Y., 2013. Arabidopsis AtRRP44A is the functional homolog of Rrp44/Dis3, an exosome component, is essential for viability and is required for RNA processing and degradation. PLoS ONE 8, e79219.

Kurihara, Y., Schmitz, R.J., Nery, J.R., Schultz, M.D., Okubo-Kurihara, E., Morosawa, T., Tanaka, M., Toyoda, T., Seki, M., Ecker, J.R., 2012. Surveillance of 3’ Noncoding Transcripts Requires FIERY1 and XRN3 in Arabidopsis. G3 (Bethesda) 2, 487–98.

LaCava, J., Houseley, J., Saveanu, C., Petfalski, E., Thompson, E., Jacquier, A., Tollervey, D., 2005. RNA degradation by the exosome is promoted by a nuclear polyadenylation complex. Cell 121, 713–24.

Lafontaine, D.L., 2010. A “garbage can” for ribosomes: how eukaryotes degrade their ribosomes. Trends Biochem. Sci. 35, 267–77.

Lamanna, A.C., Karbstein, K., 2009. Nob1 binds the single-stranded cleavage site D at the 3’-end of 18S rRNA with its PIN domain. Proc. Natl. Acad. Sci. U.S.A. 106, 14259–64.

Lange, H., Gagliardi, D., 2012. Plant Exosomes and Cofactors. Enzymes 31, 31–52.

Lange, H., Holec, S., Cognat, V., Pieuchot, L., Ret, M. Le, Canaday, J., Gagliardi, D., 2008. Degradation of a polyadenylated rRNA maturation by-product involves one of the three RRP6-like proteins in Arabidopsis thaliana. Mol. Cell. Biol. 28, 3038–44.

Lange, H., Sement, F.M.M., Canaday, J., Gagliardi, D., 2009. Polyadenylation-assisted RNA degradation processes in plants. Trends Plant Sci. 14, 497–504.

Lange, H., Sement, F.M.M., Gagliardi, D., 2011. MTR4, a putative RNA helicase and exosome co-factor, is required for proper rRNA biogenesis and development in Arabidopsis thaliana. Plant J. 68, 51–63.

Lange, H., Zuber, H., Sement, F.M.M., Chicher, J., Kuhn, L., Hammann, P., Brunaud, V., Bérard, C., Bouteiller, N., Balzergue, S., Aubourg, S., Martin-Magniette, M.-L.L., Vaucheret, H., Gagliardi, D., 2014. The RNA helicases AtMTR4 and HEN2 target specific subsets of nuclear transcripts for degradation by the nuclear exosome in Arabidopsis thaliana. PLoS Genet. 10, e1004564.

Lebreton, A., Tomecki, R., Dziembowski, A., Séraphin, B., 2008. Endonucleolytic RNA cleavage by a eukaryotic exosome. Nature 456, 993–6.

Li, J., Yang, Z., Yu, B., Liu, J., Chen, X., 2005. Methylation protects miRNAs and siRNAs from a 3'-end uridylation activity in Arabidopsis. Curr. Biol. 15, 1501–7.

Li, W., Zhang, Y., Zhang, C., Pei, X., Wang, Z., Jia, S., 2014. Presence of poly(A) and poly(A)-rich tails in a positive-strand RNA virus known to lack 3′ poly(A) tails. Virology 454-455, 1–10.

Lim, J., Ha, M., Chang, H., Kwon, S.C., Simanshu, D.K., Patel, D.J., Kim, V.N., 2014. Uridylation by TUT4 and TUT7 marks mRNA for degradation. Cell 159, 1365–76.

Liou, G.-G.G., Chang, H.-Y.Y., Lin, C.-S.S., Lin-Chao, S., 2002. DEAD box RhlB RNA helicase physically associates with exoribonuclease PNPase to degrade double-stranded RNA independent of the degradosome-assembling region of RNase E. J. Biol. Chem. 277, 41157–62.

Liu, Q., Greimann, J.C., Lima, C.D., 2006. Reconstitution, activities, and structure of the eukaryotic RNA exosome. Cell 127, 1223–37.

Liu, X., Zheng, Q., Vrettos, N., Maragkakis, M., Alexiou, P., Gregory, B.D., Mourelatos, Z., 2014. A MicroRNA precursor surveillance system in quality control of MicroRNA synthesis. Mol. Cell 55, 868–79.

Lorentzen, E., Conti, E., 2005. Structural basis of 3' end RNA recognition and exoribonucleolytic cleavage by an exosome RNase PH core. Mol. Cell 20, 473–81.

Lorentzen, E., Conti, E., 2012. Crystal structure of a 9-subunit archaeal exosome in pre-catalytic states of the phosphorolytic reaction. Archaea 2012, 721869.

Lorentzen, E., Walter, P., Fribourg, S., Evguenieva-Hackenberg, E., Klug, G., Conti, E., 2005. The archaeal exosome core is a hexameric ring structure with three catalytic subunits. Nat. Struct. Mol. Biol. 12, 575–81.

Lubas, M., Andersen, P.R., Schein, A., Dziembowski, A., Kudla, G., Jensen, T.H., 2015. The human nuclear exosome targeting complex is loaded onto newly synthesized RNA to direct

early ribonucleolysis. Cell Rep 10, 178–92.

Lubas, M., Chlebowski, A., Dziembowski, A., Jensen, T.H., 2012. Biochemistry and Function of RNA Exosomes. Enzymes 31, 1–30.

Lubas, M., Christensen, M.S., Kristiansen, M.S., Domanski, M., Falkenby, L.G., Lykke-Andersen, S., Andersen, J.S., Dziembowski, A., Jensen, T.H., 2011. Interaction profiling identifies the human nuclear exosome targeting complex. Mol. Cell 43, 624–37.

Lubas, M., Damgaard, C.K., Tomecki, R., Cysewski, D., Jensen, T.H., Dziembowski, A., 2013. Exonuclease hDIS3L2 specifies an exosome-independent 3'-5' degradation pathway of human cytoplasmic mRNA. EMBO J. 32, 1855–68.

Luo, W., Johnson, A.W., Bentley, D.L., 2006. The role of Rat1 in coupling mRNA 3'-end processing to transcription termination: implications for a unified allosteric-torpedo model. Genes Dev. 20, 954–65.

Lykke-Andersen, S., Brodersen, D.E., Jensen, T.H., 2009. Origins and activities of the eukaryotic exosome. J. Cell. Sci. 122, 1487–94.

Maathuis, F.J., 2009. Physiological functions of mineral macronutrients. Curr. Opin. Plant Biol. 12, 250–8.

Makino, D.L., Baumgärtner, M., Conti, E., 2013. Crystal structure of an RNA-bound 11-subunit eukaryotic exosome complex. Nature 495, 70–5.

Makino, D.L., Schuch, B., Stegmann, E., Baumgärtner, M., Basquin, C., Conti, E., 2015. RNA degradation paths in a 12-subunit nuclear exosome complex. Nature 524, 54–8.

Malecki, M., Viegas, S.C., Carneiro, T., Golik, P., Dressaire, C., Ferreira, M.G., Arraiano, C.M.M., 2013. The exoribonuclease Dis3L2 defines a novel eukaryotic RNA degradation pathway. EMBO J. 32, 1842–54.

Merret, R., Nagarajan, V.K., Carpentier, M.-C.C., Park, S., Favory, J.-J.J., Descombin, J., Picart, C., Charng, Y.-Y.Y., Green, P.J., Deragon, J.-M.M., Bousquet-Antonelli, C., 2015. Heat-induced ribosome pausing triggers mRNA co-translational decay in Arabidopsis thaliana. Nucleic Acids Res. 43, 4121–32.

Missbach S., Weis B.L., Martin R., Simm S., Bohnsack M.T., Schleiff E., 2013. 40S ribosome biogenesis co-factors are essential for gametophyte and embryo development. PLoS One, 8(1):e54084

Mitchell, P., 2014. Exosome substrate targeting: the long and short of it. Biochem. Soc. Trans. 42, 1129–34.

Mitchell, P., Tollervey, D., 2003. An NMD pathway in yeast involving accelerated deadenylation and exosome-mediated 3'-->5' degradation. Mol. Cell 11, 1405–13.

Mitchell, P., Petfalski, E., Shevchenko, A., Mann, M., Tollervey, D., 1997. The exosome: a conserved eukaryotic RNA processing complex containing multiple 3’-->5' exoribonucleases. Cell 91, 457–66.

Mitchell, P., Petfalski, E., Tollervey, D., 1996. The 3’ end of yeast 5.8S rRNA is generated by an exonuclease processing mechanism. Genes Dev. 10, 502–13.

Mohanty, B.K., Kushner, S.R., 2000. Polynucleotide phosphorylase functions both as a 3’ right-arrow 5' exonuclease and a poly(A) polymerase in Escherichia coli. Proc. Natl. Acad. Sci. U.S.A. 97, 11966–71.

Mohanty, B.K., Kushner, S.R., 2002. Polyadenylation of Escherichia coli transcripts plays an integral role in regulating intracellular levels of polynucleotide phosphorylase and RNase E. Mol. Microbiol. 45, 1315–24.

Mohanty, B.K., Kushner, S.R., 2016. Regulation of mRNA Decay in Bacteria. Annu. Rev. Microbiol.

Moomaw, A.S., Maguire, M.E., 2008. The unique nature of mg2+ channels. Physiology (Bethesda) 23, 275–85.

Mullineux S.T., Lafontaine D.L., 2012. Mapping the cleavage sites on mammalian pre-rRNAs: where do we stand? Biochimie, 94(7):1521-32.

Nagarajan, V.K., Jones, C.I., Newbury, S.F., Green, P.J., 2013. XRN 5’→3' exoribonucleases: structure, mechanisms and functions. Biochim. Biophys. Acta 1829, 590–603.

Nakamura, R., Takeuchi, R., Takata, K., Shimanouchi, K., Abe, Y., Kanai, Y., Ruike, T., Ihara, A., Sakaguchi, K., 2008. TRF4 is involved in polyadenylation of snRNAs in Drosophila melanogaster. Mol. Cell. Biol. 28, 6620–31.

Neil, H., Malabat, C., Aubenton-Carafa, Y. d’, Xu, Z., Steinmetz, L.M., Jacquier, A., 2009. Widespread bidirectional promoters are the major source of cryptic transcripts in yeast. Nature 457, 1038–42.

Norbury, C.J., 2013. Cytoplasmic RNA: a case of the tail wagging the dog. Nat. Rev. Mol. Cell Biol. 14, 643–53.

Orban, T.I., Izaurralde, E., 2005. Decay of mRNAs targeted by RISC requires XRN1, the Ski complex, and the exosome. RNA 11, 459–69.

Parker, R., 2012. RNA degradation in Saccharomyces cerevisae. Genetics 191, 671–702.

Pertschy, B., Schneider, C., Gnädig, M., Schäfer, T., Tollervey, D., Hurt, E., 2009. RNA helicase Prp43 and its co-factor Pfa1 promote 20 to 18 S rRNA processing catalyzed by the endonuclease Nob1. J. Biol. Chem. 284, 35079–91.

Pelechano, V., Wei, W., Steinmetz, L.M., 2015. Widespread Co-translational RNA Decay Reveals Ribosome Dynamics. Cell 161, 1400–12.

Perrin, R., Meyer, E.H., Zaepfel, M., Kim, Y.-J.J., Mache, R., Grienenberger, J.-M.M., Gualberto, J.M.M., Gagliardi, D., 2004. Two exoribonucleases act sequentially to process mature 3'-ends of atp9 mRNAs in Arabidopsis mitochondria. J. Biol. Chem. 279, 25440–6.

Petfalski, E., Dandekar, T., Henry, Y., Tollervey, D., 1998. Processing of the precursors to small nucleolar RNAs and rRNAs requires common components. Mol. Cell. Biol. 18, 1181–9.

Portnoy, V., Evguenieva-Hackenberg, E., Klein, F., Walter, P., Lorentzen, E., Klug, G., Schuster, G., 2005. RNA polyadenylation in Archaea: not observed in Haloferax while the exosome polynucleotidylates RNA in Sulfolobus. EMBO Rep. 6, 1188–93.

Preker P., Nielsen J., Kammler S., Lykke-Andersen S., Christensen M.S., Mapendano C.K., Schierup M.H., Jensen T.H., 2008. RNA exosome depletion reveals transcription upstream of active human promoters. Science, 322(5909):1851-4

Preti, M., O'Donohue, M.-F.F., Montel-Lehry, N., Bortolin-Cavaillé, M.-L.L., Choesmel, V., Gleizes, P.-E.E., 2013. Gradual processing of the ITS1 from the nucleolus to the cytoplasm during synthesis of the human 18S rRNA. Nucleic Acids Res. 41, 4709–23.

Py, B., Causton, H., Mudd, E.A., Higgins, C.F., 1994. A protein complex mediating mRNA degradation in Escherichia coli. Mol. Microbiol. 14, 717–29.

Roppelt, V., Klug, G., Evguenieva-Hackenberg, E., 2010. The evolutionarily conserved subunits Rrp4 and Csl4 confer different substrate specificities to the archaeal exosome. FEBS Lett. 584, 2931–6.

Rouquette J., Choesmel V., Gleizes P.E, 2005. Nuclear export and cytoplasmic processing of precursors to the 40S ribosomal subunits in mammalian cells. EMBO J., 24(16):2862-72

Sáez-Vasquez, J., Caparros-Ruiz, D., Barneche, F., Echeverría, M., 2004. A plant snoRNP complex containing snoRNAs, fibrillarin, and nucleolin-like proteins is competent for both rRNA gene binding and pre-rRNA processing in vitro. Mol. Cell. Biol. 24, 7284–97.

Saito, S., Hosoda, N., Hoshino, S., 2013. The Hbs1-Dom34 protein complex functions in non-stop mRNA decay in mammalian cells. J. Biol. Chem. 288, 17832–43.

San Paolo S., Vanacova S., Schenk L., Scherrer T., Blank D., Keller W., Gerber A.P., 2009. Distinct roles of non-canonical poly(A) polymerases in RNA metabolism. PLoS Genet., 5(7):e1000555

Schaeffer, D., Tsanova, B., Barbas, A., Reis, F.P., Dastidar, E.G., Sanchez-Rotunno, M., Arraiano, C.M.M., Hoof, A. van, 2009. The exosome contains domains with specific endoribonuclease, exoribonuclease and cytoplasmic mRNA decay activities. Nat. Struct. Mol.

Biol. 16, 56–62.

Schilders, G., Dijk, E. van, Pruijn, G.J., 2007. C1D and hMtr4p associate with the human exosome subunit PM/Scl-100 and are involved in pre-rRNA processing. Nucleic Acids Res. 35, 2564–72.

Schmidt, K., Xu, Z., Mathews, D.H., Butler, J.S., 2012. Air proteins control differential TRAMP substrate specificity for nuclear RNA surveillance. RNA 18, 1934–45.

Schneider, C., Kudla, G., Wlotzka, W., Tuck, A., Tollervey, D., 2012. Transcriptome-wide analysis of exosome targets. Mol. Cell 48, 422–33.

Schneider, C., Leung, E., Brown, J., Tollervey, D., 2009. The N-terminal PIN domain of the exosome subunit Rrp44 harbors endonuclease activity and tethers Rrp44 to the yeast core exosome. Nucleic Acids Res. 37, 1127–40.

Schneider, C., Tollervey, D., 2013. Threading the barrel of the RNA exosome. Trends Biochem. Sci. 38, 485–93.

Schuch, B., Feigenbutz, M., Makino, D.L., Falk, S., Basquin, C., Mitchell, P., Conti, E., 2014. The exosome-binding factors Rrp6 and Rrp47 form a composite surface for recruiting the Mtr4 helicase. EMBO J. 33, 2829–46.

Schuster, G., Lisitsky, I., Klaff, P., 1999. Polyadenylation and degradation of mRNA in the chloroplast. Plant Physiol. 120, 937–44.

Schuster, G., Stern, D., 2009. RNA polyadenylation and decay in mitochondria and chloroplasts. Prog Mol Biol Transl Sci 85, 393–422.

Shi, Z., Yang, W.-Z.Z., Lin-Chao, S., Chak, K.-F.F., Yuan, H.S., 2008. Crystal structure of Escherichia coli PNPase: central channel residues are involved in processive RNA degradation. RNA 14, 2361–71.

Shin, J.-H.H., Chekanova, J.A., 2014. Arabidopsis RRP6L1 and RRP6L2 function in FLOWERING LOCUS C silencing via regulation of antisense RNA synthesis. PLoS Genet. 10, e1004612.

Shin, J.-H.H., Wang, H.-L.V.L., Lee, J., Dinwiddie, B.L., Belostotsky, D.A., Chekanova, J.A., 2013. The role of the Arabidopsis Exosome in siRNA-independent silencing of heterochromatic loci. PLoS Genet. 9, e1003411.

Sikorski, P.J., Zuber, H., Philippe, L., Sement, F.M.M., Canaday, J., Kufel, J., Gagliardi, D., Lange, H., 2015. Distinct 18S rRNA precursors are targets of the exosome complex, the exoribonuclease RRP6L2 and the terminal nucleotidyltransferase TRL in Arabidopsis thaliana. Plant J. 83, 991–1004.

Siwaszek, A., Ukleja, M., Dziembowski, A., 2014. Proteins involved in the degradation of cytoplasmic mRNA in the major eukaryotic model systems. RNA Biol 11, 1122–36.

Sloan, K.E., Mattijssen, S., Lebaron, S., Tollervey, D., Pruijn, G.J., Watkins, N.J., 2013. Both endonucleolytic and exonucleolytic cleavage mediate ITS1 removal during human ribosomal RNA processing. J. Cell Biol. 200, 577–88.

Slomovic, S., Laufer, D., Geiger, D., Schuster, G., 2005. Polyadenylation and degradation of human mitochondrial RNA: the prokaryotic past leaves its mark. Mol. Cell. Biol. 25, 6427–35.

Slomovic, S., Portnoy, V., Liveanu, V., Schuster, G, 2006. RNA Polyadenylation in Prokaryotes and Organelles; Different Tails Tell Different Tales. Critical Reviews in Plant Sciences Vol. 25 , Iss. 1.

Slomovic, S., Laufer, D., Geiger, D., Schuster, G., 2006. Polyadenylation of ribosomal RNA in human cells. Nucleic Acids Res. 34, 2966–75.
Slomovic, S., Portnoy, V., Yehudai-Resheff, S., Bronshtein, E., Schuster, G., 2008. Polynucleotide phosphorylase and the archaeal exosome as poly(A)-polymerases. Biochim. Biophys. Acta 1779, 247–55.

Soreq, H., Littauer, U.Z., 1977. Purification and characterization of polynucleotide phosphorylase from Escherichia coli. Probe for the analysis of 3’ sequences of RNA. J. Biol. Chem. 252, 6885–8.

Souret, F.F.F., Kastenmayer, J.P., Green, P.J., 2004. AtXRN4 degrades mRNA in Arabidopsis and its substrates include selected miRNA targets. Mol. Cell 15, 173–83.

Staals, R.H., Bronkhorst, A.W., Schilders, G., Slomovic, S., Schuster, G., Heck, A.J., Raijmakers, R., Pruijn, G.J., 2010. Dis3-like 1: a novel exoribonuclease associated with the human exosome. EMBO J. 29, 2358–67.

Stickney, L.M., Hankins, J.S., Miao, X., Mackie, G.A., 2005. Function of the conserved S1 and KH domains in polynucleotide phosphorylase. J. Bacteriol. 187, 7214–21.

Tafforeau, L., Zorbas, C., Langhendries, J.-L.L., Mullineux, S.-T.T., Stamatopoulou, V., Mullier, R., Wacheul, L., Lafontaine, D.L., 2013. The complexity of human ribosome biogenesis revealed by systematic nucleolar screening of Pre-rRNA processing factors. Mol. Cell 51, 539–51.

Thoms, M., Thomson, E., Baßler, J., Gnädig, M., Griesel, S., Hurt, E., 2015. The Exosome Is Recruited to RNA Substrates through Specific Adaptor Proteins. Cell 162, 1029–38.

Thomson, E., Tollervey, D., 2010. The final step in 5.8S rRNA processing is cytoplasmic in Saccharomyces cerevisiae. Mol. Cell. Biol. 30, 976–84.

Toh-E, A., Guerry, P., Wickner, R.B., 1978. Chromosomal superkiller mutants of Saccharomyces cerevisiae. J. Bacteriol. 136, 1002–7.

Tomecki, R., Drazkowska, K., Kucinski, I., Stodus, K., Szczesny, R.J., Gruchota, J., Owczarek,

E.P., Kalisiak, K., Dziembowski, A., 2014. Multiple myeloma-associated hDIS3 mutations cause perturbations in cellular RNA metabolism and suggest hDIS3 PIN domain as a potential drug target. Nucleic Acids Res. 42, 1270–90.

Tomecki, R., Kristiansen, M.S., Lykke-Andersen, S., Chlebowski, A., Larsen, K.M., Szczesny, R.J., Drazkowska, K., Pastula, A., Andersen, J.S., Stepien, P.P., Dziembowski, A., Jensen, T.H., 2010. The human core exosome interacts with differentially localized processive RNases: hDIS3 and hDIS3L. EMBO J. 29, 2342–57.

Tu, B., Liu, L., Xu, C., Zhai, J., Li, S., Lopez, M.A., Zhao, Y., Yu, Y., Ramachandran, V., Ren, G., Yu, B., Li, S., Meyers, B.C., Mo, B., Chen, X., 2015. Distinct and cooperative activities of HESO1 and URT1 nucleotidyl transferases in microRNA turnover in Arabidopsis. PLoS Genet. 11, e1005119.

Tudek, A., Porrua, O., Kabzinski, T., Lidschreiber, M., Kubicek, K., Fortova, A., Lacroute, F., Vanacova, S., Cramer, P., Stefl, R., Libri, D., 2014. Molecular basis for coordinating transcription termination with noncoding RNA degradation. Mol. Cell 55, 467–81.

Turowski, T.W., Tollervey, D., 2015. Cotranscriptional events in eukaryotic ribosome synthesis. Wiley Interdiscip Rev RNA 6, 129–39.

Vanácová, S., Wolf, J., Martin, G., Blank, D., Dettwiler, S., Friedlein, A., Langen, H., Keith, G., Keller, W., 2005. A new yeast poly(A) polymerase complex involved in RNA quality control. PLoS Biol. 3, e189.

van Hoof, A., Frischmeyer, P.A., Dietz, H.C., Parker, R., 2002. Exosome-mediated recognition and degradation of mRNAs lacking a termination codon. Science 295, 2262–4.

van Hoof, A., Lennertz, P., Parker, R., 2000a. Yeast exosome mutants accumulate 3’-extended polyadenylated forms of U4 small nuclear RNA and small nucleolar RNAs. Mol. Cell. Biol. 20, 441–52.

van Hoof A., Staples R.R., Baker R.E., Parker R., 2000b. Function of the ski4p (Csl4p) and Ski7p proteins in 3'-to-5' degradation of mRNA. Mol Cell Biol. 20(21):8230-43.

Wang H.W., Wang J., Ding F., Callahan K., Bratkowski M.A., Butler J.S., Nogales E., Ke A., 2007. Architecture of the yeast Rrp44 exosome complex suggests routes of RNA recruitment for 3' end processing. Proc Natl Acad Sci U S A, 104(43):16844-9.

Wasmuth, E.V., Januszyk, K., Lima, C.D., 2014. Structure of an Rrp6-RNA exosome complex bound to poly(A) RNA. Nature 511, 435–9.

Wasmuth, E.V., Lima, C.D., 2012a. Exo- and endoribonucleolytic activities of yeast cytoplasmic and nuclear RNA exosomes are dependent on the noncatalytic core and central channel. Mol. Cell 48, 133–44.

Wasmuth, E.V., Lima, C.D., 2012b. Structure and Activities of the Eukaryotic RNA Exosome.

Enzymes 31, 53–75.

Weir, J.R., Bonneau, F., Hentschel, J., Conti, E., 2010. Structural analysis reveals the characteristic features of Mtr4, a DExH helicase involved in nuclear RNA processing and surveillance. Proc. Natl. Acad. Sci. U.S.A. 107, 12139–44.

Weis, B.L., Kovacevic, J., Missbach, S., Schleiff, E., 2015. Plant-Specific Features of Ribosome Biogenesis. Trends Plant Sci. 20, 729–40.

Weißbach, S., Langer, C., Puppe, B., Nedeva, T., Bach, E., Kull, M., Bargou, R., Einsele, H., Rosenwald, A., Knop, S., Leich, E., 2015. The molecular spectrum and clinical impact of DIS3 mutations in multiple myeloma. Br. J. Haematol. 169, 57–70.

West, S., Gromak, N., Norbury, C.J., Proudfoot, N.J., 2006. Adenylation and exosome-mediated degradation of cotranscriptionally cleaved pre-messenger RNA in human cells. Mol. Cell 21, 437–43.

Woolford, J.L., Baserga, S.J., 2013. Ribosome biogenesis in the yeast Saccharomyces cerevisiae. Genetics 195, 643–81.

Wyers, F., Rougemaille, M., Badis, G., Rousselle, J.-C.C., Dufour, M.-E.E., Boulay, J., Régnault, B., Devaux, F., Namane, A., Séraphin, B., Libri, D., Jacquier, A., 2005. Cryptic pol II transcripts are degraded by a nuclear quality control pathway involving a new poly(A) polymerase. Cell 121, 725–37.

Xi, L., Moscou, M.J., Meng, Y., Xu, W., Caldo, R.A., Shaver, M., Nettleton, D., Wise, R.P., 2009. Transcript-based cloning of RRP46, a regulator of rRNA processing and R gene-independent cell death in barley-powdery mildew interactions. Plant Cell 21, 3280–95.

Yang, M., Zhang, B., Jia, J., Yan, C., Habaike, A., Han, Y., 2013. RRP41L, a putative core subunit of the exosome, plays an important role in seed germination and early seedling growth in Arabidopsis. Plant Physiol. 161, 165–78.

Ye, R., Chen, Z., Lian, B., Rowley, M.J., Xia, N., Chai, J., Li, Y., He, X.-J.J., Wierzbicki, A.T., Qi, Y., 2016. A Dicer-Independent Route for Biogenesis of siRNAs that Direct DNA Methylation in Arabidopsis. Mol. Cell 61, 222–35.

Zakrzewska-Placzek, M., Souret, F.F., Sobczyk, G.J., Green, P.J., Kufel, J., 2010. Arabidopsis thaliana XRN2 is required for primary cleavage in the pre-ribosomal RNA. Nucleic Acids Res. 38, 4487–502.

Zhang, H., Tang, K., Qian, W., Duan, C.-G.G., Wang, B., Zhang, H., Wang, P., Zhu, X., Lang, Z., Yang, Y., Zhu, J.-K.K., 2014. An Rrp6-like protein positively regulates noncoding RNA levels and DNA methylation in Arabidopsis. Mol. Cell 54, 418–30.

Zhang, W., Murphy, C., Sieburth, L.E., 2010. Conserved RNaseII domain protein functions in cytoplasmic mRNA decay and suppresses Arabidopsis decapping mutant phenotypes. Proc.

Natl. Acad. Sci. U.S.A. 107, 15981–5.

Zhao, Y., Yu, Y., Zhai, J., Ramachandran, V., Dinh, T.T., Meyers, B.C., Mo, B., Chen, X., 2012. The Arabidopsis nucleotidyl transferase HESO1 uridylates unmethylated small RNAs to trigger their degradation. Curr. Biol. 22, 689–94.

Zhou, Y., Zhu, J., Schermann, G., Ohle, C., Bendrin, K., Sugioka-Sugiyama, R., Sugiyama, T., Fischer, T., 2015. The fission yeast MTREC complex targets CUTs and unspliced pre-mRNAs to the nuclear exosome. Nat Commun 6, 7050.

Zuber, H., Scheer, H., Ferrier, E., Sement, F.M.M., Mercier, P., Stupfler, B., Gagliardi, D., 2016. Uridylation and PABP Cooperate to Repair mRNA Deadenylated Ends in Arabidopsis. Cell Rep 14, 2707–17.

Natalia Sikorska

The phosphorolytic activity of the exosome core complex contributes to rRNA maturation in *Arabidopsis*

Résumé

L'exosome joue un rôle fondamental dans la dégradation de 3' en 5' et la maturation des ARNs chez les eucaryotes. Le "cœur" de l'exosome est composé de 9 sous-unités (EXO9). EXO9 est catalytiquement inactif chez l'homme et la levure, et est associé à deux RNases, Rrp6 et Rrp44, responsables de l'activité exonucléolytique de l'exosome.
Mes travaux de thèse démontrent que chez *Arabidopsis*, le cœur de l'exosome EXO9 possède une activité catalytique intrinsèque. Cette activité est dépendante de la présence de phosphate, produit des nucléosides diphosphates et est réversible. Elle possède de ce fait toutes les caractéristiques d'une **activité phosphorolytique**. L'activité d'EXO9 est impliquée dans l'élimination de sous-produits de la maturation des ARNr et dans la maturation de l'ARNr 5.8S, deux fonctions typiques de l'exosome. Mes travaux révèlent également que AtRRP44, EXO9 et AtRRP6L2 coopèrent de manière séquentielle pour la maturation de l'ARN 5.8S.
Mes travaux de thèse constituent la base de travaux futurs visant à comprendre les rôles de l'activité phosphorolytique de l'exosome chez un organisme eucaryote.

Mots-clés : dégradation des ARNs, exosome, EXO9, exoribonucléase phosphorolytique, *Arabidopsis thaliana*

Abstract

The **eukaryotic RNA exosome** complex is the main 3'-5' degradation machinery that plays an essential role in RNA decay, quality control and maturation. The exosome core complex (EXO9) is catalytically inert in yeast and humans, and therefore relies on the catalytic activity of associated RNases, Rrp6 and Rrp44.
In this study I demonstrated that EXO9 is catalytically active in *Arabidopsis*. EXO9's activity is phosphate-dependent, releases nucleoside diphosphates and is reversible, meeting all criteria of a **phosphorolytic activity**. Importantly, EXO9's *in vivo* substrates include the archetypical exosome substrates, rRNA maturation by-products and 5.8S rRNA precursors. My data show that AtRRP44, EXO9 and AtRRP6L2 sequentially cooperate for the processing of 5.8S rRNA.
This work sets a basis for studies aiming at further understanding the biological functions of EXO9's phosphorolytic activity in a eukaryotic organism.

Keywords: RNA degradation, exosome, EXO9, phosphorolytic exoribonuclease, *Arabidopsis thaliana*